The cytoskeletal linker protein, Ezrin, inhibits α-synuclein fibrillization and toxicity by a novel mechanism

Dissertation zur Erlangung des akademischen Grades des

Doktors der Naturwissenschaften (Dr. rer. nat.)

eingereicht im Fachbereich Biologie, Chemie, Pharmazie

der Freien Universität Berlin

vorgelegt von

Maliha Shah
aus Mumbai, Indien

Berlin, 2013

Die Arbeit wurde im Zeitraum von September 2008 bis September 2012 unter der Leitung von Herrn Prof. Dr. Erich E. Wanker am Max Delbrück Centrum für Molekulare Medizin Berlin-Buch angefertigt.

1. Gutachter: Prof. Dr. Erich E. Wanker

2. Gutachter: Prof. Dr. Fritz G. Rathjen

Disputation am 04.04.14

ACKNOWLEDGEMENTS

This work was made possible by the financial support of the Helmholtz Gemeinschaft and my supervisor, Prof. Erich Wanker, to whom I am grateful for the resources, guidance and freedom to pursue different avenues throughout my time in lab. I would also like to thank Dr. Jan Bieschke for the immeasurable contribution throughout my PhD.

To Dr. Philipp Selenko and Dr. Silvia Verzini (my friend and colleague) I will be eternally grateful for the interest, effort and sheer work that accompanied the unlimited hours of spectrometer-usage.

To my colleagues and labmates, particularly Anup Arumughan and Anne Wagner, I cannot express how much I value the help, advice and patience. The most heartfelt thanks go to all my friends at the MDC (and outside it), who are too numerous to list on a single page, but whose care and concern I have not forgotten.

To my family both in India and in Germany, I am indebted: Christian Minaty and family, Damir Omerbasic, Manisha Juneja, Vaishnavi Raghunathan, Mayur Vadhvani, my MolNeuro friends, Indubai Laigude, Ranga Devadiga and everyone else, thank you for everything.

And last of all, for their unparalleled faith, support and love, I owe the deepest gratitude of all to my parents, to whom I dedicate my thesis.

TABLE OF CONTENTS

1. INTRODUCTION

1.1 A background on Parkinson's disease

Parkinson's disease (PD) is a progressive, neurodegenerative, aging disorder, named after the man who first described it in 1817 in *An Essay on the Shaking Palsy*, Dr. James Parkinson (Parkinson, 2002). PD is the second most common neurodegenerative disease, after Alzheimer's disease, affecting 1% of the population over the age of 60 years (Samii et al., 2004). While disease symptoms appear at a mean age of onset of 57 years (Koller et al. (1987), about 5% of the individuals diagnosed with PD are younger than 40 years of age (early-onset PD) (Gershanik and Nygaard, 1990).

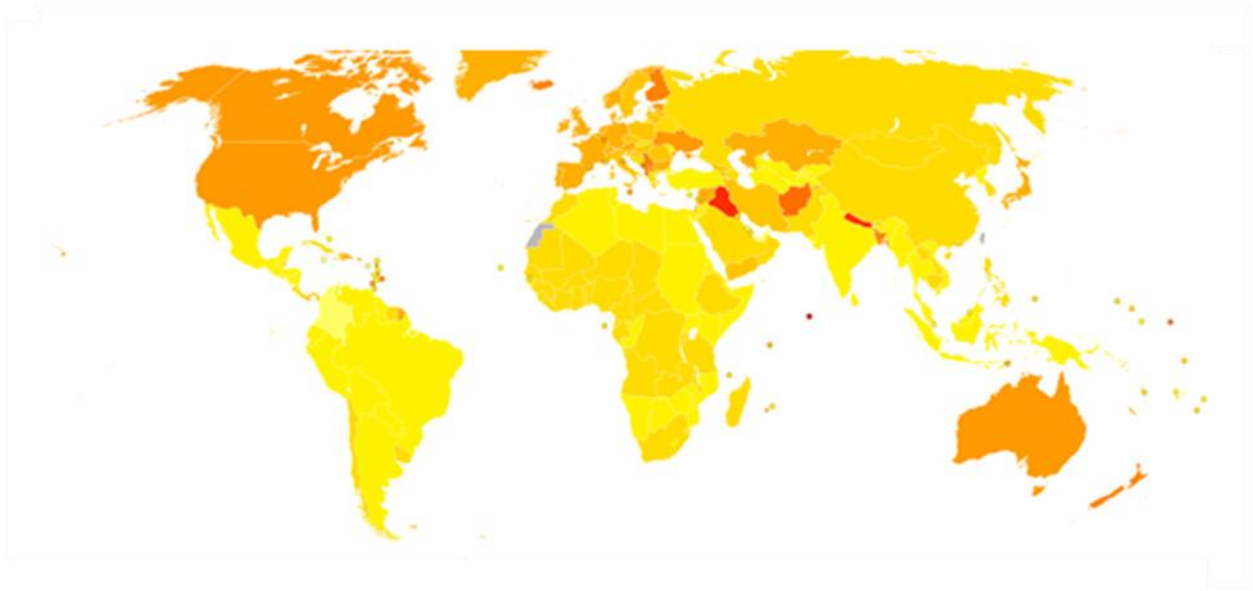

Fig 1.1 Global burden of Parkinson's disease, measured in disability-adjusted life years per 100,000 inhabitants in 2004 [adapted from *Death and DALY estimates for 2004 by cause for WHO Member States (Persons, all ages)* (2009-11-12), World Health Organisation, Department of Measurement and Health Information (((WHO), 2009)].

1.1.1 Clinical symptoms of PD

The motor symptoms of PD are collectively termed 'parkinsonism'. They include the hallmark 'resting tremor', involuntary shaking, akinesia, bradykinesia (slowness of movement), reduced spontaneous movement, rigidity, balance problems, difficulty in walking, disturbances to posture and hypomimia (reduced facial expression). Other non-motor symptoms include fatigue, sleep abnormalities, constipation and gastric dysmotility (Tanner et al., 2009). As the disease advances, PD patients may also show autonomic, behavioural

and psychiatric problems, such as depression and anxiety (Chaudhuri and Schapira, 2009). Cognitive impairment e.g. slowness in memory and thought, increases with age and disease progression (Levy, 2007).

Fig 1.1.1 Illustration of Parkinson's disease by William Richard Gowers, first published in A Manual of Diseases of the Nervous System (1886) [adapted from (Gowers and Barker, 1886)].

1.1.2 Pathology of PD

Lewy Body formation: The hallmark pathological characteristic of PD is the presence of intracellular proteinaceous inclusions or deposits, termed Lewy bodies (LB), first described in 1912 by Frederic Lewy (Lewy, 1912). The analysis of LBs reveals their major constituent to be amyloid fibrils made up of the protein, α-synuclein (Spillantini et al., 1997), which is strongly expressed in presynaptic terminals of the central nervous system (CNS). Another pathological feature of PD is the appearance of Lewy neurites, which correspond to abnormal neurites containing inclusions similar to those found in LBs (Dickson et al., 1991). LBs are particularly abundant in the area of the mid-brain called the substantia nigra (Tretiakoff, 1919), which plays a role in the control of voluntary movement, learning, reward-seeking and addiction, specifically in the substantia nigra pars compacta (SNpc) (Braak and Braak, 2000), the most prominent function of which is motor control (Banich MT, 2011). Parts of the substantia nigra appear darker than neighbouring areas due to high levels of melanin in the constituent dopaminergic neurons, lending this region its name, which is Latin for “black substance”.

Loss of dopaminergic neurons: Aside from the formation of LBs, PD is characterized by the progressive loss of dopaminergic neurons in the SNpc of PD patients (Braak and Braak, 2000), and such neuronal degeneration leads to a depigmentation of the area in post-mortem brains of PD patients (Figure 1.1.2.1) (Forno, 1974). The cause of death of dopaminergic neurons in the pars compacta is unknown. However, some contributions to the unique susceptibility of dopaminergic neurons in the pars compacta have been identified. For one, dopaminergic neurons show abnormalities in mitochondrial complex 1, which may cause aggregation of α-synuclein. This could result in abnormal protein handling and neuronal death (Betarbet et al., 2000). Regardless of the cause of neuronal death, the plasticity of the pars compacta is very robust; Parkinsonian symptoms do not appear until up to 50-80% of pars compacta dopaminergic neurons have died (Sherer et al., 2003). Most of this plasticity occurs at the neurochemical level; dopamine transport systems are slowed, allowing dopamine to linger for longer periods of time in the chemical synapses in the striatum (Sherer et al., 2003), probably accounting for many of the symptoms previously described for PD.

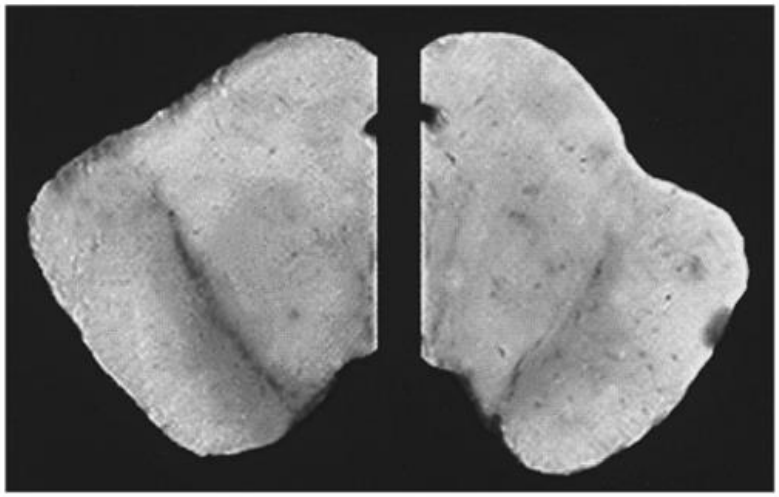

Fig 1.1.2.1 Melanized dopaminergic neurons of the substantia nigra from post mortem human brain. Brain sections taken through the mid-brain of a normal (left) and a Parkinson's disease patient (right). The Parkinson's diseased hemisphere on the right shows a loss of the melanized neurons in the substantia nigra in the ventral midbrain (Alexi et al., 2000; Mazzio et al., 2011)

Neurons in the SNpc display characteristics which make them highly susceptible to cell death (as shown in Fig. 1.1.2.2. below), for example a higher dopamine transporter (DAT)/vesicular monoamine transporter 2 (VMAT2) ratio and the use of CaV1.3 calcium (Ca2+) channels for autonomous pacemaking (Venda et al., 2010). Subtle increases in Ca2+ levels in the cytoplasm activate dopamine (DA) synthesis. Impairment of vesicle docking and recycling due to α-synuclein dysfunction could prevent incorporation of newly synthesized

and newly taken up DA into vesicles. This could lead to an increase in cytosolic DA concentration (DAcyt), which causes increased generation of toxic reactive species and ultimately contributes to dopaminergic neurodegeneration. Thus, the combined action of α-synuclein dysfunction and increased dopamine in the cytosol of SNpc neurons could drive cell death in Parkinson's disease (PD).

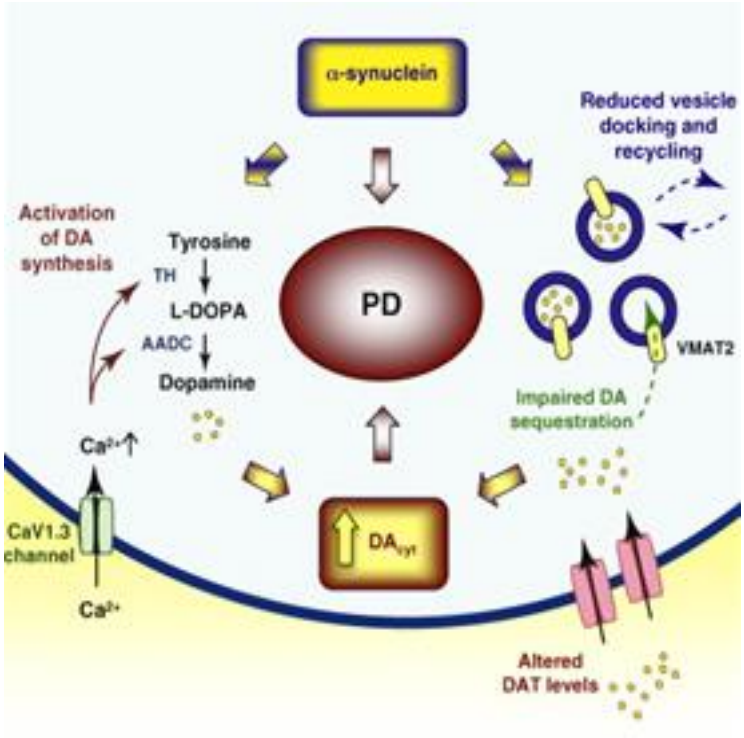

Fig 1.1.2.2. A schematic working model illustrating various proposed cellular mechanisms for how preferential neurodegeneration of substantia nigra pars compacta (SNpc) dopaminergic neurons could take place [adapted from (Venda et al., 2010)].

Although dopaminergic neurons represent less than 1% of the total amount of neurons in the human brain, these cells play an important role in the regulation of basic brain functions (Chinta and Andersen, 2005). While major disease symptoms become evident after significant loss of dopaminergic neurons projecting from the SNpc to the striatum (Samii et al., 2004), PD pathology is not limited to the nigrostriatal pathway, as LBs have also been found in the cortex, amygdala, locus coeruleus, peripheral autonomic system and particularly, the enteric nervous system innervating the gut (Dickson et al., 2009; Wolters, 2009).

1.1.3 Treatment options

There is presently no cure for Parkinson's disease. Neither effective treatments nor preventive measures have been identified so far, and slowing down the disease on a cellular level is not possible as of yet. Available medication is directed mainly at treating the

symptoms (low dopamine levels), rather than the underlying problem (the death of dopaminergic neurons in the substantia nigra), since the initial onset of the disease is not completely understood and patients often present only after the symptoms have become strikingly evident and/or cause noticeable disability. Thus, medicine is often first prescribed at an already advanced stage of the disease. The major focus of treatment is the replacement of the neurotransmitter dopamine, which is lost due to the death of the dopaminergic neurons. PD is generally treated with dopamine agonists that stimulate dopamine receptors in the brain and thus mimic the action of dopamine, or chemical therapeutics such as levodopa (L-DOPA, the dopamine precursor), which directly replaces dopamine (Foley et al., 2004).

Levodopa treatment: Levodopa (commonly referred to as L-DOPA) can cross the blood–brain barrier and increase dopamine levels in the substantia nigra, thus alleviating the symptoms of PD. As the disease progresses and dopamine neurons continue to be lost, eventually levodopa - like other drugs - can become ineffective at treatment, and may even produce complications such as involuntary movements (Zhang et al., 2000). Additional undesirable side-effects of chronic levodopa administration include end-of-dose deterioration of function, on/off oscillations, freezing during movement, dose failure (drug resistance), dyskinesia at peak dose, possible serotonin depletion and possible dopamine dysregulation. Despite controversy concerning the neurotoxicity of dopamine and L-DOPA (Wood-Kaczmar et al., 2006), it remains the most potent and most commonly prescribed anti-parkinson drug.

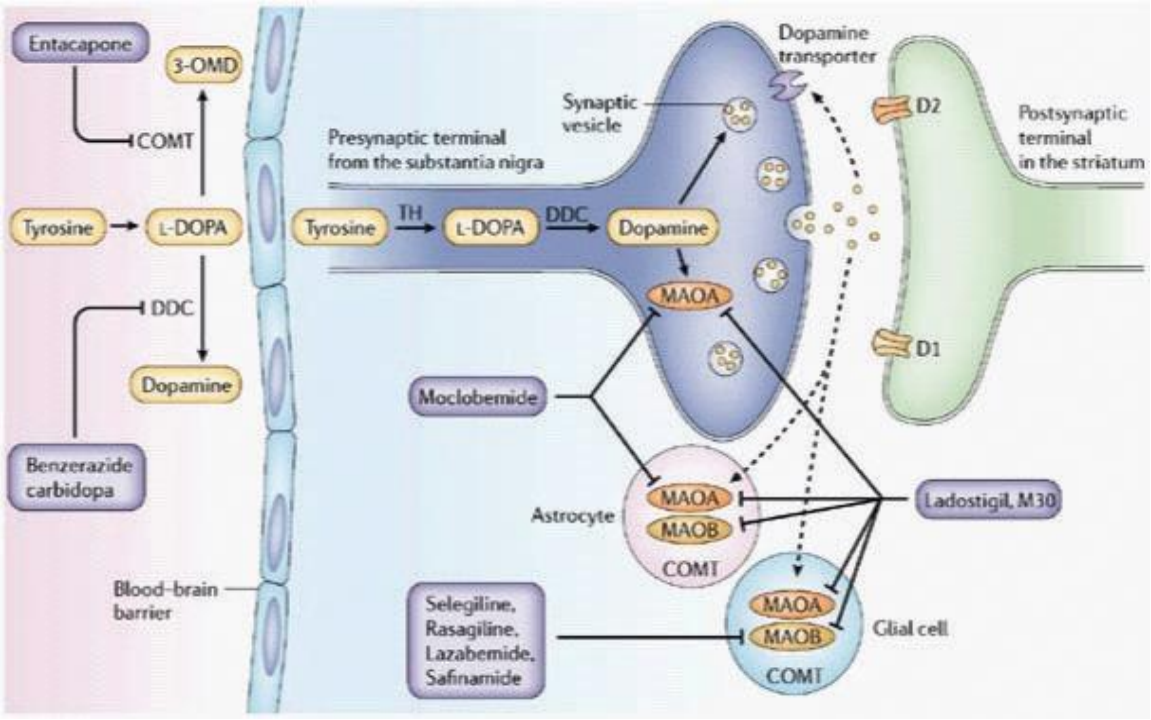

Fig 1.1.3 The pathway of dopamine synthesis proceeds from tyrosine via tyrosine hydroxylase (TH) catalysis to levodopa (L-DOPA), and subsequent decarboxylation by dopa decarboxylase (DDC) to dopamine [adapted from (Youdim et al., 2006)]. Dopamine is metabolized by intraneuronal monoamine oxidase A (MAOA) and by glial and astrocyte MAOA and MAOB1. Selective inhibitors of MAOA (for example, moclobemide) and MAOB (selegiline, rasagiline and safinamide) do not alter the steady-state striatal dopamine levels, although chronic treatment with these drugs does enhance dopamine release, possibly due to the elevation of endogenous brain amines or receptor modulation. However, non-selective MAOA/B inhibitors (such as ladostigil) do induce highly significant increases in the levels of dopamine in the striatum and other regions. Although dopamine does not pass the blood–brain barrier (BBB), L-DOPA can, and DDC inhibitors that do not pass the BBB, such as benzerazide (benserazide) and carbidopa, increase its availability to the brain. Inhibitors of catechol-O-methyltransferase (COMT), such as entacapone, also enhance L-DOPA availability and prevent the inactivation of dopamine by COMT. 3-OMD, 3-O-methyl dopa; D1, D2, dopamine receptors.

Intensive measures: Surgery and deep brain stimulation (DBS) are used to reduce motor symptoms as a last resort in severe cases where drugs are ineffective. Surgical options for treatment were far more common before the introduction of levodopa in the 1960s (Samii et al., 2004). DBS involves the implantation of a medical device called a brain pacemaker, which sends electrical impulses to specific parts of the brain. DBS is recommended for people who have PD who suffer from motor fluctuations and tremor inadequately controlled by medication, or to those who are intolerant to medication, as long as they do not have severe neuropsychiatric problems (Bonifati et al., 2003). Fetal nigral tissue transplantation has been shown to result in the survival of dopamine neurons, however, either no relevant motor improvement was noted (Olanow et al., 2003) or severe side-effects occurred (Freed et al., 1992), which excludes transplantation from the list of treatment options for PD at present.

Additional protective factors: Caffeine consumption protects against PD (Gosavi et al., 2002). "Prospective epidemiologic studies performed in large cohorts of men (total: 374,003 subjects) suggest that the risk for PD diminishes progressively as the consumption of coffee and other caffeinated beverages increases" (Conway et al., 2001). Tobacco smoking has been related to a reduced risk of having PD. Smokers' risk of having PD may be reduced down to a third when compared to non-smokers (Beyer, 2006). The basis for this effect is not known, but possibilities include an effect of nicotine as a dopamine stimulant (Beyer, 2006; Conway et al., 2000c). Tobacco smoke contains compounds that act as MAO inhibitors that also might contribute to this effect (Dev et al., 2003).

1.1.4 Factors contributing to PD

Over 90% of PD cases are considered to be idiopathic or sporadic, i.e. having no specific known cause or an unknown origin of the disease, hence PD traditionally has been considered a non-genetic disorder. However, an estimated 5-10% of all parkinsonian cases are familial; ~15% of individuals with PD have a first-degree relative who has the disease (Koller et al., 1987). At least 5% of people are now known to have forms of the disease that occur because of a mutation of one of several specific genes (Norris et al., 2007).

1.1.4.1 Factors contributing to idiopathic PD [environmental factors]

As the underlying cause of this form of PD is still unknown, various hypotheses have been put forward to explain its appearance, and the role of environmental factors has been particularly examined. An association between pesticide exposure and PD has been demonstrated by several studies (Dick et al., 2007; Frigerio et al., 2006; Tanner et al., 2009). Exposure to paraquat and rotenone leads to development of neurodegenerative phenotypes resembling PD in mice, rats and primates (Betarbet et al., 2000; Norris et al., 2007; Sherer et al., 2003). The herbicide paraquat is used to eliminate weeds, and rotenone is used as insecticide, piscicide and pesticide. Exposure to 1-methyl-4-phenyl-1,2,3,6-tetrahydropyridine (MPTP) directly causes parkinsonism (Davis et al., 1979; Langston et al., 1983). MPTP is a contaminant of artificial heroin (1-methyl-4-phenyl-propionoxypiperidine (MPPP) and has a similar structure to paraquat. Both paraquat and MPTP bind to the mitochondrial complex I and interfere with oxidative phosphorylation, leading to mitochondrial dysfunction (Ayala et al., 2007). As previously mentioned, abnormalities in mitochondrial complex I are associated with α-synuclein aggregation and are detrimental to the health of cells. Furthermore, disturbed mitochondrial function leads to an increase in reactive oxygen species (ROS), which oxidize and damage different components of a cell, thereby giving rise to toxicity. Heavy metal exposure, particularly excessive exposure to iron, has been proposed to be a risk factor, through possible accumulation in the substantia nigra.

1.1.4.2 Factors contributing to familial PD [genetic factors]

Most of the familial cases are caused by mutations in the genes SNCA, PARK2, PINK1, DJ1 and LRRK2 (Wood-Kaczmar et al., 2006). Fig 1.1.4.2 below shows a diagrammatic representation of the various domains of the 5 proteins expressed by these genes.

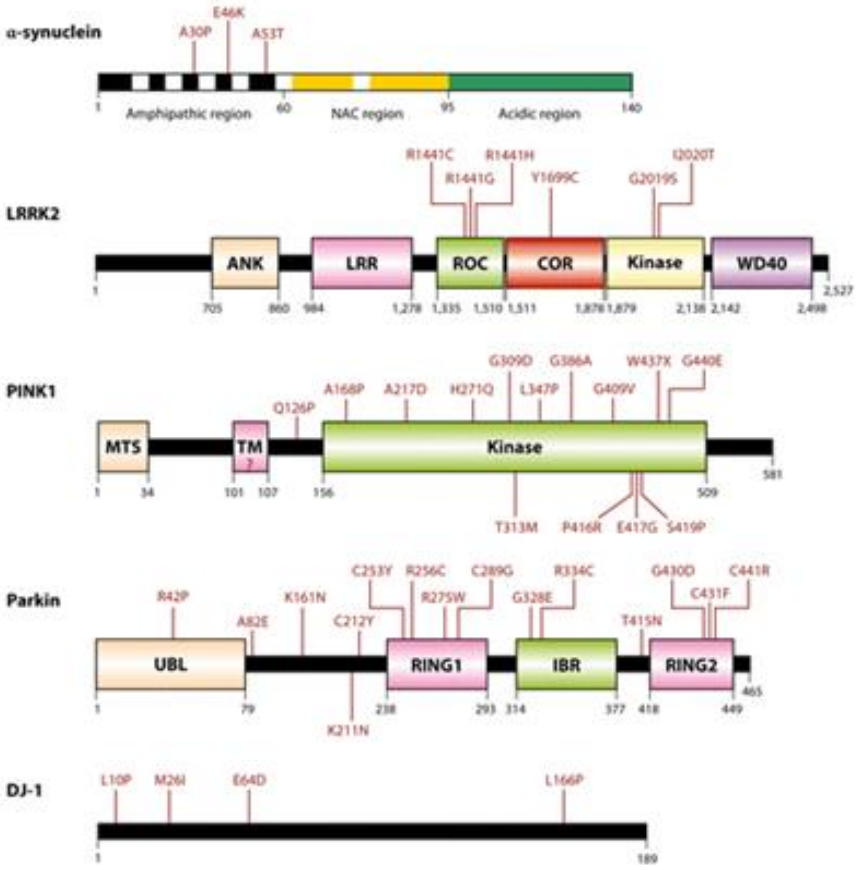

Fig 1.1.4.2 Diagrammatic representation of the different domains of the proteins expressed by the 5 principal genes known to be involved in Parkinson's disease (Martin et al., 2011).

The best studied gene in PD is SNCA, the gene encoding α-synuclein, which is in the focus of this doctoral work. The E3 ubiquitin protein ligase parkin encoded by the gene PARK2 targets misfolded proteins for degradation by the ubiquitin proteasome pathway (Zhang et al., 2000). Mutations in the PARK2 gene are linked to autosomal recessive early-onset PD (Kitada et al., 1998; Shimura et al., 2000; Zhang et al., 2000). The serine/threonine-protein kinase PINK1 accumulates within the intermembrane space of mitochondria (Silvestri et al., 2005). Some rare forms of familial PD are correlated to mutated PINK1 (Silvestri et al., 2005). Overexpression of wild-type PINK1 in cell lines prevents the release of mitochondrial cytochrome c and subsequent apoptosis, but this function is abolished in cells expressing familial PD-linked PINK1 mutants (Petit et al., 2005). Loss-of-function mutations in the DJ-1 gene have been associated with rare forms of autosomal recessive early-onset parkinsonism (Bonifati et al., 2003). The homodimeric protein may function as a scavenger of reactive oxygen species (ROS) (Canet-Aviles et al., 2004; Taira et al., 2004). It was also suggested that oxidized DJ-1 acts as a chaperone and might prevent early steps in the formation of α-synuclein aggregates (Shendelman et al., 2004). Mutations in the leucine-rich repeat kinase

2 (LRRK2) cause autosomal dominant PD (Paisan-Ruiz et al., 2004; Zimprich et al., 2004). Furthermore, LRRK2 point mutations have been associated with 1-2% of the idiopathic PD cases (Di Fonzo et al., 2005; Gilks et al., 2005). A role for LRRK2 as a modulator in a mitochondrial dependent cell death pathway has been suggested (Paisan-Ruiz et al., 2004). In summary, the number of genes associated with PD is growing constantly (Nalls et al., 2011); in fact, according to the PDGene database (a database for Parkinson's disease genetic association studies developed by the Max Planck institute for Molecular Genetics Berlin, the Michael J. Fox Foundation and the Alzheimer Research Forum), 881 different studies have revealed 915 genes that are thought to be involved in Parkinson's disease (Lill et al., 2012).

1.2 The role of α-synuclein in PD

PD, along with dementia with LBs and multiple system atrophy, is referred to as a synucleinopathy (Jellinger, 2003). Synucleinopathies are a heterogeneous group of neurodegenerative disorders characterized by LBs containing large amounts of aggregated α-synuclein (hereafter referred to as SNCA in case of the corresponding gene/DNA) (Jellinger, 2003). Several mutations identified in the SNCA locus have linked α-synuclein to familial PD. The first mutations were found in Italian and Greek families with a dominantly inherited form of PD (Polymeropoulos et al., 1997). The authors identified the G209A missense mutation leading to an A53T (alanine to threonine) amino acid exchange. The age of disease onset in affected patients was around 40 years. Subsequently, additional point mutations associated with autosomal dominant PD were identified in the SNCA gene. The G88C missense mutation leads to an A30P (alanine to proline) amino acid exchange in German PD patients (Kruger et al., 1998). The third missense mutation was discovered in a Spanish family (Zarranz et al., 2004). In these patients, the G188A mutation caused the E46K (glutamic acid to lysine) amino acid exchange, leading to autosomal dominant PD (Zarranz et al., 2004). In addition, duplication and triplication of the SNCA locus has been reported in families with an autosomal dominant inheritance pattern (Chartier-Harlin et al., 2004; Singleton et al., 2003), further confirming the important role of α-synuclein in the pathogenesis of the disease. Strikingly, a gene dosage effect was identified, as an earlier disease onset and more severe symptoms were observed in the cases with SNCA triplication (Fuchs et al., 2007). Several genome-wide association studies (GWAS) performed recently have associated polymorphisms in the SNCA locus with PD (Latourelle et al., 2009; Satake et al., 2009; Simon-Sanchez et al., 2009). Taken together, these studies suggest that α-synuclein also plays an important role in sporadic PD. Consistent with this hypothesis, SNCA transcript levels are increased in PD brains (Chiba-Falek et al., 2006) and LBs containing aggregated α-synuclein are also present in the sporadic cases of the disease (Baba et al., 1998).

Identification of α-synuclein: α-synuclein was first isolated in 1988 from *Torpedo californica* (an electric ray) using an antiserum against cholinergic vesicles (Maroteaux et al., 1988). The protein was localized to the nuclear envelope and presynaptic nerve terminals of neurons and was thus named synuclein (Maroteaux et al., 1988). Later, a peptide termed NAC (Non-Amyloid Component of AD amyloid) was found in amyloid plaques of Alzheimer's disease (AD) patients. The precursor protein of this peptide (NACP) was identified as a homolog of rat α-synuclein (Ueda et al., 1993).

INTRODUCTION

Evolutionary conservation and expression of synuclein: α-synuclein belongs to the family of synucleins, which also includes beta-synuclein and gamma-synuclein (George, 2002). The members of the family have a similar domain organization and are 55-62% identical in sequence (Goedert, 2001). Synucleins are highly conserved between vertebrate species (Clayton and George, 1998). All members of the synuclein family are abundantly present in the human brain, but their exact physiological function remains to be determined. α-synuclein is primarily found in neural tissue and comprises 1% of total cytosolic protein.

Genetic aspects of α-synuclein: The human SNCA gene is located on chromosome 4q21.3-q22 and spans a region of 111 kb. The gene consists of seven exons, but only five of them correspond to a region encoding the 140 amino acid α-synuclein protein.

Recent genetic studies have identified common variants at the SNCA locus which are associated with sporadic PD, as depicted in Fig 1.2 below (Venda et al., 2010). In these studies, three single nucleotide polymorphisms (SNPs) were found to be most highly associated with PD, namely, rs2736990, rs3857059 and rs11931074, as shown in Fig.1.2.A. Such variants could affect α-synuclein function and contribute to PD etiology by altering levels of gene transcription, altering mRNA stability (via altered miRNA binding) or by altering the generation of alternative splice isoforms. Some of the 3′ SNPs have been shown to be in linkage disequilibrium (LD) with the REP1 dinucleotide repeat in the promoter region, previously found to regulate SNCA expression.

Other studies have reported four different α-synuclein isoforms (SNCA140, SNCA126, SNCA112, and SNCA98) that are generated by alternative splicing of exons 3 and 5 (Beyer, 2006). One of these isoforms, SNCA112 (shown in Fig.1.2.B), is only found in brains from patients with LB disease (Kalivendi et al., 2010). In addition, this isoform is upregulated in PD cell culture models using MPTP or rotenone (Kalivendi et al., 2010).

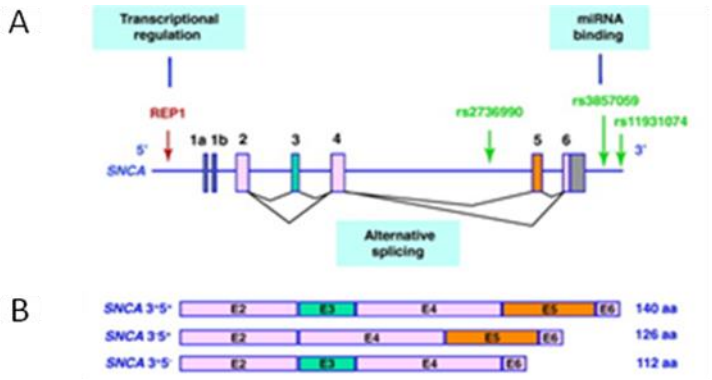

Fig 1.2. Possible *SNCA*-associated disease mechanisms [adapted from (Venda et al., 2010)]. (A) The three single nucleotide polymorphisms (SNPs) that were found to be most highly associated with PD (rs2736990, rs3857059 and rs11931074) are indicated by green arrows, while the REP1 dinucleotide repeat in the promoter region is indicated in red. (B) Alternative splicing of exons 3 and 5 generates four SNCA isoforms of different lengths, one of which (SNCA112; exon 3+5−) has been implicated in Lewy body formation and neurotoxicity.

1.2.1 Function of α-synuclein

Recently, Burre and colleagues demonstrated that α-synuclein binds directly to the SNARE-protein synaptobrevin-2/vesicle-associated membrane protein 2 (VAMP2) and promotes SNARE-complex assembly, both *in vitro* and *in vivo* (Burre et al., 2010). Prior to this, no specific function had been assigned to α-synuclein for the longest time, although it had been implicated in a variety of roles, e.g. vesicular transport, interactions with membranes and lipids, and interactions with other proteins, e.g. phospholipase D2. These three broad categories have been examined in greater detail, below:

Vesicular transport: In pre-synaptic termini, monomeric α-synuclein exists in an equilibrium between free and plasma membrane- or vesicle-bound states (McLean et al., 2000), with approximately 15% of α-synuclein being membrane-bound (Lee et al., 2002a). This close association with vesicular structures has led to the hypothesis that α-synuclein may regulate vesicular release and/or turnover and other synaptic functions in the central nervous system - a hypothesis which was later confirmed by Burre et al. (Burre et al., 2010; Clayton and George, 1998; Clayton and George, 1999; Davidson et al., 1998; Lavedan, 1998; Ueda et al., 1993). As depicted in Fig. 1.2.1 below, (a) When α-synuclein levels are reduced, the availability of vesicles in the reserve pool is decreased (Latourelle et al., 2009; Satake et al., 2009) and more vesicles are readily available to be released (Chiba-Falek et al., 2006), which can lead to an increase in dopamine release. (b) Under normal conditions α-synuclein is thought to play a physiological role in regulating vesicle availability in the different pools and influences vesicle docking and fusion. (c) By contrast, elevated α-synuclein levels or mutated E46K or A53T α-synuclein can lead to a reduction in dopamine release (Clayton and George, 1998) possibly by affecting a late step in exocytosis (Maroteaux et al., 1988) or by decreasing vesicle availability in the recycling pool due to impaired vesicle endocytosis (Simon-Sanchez et al., 2009).

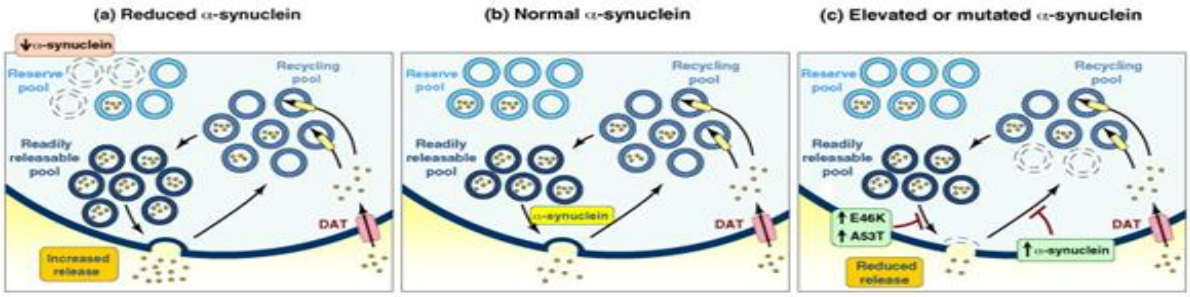

Fig 1.2.1. Schematic model of α-synuclein's proposed roles in regulating presynaptic vesicle cycling in situations of different α-synuclein levels [adapted from (Venda et al., 2010).

Genome-wide screening in yeast showed that nearly one-third of genes that enhance the toxicity of α-synuclein are functionally related to lipid metabolism and vesicle trafficking (Willingham et al., 2003). Expression profiling of transgenic flies revealed that expression of lipid and membrane transport genes were associated with α-synuclein expression (Scherzer et al., 2003). To prevent neurodegeneration, α-synuclein cooperates with cysteine string protein-a (CSPa), an abundant synaptic vesicle protein, which possesses a co-chaperone function and is essential for neuronal survival (Chandra et al., 2005). This cooperation is accomplished via a downstream mechanism that requires phospholipid binding by α-synuclein (Chandra et al., 2005). Based on these observations, it has been concluded that one of the crucial α-synuclein functions *in vivo* is the protection of the nerve terminals against injury via cooperation with CSPa and soluble NSF (N-ethylmaleimide sensitive factor) attachment receptor proteins on the presynaptic membrane interface (Bonini and Giasson, 2005; Chandra et al., 2005). Finally, a more recent study revealed that α-synuclein regulates catecholamine release from synaptic vesicles (Larsen et al., 2006).

Interaction with membranes and lipids: α-synuclein interacts stably with synthetic phospholipid vesicles containing negatively-charged head groups (Davidson et al., 1998; Jo et al., 2000; Ramakrishnan et al., 2003), various phospholipid membranes, fatty acids, detergent micelles (Cole et al., 2002; Jo et al., 2004; Jo et al., 2000; Kim et al., 2006; Necula et al., 2003; Perrin et al., 2001; Sharon et al., 2003; Zhu and Fink, 2003; Zhu et al., 2003) and with biological membranes, such as crude brain vesicles (Jensen et al., 1998), general cellular membranes (McLean et al., 2000), lipid rafts (Fortin et al., 2004), and lipid droplets (Cole et al., 2002). The protein has a higher affinity for small vesicles than for vesicles of larger diameter, possibly because of the higher surface-to-volume ratio of small vesicles (Davidson et al., 1998; Zhu and Fink, 2003). The association of α-synuclein with negatively charged membranes of multilamellar vesicles has a profound effect on the integrity of these bilayers and causes the formation of non-bilayer or small vesicular structures (Madine et al., 2006). These observations suggest that α-synuclein plays a role in modulating the

organization of membrane lipid components. Additionally, lipid packing in small unilamellar vesicles is apparently affected by interaction with α-synuclein (Kamp and Beyer, 2006). Finally, it has been found that monomeric α-synuclein bound to the lipid membrane can efficiently prevent lipid oxidation, possibly suggesting that the inhibition of lipid oxidation is a physiological function of the protein (Zhu et al., 2006).

Interaction with other proteins: α-synuclein was shown to act as a high affinity inhibitor of phospholipase D2, which hydrolyzes phosphatidylcholine to phosphatidic acid (Jenco et al., 1998). α-synuclein is also involved in regulation of certain enzymes, transporters, and neurotransmitter vesicles (Dev et al., 2003). Indeed, α-synuclein can act as a molecular chaperone assisting in the folding and refolding of synaptic proteins such as NSF (N-ethylmaleimide sensitive factor) and attachment receptors (Chandra et al., 2005). In case-by-case studies, α-synuclein has been shown to interact with at least 50 proteins and other ligands (Dev et al., 2003). In a recent proteomic analysis, 587 proteins were found to be involved in the formation of complexes with α-synuclein in dopaminergic substantia nigra and neuroblastoma hybrid cell lines (MES 23.5 or MES) and 141 proteins displayed significant changes in their relative abundance (increase or decrease) after the substantia nigra/neuroblastoma hybrid cells (MES cells) were treated with rotenone (Jin et al., 2007). It is important to note that this large number of α-synuclein-binding partners might be an overestimate, as some of the proteins could be enriched due to high concentrations of sodium dodecyl sulfate micelles to which both α-synuclein and its partner proteins can bind.

1.2.2 The role of α-synuclein in cellular dysfunction

In keeping with the variety of functions attributed to α-synuclein (as described above), the protein also leads to several forms of cellular dysfunction, as detailed below:

1.2.2.1 Evidence from cell-culture studies

Overexpression of α-synuclein in a neuronal cell line and homozygous deletions of α-synuclein in mice were both accompanied by noticeable changes in membrane fluidity and cellular fatty acid uptake and metabolism (Castagnet et al., 2005; Golovko et al., 2005; Sharon et al., 2003). α-synuclein has been shown to regulate the production of dopamine in cell culture by physically interacting with tyroxine hydroxylase (TH), a rate-limiting enzyme in the dopamine synthesis pathway (Liu et al., 2008; Perez et al., 2002). α-synuclein binds TH, prevents its phosphorylation and inhibits TH activation by increasing protein phosphatase 2A activity (Peng et al., 2005; Perez et al., 2002). In agreement with these findings, suppression of α-synuclein in cell culture models leads to increased TH phosphorylation and activity (Liu

et al., 2008). Consistent with a role of α-synuclein in dopamine biosynthesis, reduced TH activity has also been demonstrated in mouse models overexpressing α-synuclein (Kirik et al., 2002; Masliah et al., 2000). Finally, it was shown that α-synuclein can reduce histone acetylation in the nucleus and thereby promote neurotoxicity (Kontopoulos et al., 2006).

1.2.2.2 Evidence from other studies

Role in synaptic vesicle dysfunction: Various studies show that increased α-synuclein levels lead to decreased neurotransmitter release, loss of presynaptic proteins, redistribution of SNARE proteins, enlargement of synaptic vesicles as well as the inhibition of vesicle recycling, all of which are consistent with a role for α-synuclein in SNARE-complex assembly (Garcia-Reitbock et al., 2010; Nemani et al., 2010; Scott et al., 2010). Another study (Larsen et al., 2006) showed that overexpression of α-synuclein inhibits a vesicle 'priming' step that occurs after secretory vesicle trafficking to 'docking' sites but before calcium-dependent vesicle membrane fusion.

Role in endoplasmic reticular dysfunction: A recent analysis of a yeast PD model with dosage sensitivity for α-synuclein expression (Outeiro and Lindquist, 2003) revealed that the earliest defects following α-synuclein expression were an inhibition of the endoplasmic-reticulum-to-Golgi vesicular trafficking and an impairment of the endoplasmic-reticulum-associated-degradation pathway, ERAD (Cooper et al., 2006). Other studies in yeast, worms and mammalian cells described ER/Golgi stress and impaired transport caused by α-synuclein (Cooper et al., 2006; Gitler et al., 2008; Thayanidhi et al., 2010).

Role in mitochondrial dysfunction: α-synuclein localizes to mitochondria and causes down-regulation of complex I activity, similar to mitochondrial toxins (Devi et al., 2008; Li et al., 2007a; Loeb et al., 2010). In addition, mice overexpressing α-synuclein show aberrant mitochondrial morphology (Martin et al., 2006). Mitochondrial dysfunction might generate reactive oxygen species (ROS) and induce neuronal death (Hsu et al., 2000).

Role in other types of dysfunction: α-synuclein might also impair cytoskeletal dynamics, as it interacts with and influences the polymerization of tubulin (Alim et al., 2004; Zhou et al., 2010). Furthermore, several studies demonstrated that aberrant α-synuclein can induce proteasomal dysfunction (Petrucelli et al., 2002; Snyder et al., 2003; Stefanis et al., 2001; Tanaka et al., 2001) and impair the function of the lysosomal degradation system (Alvarez-Erviti et al., 2010; Cuervo et al., 2004; Xilouri et al., 2009).

Despite the several forms of cellular dysfunction caused by α-synuclein, its exact role in the pathogenesis of Parkinson's disease remains to be identified. In order to approach the question of how one small protein can have such a diverse set of functions, dysfunctions and interactions, it is essential to structurally examine α-synuclein, which is a chameleon-like molecule (i.e. it is extremely sensitive to its environment and can be easily modulated by a change in conditions) and thereby lacks a single unique or rigid structure (Drescher et al., 2012; Silva et al., 2012; Uversky, 2003).

1.2.3 Structure of α-synuclein

In order to better understand the structure and function of α-synuclein, it is necessary to analyze the protein in greater detail at several levels: 1) at a holistic level, i.e. discussing structural models of the entire α-synuclein protein under various conditions, and 2) at a deeper level of resolution, i.e. examining the properties and characteristics of individual regions or domains of the protein.

1.2.3.1 Whole-molecule structural analysis of α-synuclein

α-synuclein is a typical intrinsically disordered (or natively unfolded) protein, which possesses little or no ordered structure under physiological conditions *in vitro* (it exists in a random-coil conformation), as shown by far-UV circular dichroism and Fourier transform infra red spectroscopy, sedimentation, gel-filtration, dynamic light scattering, and SAXS (Eliezer et al., 2001; Uversky, 2003; Uversky et al., 2001b; Weinreb et al., 1996). This is in agreement with computational predictions, and high-resolution NMR which revealed that α-synuclein is largely unfolded in solution, but exhibits a region with a preference for helical conformation (Eliezer et al., 2001). While it has recently been proposed (Bartels et al., 2011; Wang et al., 2011) that α-synuclein, in its native form, may actually exist as a helical tetramer, there have been hardly any following studies that support this hypothesis. In fact, counter-reports (Fauvet et al., 2012) have provided comprehensive evidence to the contrary; namely that the protein lacks a defined tertiary structure in solution and adopts a random-coil conformation in its monomeric state under native conditions, in keeping with previous studies (Uversky, 2003; Uversky et al., 2002). Intrinsically disordered proteins have recently been recognized as a new protein class, and are gaining considerable attention due to the capability of these proteins to perform numerous biological functions despite the lack of unique structure (Dunker et al., 2001; Tompa, 2002; Uversky, 2003). These proteins exist as dynamic and highly flexible ensembles, commonly referred to as monomers that undergo a number of distinct inter-conversions on different time scales.

As mentioned in the previous section, α-synuclein is referred to as a protein-chameleon, which can alter its conformation due to environmental changes. Thus α-synuclein possesses a remarkable conformational plasticity, being able to adopt structurally unrelated conformations, described in greater detail in Table 1.2.3.1 (Uversky et al., 2002a). The natively-monomeric, random-coil forms of the protein can also form several morphologically different types of aggregates, including amyloid fibrils, which are the main components of the large proteinaceous inclusions seen in PD and other synucleinopathies (described in Table 1.2.3.1) (Uversky, 2003; Uversky et al., 2002a). These amyloid fibrils represent major building blocks of pathology-related inclusions, such as Lewy bodies (LBs), Lewy neurites (LNs), glial cytoplasmic inclusions (GCIs), neuronal cytoplasmic inclusions, and axonal spheroids, which have all been found in neurons affected by synucleinopathies. A summary of the major known α-synuclein conformations and aggregates is shown in Table 1.2.3.1.

Table 1.2.3.1 Summary of the major known conformations of α-synuclein and the conditions required to generate them.

State of the protein	Environment or conditions	References
Extended or intrinsic state of α-synuclein	Physiological conditions *in vitro* and *in vivo.*	(McNulty et al., 2006; Uversky, Li, et al., 2001a; Weinreb et al., 1996)
Pre-molten globule state	Low pH, high temperature, low concentrations of organic solvents, trimethylamine N-oxide, various metal ions & salts, several pesticides, herbicides & other glycosoaminoglycans, some polycations, also stabilized by spontaneous oligomerization *in vitro & in vivo.*	(Cohlberg, Li, Uversky, & Fink, 2002; Goers, Uversky, & Fink, 2003; Abedini & Raleigh, 2009; Manning-Bog et al., 2002; Munishkina, Henriques, Uversky, & Fink, 2004; Munishkina, Phelan, Uversky, & Fink, 2003; Uversky, Lee, Li, Fink, & Lee, 2001; Uversky, Li, et al., 2001b; Uversky, Li, & Fink, 2001c, 2001d)
α-helical membrane bound form	In the presence of synthetic vesicles containing acidic phospholipids, e.g. small unilamellar vesicles containing 30% phosphatidylserine and 70% phosphatidylcholine, and synaptic vesicle- proteins such as SNARE proteins.	(Chandra, Chen, Rizo, Jahn, & Sudhof, 2003; Davidson et al., 1998; Perrin, Woods, Clayton, & George, 2000)
Dimers	Prolonged incubation at high temperatures results in progressive aggregation, where dimers are formed first (non-covalent).	(Uversky, Lee, et al., 2001)
Oxidative dimers & higher-order oligomers with di-tyrosine cross-links	Under oxidative stress, e.g. UV-irradiation, or via cross-linking agents, e.g. BS3, DSS, PICUP, etc. (covalent).	(Souza et al., 2000)

Oligomers (without covalent aspects)	Nitration of α-synuclein, incubation with different metals, such as Cu2+, Fe3+, Ni2+, Mg2+, Cd2+, Zn2+, Co2+ and Ca2+.	(Lowe et al., 2004; Yamin, Glaser, Uversky, & Fink, 2003; Yamin, Uversky, & Fink, 2003)
Protofibrils	Incubation of spherical α-synuclein oligomers with brain-derived membranes produces pore-like ring-type protofibrils.	(Ding, Lee, Rochet, & Lansbury, 2002)
Insoluble amorphous aggregates	Solution conditions, presence of small molecules e.g. EGCG, effect of modifying proteins, amongst other factors.	(Ehrnhoefer et al., 2008)
Insoluble amyloid fibrils	*In vitro*: under conditions of body temperature, physiological pH, physiological salt concentrations, constant shaking, presence of a glass bead, high concentrations of α-synuclein. *In vivo*: during the course of the disease, as the main component of pathological protein inclusions (Lewy bodies)	(Farrer et al., 2004; A. Singleton, Myers, & Hardy, 2004; A. B. Singleton et al., 2003; Uversky, Li, et al., 2001b)

1.2.3.2 Region-based structural analysis of α-synuclein

The full-length α-synuclein protein can be divided into three domains: the N-terminal domain, the NAC region and the C-terminal domain (Cookson, 2005).

N-terminal domain: The highly conserved amphipathic N-terminal domain (residues 1-60) contains a series of imperfect 11-amino acid repeats. These repeats include the consensus sequence KTKEGV, which has a structural α-helix propensity and is highly similar to apolipoprotein lipid-binding motifs. Thus this region adopts an α-helical secondary structure when bound to phospholipids (Davidson et al., 1998). The three missense mutations associated with familial PD (A30P, E46K and A53T) are located in this domain.

NAC region: The central hydrophobic NAC domain (Non-Amyloid Component, residues 61-95) of α-synuclein is associated with an increased propensity of the protein to assume a ß-sheet conformation and to form amyloid fibrils (Bodles et al., 2001). Other members of the α-synuclein family lack the NAC region and do not efficiently form aggregates (Goedert, 2001), further underlining the importance of this region for α-synuclein aggregation.

C-terminal domain: The highly acidic and proline-rich C-terminal tail (residues 96-140) contains mostly negatively charged residues and has no distinct structural propensity. The acidic glutamate-rich C-terminal region (Asp98–Ala140) was shown to behave as a highly mobile tail. It remained unstructured even in the presence of membranes (Jao et al., 2004; Ulmer and Bax, 2005; Ulmer et al., 2005), becoming insensitive to protease digestion when the micelle bound α-synuclein is exposed to calcium (de Laureto et al., 2006).

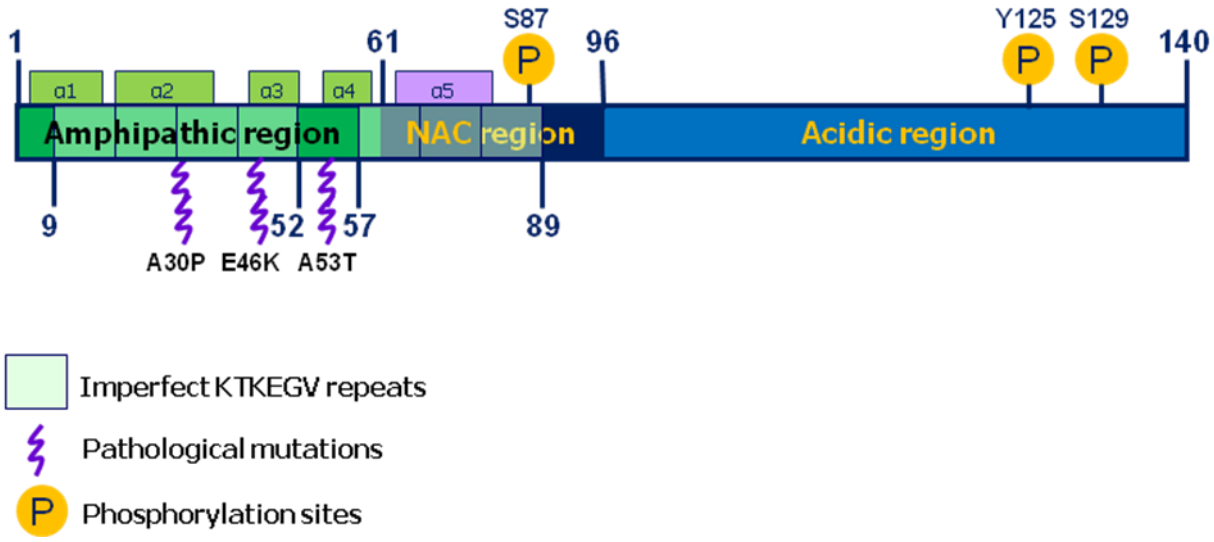

Fig 1.2.3.2 Modular domain structure of α-synuclein. The α-helices in the N-terminal amphipathic region (α1- α4) are required for phospholipid binding. The non-amyloid component (NAC) region confers the ß-sheet potential of the protein. The highly acidic C-terminal region is unstructured and subject to post-translational modifications. Amino-acid positions are indicated above the regions. The imperfect KTKEGV repeats that form amphipathic α-helices are also shown. Pathological mutations and the major (S129) and minor (Y125) phosphorylation sites are also indicated. The figure is based on published information (Cookson, 2005).

1.3 Aggregation of α-synuclein

Since amyloid fibrils of α-synuclein play an important role in the pathology of PD, it is crucial to understand the underlying process of soluble protein aggregation into amyloid fibrils, referred to in the scientific literature as the amyloid cascade or amyloid hypothesis of α-synuclein aggregation (Hardy and Higgins, 1992; Kisilevsky and Axelrad, 1976).

1.3.1 Amyloid hypothesis of α-synuclein aggregation

The term amyloid is derived from the early mistaken identification of pathological aggregates as starch (*amylum* in Latin) based on crude iodine-staining techniques. 'Amyloid' was originally used to describe the extracellular protein deposits found in Alzheimer's disease and systemic amyloid disorders (Kisilevsky and Axelrad, 1976). Recently, it has been extended to describe intracellular aggregates as well. Amyloid refers to protein aggregates organized in a cross-β-sheet structure, bound specifically by dyes such as Congo red and Thioflavin S. They are known to exhibit a high resistance to proteolytic degradation and heat denaturation, and were shown to have a fibrillar morphology observed by electron microscopy (Soto, 2003). The following mechanism - commonly referred to as the *amyloid hypothesis* of aggregation (see Fig. 1.3.1) - has been put forward to explain the process of α-synuclein fibrillization:

As α-synuclein is unfolded in aqueous solution with a random coil structure (Li et al., 2002a; Masino and Pastore, 2002) it may expose hydrophobic surfaces (which would otherwise be hidden or masked within structured proteins) which can potentially interact with each other or with other proteins in the surroundings. *In vitro* studies suggest that the initiation of aggregation depends on specific intermolecular interactions between folding intermediates (Wetzel, 1996), or on the disruption of equilibria between unfolded monomeric α-synuclein and its other intermediate conformations, such as the globular pre-molten state referred to above. Additionally, point mutations associated with familial variants of the disease, such as the A53T and A30P α-synuclein mutants in PD, can destabilize the native conformation of the protein and increase the likelihood of self-association and aggregation (Bertoncini et al., 2005). This destabilization of monomeric α-synuclein, along with certain interactions between intermediate conformations, could increase the propensity of the molecule to form microaggregates, such as dimers, oligomers, tiny spherical particles or protofibrils, which eventually group together into larger, macromolecular deposits, such as the highly ordered amyloid fibrils (refer to Fig. 1.3.1). Furthermore, microaggregates often act as 'seeds' for the aggregation reaction, increasing the propensity of the various molecules to aggregate into amyloid fibrils, thereby arriving at an energetically-favourable equilibrium.

Thus, the formation of α-synuclein amyloid fibrils is a complex process, involving one or more discrete intermediates, including small oligomers, protofibrils and finally mature fibrils, all of which have been shown to produce toxicity, to varying levels (Conway et al., 2000a; Harper et al., 1999; Poirier et al., 2002). The amyloid fibrils are the most energetically stable (or nearly irreversible) structures generated in this entire process. They are also, understandably, the most commonly and easily detected aggregates in PD brain tissue.

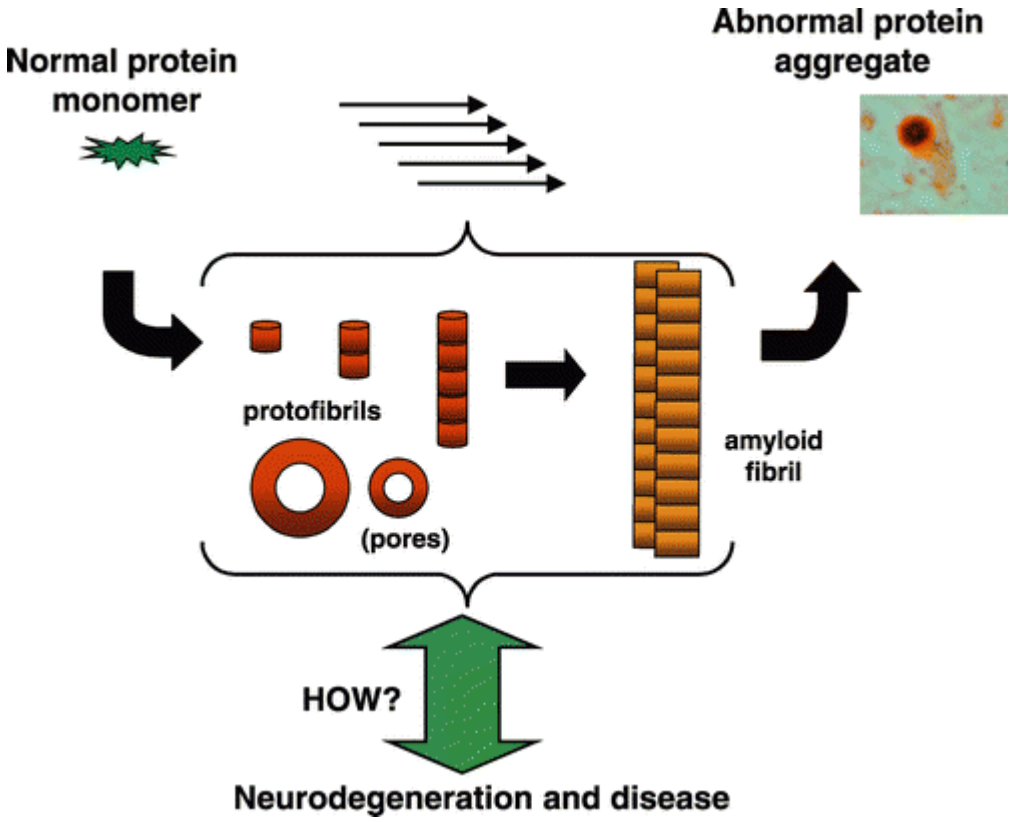

Fig 1.3.1 The amyloid hypothesis of α-synuclein aggregation [adapted from (Caughey and Lansbury, 2003)]. A general mechanistic scheme combining information from studies of *ex vivo* and *in vitro* protein aggregation. The conversion of normal α-synuclein protein into disease-associated deposits, such as Lewy bodies in PD (image at *right*), occurs via a multi-step process involving the intermediacy of oligomeric forms that are less stable but potentially more toxic than the end-product fibril. The mechanism by which these intermediates may cause neuronal dysfunction and death is not clear.

1.3.2 α-synuclein aggregation and cell death

Although the presence of pathological inclusions in neurodegenerative disease brains has been known for many years, it is still under discussion whether inclusions are the direct cause and primary toxic species leading to neurodegeneration or rather the result of some other underlying mechanism. The neuropathological link between protein aggregation and disease is confused by sometimes poor correlations between the load of amyloid deposits in

the brain and the severity of disease (Forno, 1996; Gutekunst et al., 1999). Hence, the question arises whether it is the amyloid fibril that is toxic to cells or perhaps one of the other intermediate conformations of the α-synuclein protein, e.g. oligomers formed early in the aggregation process (Volles and Lansbury, 2003).

Some α-synuclein oligomers may serve as neuron killers. Oligomeric α-synuclein was shown to be deposited in detergent insoluble fractions in the brains of patients with the gene triplication mutation (Miller et al., 2004). The observation that the A30P mutation dramatically accelerates the initial oligomerization of α-synuclein and significantly retards the formation of mature fibrils (Conway et al., 2000a; Conway et al., 2000b; Conway et al., 2000c; Li et al., 2001; Li et al., 2002b) represents a key result leading to the theory that oligomeric intermediates of α-synuclein, rather than mature fibrils, may in fact be the disease-associated aggregate species in PD (Lansbury, 1999). Annular (doughnut-like) oligomers - which not only are stabilized during the *in vitro* studies, but have also been isolated from human brain samples (Pountney et al., 2004) - may have pore-like properties and may damage membranes in mammalian cells (Volles and Lansbury, 2002). Additionally, oligomer toxicity is suggested to be critical in cell model studies, where toxicity is usually seen without heavily aggregated α-synuclein, leading to the suggestion that soluble species mediate toxicity (Xu et al., 2002). Proteins that are not associated with amyloid disease but are able to aggregate into fibrils *in vitro*, are toxic to cells in culture while they still possess a non-fibrillar, oligomeric morphology (Bucciantini et al., 2004; Bucciantini et al., 2002). Although these studies seem to suggest that only the oligomeric species are toxic to cells, there is also contradictory evidence, described below.

The investigation of amyloid plaques in a transgenic mouse model (Tsai et al., 2004) revealed that fibrillar amyloid deposits lead to synaptic abnormalities and breakage of neuronal branches. Interactions with all kinds of exposed hydrophobic surfaces also enable amyloid fibrils to recruit other proteins, a process that might significantly contribute to the toxicity of formed aggregates (Busch et al., 2003; Charles et al., 2000; Perutz et al., 1994; Trojanowski and Lee, 2000). Studies in cell culture models have shown that inclusion bodies have a very complex structure and include different proteins such as chaperones, parts of the ubiquitin-proteasome-system, proteins of the centrosome and the cytoskeleton (Rajan et al., 2001; Waelter et al., 2001), as well as different transcription factors such as TCERG1 (also known as CA150) (Holbert et al., 2001), CTBP6 (Kegel et al., 2002) and p53 (Steffan et al., 2000). The co-aggregation of misfolded proteins with normal proteins could therefore be responsible for the toxicity of protein aggregates (Nucifora et al., 2001). It remains unclear,

however, how these complex inclusions are formed and to which extent fibrillar aggregates and oligomers individually contribute to the cytotoxicity observed in the disease state.

Numerous disease models of PD primarily based on the transgenic overexpression of wild-type or mutant α-synuclein have been developed. These include cell models of primary neurons and neuroblastoma-derived cell lines (Falkenburger and Schulz, 2006). Recently, pluripotent stem cells were derived from a PD patient with triplication of the SNCA locus, which better mimics the disease phenotype (Devine et al., 2011). Overexpression of wild-type and mutant α-synuclein in yeast generates large intracellular aggregates and reduces cell growth (Outeiro and Lindquist, 2003). α-synuclein overexpression also induces loss of dopaminergic neurons in invertebrates like *D. melanogaster* (Feany and Bender, 2000). Furthermore, *C. elegans* has been used to examine the toxic effects of α-synuclein on neurons in an *in vivo* setting and aggregates of α-synuclein have also been detected in this model organism (Lakso et al., 2003).

Interestingly, α-synuclein aggregation occurs in mouse and primate models of MPTP-induced parkinsonism (Fornai et al., 2005; Kowall et al., 2000; Meredith et al., 2002; Thomas et al., 2011), an animal model of parkinsonism which utilizes the selective dopaminergic neurotoxin MPTP that reproduces the selective neuronal loss seen in PD (Bergman and Deuschl, 2002; Fornai et al., 2005; Fukuda, 2001). However, studies using rodents with increased expression of human α-synuclein have led to conflicting results where some studies show lack of increased sensitivity to MPTP with human α-synuclein expression (Dong et al., 2002; Rathke-Hartlieb et al., 2001) and other studies show increased sensitivity associated with MPTP in human α-synuclein transgenic mice (Nieto et al., 2006; Song et al., 2004). Overexpression of human α-synuclein in rodents has also been shown to produce varying degrees of neuronal dysfunction and degeneration (Daher et al., 2009; Giasson et al., 2002a; Lee et al., 2002b; Masliah et al., 2000; Neumann et al., 2002) including dopaminergic degeneration (Kirik et al., 2003; Kirik et al., 2002; St Martin et al., 2007; Tofaris et al., 2006; Yamada et al., 2004). However, a variety of human α-synuclein transgenic mice with increased α-synuclein aggregation, motor dysfunction, and neurodegeneration have failed to show overt neurodegeneration of dopaminergic neurons (Giasson et al., 2002a; Lee et al., 2002b; Neumann et al., 2002). In addition to rodent models of α-synuclein overexpression, various knock-out models of this protein have also been generated, e.g. the ‘α-synuclein null mouse’, which is viable and shows a distinctive phenotype of dopaminergic-neuron-selective MPTP resistance. Several studies show that the expression of endogenous

mouse α-synuclein is required to sensitize dopaminergic neurons to MPTP (Dauer et al., 2002; Drolet et al., 2004; Fornai et al., 2005; Robertson et al., 2004; Schluter et al., 2003).

As the relationship of α-synuclein abnormalities to rodent models of PD remains controversial, many studies focus on *in vitro* avenues of research, which are particularly ideal for the modelling of an intrinsically disordered, multi-functional protein, whose behaviour depends to a large extent on the nature of its environment, something which can precisely, reproducibly and easily be controlled *in vitro*. Thus, there is an interest in developing therapeutic strategies for PD by using *in vitro* assays, screens and cellular toxicity models, which are free from some of the drawbacks plaguing animal models of the disease.

1.4 Modulation of α-synuclein's tendency to aggregate into fibrils, as a potential neuroprotective therapy

A reasonable approach for finding an effective anti-synucleinopathy drug is a search for molecules that are able to stabilize the natively unfolded conformation of α-synuclein, completely blocking its aggregation, or to mediate its off-pathway aggregation into non-toxic, amorphous aggregates whose characteristics and effects on cells are vastly different from those of the β-sheet amyloid fibril. The latter option has been previously suggested as an alternative approach to treat neurodegenerative diseases (Bodner et al., 2006a; Bodner et al., 2006b). Screening for compounds that *promote* protein aggregation, accelerate formation of large inclusions, and eliminate the toxic effects of intermediate misfolded protein conformations (Bodner et al., 2006a; Bodner et al., 2006b) could indeed provide a viable therapy. In fact, a very potent compound (5-[4-(4-chlorobenzoyl)-1-piperazinyl]-8-nitroquinoline or 'B2') that promotes the formation of inclusions and attenuates pathological features in models of both Huntington's disease and PD was found (Bodner et al., 2006b). Additionally, studies by Ernhoefer and colleagues (Ehrnhoefer et al., 2008) showed that EGCG, a component of green tea, actually induces the formation of off-pathway amorphous aggregates of both α-synuclein and amyloid-β, which show reduced toxicity in cells as compared to the β-sheet-rich amyloid fibrils. Based on these observations, it has been concluded that generating larger deposits of off-pathway aggregated protein could represent a therapy for affected neurons (Bodner et al., 2006b).

At this point, it is necessary to make a distinction between the terms *aggregate* and *fibril*. The term *aggregate* includes all types of protein assemblies comprised of more than one protein molecule, spanning a wide range of differing structures, morphologies, sizes, and other physical properties. *Aggregates* may be toxic or non-toxic, dimeric, oligomeric or multi-meric (e.g. protofibrils), formed as on- or off-pathway products, generated *in vitro* or detected in Lewy bodies in pathological brain tissue, amorphous in nature or highly-ordered with a definite structure, such as amyloid *fibrils*. The term *fibril* is more specific and refers to a special type of aggregate, which is highly ordered, has a β-pleated sheet structure, and a fibre-like morphology. *In vivo* fibrils of α-synuclein have been detected as the main component of Lewy bodies in PD (Bagchi et al., 2013; Sampathu et al., 2003; Trojanowski et al., 1998), while fibrils of the amyloid-β protein (Aβ) have been detected as the main components of amyloid plaques in Alzheimer's disease (AD) (Glenner and Murphy, 1989; Gouras et al., 2010). *In vitro*, fibrils can also be induced spontaneously when high concentrations of α-synuclein are incubated at 37°C for long periods of time (Lee et al.,

2009; Wood et al., 1999; Yagi et al., 2005). While all *fibrils* are a type of *aggregate* by definition, all *aggregates* are not necessarily *fibrils*!

Since amyloid *fibrils* are a hallmark of PD neuropathology, it would be more accurate to say that modulation of α-synuclein *fibrillization* could be a potential neuroprotective therapy. This is supported by the following studies: 1) In Alzheimer's disease, a strategy using immunization against the Aß-peptide reduces the deposition of fibrillar Aß in the brain and ameliorates the behavioural impairment in a transgenic mouse model (Janus et al., 2000). 2) Small molecules that inhibit the fibrillogenesis of synthetic Aß-peptide rescue long-term potentiation in brain slice culture models, which is blocked by soluble Aß oligomers (Walsh et al., 2005). Hence, the focus of this study is to identify novel and potent modulators of α-synuclein *fibrillization*, rather than α-synuclein aggregation.

1.4.1 Modulation of α-synuclein fibrillization by proteins and small molecules

It has been demonstrated that several proteins can modulate α-synuclein fibrillization and toxicity, as described below.

1.4.1.1 Directly-interacting, non-chaperone protein modulators

Various proteins which are not known to have any chaperone or neuroprotective activity, have nonetheless been shown to modulate α-synuclein fibrillization through direct interaction, for example, synphilin-1, which was initially identified in a yeast-2-hybrid screen as an interaction partner of α-synuclein (Engelender et al., 1999). Synphilin-1 was found to promote α-synuclein aggregation and inclusion body formation in cell model systems (Engelender et al., 1999). Strikingly, expression of synphilin-1 in an A53T α-synuclein expressing mouse strain reduces neurodegeneration, while enhancing the formation of insoluble α-synuclein inclusions, further supporting the hypothesis that formation of insoluble aggregate species might represent a cytoprotective mechanism (Smith et al., 2010). The E3 ubiquitin ligase Siah-1 interacts with and facilitates mono- and di-ubiquitination of α-synuclein *in vivo* (Lee et al., 2008). However, ubiquitination by Siah-1 does not target α-synuclein for the degradation by the proteasome but promotes its aggregation and increases apoptotic cell death (Lee et al., 2008; Samii et al., 2004).

1.4.1.2 Chaperones as modulators of α-synuclein aggregation

Stress or heat shock proteins (HSPs) were first discovered in 1962 as a set of highly conserved proteins whose expression was induced by different kinds of stress (Ritossa, 1962). It has subsequently been shown that most HSPs have strong cytoprotective effects

and behave as molecular chaperones for other cellular proteins (Schmitt et al., 2007). Inappropriate activation of signaling pathways could occur during acute or chronic stress as a result of protein misfolding, protein aggregation, or disruption of regulatory complexes (Schmitt et al., 2007). The action of chaperones, through their properties in protein homeostasis, is thought to restore balance (Schmitt et al., 2007).

Chaperones suppress protein aggregation and participate in protein refolding and/or degradation. Several chaperones, including torsin A, a protein with homology to the yeast heat shock protein 104 (Shashidharan et al., 2000a; Shashidharan et al., 2000b; Walker et al., 2001), αB-crystallin, a small chaperone that binds to unfolded proteins and inhibits aggregation (Pountney et al., 2005), and Hsp70 and Hsp40 (Auluck et al., 2002) are prominent components of LBs with α-synuclein. The over-expression of torsin A and heat shock proteins suppressed α-synuclein aggregation in a cellular models (McLean et al., 2002). *In vitro* analysis revealed that αB-crystallin serves as a potent inhibitor of WT, A30P and A53T α-synuclein fibrillation (Rekas et al., 2004). Directed expression of the molecular chaperone Hsp70 prevented dopaminergic neuronal loss associated with α-synuclein in *Drosophila*, whereas the interference with endogenous chaperone activity accelerated α-synuclein toxicity (Auluck et al., 2002). These data suggest a critical role for chaperones in pathologies involving α-synuclein in humans, such that they may be a critical part of the neuronal arsenal that mitigates α-synuclein toxicity (Uversky, 2007).

1.5 Summary

In brief, various proteins that influence α-synuclein fibrillization have been previously identified and studied in great depth. However, cells are complex and carry a multitude of different proteins; hence, there is always the possibility that additional proteins may be identified through large-scale screening, as novel modifiers of α-synuclein fibrillization, thereby providing potential for therapeutic intervention. In fact, aggregation inhibitor screens with purified proteins have been performed on model systems for different diseases such as HD (Heiser et al., 2002), PD (Conway et al., 2001) or AD (Esler et al., 1997). *In vitro* model systems allow the detection of substances that interfere directly with the protein aggregation process. The purified proteins (e.g. α-synuclein and the candidate protein) are present in a buffered solution- a system which is extremely simplified compared to the complex environment of a brain cell. Thus, limiting the number of possible interaction partners for the molecules in solution shows clearly with which proteins α-synuclein does or does not interact. 'Hits' derived from such a screen are then further validated in cell culture and animal models, since *in vitro* effects may not necessarily be representative of a cellular environment. Within this scope, *in vitro* screening methods, complemented by downstream biochemical, biophysical, microscopy-based and cell-assay-focused techniques, are well suited for the study of direct effects of candidate proteins on α-synuclein fibrillization, and the molecular mechanisms by which the aggregation process might be influenced. This is what is aimed at in this study.

1.6 Aims of the doctoral thesis

1.6.1 To identify novel protein inhibitors of α-synuclein fibrillization by screening a library of 13,824 proteins

As described above, the detection of proteins that modulate the aggregation of α-synuclein is of high importance. The identification of proteins that influence α-synuclein aggregation in vitro suggests that endogenous proteins in vivo might also have such an effect (Lundvig et al., 2005). Hence, this doctoral work starts with the screening of a library of 13,824 human proteins, in order to detect novel and potent inhibitors of α-synuclein fibrillization.

1.6.2 To comprehensively characterize the effect of the most potent modifier using biochemical, biophysical and microscopy-based methods

In order to completely characterize the effect of the most potent inhibitor of α-synuclein fibrillization to emerge from the screen, an arsenal of biochemical, biophysical and microscopy-based techniques was employed.

1.6.3 To elucidate the mechanism by which the modifier inhibits fibrillization

In order to understand how the most potent modifier exerts its effect on α-synuclein, it is important to know the mechanism underlying its effect. For this, a cutting-edge structural technique, i.e. Nuclear Magnetic Resonance (NMR) has been employed. Time-resolved NMR is used to reveal the most intricate aspects of α-synuclein aggregation in the presence of the modifier, at both a residue-specific and region-specific level of information.

1.6.4 To evaluate the effect of the modifier on α-synuclein-mediated toxicity in cells and in an in vivo system

In vitro studies do not encompass all aspects of the environment within a cell or even in an organismal context, where multiple biomolecules and overarching processes are constantly underway. To account for these additional factors, and to establish whether the work carried out is relevant in a cellular and organismal context, the doctoral work concludes with an examination of the effect of the modifier on α-synuclein toxicity within rat primary cortical neurons and a S. cerevisiae model of α-synuclein toxicity.

2. MATERIALS & METHODS

2.1 Materials

2.1.1 Biological stocks

2.1.1.1 Bacterial strains

(i) Mach1™ T1®

E. coli F– Φ80lacZΔM15 ΔlacX74 hsdR(r_k^+, m_k^+) ΔrecA1398 endA1 tonA (Invitrogen), recommended strain for use with the Gateway ® Cloning System.

(ii) BL21-CodonPlus(DE3)-RP

E. coli B F$^-$ ompT hsdS(rB^- mB^-) dcm+ Tet^r gal λ(DE3) endA Hte [argU proL Cam^-] strain (Statagene); for high level protein expression following IPTG (Isopropyl-1-thio-β-D-galacto-pyranoside) induction of T7 polymerase driven by lacUV5 promoter.

(iii) Rosetta™

E. coli F$^-$ ompT hsdS_B(r_B^- m_B^-) gal dcm pRARE (Cam^R); BL21 derivatives designed to enhance the expression of eukaryotic proteins that contain codons rarely used in E. coli. These strains supply tRNAs for AGG, AGA, AUA, CUA, CCC, GGA codons on a compatible chloramphenicol-resistant plasmid. Thus, the Rosetta strains provide for "universal" translation which is otherwise limited by the codon usage of *E. coli*. The tRNA genes are driven by their native promoters.

2.1.1.2 Yeast strain

W303-1A (CRY1) GAL+ MATa ura3-1 trp1-1 his3-11, 15 leu2-3,112 ade2-1 can1-100

2.1.1.3 Mammalian cell

C57BL/6 mouse primary neuronal cells (a kind gift from Prof. Jochen Meier, Max-Delbrück-Centrum)

2.1.2 Expression vectors and plasmids

(i) pDONR^{TM}221

A Gateway® vector containing attP sites, this vector is used for cloning PCR products and genes of interest flanked by attB sites (expression clones) to generate entry clones. It contains the ccdB gene for negative selection and the kanamycin resistance gene for selection in *E.coli* (Invitrogen).

(ii) pDESTco

A Gateway® vector containing attR sites, with an insert size of 2342, designed for bacterial expression. A sequence of 6x-His residues on the N-terminal acts as a tag, which is of

extreme importance during purification of the recombinant protein. The vector backbone, pQE-2, is manufactured by Qiagen. This vector confers resistance to ampicillin and chloramphenicol when present in cells (recommended growth strain: DB3.1)

(iii) pAG425-GAL

A yeast expression plasmid designed to enable the expression of human genes within yeast cells, in order to examine the function, localization, interaction partners, etc. of the protein of interest, in *S. cerevisiae*. Upon addition of galactose to the growth medium, expression of the protein encoded by the plasmid is turned on. In conjunction with the yeast strain described above, this plasmid enables the simultaneous over-expression of α-synuclein (integrated into the yeast genome behind a galactose promoter) and the protein of interest (in this study, a modifier of α-synuclein fibrillization).

2.1.3 Media

2.1.3.1 Bacterial media

Bacterial media	Composition
LB-medium	10 g/l Bacto peptone, 5 g/l yeast-extract, 10 g/l NaCl, set pH to 7.2
Antibiotics:	
Ampicillin	100 mg/ml in ddH_2O (stock), final concentration: 100 µg/ml
Tetracycline	12.5 mg/ml in 50% EtOH (stock), final concentration: 20 µg/ml
Kanamycin	30 mg/ml in ddH_2O (stock), final concentration: 15 µg/ml
Spectinomycin	25 mg/ml in ddH_2O (stock), final concentration: 50 µg/ml
SOB-medium	20 g Bacto tryptone, 5 g Bacto yeast extract, 0.5 g NaCl, add 1000 ml ddH_2O, after autoclaving add: 10 ml 1 M $MgCl_2$,10 ml 1 M $MgSO_4$
SOC-medium	99 ml SOB-medium, 1 ml 20% glucose

2.1.3.2 Yeast Media

Yeast media	Composition
YPD (liquid)	10 g/l Bacto yeast extract, 20 g/l Bacto peptone, 20 g/l glucose
SD (liquid)	6.7 g/l Yeast Nitrogen Base, 20 g/l glucose, add 10 ml supplemental amino acids (100x stock solutions) to 1 l SD medium
Supplemental amino acids (100X stock solutions):	
Adenine (Ade)	2 g/l (stock), final concentration: 20 mg/l
Histidine (His)	2 g/l (stock), final concentration: 20 mg/l
Leucine (Leu)	10 g/l (stock), final concentration: 100 mg/l
Tryptophan (Trp)	2 g/l (stock), final concentration: 20 mg/l
Uracil (Ura)	2 g/l (stock), final concentration: 20 mg/l
Note: SD medium contains all essential amino acids except for the ones listed above. The media are named after the missing and required amino acids or nucleosides: Anabolytes omitted are marked by a minus sign, while those that are added to the medium are separated by a slash. For example, SD -ut/ahl lacks uracil and tryptophan, but contains adenine, histidine and leucine.	
NBG (yeast storage medium)	6,7 g/l Yeast Nitrogen Base, 20 g/l glucose, 5 % glycerol, 0,5 M betaine, add 10 ml supplemental amino acids (100x stock solutions) to 1 l SD medium.
Note: For solid SD, NBG or YPD media, 17 g/l agar is added to the media above.	
Yeast Lysis Buffer	25 mM TRIS pH 7.5, 50 mM DTT, 2 mM $MgCl_2$, 2% SDS

Benzonase solution	285 µl buffer, 15 µl Benzonase (Benzonase 20 U/ml)

2.1.3.3 Cell culture media and supplements

Cell culture media and supplements	Supplier
Dulbecco's modifed Eagle medium (DMEM) with 4.5 g/L	Gibco
D-Glucose, Sodium Pyruvate, without L-Glutamine	Gibco
0.5% Trypsin and 0.53 mM Na-EDTA in Hanks' B.S.S.	Gibco
Fetal calf serum (FBS) from E.G. approved countries	Gibco
Dulbecco's phosphate buffered saline (D-PBS) without calcium, magnesium	Gibco

2.1.4 Buffers & Solutions

Buffers and solutions	Composition
1000x Ampicillin	stock 100 mg/ml dissolved in 50% ethanol, stored at -20°C
AttoPhos™ buffer	50 mM Tris-HCl pH 9.0, 500 mM NaCl, 1 mM $MgCl_2$
AttoPhos™ reagent	10 mM AttoPhos reagent dissolved in 100 mM Tris pH 9.0

1% BSA	Bovine serum albumin was dissolved in 1x PBS to a final concentration of 1% (w/v)
Coomassie destaining	45% methanol, 10% acetic acid solution
Coomassie staining	45% methanol, 10% acetic acid, 0.05% Coomassie brilliant blue solution R250
4x DNA sample buffer	0.25% bromophenol blue, 0.25% xylene cyanole FF, 30% glycerol
1000x Kanamycin	stock 25 mg/ml dissolved in distilled water, stored at -20°C
LB (Luria Bertani) medium	10 g/l Bacto Peptone, 5g/l yeast-extract, 10 g/l NaCl, pH 7.2
MTT-stop buffer	47.75% DMF, 20% SDS, 2% acetic acid, 25 mM HCl
NaP buffer	20mM NaCl, 200 mM NaP (pH 7.2), final pH 7.5
4% paraformaldehyde	4 g of paraformaldehyde dissolved in 100 ml PBS and heated at 50°C for 5 minutes to obtain a clear solution, stored at -20°C
25x Protease inhibitors	One tablet of Complete™ protease inhibitor (Roche) dissolved in 2 ml distilled water, stored at -20°C
10x PBS	80 g NaCl, 2 g KCl, 14.4 g Na_2HPO_4, 2.4 g KH_2PO_4, in distilled water upto 1 l
PBS-T	1x PBS, 0.05% Tween-20
PMSF	100 mM PMSF dissolved in isopropanol, stored at -20°C
10 % SDS resolving	2.5 ml of 40% bisacrylamide, 2.5 ml of 1.5 M Tris-HCl (pH 8.8),

gel	100 µl of 10% SDS, 4.9 ml dd H_2O, 100 µl of 10% APS, 10 µl TEMED
5% SDS stacking gel	0.75 ml of 40% acrylamide, 1.5 ml of 0.5 M Tris-HCl (pH6.8), 60 µl of 10% SDS, 3.6 ml ddH_2O, 60 µl of 10% APS, 6µl TEMED
4x SDS loading buffer	200 mM Tris-HCl pH 6.8, 400 mM DTT, 8% SDS, 4 mg/ml bromophenol blue, 40% glycerol, store at -20°C
1x SDS running buffer	1x WB-buffer, 0.1% SDS
5% milk	skimmed milk powder was dissolved in TBS-T to a final concentration of 5% (w/v)
S.O.C. Medium	2% Tryptone, 0.5% Yeast Extract,10 mM NaCl, 2.5 mM KCl, 10 mM $MgCl_2$, 10 mM $MgSO_4$, 20 mM glucose
1x TAE	40 mM Tris-Acetate, 1 mM EDTA, pH 8.0
1x TBE	45 mM Tris-Borate, 1 mM EDTA, pH 8.0
1x TBS	20 mM Tris-HCl pH 7.5, 150 mM NaCl
1x TBS-T	20 mM Tris-HCl pH 7.5, 150 mM NaCl, 0.05% Triton X-100
1x TE	10 mM Tris-HCl, pH 7.4, 1 mM EDTA, pH 8.0
10 x WB buffer	30 g/l Tris, 144 g/l Glycine
Western blot buffer	1 x WB-buffer, 10% Ethanol
Cell Lysis Buffer (His-proteins)	1.0 mg/ml Lysozyme, 300 mM NaCl, 0.5% NP-40, 1% Triton, 1 mM PMSF, 500 U Benzonase in PBS

Cell Lysis Buffer (α-synuclein)	Tris-HCl pH 8.0, 1 mM EDTA, 1 mM PMSF
Cell Lysis Buffer (Ezrin)	0.5% NP-40, 1% Triton-X, 1 mM PMSF, 300 mM NaCL, 20 mM Imidazole, 2 µl Benzonase, 1 Protease-inhibitor tablet, PBS
Washing buffer (His-fusion proteins)	20 mM NaH_2PO_4, 300 mM NaCl, 20 mM Imidazole pH 7.4
Elution buffer (His-fusion proteins)	20 mM NaH_2PO_4, 500 mM NaCl, 500 mM Imidazole pH 7.4
Elution buffer (α-synuclein)	10 mM NH_4HCO_3
Binding buffer (Ezrin)	20 mM Na_3PO_4, 0.5 M NaCl, 20-40 mM Imidazole, pH 7.4, filtered
Elution buffer (Ezrin)	20 mM Na_3PO_4, 0.5 M NaCl, 500 mM Imidazole, pH 7.4, filtered
NMR buffer	20 mM NaP, 150 mM NaCl, end-pH 6.4, filtered, de-gased
Transformation Mix 1	1 ml 1 M LiOAc, 0.5 ml 10x TE, 5 ml 2 M Sorbitol, 3.5 ml ddH_2O
Transformation Mix 2	6 ml 1 M LiOAc, 6 ml 10x TE, 40 ml 60% PEG 3350, 8 ml ddH_2O

2.1.5 Proteins and Antibodies

All primary antibodies were diluted in 5% milk in PBS-T (5% skim milk powder (w/v)).

Table 2.1.5.1: Primary antibodies

Primary antibody	Species	Dilution	Supplier
Ezrin (3C12): sc-58758	mouse	1:5000	Santa Cruz Biotechnology, Inc.
Ezrin (H-276): sc-20773	rabbit	1:5000	Santa Cruz Biotechnology, Inc.
α-synuclein (211): sc-12767	mouse	1:5000	Santa Cruz Biotechnology, Inc.
α-synuclein (C-20)-R: sc-7011-R	rabbit	1:5000	Santa Cruz Biotechnology, Inc.
Penta·His HRP Conjugate	mouse	1:5000	Qiagen

Table 2.1.5.2: Secondary antibodies

Secondary antibody	Conjugate	Species	Dilution	Supplier
Anti-rabbit IgG (# A3687)	Alkaline Phosphatase	goat	1:10,000	Sigma-Aldrich
Anti-mouse IgG (# A3562)	Alkaline Phosphatase	goat	1:10,000	Sigma-Aldrich
Anti-rabbit IgG	Peroxidase	goat	1:10,000	Chemicon

2.1.6 Enzymes, proteins and markers

Enzymes, proteins and markers	Supplier
^{15}N-labelled α-synuclein (for NMR studies)	(a kind gift from AG Selenko, FMP)
Benchmark pre-stained protein ladder	Invitrogen
Benzonase purity grade II	Merck

BSA 10 mg/ml	NEB
Herring Sperm Carrier DNA	Clontech
BP Clonase® II enzyme mix	Invitrogen
LR Clonase® II enzyme mix	Invitrogen
Ready-Load™ 1 Kb Plus DNA ladder	Invitrogen
Lysozyme	Sigma-Aldrich
Gel filtration calibration kit LMW	GE Healthcare
Gel filtration calibration kit HMW	GE Healthcare
Trypsin, Sequencing Grade, modified	Roche Applied Science
NativeMark™ Unstained Protein Standard	Invitrogen

2.1.7 Kits

Kits	Supplier
BCA Protein assay reagent	Pierce
Chemi-Glow West	Cell Biosciences
QIAprep spin miniprep kit	Qiagen

QIAquick gel extraction kit	Qiagen
LDH-Cytotoxicity colorimetric assay kit	Biovision

2.1.8 Chemicals and consumables

Chemicals and consumables	Supplier
3-(4,5-dimethylthiazol-2-yl)-2,5-diphenyltetrazolium bromide (MTT)	Promega
386-well microtiter plates	Nunc
96-well Fluoronunc plates	Nunc
96-well NiNTA-agarose plates	Multitrap HP/ Healthcare
96-well PCR plates	Thermo Scientific
Agarose	Invitrogen
Amicon™ centrifugal filter units, cutoff 10 kDa	Millipore
Amicon™ Ultra-15 centrifugal filter units	Millipore
Ammonium persulphate	Bio-Rad Laboratories
Ammonium sulphate	Merck
Attophos powder	Europa Bioproducts Ltd.

Bacto peptone	Becton Dickinson
Bacto tryptone	Becton Dickinson
Bacto yeast	Becton Dickinson
Bromophenol blue	Merck Eurolab GmbH
Cell culture flasks	DB Falcon
Cellulose acetate membrane 0.2µm	Schleicher and Schuell
Chloramphenicol	Sigma-Aldrich
Complete™ protease inhibitor cocktail	Roche Applied Science
Congo Red, analytical standard	Sigma-Aldrich
Coomassie brilliant blue G-250	Merck
Dialysis membrane, 10,000 kDa cutoff	SpectraPor® Dialysis
Deoxyribonucleotides (dNTPs)	Fermentas
Dithiothreitol (DTT)	Serva
Dimethyl sulphoxide (DMSO)	Sigma-Aldrich
Ethidium bromide solution (10mg/ml)	Sigma-Aldrich

Ethylenediamine tetraacetic acid	Merck Eurolab GmbH
Filter paper GB005	Schleicher and Schuell
Glass beads, acid-washed	Sigma-Aldrich
Glycerol	Merck Eurolab GmbH
HisTrap FF Crude Lysate 1 ml affinity column with precharged Ni-Sepharose 6 Fast Flow	GE Healthcare
Isopropyl-1-thio-β-D-galactoside (IPTG)	Applichem
Kanamycin A monosulfate	Sigma-Aldrich
Methylene blue	Sigma-Aldrich
NiNTA-agarose	Qiagen
Nitrocellulose membrane 0.2µm	Schleicher and Schuell
NMR tubes (5mm diameter)	Shigemi (a kind gift from AG Selenko, FMP)
NP-40 (IGEPAL CA 630)	Sigma-Aldrich
p-t-Octylphenyl-polyoxyethylen (Triton X-100)	Sigma-Aldrich
Paraformaldehyde	Sigma-Aldrich

PD-10 desalting columns	GE Healthcare
Phenylmethylsulphonylfluoride (PMSF)	Sigma-Aldrich
Polyethylene Glycol 3350 (PEG 3350)	Biomatik
Polyoxyethylensorbitan-Monolaureat (Tween 20)	Sigma-Aldrich
Polypropylene columns (1 ml and 5 ml)	Qiagen
Ponceau S-solution, 0.1%	Sigma-Aldrich
Protein LoBind tubes	Eppendorf
Quartz glass cuvettes	Hellmer
Quartz glass cuvettes 100-QS	neoLab
Sodium glycinate	Sigma-Aldrich
Streptomycin sulphate	Serva
Superdex 30/100_GL column	GE Healthcare
TEMED	Life Technologies
Tetracycline	Sigma-Aldrich
Thiamine	Sigma-Aldrich

Thioflavin T	Merck
Trichloroacetic acid	Merck
TrypanBlue solution (0.4%)	Sigma-Aldrich
Uranyl acetate dehydrate	Serva
Vacuum applicator	Qiagen
Whatman chromatography paper 3MM	Whatman
Yeast Nitrogen Base	Sigma-Aldrich
All other chemicals, salts, buffer substances, solvents, acids and bases were purchased from Carl Roth GmbH.	

.

2.1.9 Laboratory equipment

Laboratory equipment	Supplier
Äkta purifier	Amersham Biosciences
ArrayScan VTI	Thermo Scientific
Avance III HD NMR spectrometer	Bruker (collaboration with AG Selenko, FMP) [part of a core facility]
BioAnalyzer (2100)	Agilent

Biomek® FXP pipetting robot	Beckman Coulter
Biophotometer	Eppendorf
Centrifuge 5810R	Eppendorf
Criterion cell for SDS-PAGE	Bio-Rad
DNA electrophoresis chamber	Bio-Rad
Electrophoresis Power Supply EPS 601	Amersham
EM910	Zeiss
Freedom EVO pipetting robot	TECAN
Gene Genius UV imager	Bio Imaging Systems/ Syngene
HybriDot Manifold vacuum fitration unit	Whatman
Infinite M200 microplate reader	TECAN
Infinite M1000 microplate reader	TECAN
Innova 4430 incubator shaker	New Brunswick Scientific
K4 stamping robot	KBiosystems
LAS-3000 photo imager	Fujifilm
Leica TCS SP2	Leica
Micro 22R centrifuge	Hettich

MX40 Light microscope	Olympus
NanoDrop 8000	Thermo Scientific/ peQlab
Nanowizard AFM with Zeiss Axiovert 200	JPK Instruments AG
Optima TLX Ultracentrifuge	Beckman Coulter
PTC200 Peltier Thermal Cycler	MJ Research
Shaking Incubator	Infors Unitron
Thermomixer comfort	Eppendorf
Trans-Blot SD Semi-Dry Electrophoretic Transfer Cell	Bio-Rad
TW8 Water Bath	Julabo
XCell SureLock™ Mini	Invitrogen
Zetasizer Nano	Malvern Instruments

2.1.10 Software

Software	Source
AIDA 1.0	AIDA, Deutschland
CDNN 2.1 software	http://bioinformatik.biochemtech.uni-halle.de/cdnn

Lasergene	DNA star Inc.
Generunner	http://www.generunner.com
JPK Data Processing software	JPK Instruments AG
ProtParam	http://au.expasy.org/tools/protparam.html
Sparky 3.114- NMR Assignment and Integration Software	T. D. Goddard and D. G. Kneller, SPARKY 3, University of California, San Francisco
TopSpin™ Software for NMR data analysis	Bruker

2.2 Methods

2.2.1 Molecular biology

2.2.1.1 Plasmid preparation from E.coli

For plasmid amplification, LB medium containing the appropriate antibiotics was inoculated with *E. coli* colonies harbouring the plasmid of interest and grown to saturation over night at 37°C in an incubator-shaker. Cells were harvested by centrifugation and plasmids were purified using the Qiaprep Spin Miniprep Kit for small quantities or the Qiagen Midi Kit for larger quantities of DNA according to the manufacturer's instructions.

2.2.1.2 Determination of DNA concentration

DNA concentration of purified plasmid DNA was measured by UV absorption spectroscopy at a wavelength of 260 nm. In H_2O, a solution of 50 µg/ml of double stranded DNA exhibits an absorbance of 1.0.

2.2.1.3 Restriction digestion of DNA

Restriction digestion was performed as recommended by the manufacturer. Reactions were incubated at 37°C for 1-2 h. Reactions were stopped by adding 4x DNA loading buffer and separated by agarose gel electrophoresis for DNA fragment analysis. For further cloning the enzymes were heat-inactivated for 20 min at 65°C.

2.2.1.4 DNA agarose gel electrophoresis

For separation of DNA fragments, loading buffer was added to the samples and samples were loaded onto a 0.8-1.2% (w/v) agarose gel, depending on the size of the DNA fragment. 0.5x TBE was used as the running buffer. The gels were supplemented with 0.5 g/ml ethidium bromide to visualize the DNA under UV light after separation. A DNA mass standard was used for identification of DNA length.

2.2.1.5 Creating cDNA entries using the BP recombination reaction (BP reaction)

150 ng of polymerase chain reaction product containing the attB cloning sites were mixed with 75 ng of pDONR221. The volume was adjusted to 8 µl with TE buffer at pH 8.0 and 2 µl BP clonase was added. The reaction was incubated at 25°C for 2 h and transformed into 12 µl commercial Mach1 cells (Invitrogen).

2.2.1.6 Gateway shuttling of cDNA into expression vectors (LR reaction)

cDNA was integrated into expression vectors using the Gateway technology (Invitrogen). 1 µl of the entry clone (25 ng/µl), 1 µl of destination vector (150 ng/µl) and 2 µl of TE-buffer

at pH 8.0 were incubated with 1 µl of LR clonase at 25°C for 3 h. The DNA was transformed into 10 µl commercial Mach1 cells (Invitrogen), for selection of positive clones.

2.2.1.7 DNA extraction from agarose gels

After separation by agarose gel electrophoresis, bands of interest were excised with a scalpel and purified using the QIAquick gel extraction kit according to the manufacturer's instructions.

2.2.1.8 Preparation of chemically competent E. coli

50 ml of LB medium were inoculated with a single colony and grown overnight to saturation at 37°C with shaking at 200 rpm. 10 ml of this overnight culture were used to inoculate 1 l of LB medium. The culture was grown at 37°C to an optical density of 0.4-0.6 measured at 600 nm. All the following steps were performed on ice and with pre-chilled solutions. Cells were centrifuged at 2500 rpm for 20 min, washed with 500 ml 0.1 M $MgCl_2$ solution, again centrifuged and washed with 250 ml 0.1 M $CaCl_2$ solution. After another centrifugation step the cells were resuspended in 10 ml 0.07 M $CaCl_2$ solution containing 30 % glycerol. Aliquots were frozen in liquid nitrogen and stored at -80°C.

2.2.1.9 Chemical transformation of E. coli

Frozen chemically competent cells were thawed on ice for 5 min. For transformation, 30 µl of DH10B or BL21-RP *E. coli* strains were mixed with 1 µl of plasmid DNA and incubated on ice for 30 min. The cells were then heat-shocked at 42°C for 45 sec and cooled on ice for 5 min. After addition of 1 ml pre-warmed SOC medium the cells were incubated at 37°C for 1 h with shaking. Subsequently, aliquots of cells were plated on LB agar plates containing the appropriate antibiotics and incubated overnight at 37°C. In case of BP or LR reactions, the reaction mix was transformed into 10 µl of Mach1 cells, subjected to heat-shock as described before and grown in 100 µl SOC medium. All cells were plated on LB agar plates containing the appropriate antibiotics.

2.2.2 Protein biochemistry

2.2.2.1 Expression of His-fusion proteins in E.coli in a 96-well format

For the expression of His-tagged fusion proteins in a 96-well format, a single colony of *E. coli* containing the expression vector of interest was inoculated in 1.5 ml TB media containing the appropriate antibiotics, in one well of a micro-titre plate. Thus, the 96 wells of the plate contained 96 different *E. coli* colonies, each carrying a vector for the expression of a different construct or gene. These cultures were grown overnight in an incubator-shaker at 37°C, 200 rpm. The next day, 150 µl of the overnight culture from each well were inoculated into 1.4 ml

of fresh TB medium (containing the appropriate antibiotics) in a deep-well plate, and incubated for 1.5 h at 37°C, 200 rpm. Expression was induced by adding 1 mM isopropyl-1-thio-β-D-galactoside (IPTG) and cells were then incubated overnight at 30°C, 200 rpm. The next morning, the deep-well plate was centrifuged at 4000 rpm for 10 min at 4°C, and washed with PBS (on ice) twice. The deep-well plate containing the harvested cell-pellets was then frozen at -80°C.

2.2.2.2 Purification of His-fusion proteins in a 96-well format

For the purification of His-fusion proteins in a 96-well format, the pellets in the deep-well plate were resuspended in 100 µl Cell Lysis buffer supplied with benzonase and 1 mg/ml lysozyme. Lysis was allowed to proceed for 1 h on ice, with vortexing being carried out at 15-minute intervals. The lysates were then transferred to a 96-well plate containing a suspension of NiNTA-agarose, which had been pre-washed and pre-equilibrated with water and washing-buffer, respectively, and allowed to stand for 5 min. The lysates were then washed thrice before the proteins were eluted using an elution-buffer supplied with 500 mM imidazole (pH 7.4) into a fresh 96-well plate. After the contents were spun down (2 min, 1000 rpm, 4°C), the protein-containing plate was stored at -20°C.

2.2.2.3 Expression of His-fusion proteins in E. coli in larger volumes (250 ml volume)

For the expression of His-tagged fusion proteins, a single colony of *E. coli* containing the expression vector was inoculated in 10 ml TB media containing the appropriate antibiotics. The culture was grown overnight in an incubator-shaker at 37°C, 200 rpm. The optical density was measured at 600 nm and 250 ml of fresh TB media with the appropriate antibiotics were inoculated with overnight culture to a final concentration of 0.1 OD_{600}. This culture was grown until an optical density of 0.4-0.6 measured at 600 nm was reached. Expression was induced by adding 1 mM IPTG and cells were then incubated overnight at 30°C, 200 rpm. The next morning, cells were centrifuged at 4000 rpm for 10 min at 4°C and washed with PBS (on ice) twice. The harvested cell pellet was frozen at -80°C.

2.2.2.4 Purification of His-fusion proteins in larger volumes (250ml)

For the purification of His-fusion proteins in larger volumes, the pellets were resuspended in 5 ml Cell Lysis buffer supplied with benzonase and 1 mg/ml lysozyme. Lysis was allowed to proceed for 1 h on ice, with vortexing being carried out at 15-minute intervals. The lysed cell-pellets were then centrifuged at 4000 rpm for 1 h at 4°C. The supernatants were then transferred to 2 ml Eppendorf tubes containing a 300 µl suspension of NiNTA-agarose, which had been pre-washed and pre-equilibrated with water and washing-buffer, respectively. The tubes were then placed on a rotating wheel for 1 h at 4°C to allow binding

of the His-tagged proteins to the NiNTA-agarose suspension. The lysates were then delivered onto filter-columns (pre-washed and pre-equilibrated with water and washing-buffer, respectively) and washed four times with washing buffer. The proteins were then eluted using an elution-buffer supplied with 500 mM imidazole (pH 7.4) into fresh 2 ml Eppendorf tubes. The proteins were stored at -20°C.

2.2.2.5 Expression of wild-type α-synuclein

For the expression of wild-type, untagged α-synuclein, a single colony of *E. coli* containing the expression vector was inoculated in 100 ml LB media containing the appropriate antibiotics. The culture was grown overnight in an incubator-shaker at 37°C, 200 rpm. The optical density was measured at 600 nm and 2 l of fresh LB media with the appropriate antibiotics were inoculated with overnight culture to a final concentration of 0.1 OD_{600}. This culture was grown until an optical density of 0.4-0.6 measured at 600 nm was reached. Expression was induced by adding 1 mM IPTG and cells were then incubated overnight at 30°C, 200 rpm. The next morning, cells were centrifuged twice at 4000 rpm for 30 min at 4°C. The harvested cell pellet was frozen at -80°C.

2.2.2.6 Purification of wild-type α-synuclein

For the purification of wild-type α-synuclein, the pellet was resuspended in 20 ml Cell Lysis buffer and lysed by ultrasound, vortexing and sonification. The lysed cell-pellet was then boiled at 90°C for 20 min followed by centrifugation at 11,000 rpm for 30 min at 4°C to precipitate heat-sensitive proteins. The supernatant was then subjected to treatment with 10 mg/ml streptomycin-sulphate and centrifugation at 10,000 rpm for 30 min at 4°C to precipitate the DNA from the solution. The resulting supernatant was then treated with 361 mg/ml ammonium-sulphate for 15 min at 4°C on a rotating-wheel before centrifugation at 10,000 rpm for 30 min at 4°C to precipitate the α-synuclein from the solution. The pellet was then stored at 4°C, before being subjected to anion-exchange chromatography, desalting, flash-freezing and lyophilisation, as described below.

2.2.2.7 Anion-exchange chromatography of α-synuclein

The protein-pellet was re-suspended in 6 ml 25 mM Tris-HCl pH 7.7 and filtered through a 0.2 µm-filter. 2.5 ml of the filtered mixture was loaded onto a ResourceQ- 6 ml column fitted to an Äkta purifier system and eluted at a flow-rate of 2 ml/min. The fractionation was carried out in 1 ml volumes, before the rest of the mixture was loaded onto the column for purification. 10 µl from each of the collected fractions were then denatured with 5 µl of loading buffer before being subjected to SDS-PAGE on a 10%-gel followed by Coomassie staining (as described in sections 2.2.2.12. and 2.2.2.15, below). Finally, the concentration of

the samples was determined using the Nanodrop (see section 2.2.2.11) and the selected samples were stored at - 20°C.

2.2.2.8 De-salting of α-synuclein and final steps of purification

The samples selected in section 2.2.2.7 above were then pooled into 2.5 ml volumes and delivered onto PD-10 desalting columns (pre-equilibrated with Elution buffer). After the flowthrough had been discarded, the proteins were eluted in 1 ml volumes using the Elution buffer and the absorption of each eluent at 280 nm was measured. Suitably concentrated samples were then pooled into 1 ml aliquots, flash-frozen in liquid nitrogen and lyophilized overnight. The lyophilized samples were then stored at -80°C.

2.2.2.9 Expression of Ezrin

For the expression of Ezrin, a single colony of *E. coli* containing the expression vector was inoculated in 10 ml LB media containing the appropriate antibiotics. The culture was grown overnight in an incubator-shaker at 37°C, 200 rpm. The next day, 15 ml of culture was inoculated in 1500 ml fresh media with the appropriate antibiotics, allowed to grow at 37°C to an OD_{600} of 0.7 and then induced with 500 µM IPTG overnight at 18°C. The culture was then spun down at 4000 rpm, 4°C for 10 mins. The supernatant was discarded and the pellet was frozen at -80°C.

2.2.2.10 Purification of Ezrin

For the purification of Ezrin, the 1500 ml cell-pellet was re-suspended in 10-15 ml of Cell Lysis buffer, sonicated until the solution turned clear and spun down at 15,000 rpm at 4°C for 30 mins. The supernatant was then passed through a 0.22 µm filter, pre-equilibrated with the Cell Lysis buffer, before being loaded onto a HisTrap FF Crude Lysate 1 ml affinity column with precharged Ni Sepharose 6 Fast Flow at 4°C and run at a flow-rate of 1 mg/ml using step-gradients for 10%, 60%, 70%, 80% and 100% Elution-buffer, each gradient lasting 5 column-volumes. Samples were eluted into transparent 96-well plates in volumes of 250 µl. Samples were selected for pooling based on an elution-peak at the expected imidazole concentration and thereafter subjected to size-exclusion chromatography or gel-filtration into NMR buffer on a Superdex 30/100_GL column at a flow rate of 300 µl/min at 4°C. The eluate was collected in fractions of 1.5 ml and samples eluting at the expected size for Ezrin were selected for pooling. The protein concentrations of the final pooled samples were determined by measuring the absorbance at 280 nm, before the samples were aliquoted into 1.5 ml volumes and stored at -20°C.

2.2.2.11 Determination of the protein concentration

The protein concentration of His-fusion proteins, α-synuclein and Ezrin was determined spectrophotometrically based on the absorption at 280 nm, as determined using the Nanodrop. In order to calculate the concentration from the measured absorbance the theoretical extinction coefficients were calculated for the respective amino acid sequences (http://au.expasy.org/tools/protparam.html). The protein concentration of crude cell-lysates was determined using a BCA protein assay kit. The assay was carried out as per the manufacturer's instructions.

2.2.2.12 SDS-polyacrylamide gel electrophoresis (SDS-PAGE)

Proteins were separated by SDS-PAGE using a discontinuous buffer system under denaturing and reducing conditions according to Laemmli (Laemmli, 1970). Prior to loading the samples onto the gel, a 4x loading buffer was added to them and proteins were denatured at 96°C for 5 min. SDS-PAGE was performed with resolving gels containing 10% polyacrylamide, and stacking gels containing 5% polyacrylamide. As a protein standard, the Benchmark™ pre-stained protein ladder from Invitrogen was used. Gels were run in SDS running-buffer for 15 min at 120 V, followed by 40 min at 180 V.

2.2.2.13 Western blotting

Proteins, separated by SDS-PAGE, were transferred onto a nitrocellulose membrane in a semi-dry Transblot apparatus at 20 V for 1 h. The gel was placed on a nitrocellulose membrane, sandwiched between two layers of Schleicher and Schuell GB005 Whatman paper. The membrane was placed on the side of the gel facing the anode.

2.2.2.14 Immunodetection of proteins on nitrocellulose or cellulose acetate membranes

Membranes were blocked in 5% milk in TBS-T for 30 min at room temperature or overnight at 4°C. The first antibody was diluted in 5% milk in TBS-T, if not stated otherwise, and incubated with the membrane at room temperature for 1 h or overnight at 4°C. After washing the membrane three times for 5 min each with TBS-T, the secondary antibody, also diluted in 5% milk in TBS-T, was added and the membrane was incubated for 30 min at room temperature.

For alkaline phosphatase conjugated secondary antibodies, the membranes were washed twice with TBS-T, once with TBS and finally once with attophos buffer, for 5 min each. The membranes were then incubated for 1 min in a 200-fold dilution of AttoPhos reagent in attophos buffer. Protein bands or dots were visualized by fluorescence under 460 nm UV-light in a LAS3000 Image reader and quantified using the AIDA software.

If the secondary antibody was conjugated to peroxidase the membranes were washed twice with TBS-T and once with TBS, for 5 min each. Chemiluminescence was measured using the Western Lightning™ kit from PerkinElmer using a LAS3000 Image reader according to the manufacturer's protocol.

2.2.2.15 Coomassie staining of SDS gels

Coomassie Brilliant Blue is a dye that forms strong non-covalent complexes with proteins. The dye is used to stain proteins in SDS-polyacrylamide gels. After SDS-PAGE, the gels were incubated for 1 h in Coomassie staining solution on a horizontal shaker at room temperature. To reduce background staining the gels were then washed in de-staining solution until the bands were clearly visible. For documentation the gel was scanned using a tabletop scanner.

2.2.2.16 In vitro Thioflavin-T aggregation assay

Thioflavin-T fluorescence was recorded from triplicate experiments of 50 µM α-synuclein aggregation reactions (in the presence and absence of modifier proteins, at varying concentrations spanning a range from 10 µM to 0.16 µM). α-synuclein was incubated along with the appropriate amounts of modifier protein(s) in a NaP buffer, pH 7.4, with 2 µM Thioflavin-T and a 2 mm glass-bead for enhanced stirring, in a black-walled, transparent-bottom 96-well plate, at 37°C, shaking at 200 rpm. Every 2 h for a total time-period of 70 h, the plate was removed from the incubator to allow for the recording of Thioflavin-T fluorescence in a fluorescence plate reader (InfinitE M200, Tecan) with 3 s shaking before each read. The shift in fluorescence was monitored continuously at an excitation wavelength of 450 nm and an emission wavelength of 485 nm.

2.2.2.17 Filter retardation assay

To detect SDS-insoluble aggregates, 50 µl of 50 µM α-synuclein *in vitro* aggregation reactions were mixed with an equal volume of denaturing buffer containing 0.4% SDS and 100 mM DTT and denatured at 96°C for 5 min, followed by filtration through a previously-equilibrated cellulose acetate membrane with a pore size of 0.2 µm. Blots were washed twice with 100 µl 0.2% SDS solution. Aggregates were detected with α-synuclein (211): sc-12767, Ezrin (3C12): sc-58758, and/or penta·His HRP Conjugate antibody using the standard immunodetection protocol.

2.2.3 Analytical and structural methods

2.2.3.1 Atomic force microscopy (AFM)

20 µl aliquots of 1:5 diluted *in vitro* aggregation reactions of α-synuclein with and without Ezrin were spotted immediately on freshly cleaved mica, allowed to adhere for 5 min and then washed five times with 50 µl distilled water. The samples were dried overnight at room temperature. The samples were then imaged in air with a digital multimode Nano Wizard® II atomic force microscope operating in intermittent contact mode.

2.2.3.2 Nuclear Magnetic Resonance spectroscopy

^{15}N-labelled α-synuclein (as well as spectrometer-time) was a generous gift from Dr. Philipp Selenko (FMP). Spectrometer-operation, spectra-generation and raw-data conversion were done in collaboration with Dr. Silvia Verzini (FMP), without whom this work would not be possible. Both Dr. Philipp Selenko and Dr. Andres Binolfi contributed significantly to data-interpretation**.**

(i) Sample preparation and measurement

Test and experimental samples contained 50 µM of ^{15}N-labeled recombinant α-synuclein in the presence and absence of 10 µM Ezrin and 10% (v/v) D_2O in 20 mM potassium phosphate buffer pH 7.5 with 150 mM NaCl, in a total volume of 300 µl each. These samples were aliquoted into 3 wells of a 96-well plate, in volumes of 100 µl each, to simulate the exact conditions of the *in vitro* Thioflavin-T aggregation assays described previously. This plate was incubated at 37°C, 200 rpm, and samples were removed at regular 4-5 h intervals, pooled back into 300 µl volumes, loaded in Shigemi NMR tubes (5 mm diameter) and measured in the NMR spectrophotometer, as described below. After measurement, the samples were returned to the appropriate wells of the 96-well plate, which was then replaced in the incubator. The total incubation time of the samples, not including the time spent outside the incubator (i.e. NMR-measurement and sample-processing time), was 42 h. A duplicate aggregation assay containing Thioflavin-T was allowed to run as a simultaneous control, wherein the samples were measured in a Tecan Infinite M200 plate reader at the exact same time-points as the NMR measurements, to provide corresponding Thioflavin-T-fluorescence readouts.

(ii) Data collection

All NMR measurements were operated at 298K on either a 600 MHz or 750 MHz Bruker Avance III HD NMR Spectrometer equipped with a {^{1}H/^{13}C, ^{15}N} cryoprobe. 1D ^{15}N/^{1}H correlation NMR spectra were recorded with 1024 (^{1}H) and acquisition time per experiment

was approximately 1.5 min. 2D $^{15}N/^{1}H$ SOFAST-HMQC correlation spectra of uniformly ^{15}N-labeled recombinant α-synuclein (with and without Ezrin) were recorded with 8 transients and 2048 (^{1}H) x 256 (^{15}N) complex points (interscan delay=60 ms, 6 min per acquisition time). Time-resolved NMR data were recorded in an identical setup for the experimental and the test conditions, across all the different time-points.

(iii) NMR spectra analysis

NMR spectra were processed by zero-filling (ZF) to 2 K and 256 points in the proton and nitrogen dimension, respectively. 90º (1H) and 90º bell-sine window functions were used for apodization. All data were processed with TopSpin™ software for NMR data analysis and the acquisition and processing of NMR spectra, while chemical shift variation analyses were carried out using the Sparky 3.114 - NMR Assignment and Integration software.

2.2.4 Cell biology

2.2.4.1 Rat primary neuronal cells

Plated primary neuronal cells from rat hippocampus and cortex were obtained as a kind gift from AG Meier, on the day before the corresponding toxicity assay (i.e. LDH or MTT) was to be carried out. The cells were maintained in an incubator at conditions of 37°C and 5% CO_2.

2.2.4.2 LDH Assays for determination of cell survival

Lactate dehydrogenase (LDH), which is a soluble cytosolic enzyme present in most eukaryotic cells, is released into culture medium upon cell death due to the damage of the plasma membrane. The increase of the LDH activity in culture supernatant is proportional to the number of lysed cells. The LDH assay provides a colorimetric method to measure LDH activity using a reaction cocktail containing lactate and NAD+, among other components. LDH catalyses the reduction of NAD+ to NADH in the presence of L-lactate, while the formation of NADH can be measured in a coupled reaction in which the tetrazolium salt INT is reduced to a red formazan product. The amount of the highly colored and soluble formazan can be measured at 490 nm spectrophotometrically.

For the LDH assay, fresh LDH Reaction Mix was prepared. After a 2-day incubation of the cells with the appropriate samples (e.g. α-synuclein alone, or Ezrin + α-synuclein) in a 96-well format, 10 µl of the supernatant were removed from each well and pipetted into another transparent 96-well plate. 1 µl of LDH positive control was added to the appropriate wells, after which 100 µl/well of freshly prepared LDH Reaction Mix (200 µl of WST Substrate Mix + 10 ml LDH Assay Buffer) was delivered to the samples. The 96-well plate was then

incubated for 20 min shielded from light, before the absorption of the formazan solution at 490 nm was measured using the Tecan Infinite M200 plate reader.

2.2.4.3 MTT Assays for determination of cell survival

The MTT assay is another colorimetric assay for detection of cellular growth and survival. It is based on the reduction of the tetrazole MTT to formazan by cellular redox enzymes in living cells. Following lysis of the cells, the absorption of the formazan solution at 570 nm can be analyzed spectrometrically. After a 2-day incubation of the cells with the appropriate samples (e.g. α-synuclein alone, or Ezrin + α-synuclein) in a 96-well format, 15 µl of MTT reagent (Methylthiazolyldiphenyl-tetrazolium bromide) was added to each well and the plates were incubated for 2 hours at 37°C. The cells were then lysed by adding 100 µl MTT stop solution per well and incubating for another 2 h at 37°C. The absorption of the formazan solution at 570 nm was then measured using the Tecan Infinite M200 plate reader.

2.2.5 Yeast Biology

2.2.5.1 Gateway™ cloning reaction

Gateway™ LR cloning reactions were performed to rapidly transfer open reading frames (ORFs) from entry clones into expression vectors. Each reaction was composed of 1 µl destination vector (75 ng/µl), 1 µl entry vector (25 ng/µl), 0.5 µl Gateway™ LR Clonase II Enzyme mix (Invitrogen) and 2.5 µl with TE buffer (pH 8.0). To allow site-specific recombination, the reaction was incubated at 25°C for 2 h. Reactions were directly used for chemical *E.coli* transformation or stored at -20°C.

2.2.5.2 Chemical E. coli transformation

This protocol was used for a 96-well format chemical transformation of *E. coli* cells with LR reaction products or other plasmid DNA. Competent bacterial cells were thawed on ice for 15 min. 8 µl cells were distributed into each well of 96-well PCR plates, each well containing 5 µl LR reaction solution. PCR plates were sealed, vortexed at low speed and incubated on ice for 15 min. The plates were incubated at 42°C for 45 sec and kept on ice for an additional 5 min. 100 µl SOC-medium (37°C) were added to each well and the plate was incubated at 37°C for 1 h. 25 µl from each well were streaked out as a line on selective LB plates including the appropriate antibiotic. Plates were incubated for 16 h at 37°C. Subsequently, single colonies were transferred into 96-well deep well plates, each well containing 1.2 ml liquid LB medium including the appropriate antibiotic. The deep well plates were incubated with shaking for 16 h at 37°C.

2.2.5.3 Chemical S.cerevisiae *transformation*

This protocol was used for 96-well format chemical transformation of *S. cerevisiae* cells with expression plasmids generated by Gateway™ LR cloning or other plasmid DNA. The W303-1A yeast strain was used, with the following constructs integrated into the yeast genome: wild-type-α-synuclein-GFP, A53T-α-synuclein-GFP, and the blank vector-GFP. As A53T α-synuclein is known to be more toxic when expressed than wild-type α-synuclein, all the yeast studies in this project were carried out using the A53T-α-synuclein-GFP-containing yeast strain (with the blank-vector-GFP-containing strain being the control).

A 3 ml overnight culture of the yeast was incubated with shaking at 30°C for 16 h. From this culture, 30 ml NBG –ut/ahl were inoculated at 0.1 OD_{600} and grown with shaking to an OD_{600} of 0.5 at 30°C (~4 h). Cells were centrifuged for 5 min at 1300 g, washed with 10 ml TE buffer and incubated with 1100 µl Transformation Mix 1. Herring Sperm Carrier DNA (Clontech) was boiled for 10 min, cooled on ice for 2 min and 1.5 µl were distributed to each well of a 96-well PCR plate. 5 µl mini-prep plasmid DNA, 12 µl yeast in Transformation Mix 1 and 60 µl Transformation Mix 2 were distributed to each well. The PCR plates were sealed and incubated at 30 °C for 30 min. 8 µl DMSO were added to each well and the cells were heat-shocked at 42 °C for 7 min. Subsequently, yeast cells were stamped onto NBG –ut/ahl media. After incubation at 30°C for 72 h, several clones were transferred into liquid NBG -ut/ahl media.

2.2.5.4 Modifiers of α-synuclein induced toxicity

ORFs encoding Ezrin were Gateway™ cloned into the yeast expression vector pAG425-FLAG. The generated plasmid, along with known suppressors and known enhancers of toxicity and the empty pAG425-FLAG vector were transformed into the yeast, as described above. Several yeast clones per construct were used to inoculate liquid NBG -ut/ahl (-ura-trp/+ade+his+leu) cultures (carbon source: glucose) that were grown with shaking for 48 h at 30°C. Glycerol stocks were then prepared and stored at -80°C.

2.2.5.5 Yeast growth tests on solid agar and in liquid culture

The cultures described above were then used to inoculate liquid NBG –ut/ahl media (carbon source: raffinose). These cultures were then allowed to grow at 30 °C, 200 rpm, to an OD_{600} of 1, before being used in:

(i) Growth tests on solid agar:

1:5 serial dilutions of the yeast cultures were prepared in 96-well MTPs and stamped onto NBG -ut/ahl agar plates containing the carbon sources glucose or galactose. Plating on

galactose activates the GAL-promoter that precedes the α-synuclein-GFP and the blank-vector-GFP constructs integrated into the yeast genome, as well as the N-terminally FLAG-tagged gene-containing plasmids transformed into the yeast, resulting in expression of α-synuclein-GFP and/or N-terminally FLAG-tagged fusion proteins. Upon suitable over-expression of α-synuclein-GFP, large aggregates of α-synuclein-GFP are formed, which are toxic to the growth of the yeast cells carrying them, particularly yeast strains expressing A53T-α-synuclein-GFP (Outeiro and Lindquist, 2003). Plating on glucose, however, does not activate the GAL-promoter or α-synuclein-GFP expression, resulting in neither aggregate formation nor ensuing cellular toxicity. The plates were incubated at 30 °C for 120 h and digital images of yeast colonies were taken. The experiment was performed in triplicate.

(ii) Growth tests in liquid culture:

100 ml each of glucose-containing and galactose-containing NBG -ut/ahl media were inoculated with the yeast cultures at a starting OD_{600} of 0.01 and incubated at 30 °C for 72 h, before the final OD_{600} was measured. The experiment was performed in triplicate.

2.2.5.6 Yeast microscopy and quantification of aggregates

25 µl samples were extracted from the liquid cultures described above and dropped onto a glass slide for examination under an Olympus MX40 light microscope with the following objectives: 20X, 40X and 80X, using a GFP filter. For α-synuclein-GFP aggregate quantification purposes, a minimum of 100 cells per test condition was evaluated.

2.2.5.7 Yeast lysis

25 ml of each yeast strain of interest were grown at 30°C to an OD_{600} of 1, before being centrifuged for 5 min at 3000 g and washed with PBS. Upon addition of 200 µl lysis buffer and glass beads, the samples were vortexed for 2 min, before being subjected to 30 seconds in liquid nitrogen, followed by a heat-shock at 50°C (treatment repeated thrice). The samples were then spun down at 3000 rpm for 5 min, and the supernatant was transferred to a new tube for treatment with 5 µl benzonase solution and incubation for 30 min at 37°C. For SDS-PAGE, 55 µl 10% SDS were added, along with 4X loading-buffer and the samples were then incubated for 10 min at 99°C with shaking. SDS-PAGE and immunoblotting were carried out as previously described.

3. RESULTS

3.1 Screening of 13,824 proteins reveals potent modifiers of α-synuclein fibrillization

In order to indentify novel modulators of α-synuclein fibrillization, we screened a library of 13,824 proteins using a fluorescence-based fibrillization assay. The production of both α-synuclein and library proteins along with the establishment of a fibrillization assay with a protein-pooling approach have been detailed below. The screening process and downstream deconvolution strategy have been represented diagrammatically, followed by the outcome of the screen. Information on the novel modulators discovered and their behavior in dose-dependence assays has also been provided, leading to the ultimate identification of Ezrin as the protein modifier of choice for further study.

3.1.1 Expression and purification of α-synuclein

α-synuclein was expressed from the pRK172 vector present in the BL21(DE)3 strain of *E. coli* using the protocol first described by the Lansbury group (Weinreb et al., 1996). As described in Section 2.2.2.5, protein expression was induced by addition of IPTG to the growth medium overnight at 30°C. The following day, cells were harvested, lysed and subjected to purification, first by eluting the protein from a Resource Q-6ml anion-exchange column and then by size-exclusion chromatography. These samples were analyzed by SDS-PAGE and Coomassie staining (Fig 3.1.1), before pooling of the fractions 18-23, overnight lyophilisation and storage at -80°C. Using this approach, α-synuclein with a purity of over 90% was produced (gauged by determining the ratio of α-synuclein-bands to the total amount of protein detected on the Coomassie gel using the AIDA quantification software). As the purification process for α-synuclein involves multiple stringent steps as well as the use of various buffers and only the highest purity α-synuclein was desired for use in experiments, the protein loss during the purification process was not altogether insignificant. Roughly, 20 l of protein-expressing bacterial culture yielded 200 mg of purified, buffer-exchanged and lyophilized α-synuclein.

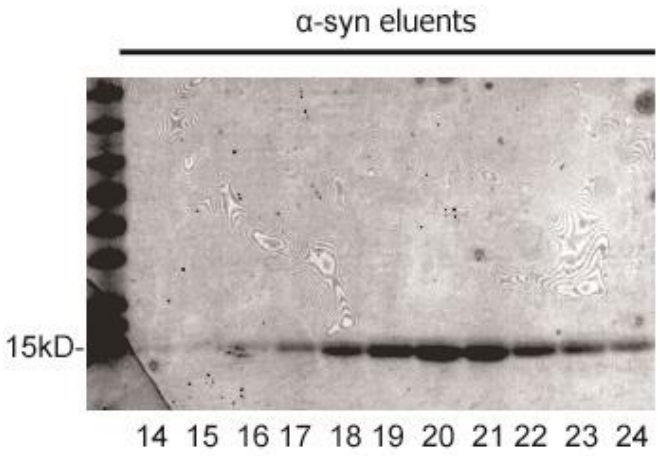

Figure 3.1.1 Confirmation of the purity of gel-filtered α-synuclein by SDS-PAGE (on a 10% gel) and Coomassie staining.

3.1.2 Establishment of a cell-free α-synuclein fibrillization assay

In order to establish a cell-free assay with optimal conditions for the detection of modulator proteins that inhibit α-synuclein fibrillization, a large number of assay conditions were investigated. These included different multi-well plate formats (384-well vs. 96-well), PBS and sodium phosphate (NaP) buffers, varying pH values of 6, 6.5, 7 and 7.5, wild-type, A53T and E46K α-synucleins, room temperature (25 ˚C) and physiological body temperature (37 ˚C) conditions, and three different sub-stoichiometric concentrations of control modifier proteins relative to α-synuclein concentration (i.e. 5μM, 10μM and 15μM). Fig. 3.1.2 depicts two different assay parameters that were optimized, namely, varying temperatures and various forms of α-synuclein. Only after optimization of the various conditions was the final assay established and employed in systematic modulator screening, as described below.

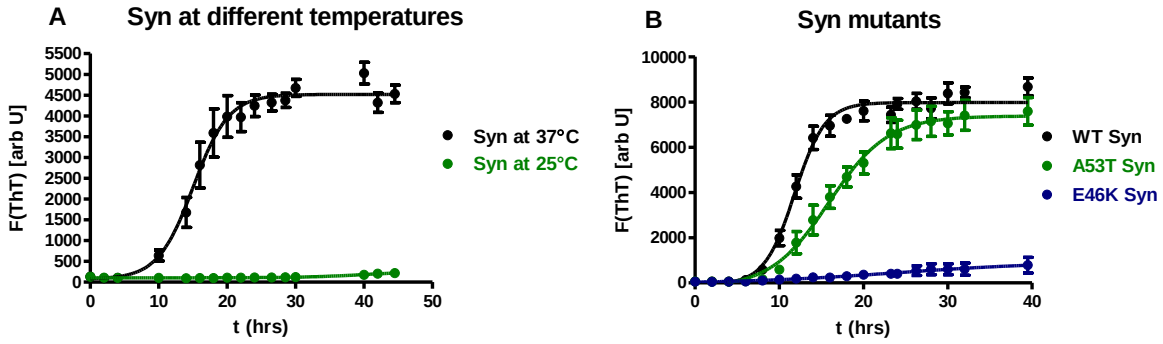

Fig. 3.1.2 Optimization of parameters for the establishment of a cell-free fibrillization assay. (A) Thioflavin-T fluorescence traces of α-synuclein (Syn) incubated at physiological temperature (37˚C) and room temperature (25˚C). (B) Thioflavin-T fluorescence traces of wild-type α-synuclein (WT Syn), A53T mutant α-synuclein (A53T Syn) and E46K mutant α-synuclein (E46K Syn) incubated at 37˚C.

50 µM of wild-type α-synuclein were incubated in NaP buffer (pH 7.5) in 96-well plates with 5 µM modifier protein at 37 ˚C, shaking at 200 rpm, in the presence of a glass bead and the fluorescent dye, Thioflavin-T. Fluorescence-measurements were taken every 2 hours for a minimum period of 24 hours up to a maximum period of 70 hours. The glass bead was included to increase the shearing forces within the solution as well as to act as a nucleating point within the well, thereby speeding up the fibrillization process, such that the assay usually reached completion within 70 h after the start of incubation. The fibrillization assay is based upon the property of the dye Thioflavin-T to emit fluorescence when bound to ß-pleated sheet structures, such as α-synuclein fibrils (LeVine, 1999). In the presence of an inhibitor, a reduction in fluorescence should be observed, either as a decreased amplitude of fluorescence or as a delayed lag phase or both, thereby enabling a quick-and-easy first-level identification of novel modifiers of α-synuclein aggregation.

3.1.3 Validation of the assay using test set proteins

In order to establish an effective high-throughput screen for modifiers of α-synuclein fibrillization, a pilot screen was first carried out using a test set of 32 proteins expressed in triplicate in a 96-well plate format. Of these proteins, some were known inhibitors of α-synuclein aggregation, such as heat-shock proteins 70 and 90, and others, such as superoxide dismutase 1, were known to have no effect on α-synuclein fibril formation (Andrekopoulos et al., 2004; Fan et al., 2006; Hinault et al., 2010; Hyun et al., 2003; Luk et al., 2008). Thus, by adding known inhibitor proteins to the cell-free assay described above and evaluating their effect on α-synuclein fibrillization, the suitability of this assay as a means of identifying novel inhibitor proteins could be gauged.

3.1.3.1 Expression and purification of the protein test set

The proteins used in this study were tagged at their N-terminal end with a six-residue His sequence. For the production of proteins, *E. coli* cells carrying the cDNA of interest in the pDESTco expression plasmid were induced by addition of IPTG to the growth medium. The following day, cells were harvested, lysed and subjected to purification via the 6xHis-tags by using Ni-NTA beads (as described in Section 2.2.2.2). The resulting samples were analyzed by SDS-PAGE and Coomassie staining, before storage at -20°C (a representative sample of His-tagged and purified proteins is shown in Fig. 3.1.3.1). Due to the heterogeneity of expression of single clones in small volumes such as 1.3 ml (which is the case in 96-well plates) each clone was expressed and purified in triplicate, prior to analysis by SDS-PAGE. As can be seen in Fig. 3.1.3.1, a single clone, e.g. APP-B (amyloid precursor protein-binding protein 1), shows highly varying expression levels in 3 individual wells. Thus, such a

'triplicate' approach ensured the selection and downstream usage of only the most suitable clone.

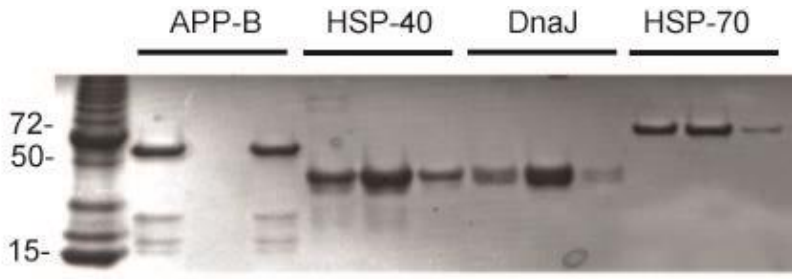

Fig. 3.1.3.1. Confirmation of the purity of a representative sample of test set proteins by SDS-PAGE (on a 10% gel) followed by Coomassie staining. The individual proteins were run on gels in triplicate to overcome any expressional heterogeneity (as described above). APP-B: amyloid precursor protein-binding protein 1; HSP-40: heat shock protein 40; DnaJ: a heat-shock protein family member; HSP-70: heat shock protein 70.

3.1.3.2 Validating the cell-free fibrillization assay using test proteins

In order to validate whether the cell-free assay provides a suitable setting for the detection of inhibitors of α-synuclein fibrillization, known inhibitors of α-synuclein fibrillization, e.g. HSP-70 and other proteins described above, were tested in the assay. Fig. 3.1.3.2 depicts the data from a validation assay where 50 μM α-synuclein were incubated either alone or together with HSP-40, HSP-70, or SOD1. As expected, α-synuclein fibrillization (as detected by an increase in Thioflavin-T fluorescence) was significantly reduced in the presence of the known inhibitors, HSP-40 and HSP-70, while the presence of SOD1 in the incubation mixture had no effect on the fibrillization of α-synuclein. Thus, the assay proved to be optimal for the detection of novel protein modulators, as established fibrillization-inhibitors clearly showed an effect within this experimental set-up.

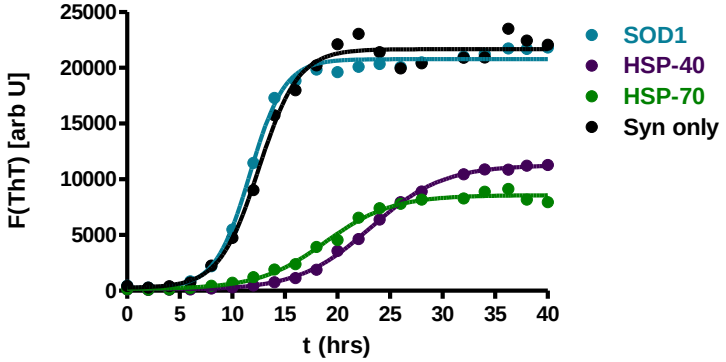

Figure 3.1.3.2 Validation of a cell-free assay to detect inhibitors of α-synuclein fibrillization. Thioflavin-T assay of α-synuclein incubated either alone (Syn only) or in the presence of superoxide dismutase 1 (SOD1), heat-shock proteins 40 and 70 (HSP-40 & HSP-70). The positive controls, HSP-40 and HSP-70,

reduce the thioflavin-T signal indicative of inhibition of fibril formation, while the negative control, SOD1, has little effect on the aggregation of α-synuclein. [Concentration of each of the control proteins relative to α-synuclein was 10:1].

3.1.3.3 Rationale for the selection of test proteins

The heat-shock proteins as well as superoxide dismutase 1 were selected as controls for assay development as previous studies within the scientific literature indicated that these proteins may influence protein misfolding and/or aggregation. Studies have shown that in neurons, the HSP70s and their HSP40-like J-domain co-chaperones are the only known components of the chaperone network that can use ATP to convert cytotoxic protein aggregates into harmless natively refolded polypeptides. J-domain co-chaperones may preferably bind to exposed bulky misfolded structures in misfolded proteins and, thus, complement HSP70s that bind to extended segments (Hinault et al., 2010). Additionally, interactions between HSP70 and the hydrophobic core of α-synuclein inhibit fibril assembly (Luk et al., 2008).

Conversely, one of the proposed mechanisms for aggregation of α-synuclein involves oxidative and nitrative modifications. Bicarbonate-dependent peroxidase activity of Cu,Zn-superoxide dismutase (SOD1) has been shown to induce covalent aggregation of α-synuclein via a CO_3*--dependent mechanism (Andrekopoulos et al., 2004). Similarly, the frequency of cells showing immunoreactivity against ubiquitinated- or nitrated- proteins is enhanced when wild-type and mutant SOD1 are overexpressed, as a result of which ubiquitinated or nitrated SOD-1 and α-synuclein are observed in aggregates (Hyun et al., 2003). Such α-synuclein and SOD1 aggregates are also observed in cells overexpressing mutant Parkin (Del3-5, T240R and Q311'X) (Hyun et al., 2003). For this reason, HSP40, HSP70 and the SOD1 protein were chosen as appropriate controls for establishment and validation of the cell-free assay to detect inhibitors of α-synuclein fibrillization.

3.1.4 Optimization of the fibrillization assay for high-throughput screening

The next step towards the identification of novel inhibitors of α-synuclein fibrillization was to optimize the assay for use in a large-scale screening format. Since the library to be screened consisted of 13,824 proteins, a high-throughput format was sought so that in just a few rounds of screening, large numbers of proteins could be sorted through. The following sub-sections describe how this requirement was met.

3.1.4.1 Adopting a pooling strategy for high-throughput compatibility

In order to accomplish the goal of resource-efficient high-throughput screening, a pooling strategy was devised. A library consisting of 36 X ‘384-well’ microtiter plates was used, with

each well containing an *E. coli* clone carrying the cDNA of interest in the pDESTco expression plasmid. In brief, 8 *E. coli* clones were picked and pooled at random into one well of a 96-well plate in order to reduce the total number of plates (and thereby, samples) in the initial screen from *144* X 96-well plates to *18* X 96-well plates. Expression of the eight library proteins per pool was then induced in the usual way, by addition of IPTG to the growth medium followed by downstream protein purification methods involving Ni-NTA beads (as described in Section 2.2.2.2). Each pool was then treated as one test sample and examined in the cell-free fibrillization assay as such. Hence, one 96-well plate contained 96 test samples from which 96 distinct Thioflavin-T fluorescence traces were generated. Thus, test samples, i.e. entire pools which showed no decrease in fluorescence, could be discarded in the first screening round, minimizing the amount of work that would otherwise be required to screen 13,824 proteins individually. It should be noted here that the screening assay is blind to false-negatives such as poorly expressed proteins, proteins without functional fold, cross-inhibition of protein activity by other proteins in the pool, etc. However, although potential false-negatives may be overlooked via such a process, this 'pooling-based approach' allows for the processing of the whole protein library in just a few screening rounds and significantly speeds up identification of those proteins that appear to function as inhibitors of α-synuclein fibrillization.

3.1.4.2 Equivalence of 'pooled test proteins' and 'individual test proteins' when used as inhibitors in the fibrillization assay

Before directly employing the pooling strategy for a high-throughput screen, it was necessary to confirm that the results yielded by a pool of test proteins containing at least one 'hit' among them were truly equivalent to the results obtained when the individual 'hit' protein was tested in the assay alone. Fig. 3.1.4.2 below highlights the equivalence of pooled hit proteins and individually examined hit proteins for the purposes of this study.

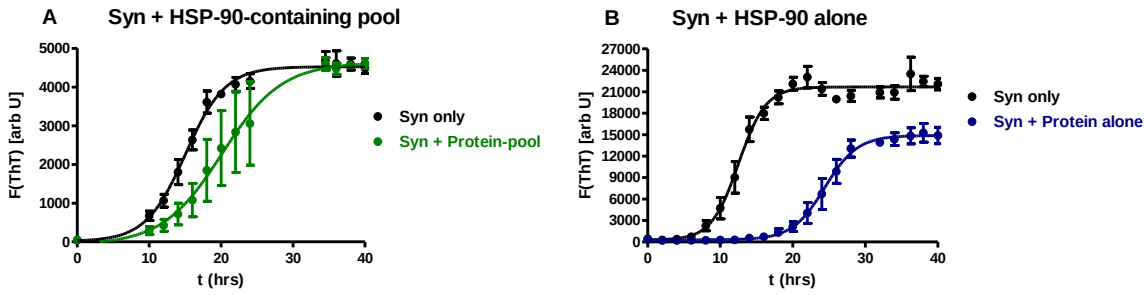

Fig. 3.1.4.2 Equivalence of protein-pools and proteins incubated alone. (A) Thioflavin-T fluorescence traces of α-synuclein incubated alone (Syn only) or with a pool of proteins, one of which is known to be HSP-90 (Syn + Protein-pool). (B) Thioflavin-T fluorescence traces of α-synuclein incubated alone (Syn only) or with a single member of the protein-pool, HSP-90 (Syn + Protein alone). N.B. The difference in

the scales of the Y-axes arises from the difference in the settings of the two TECAN fluorescence-readers that were used in the experiments.

3.1.5 High-throughput screening of 13,824 proteins using the fibrillization assay

As previously mentioned, in the very first screen (Round 1) the total number of plates was reduced from *144* to *18*, thus, 1,728 protein pools were systematically screened. After the elimination of pools of proteins which showed no change in Thioflavin-T-fluorescence in Round 1, roughly 313 pools or approximately 2,504 proteins were selected as potential modulator candidates. A potential candidate pool was defined as any pool that exhibited (i) an increase in T_{50} of ≥ 25% (where T_{50} is the time, T, taken to achieve 50% of the maximum fluorescent signal), (ii) a decrease in the maximum fluorescent signal of ≥ 25%, or (iii) both. In a subsequent round of screening (Round 2), these candidate pools were subjected to a confirmatory re-screen using a more stringent selection based only on T_{50}. In other words, only pools which showed an increase in T_{50} of ≥ 50%, i.e. pools which took twice as long to achieve half-maximum fluorescence as compared to the control α-synuclein pool were chosen. This resulted in the identification of 33 pools or 264 potential modulator candidates.

Round 3 of the screening consisted of the de-convolution of candidate pools, i.e. each of the 264 proteins was individually tested in a fibrillization assay. As before, only proteins which showed an increase in T_{50} of ≥ 50% as compared to α-synuclein alone were chosen. By using this step-by-step approach, 25 proteins were revealed to be inhibitors of α-synuclein fibrillization, of which 20 were novel and 5 were previously known from the existing scientific literature. These 5 proteins encompassed mainly HSP-protein family members and associated proteins, namely, heat shock 90 kDa protein 1 alpha, heat shock 70 kDa protein 8 isoform 1, HSPC009 protein, HSPC038 protein and ubiquitin-like protein 1 (sentrin), thereby providing positive confirmation of the accuracy and functionality of the screen. However, not being novel, they were eliminated from the pool of proteins chosen for further analyses and in Round 4 (the final round of screening) the 20 novel modulators were systematically investigated in an initial dosage study. The term initial dosage study refers to preliminary concentration-response studies carried out with only three concentrations of the modifier with respect to 50 μM α-synuclein, i.e. α-synuclein:Ezrin 2:1, 4:1, 8:1. Modifiers that succeeded in demonstrating a strong inhibition of α-synuclein fibrillization within this initial dosage study (13 in total) were then carried forward for examination in detailed concentration-response assays. Fig. 3.1.5 summarizes the various rounds of the high-throughput screen and their outcomes in a schematic form.

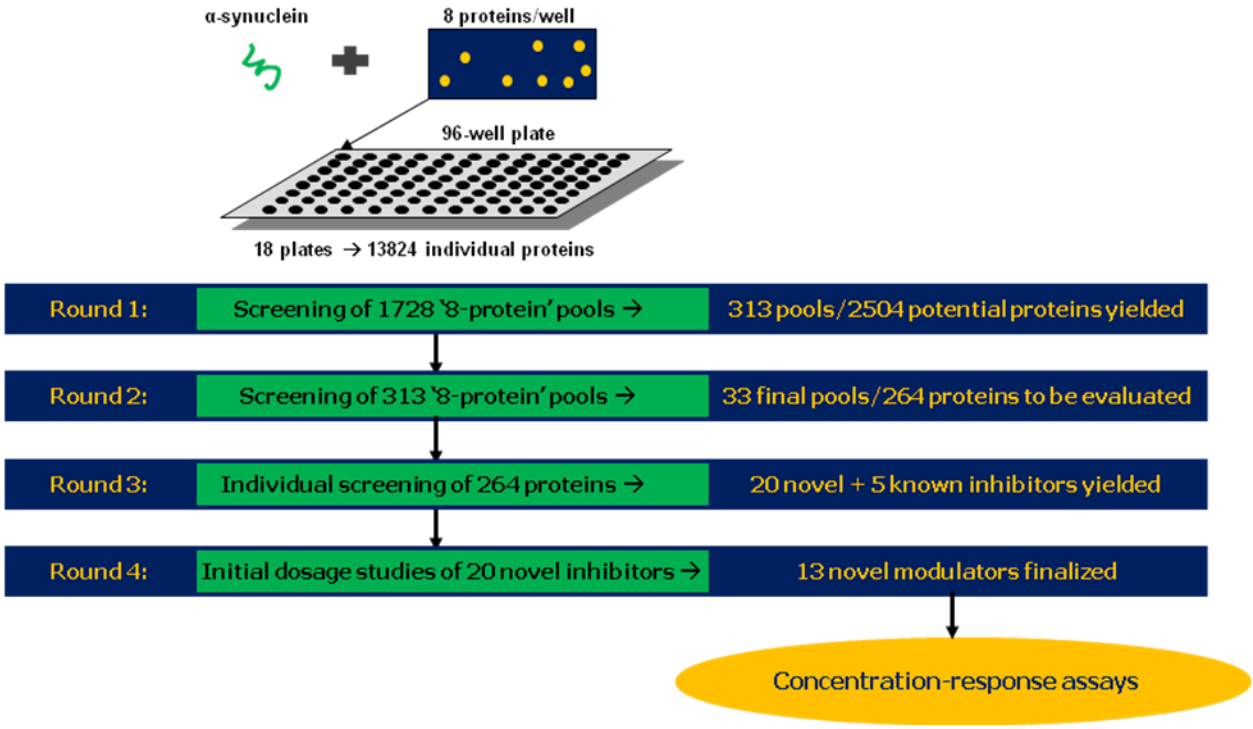

Figure 3.1.5. A diagrammatic representation of the screening process. α-synuclein was incubated in the cell-free assay with 8 randomly-pooled candidate proteins in a 96-well plate format. Screening consisted of multiple rounds, with the identification of primary pools in Round 1, confirmation of target pools in Round 2, deconvolution of pools in Round 3 and initial dosage assays of the top 20 novel hits in Round 4, before proceeding to the evaluation of the top 13 candidates in systematic concentration-response assays.

3.1.6 Thirteen novel proteins revealed as potent inhibitors of α-synuclein fibrillization

The 13 "hits" yielded by the high-throughput screen above, in alphabetical order of gene names, are: EZR (Ezrin), HMG20A (High-mobility group protein 20A), HMGN2 (High-mobility group nucleosomal binding domain 2), HNRPDL (Heterogeneous nuclear ribonucleoprotein D-like), IGSF4 (Immunoglobulin superfamily member 4), NBL1 (Neuroblastoma, suppression of tumourigenicity 1), NONO (Non-POU domain containing, octamer-binding), OTUD5 (OTU [Ovarian Tumour] domain-containing protein 5; deubiquitinating enzyme A), PABPC1 (Poly(A) binding protein, cytoplasmic 1), PFDN5 (Prefoldin 5, subunit alpha), PNMA1 (Paraneoplastic antigen, Ma1), RPL7 (Ribosomal protein L7) and RPS4X (Ribosomal protein S4, X-linked).

These proteins were next examined in concentration-response assays, using a range of concentrations relative to α-synuclein. To maintain uniformity throughout the screen and to ensure 100% reproducibility, the same modifier protein stocks used in the previous rounds of the screen were used for the concentration-response assays. Wherever enough protein was

available from the original modifier stock, higher concentrations of the modifier, such as modifier:α-synuclein 1:5, were also incorporated. Where such amounts were unavailable, concentrations towards the lower end of the range were included, e.g. modifier:α-synuclein 1:320. Thus, the range of concentrations was kept uniform for all modifiers (6 different dosages) and was always maintained at sub-stoichiometric levels. Alongside the concentration-response graph for each modifier (Fig 3.1.6.) is a representation of the T_{50} values for different concentrations of that modifier when incubated with α-synuclein.

It is important to note that some of the modifiers identified from the screen were present as protein fragments in the library, particularly ribosomal protein S4 X-linked (RPS4X) and Ezrin. However, for the validation experiments and all the downstream studies, the full-length forms of these proteins were used, as these were present in other protein libraries available in the laboratory. Hence, the data shown in Fig. 3.1.6 represent the wild-type forms of ribosomal protein S4 X-linked and Ezrin.

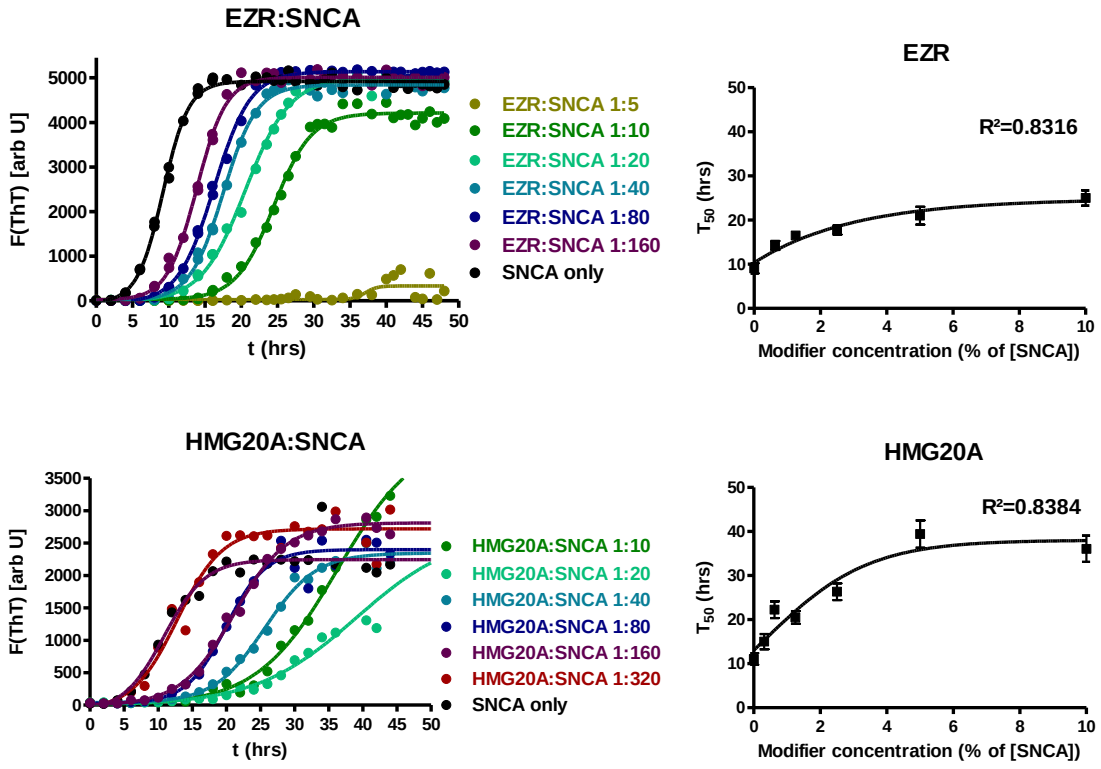

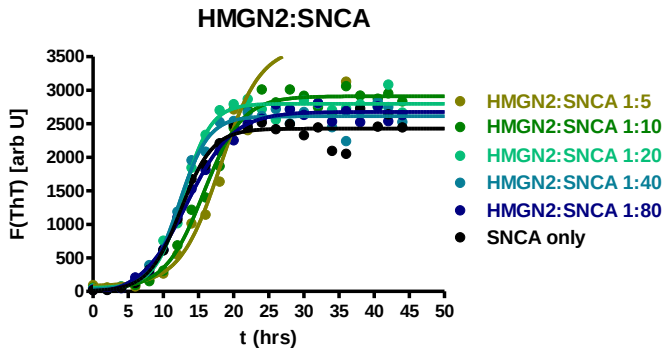
HMGN2:SNCA
F(ThT) [arb U]
t (hrs)
HMGN2:SNCA 1:5
HMGN2:SNCA 1:10
HMGN2:SNCA 1:20
HMGN2:SNCA 1:40
HMGN2:SNCA 1:80
SNCA only

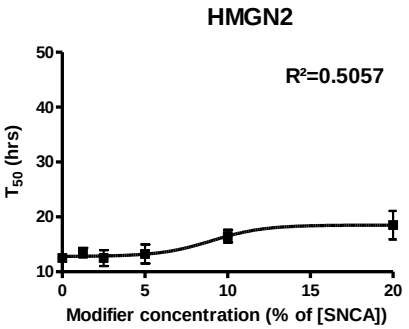
HMGN2
R²=0.5057
T50 (hrs)
Modifier concentration (% of [SNCA])

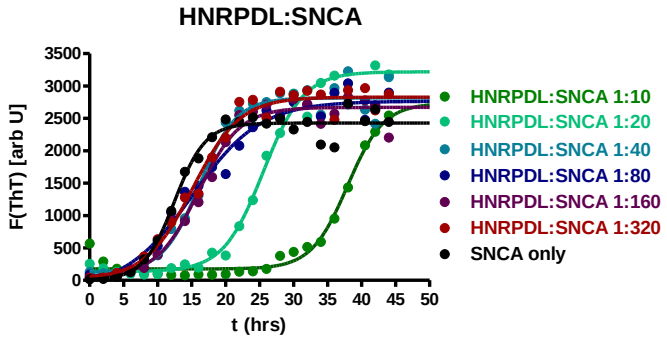
HNRPDL:SNCA
F(ThT) [arb U]
t (hrs)
HNRPDL:SNCA 1:10
HNRPDL:SNCA 1:20
HNRPDL:SNCA 1:40
HNRPDL:SNCA 1:80
HNRPDL:SNCA 1:160
HNRPDL:SNCA 1:320
SNCA only

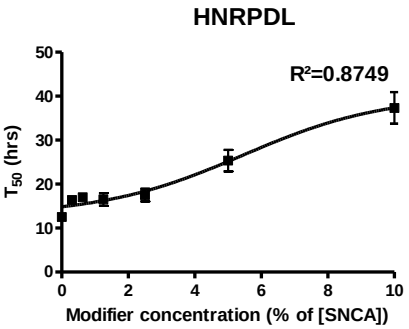
HNRPDL
R²=0.8749
T50 (hrs)
Modifier concentration (% of [SNCA])

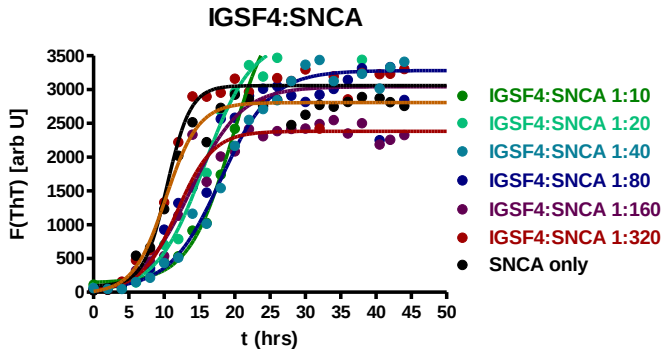
IGSF4:SNCA
F(ThT) [arb U]
t (hrs)
IGSF4:SNCA 1:10
IGSF4:SNCA 1:20
IGSF4:SNCA 1:40
IGSF4:SNCA 1:80
IGSF4:SNCA 1:160
IGSF4:SNCA 1:320
SNCA only

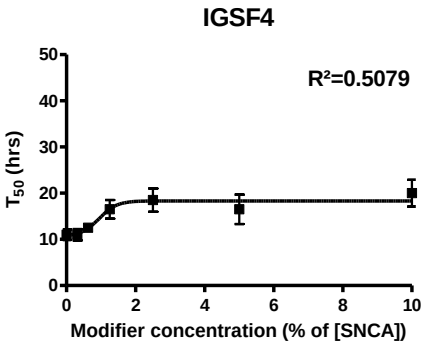
IGSF4
R²=0.5079
T50 (hrs)
Modifier concentration (% of [SNCA])

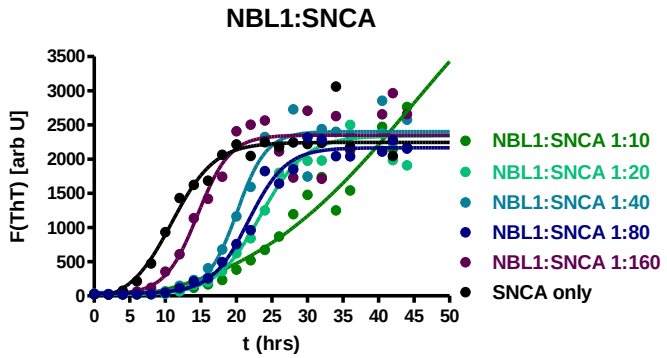
NBL1:SNCA
F(ThT) [arb U]
t (hrs)
NBL1:SNCA 1:10
NBL1:SNCA 1:20
NBL1:SNCA 1:40
NBL1:SNCA 1:80
NBL1:SNCA 1:160
SNCA only

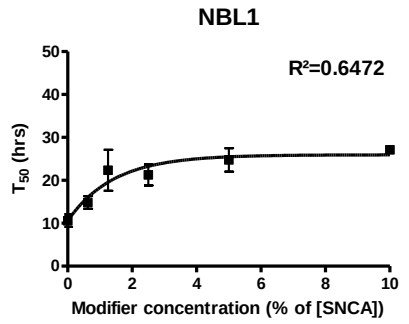
NBL1
R²=0.6472
T50 (hrs)
Modifier concentration (% of [SNCA])

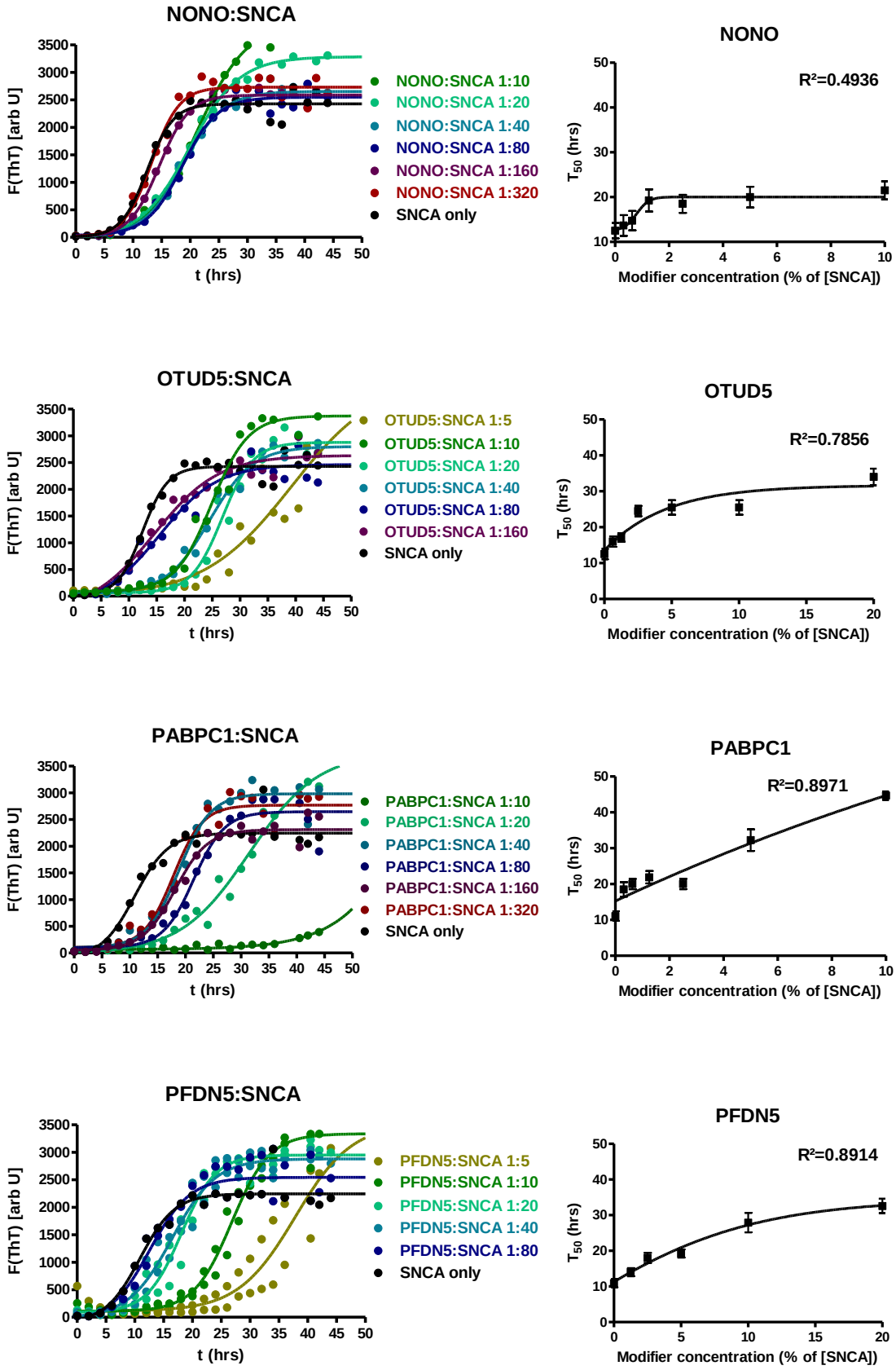
NONO:SNCA
F(ThT) [arb U]
t (hrs)
NONO:SNCA 1:10
NONO:SNCA 1:20
NONO:SNCA 1:40
NONO:SNCA 1:80
NONO:SNCA 1:160
NONO:SNCA 1:320
SNCA only
NONO
R²=0.4936
T50 (hrs)
Modifier concentration (% of [SNCA])
OTUD5:SNCA
OTUD5:SNCA 1:5
OTUD5:SNCA 1:10
OTUD5:SNCA 1:20
OTUD5:SNCA 1:40
OTUD5:SNCA 1:80
OTUD5:SNCA 1:160
SNCA only
OTUD5
R²=0.7856
PABPC1:SNCA
PABPC1:SNCA 1:10
PABPC1:SNCA 1:20
PABPC1:SNCA 1:40
PABPC1:SNCA 1:80
PABPC1:SNCA 1:160
PABPC1:SNCA 1:320
SNCA only
PABPC1
R²=0.8971
PFDN5:SNCA
PFDN5:SNCA 1:5
PFDN5:SNCA 1:10
PFDN5:SNCA 1:20
PFDN5:SNCA 1:40
PFDN5:SNCA 1:80
SNCA only
PFDN5
R²=0.8914

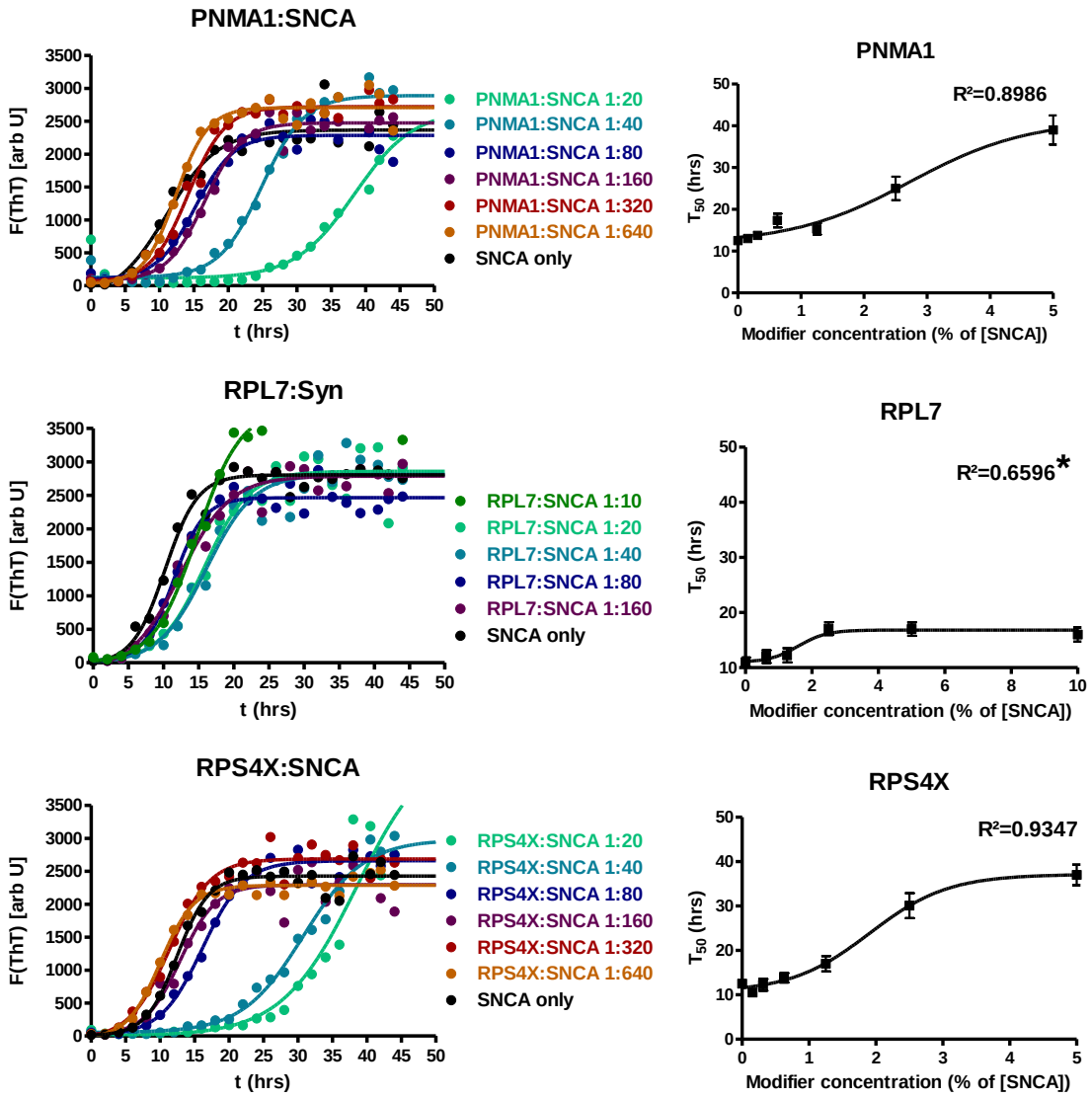

Figure 3.1.6 (Left) Concentration-response assays of various modifier proteins incubated with α-synuclein (SNCA) at sub-stoichiometric concentrations. Thioflavin-T fluorescence of SNCA in the presence or absence of EZR, HMG20A, HMGN2, HNRPDL, IGSF4, NBL1, NONO, OTUD5, PABPC1, PFDN5, PNMA1, RPL7 and RPS4X, respectively, is depicted. The concentrations of each protein relative to α-synuclein are represented for each graph. In all cases, 'sigmoidal dose-response – variable slope' curves provide the best fit to the data-points. (Right) Alongside each fluorescence assay is a depiction of the different T_{50} values corresponding to the different concentrations of the modifier with which α-synuclein is incubated (T_{50}: the time, T, taken to achieve 50% of the maximum fluorescent signal). In all cases, curves plotted for inhibitor-concentration vs. response, using a variable slope function, provide the best fit (R^2) for the data, except in the case of RPL7. Here, the variable slope function provides no R^2 value, hence, the curve is plotted without the variable slope function (R^2 for RPL7 is represented by *). Error bars represent s.e.m. n=3

While most of the proteins demonstrated a concentration-dependent decrease in the rate of α-synuclein fibrillization, none was as potent as Ezrin. Ezrin (at concentrations as low as Ezrin:α-synuclein 1:5) was the *only* protein that completely inhibited α-synuclein fibrillization,

as evidenced by the Thioflavin-T fluorescence-levels, which remained practically unaltered throughout the experiment. A detailed description of each of the modifiers, with respect to its location, site/s of expression, function and/or misfunction, involvement in disease and role in the nervous system (where relevant) is provided in Table 3.1.6.

Table 3.1.6 A detailed description of the top 13 protein modifiers revealed by systematic aggregation screens

No.	Gene Name/ ID	Protein Name	Protein Location/ Expression	Protein Function/ Misfunction
1	**EZR/ 7430**	**Ezrin**	Initially identified in the microvilli of the gut & respiratory tract lining; it is also expressed in the brain: in rat dorsal root ganglia, hippocampus & micro-vascular endothelial cells & in glial tube cells of the rostral migratory stream and sub-ventricular organ in adult mice (Cleary et al., 2006; Mooseker, 1983; Persson et al., 2010; Trofatter et al., 1993).	An actin-regulatory protein that regulates epithelial cell morphology, motility, death, migration & surface structure adhesion. A cytoplasmic peripheral membrane protein, it functions as a protein-tyrosine kinase substrate in microvilli (Bretscher et al., 2002; Crepaldi et al., 1997; Frame et al., 2010; Gould et al., 1989; Gould et al., 1986).
2	**HMG20A/ 10363**	**High-mobility group protein 20A**	Extensively poly-adenylated, it is expressed almost ubiquitously- in spleen, testis, heart, leukocytes and brain (Sumoy et al., 2000).	The HMG box encodes a conserved DNA-binding domain involved in the regulation of transcription and chromatin conformation (Artegiani et al., 2010; Sumoy et al., 2000; Wynder et al., 2005).
3	**HMGN2/ 3151**	**High mobility group nucleo-somal binding domain 2**	Cells of the thyroid gland, epididymis, alveoli, gall bladder and glial cells in the CNS show strong nuclear HMGN2 expression, while neurons show none (Lucey et al., 2008; West et al., 2001). Moderate levels of nuclear expression are seen in most normal tissues.	Like other HMGN proteins which bind to chromatin in a cell-cycle-dependent manner, HMGN2 interacts with nucleosomes. It acts in opposition to ATP-dependent chromatin remodeling factors to restrict nucleosome mobility. It also modulates global genome repair and mediates lipopolysaccharide-induced expression of β-defensins in A549 cells. HMGN2 inducibly binds a novel transactivation domain in nuclear PRLr to coordinate Stat5a-mediated transcription (Cherukuri et al., 2008; Deng et al., 2011; Fiorillo et al., 2011; Gerlitz, 2010; Rattner et al., 2009; Subramanian et al., 2009).

4	**HNRPDL/ 9987**	**Hetero-geneous nuclear ribo-nucleo-protein D-like**	The protein is ubiquitously expressed and found in the nucleus, although it may also shuttle between the nucleus and cytoplasm. It is particularly overexpressed in cells of the hematopoietic and lymphatic system (Kamei et al., 1999; Kawamura et al., 2002; Tsuchiya et al., 1998).	Belonging to the subfamily of ubiquitously expressed hnRNPs: RNA-binding proteins that complex with hnRNA, hnRNPD is associated with pre-mRNAs in the nucleus & influences pre-mRNA processing, mRNA metabolism and transport (Omnus et al., 2011; Reboll et al., 2007).
5	**IGSF4/ (also referred to as CADM1) 23705**	**Immuno-globulin superfamily member 4 or Cell adhesion molecule 1**	Neuropil in the CNS and peripheral nerves show distinct IGSF4 staining, along with granular layer cells of the cerebellum. Islets of Langerhans (pancreas) and adrenal glands, amongst a variety of other glandular cells, also show the membranous staining typical of CADM1 (Ito et al., 2008; Maekawa et al., 2011).	Also known as nectin-like protein 2, it mediates nerve-mast cell and smooth muscle-mast cell interaction. It is involved in both oncogenesis and spermatogenesis. It is a tumour-suppressor of non-small-cell lung cancer (hence, termed TSLC1) and also drives synaptic formation of neural cells (hence, termed SynCAM) (Murakami, 2008; Watabe et al., 2003).
6	**NBL1/ 4681**	**Neuro-blastoma, suppress-ion of tumouri-genicity 1**	NBL1 shows ubiquitous nuclear and cytoplasmic expression, particularly in neuronal cells of the cerebral cortex, hippocampus and lateral ventricle, all cell types within the cerebellum, lymph nodes and bone marrow, most cell types within the gastrointestinal tract, endocrine glands, skin, skeletal and smooth muscle, gall bladder, urinary tract, respiratory system, male and female reproductive system and placenta (Enomoto et al., 1994; Gerlach-Bank et al., 2002; Hayashi et al., 2013; Kim and Pleasure, 2003).	This is the founding member of the evolutionarily conserved CAN (Cerberus and DAN) family of proteins, which contain a domain resembling the CTCK (C-terminal cystine knot-like) motif found in a number of signaling molecules. These proteins are secreted and act as BMP (bone morphogenetic protein) antagonists by binding to BMPs and preventing them from interacting with their receptors. They may thus play an important role during growth and development (Enomoto et al., 1994; Hung et al., 2012; Olakowski et al., 2009; Sakiyama and Ozaki, 1997; Shinbo et al., 2002).
7	**NONO/ 4841**	**Non-POU domain containing, octamer-binding**	Localized in the nucleus, it is expressed in the heart, brain, placenta, lung, etc. and in breast tumor cell lines (Pavao et al., 2001; Schiffner et al., 2011).	DNA- and RNA- binding protein, involved in several nuclear processes; multi-functional regulator of transcription/RNA metabolism. The NONO protein blocks oxidative stress and 'mutant-α-synuclein'-induced cell death (Xu et al., 2005). It may regulate the expression of a neuroprotective genetic program in DA neurons with other coactivators (Dong et al., 2009; Yang et al., 1993).

8	**OTUD5/ 55593**	**OTU (Ovarian Tumour) domain-containing protein 5; deubiquitin- ating enzyme A**	Most normal tissues display cytoplasmic positivity. It is highly expressed in white blood cells and the amygdala (Bruzzone et al., 2008; Gousseva and Baker, 2003; Lee et al., 2006; Xu et al., 2011).	OTUD5 is a cysteine protease; it has deubiquitinating activity directed towards 'Lys-63'-linked poly-ubiquitin chains. α-synuclein stimulates the assembly of Ub-Lys-63 chains: although this is not directly involved in proteasomal degradation, it can interfere with Ub-Lys-48 chain interaction with the proteasome. Excessive stimulation of Ub-Lys-63 chain assembly by A30P, E46K & A53T could indirectly interfere with proteasome function, resulting in stabilization and aggregation of proteolytic substrates (Gonzalez-Navajas et al., 2010; Huang et al., 2012; Kayagaki et al., 2007; Todi et al., 2009; Zhang et al., 2011).
9	**PABPC1/ 26986**	**Poly(A) binding protein, cyto-plasmic 1**	PABPC1 is localized in cytoplasmic mRNP granules and shows high staining in neuronal cells of the cerebral cortex, tonsils, islets of Langerhans, appendix & naso-pharynx, among other tissues (Damrath et al., 2012; Hofmann et al., 2006; Kimura et al., 2009).	It shuttles between the granules and the nucleus. It binds the poly(A) tail of mRNA, which promotes ribosome recruitment and translation initiation. It is also required for poly(A) shortening-the first step in mRNA decay (Behm-Ansmant et al., 2007; Hosoda et al., 2006; Zekri et al., 2009).
10	**PFDN5/ 5204**	**Prefoldin 5, subunit alpha**	While it is strongly-to-moderately expressed in the cytoplasm of all normal tissues, it is particularly strongly expressed in the gastrointestinal tract and pancreatic ducts as well as in neuronal cells of the lateral ventricle (Myung et al., 2004).	One of 6 subunits of prefoldin, a molecular chaperone complex, prefoldin binds to non-native/unfolded but not native/aggregated states of the target protein. *In vivo* it directs newly synthesized/ degraded proteins to cytosolic chaperonin, preventing them from aggregation, degradation, etc. (Danno et al., 2008; Lee et al., 2011; Simons et al., 2004).
11	**PNMA1/ 9240**	**Paraneo-plastic antigen, Ma1**	Ma1 mRNA is expressed in the brain and testis (Dalmau et al., 1999; Schuller et al., 2005; Voltz et al., 1999).	Unknown function (although it is homologous to Ma2- a human neuronal protein) with a suggested role in phospho-dependent RNA processing. Some patients with paraneoplastic neurological disorders develop Ma1 antibodies (Chen and D'Mello, 2010; Hoffmann et al., 2008; Pellkofer et al., 2004; Rosenfeld et al., 2001; Schuller et al., 2005).
12	**RPL7/ 6129**	**Ribosomal protein L7** (eliminated	It is located in the cytoplasm and particularly strongly expressed in cells of the	A component of the 60S subunit, it plays a regulatory role in the translation apparatus. It is an

		from further evaluations, as no R^2 value could be generated using a variable slope function)	hematopoietic and lymphatic system, fetal brain and spinal cord, among other tissues (Biggiogera et al., 1993; Kim et al., 2009; von Mikecz et al., 1994).	autoantigen in patients with systemic autoimmune diseases, e.g. systemic lupus erythematosis (SLE). It displays an ER-binding property and is involved in ribosome-ER association. RPL7 plays a role in sexual differentiation of the zebrafinch song system (avian brain) (Duncan et al., 2009; Linke et al., 2001; Seshadri et al., 1993; Wu et al., 2008).
13	**RPS4X/ 6191**	**Ribosomal protein S4, X-linked**	While most normal cells show moderate to strong cytoplasmic expression, RPS4X levels are high in neuronal cells of the cerebral cortex, Purkinje cells of the cerebellum and various cells of the gastro-intestinal tract, among other tissues (Just et al., 1992; Omoe and Endo, 1994).	A component of the 40S subunit of cytoplasmic ribosomes that catalyze protein synthesis, belonging to the S4E family of ribosomal proteins, it is the only ribosomal protein encoded by >1 gene (RPS4X & RPS4Y). The 2 isoforms are not identical, but are functionally equivalent. This gene is not subject to X-inactivation. Haploinsufficiency may play a role in Turner syndrome (Fisher et al., 1990; Watanabe et al., 1993; Zinn et al., 1994).

3.1.7 Selection of Ezrin for further validation studies

While all the modifiers presented above showed a concentration-dependent inhibition of α-synuclein fibrillization, the extent of the effect, the kinetics of the reaction and the type of inhibition varied significantly across the different modifiers, with some appearing to be more potent than others. For instance, Ezrin was found to be the most potent modulator of α-synuclein fibrillization, because at concentrations as low as 1:5 (Ezrin:α-synuclein) fibrillization appeared to be completely inhibited. Thioflavin-T fluorescence was nearly completely absent, even at the late stages of the reaction, suggesting that Ezrin may be sufficient to completely block the formation of fibrils with a typical cross-ß-pleated sheet structure (which would readily be recognized by the Thioflavin-T dye). Although Heterogeneous nuclear ribonucleoprotein D-like, Poly(A) binding protein cytoplasmic 1, Prefoldin 5 subunit alpha, Paraneoplastic antigen Ma1, Ribosomal protein S4 X-linked and others showed robust inhibitory effects (refer to Fig. 3.1.6), at later time-points (usually by 48 hrs) the reactions proceeded to attain the full magnitude of fluorescence of the control (or showed a clear and definite increase in fluorescence in this direction). This was one of the major reasons for the selection of Ezrin as the modifier of choice for further experiments. A second major argument for Ezrin was the presence of various studies from the scientific literature which suggest a role for Ezrin not only in the nervous system but also in PD:

A role for Ezrin in the nervous system: Ezrin expression is detected in human cerebrum at 20 weeks of gestation (Johnson et al., 2002). Ezrin is abundantly expressed in the periventricular germinal matrix, extending out toward the intermediate zone in processes similar to radial glia. Columnar bundles of cells apparently migrating along these processes may represent neuronal precursors. Ezrin expression in the cerebrum at 30 weeks of gestation prominently labels the cell bodies and processes of cells within the intermediate zone in prenatal cerebral cortex (Johnson et al., 2002). Secondly, a model has been proposed for the role of the telencephalon (TLCN)–Ezrin interaction in dendritic filopodia, where Ezrin and Ezrin-like proteins are phosphorylated to the active forms that can bind TLCN in the plasma membrane. In dendritic shafts and spines, inactive Ezrin and Ezrin-like proteins are present in the cytoplasm (Furutani et al., 2007). The interaction between TLCN and phospho-Ezrin mediates the formation, elongation, and maintenance of dendritic filopodia and slows spine maturation (Furutani et al., 2007). Additionally, Rho kinase activates Ezrin and Ezrin-like proteins and mediates their function in cortical neuron growth, morphology and motility *in vitro* (Haas et al., 2007). Lastly, the cytoplasmic domain of the neural cell adhesion molecule L1 (L1CD), which mediates neurite outgrowth, plays a critical role in neurite branching through two regions that serve as ezrin-moesin-radixin-binding sites (Cheng et al., 2005). Thus, Ezrin also plays a role in L1-mediated neuritic branching.

Lastly, glutamate-receptor-mediated phosphorylation of Ezrin and Ezrin-like proteins has been implicated in filopodial protrusion of primary cultured hippocampal neuronal cells (Kim et al., 2010). The neurotransmitter glutamate induces phosphorylation of Ezrin-family proteins in cultured hippocampal cells and phosphorylated Ezrin localizes at the newly formed filopodia of neurites. This glutamate-induced phosphorylation is calcium-dependent and inhibition of protein kinase C abolishes phosphorylation as well as RhoA activation. The inhibition of RhoA and RhoA kinase also diminishes glutamate-induced phosphorylation in cultured hippocampal cells. The knock-down of the Ezrin-like protein, Moesin, or the inhibition of phosphorylation results in the reduction of glutamate-induced filopodia protrusion and diminishes the increase in active synaptic boutons induced by glutamate treatment. These results indicate that glutamate-induced phosphorylation of Ezrin-like proteins in primary cultured differentiated hippocampal neurons is mediated by calcium-dependent protein kinase C, RhoA and RhoA kinase, and that the phosphorylated Ezrin-family protein, Moesin, is necessary for the formation of filopodial protrusions and may be involved in pre-synaptic trafficking.

Thus, there is a significant amount of evidence from the scientific literature which points towards a prominent role for Ezrin within the nervous system.

A potential role for Ezrin in PD and other diseases: Variants of the leucine-rich repeat kinase 2 (LRRK2) gene are associated with an increased risk of PD (Paisan-Ruiz et al., 2004). Expression of LRRK2 mutants implicated in autosomal dominant PD causes shortening and simplification of the dendritic tree *in vivo* and in cultured neurons (MacLeod et al., 2006). The Gly2019Ser mutation in LRRK2 is a relatively common cause of familial PD in Caucasians (Gilks et al., 2005) and may also cause sporadic PD. This mutation elicits a post-synaptic calcium imbalance, leading to excess mitochondrial clearance from dendrites by mitophagy (Cherra et al., 2013). LRRK2 functions as a putative protein kinase of ezrin family proteins and the G2019S substitution in the kinase domain of LRRK2 further enhances their phosphorylation (Parisiadou et al., 2009). The phosphorylated proteins are restricted to the filopodia of growing neurites in which they tether filamentous actin (F-actin) to the cytoplasmic membrane and regulate the dynamics of filopodia protrusion. In cultured neurons derived from LRRK2 G2019S transgenic mice, the number of phosphorylated-ezrin-family proteins and F-actin-enriched filopodia is significantly increased and this correlates with the retardation of neurite outgrowth. Conversely, deletion of LRRK2, which lowers phosphorylated-ezrin-family proteins and F-actin contents in filopodia, promotes neurite outgrowth. Furthermore, inhibition of phosphorylation or actin polymerization rescues the G2019S-dependent neuronal growth defects. These data support a model in which the G2019S mutation of LRRK2 causes a gain-of-function effect that perturbs the homeostasis of phosphorylated-ezrin-family proteins and F-actin in sprouting neurites critical for neuronal morphogenesis. Thus, the phosphorylation of Ezrin and Ezrin-like proteins by LRRK2 promotes the rearrangement of the actin cytoskeleton in neuronal morphogenesis (Parisiadou et al., 2009).

Due to its strong inhibition of α-synuclein fibrillization at sub-stoichiometric concentrations, its presence in the nervous system and its potential involvement in PD, Ezrin was considered to be the most promising modifier for detailed analyses, as described in the following sections.

3.1.8 Chapter Summary

In brief, 13,824 candidate proteins were expressed in *E. coli* and purified using the 6X-His-tag system, while α-synuclein was expressed and purified using anion-exchange and gel-filtration columns prior to lyophilization. An *in vitro* fluorescence-based fibrillization assay was validated and employed in a high-throughput screen to identify novel modulators of α-

synuclein fibrillization. Candidate proteins were randomly pooled into groups of eight, incubated with α-synuclein and subjected to a second round of screening, prior to deconvolution of the pools. The individual proteins identified in this way were subjected to additional rounds of screening and successive concentration-response studies, resulting in the identification of 13 proteins that reproducibly and potently modulate α-synuclein fibrillization. Finally, Ezrin, the most potent inhibitor of α-synuclein fibrillization, was selected for further, more detailed investigations, as described in the following sections.

3.2 Confirmation of Ezrin as the modifier of choice and characterization of Ezrin-mediated inhibition of α-synuclein fibrillization

As detailed in Section 3.1, an extensive high-throughput screen for modifiers of α-synuclein fibrillization *in vitro* revealed Ezrin as being the most potent candidate. Furthermore, Ezrin has been shown to play a role in the nervous system as well as in Parkinson's disease, highlighting, once again, that Ezrin is the optimal choice for further investigations. In this chapter, additional experiments are presented to conclusively underline that Ezrin is not just the ideal screening candidate, but also a potent inhibitor of α-synuclein fibrillization in its own right. This has been shown by a variety of biophysical, biochemical and microscopy-based experiments, starting with *in vitro* aggregation assays and SDS-PAGE experiments conducted on α-synuclein incubated with additional members of the protein family to which Ezrin belongs. Following a brief description of Ezrin, the chapter continues with time-resolved SDS-PAGE, filter-retardation assays and atomic force microscopy experiments on α-synuclein incubated with Ezrin, all of which underscore the potency of Ezrin as an inhibitor of α-synuclein fibrillization.

3.2.1 Highly homologous family-members of Ezrin inhibit α-synuclein fibrillization as well

Ezrin is an evolutionarily highly conserved protein and putative homologues have been found in species as distantly related as *Arabidopsis thaliana*. In vertebrates, Ezrin is a member of a three-protein sub-family called ERM, including Ezrin, Radixin and Moesin (Membrane-Organizing Extension Spike proteIN), which share an extremely high homology to each other, as shown in Fig. 3.2.1.1 below (Polesello and Payre, 2004). Even *C.elegans* and *D. melanogaster* have one ERM protein each (CeERM-1 and Dmmoesin, respectively), with similar function and homology to the higher metazoan members (Polesello and Payre, 2004; Speck et al., 2003). Mouse Ezrin cDNA was cloned and sequenced in 1991 and shares 96.2% identity with human Ezrin cDNA (Funayama et al., 1991).

3.2.1.1 The Ezrin family

Collectively, the three vertebrate ERM proteins belong to the Band 4.1 superfamily along with their more distant cousins, Merlin (Moesin Ezrin Radixin Like proteIN) and Band 4.1 (erythrocyte band protein 4.1, the first of all these proteins to be identified). They all have a conserved domain in their N-terminal region: the FERM domain (Band Four-point-one, Ezrin, Radixin Moesin domain). Fig 3.2.1.1 below represents the homology of the Band 4.1 protein superfamily in greater detail.

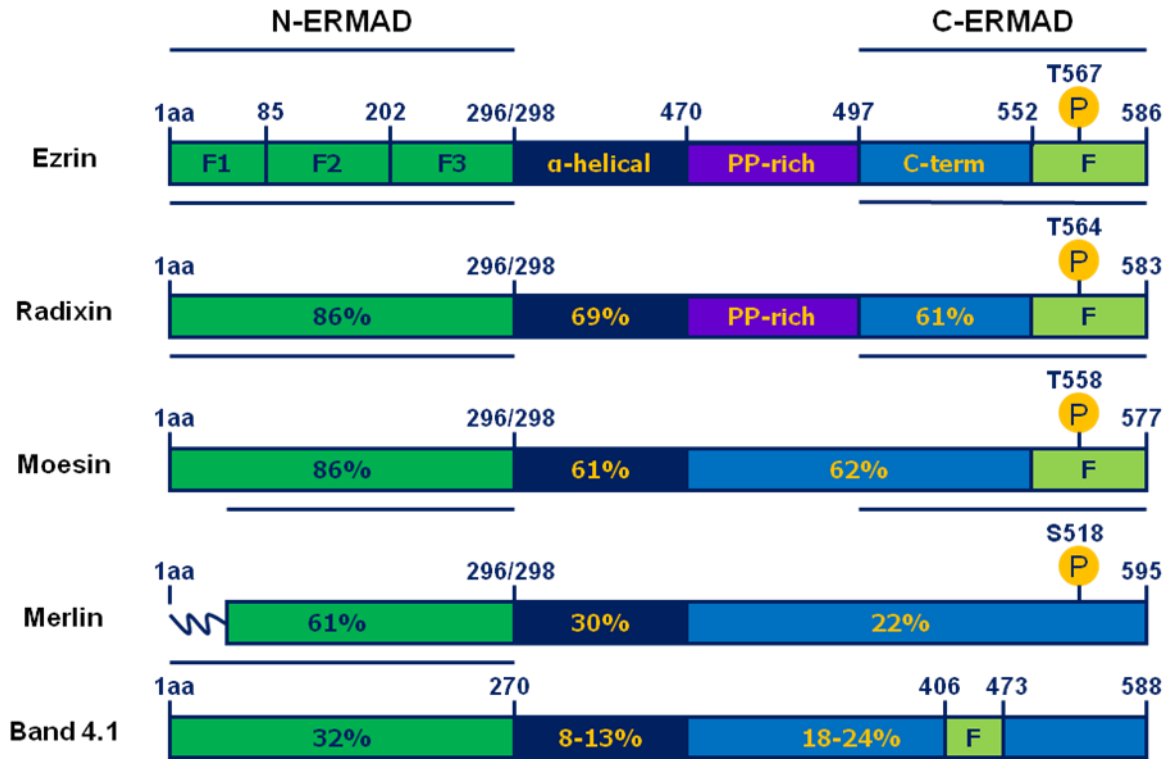

Fig 3.2.1.1 A diagrammatic representation of the homology between the various members of the Band 4.1 superfamily. Ezrin is most highly homologous to Radixin, followed by Moesin, while Merlin and, subsequently, Band 4.1 (the founding member) are relatively distant. As described in Fig. 3.2.2.2., F1, F2, F3 represent the three sub-domains of the N-terminal FERM region, followed by an α-helical stretch and a polyproline-rich region (PP-rich). The C-terminal domains of all the proteins (except Merlin) contain an F-actin binding site (F) at the very end, in which a residue is phosphorylated (P) as part of the activation process of the protein (in all cases except for Band 4.1 – the most distant family member – which is not phosphorylated at its C-terminal at all). In the case of Ezrin, this residue is T567, for Radixin it is T564, for Moesin it is T558, and for Merlin it is S518. Upon phosphorylation, the N-terminal Ezrin-Radixin-Moesin Association Domain (N-ERMAD) and the C-terminal Ezrin-Radixin-Moesin Association Domain (C-ERMAD) cease to associate with each other, resulting in complete activation of the protein into its fully opened conformation.

In mammals, Ezrin, Radixin and Moesin - the three ERMs - are encoded by three different genes. In humans, these genes are located on chromosomes 6, 11 and X, respectively (Fehon et al., 2010). The proteins show some tissue specificity: Ezrin is most abundantly expressed by epithelial cells, Moesin by endothelial cells and Radixin by hepatocytes (Fehon et al., 2010). ERMs share striking amino acid identity, but a few notable features suggest that there is possible functional diversity; for example, Ezrin can be phosphorylated on Tyr residues that are not present in Moesin or Radixin, and Moesin lacks Pro-rich sequences that are found in Ezrin and Radixin (Fehon et al., 2010). Ezrin-deficient mice die by 3 weeks of age with defects that are limited to the gastrointestinal tract, whereas inactivation of Radixin in mice yields viable animals that show subtle liver defects and Moesin-deficient

mice do not exhibit overt phenotypes at all (Fehon et al., 2010). The paucity of phenotypes in these mice suggests that other ERMs can compensate for the loss of individual ERMs in many tissues. This conservation of the protein's structure and function across multiple species led to the question: Could non-Ezrin ERM proteins also have an effect on α-synuclein fibrillization?

3.2.1.2 Highly homologous family members of Ezrin inhibit α-synuclein fibrillization, while more distant relatives do not

In order to answer the question posed in Section 3.2.1.1 above, α-synuclein was incubated with Ezrin, Radixin, Moesin or Band 4.1 protein, as described previously in Section 3.1.2: 50 µM of α-synuclein were incubated with 5 µM protein in NaP buffer, at 37 ˚C, shaking at 200 rpm in the presence of a glass bead and the fluorescent dye, Thioflavin-T. Fluorescence-measurements were made every 2 hours and revealed that Ezrin, Radixin and Moesin (all of which share an extremely high homology) are similarly potent inhibitors of α-synuclein fibrillization, while the most distant member of the family, i.e. the Band 4.1 protein, had hardly any effect on α-synuclein fibrillization. As Merlin was not present in the protein libraries available in this laboratory, it could not be used for analysis in this experiment.

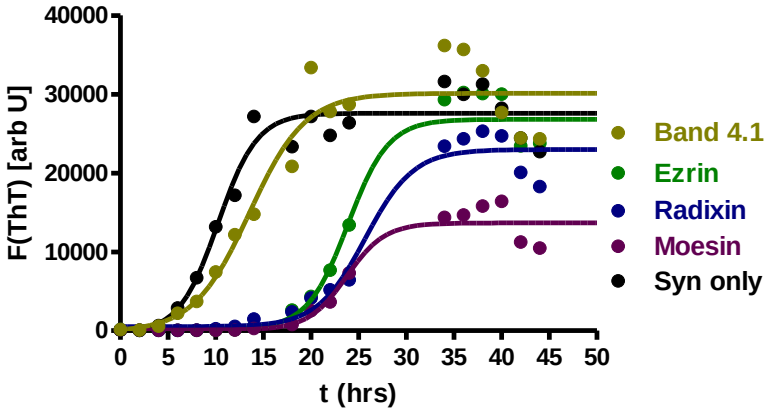

Fig 3.2.1.2 Thioflavin-T assay of α-synuclein incubated either alone (Syn only) or in the presence of Ezrin, Radixin, Moesin or Band 4.1. The highly homologous proteins Radixin and Moesin reduce the thioflavin-T signal, indicative of inhibition of ß-sheet-structured fibril formation, while Band protein 4.1 has little effect on the aggregation of α-synuclein. [The concentration of each protein relative to α-synuclein was 1:10].

3.2.1.3 A highly homologous family member, Radixin, also reduces the formation of higher-molecular-weight SDS-resistant species of α-synuclein

In a final set of experiments to determine whether highly homologous ERM proteins do, indeed, affect α-synuclein fibrillization, α-synuclein was incubated in the presence and absence of Radixin (the family member with the highest homology to Ezrin). Samples were removed at different time-points spanning the entire length of the incubation assay (i.e. 0, 4,

10, 18, 24 and 65 hrs). These samples were analyzed by SDS-PAGE followed by immunoblotting. As seen from Fig. 3.2.1.3 below, Radixin inhibits formation of the higher molecular weight, SDS-resistant α-synuclein species which form over time in fibrillization reactions of α-synuclein alone. Such inhibition of the formation of higher-molecular-weight-species of α-synuclein is also seen in the case of Ezrin incubated with α-synuclein (as described in Section 3.2.4).

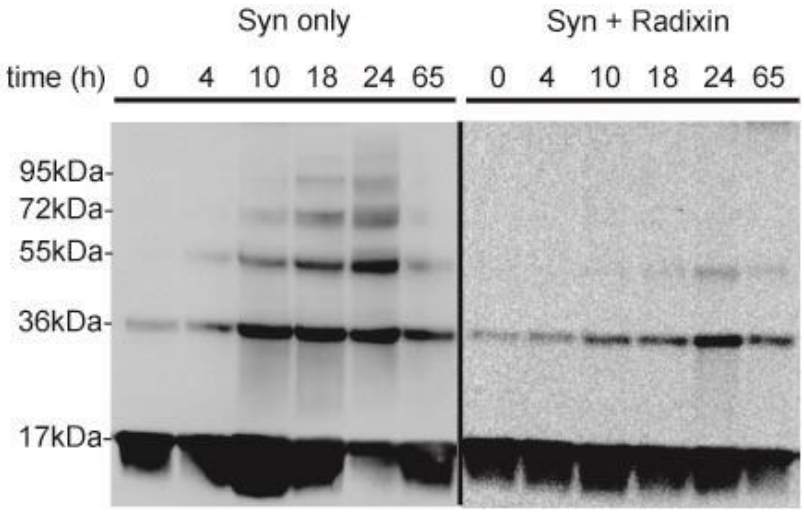

Fig 3.2.1.3 SDS-PAGE and immunoblotting of samples of α-synuclein incubated alone (Syn only) and in the presence of Radixin (Syn + Radixin) for varying periods of time. The membrane was developed with an anti-α-synuclein mouse monoclonal antibody (sc-12767; Santa Cruz Biotechnology). The sample containing α-synuclein alone shows a build-up of SDS-resistant dimeric, trimeric, tetrameric and higher-molecular weight species. The sample of α-synuclein incubated with Radixin, however, shows a significant reduction in (or complete absence of) trimeric, tetrameric and higher-molecular weight species of α-synuclein.

Proteins sharing high homology with Ezrin also inhibited α-synuclein strongly, thereby providing confirmation that Ezrin was not just the best candidate to emerge from the screen, but also a potent inhibitor in its own right. Hence, Ezrin was selected for downstream characterization experiments and also subjected to structural analyses and cell-based experiments (as described in Sections 3.3 and 1.1, respectively). In order to appreciate the effect of Ezrin on α-synuclein, however, it is important to first have a detailed understanding of Ezrin itself. This is laid out in Section 3.2.2 below, in terms of structure, function and sub-cellular localization of Ezrin.

3.2.2 Background on Ezrin

In 1981, a polypeptide of 81 kDa was shown to be rapidly phosphorylated on tyrosine residues in A-431 carcinoma cells in response to the addition of epidermal growth factor (EGF) (Hunter and Cooper, 1981). During the characterization of the components of

microvilli, a minor component of 80 kDa was purified (Bretscher, 1983). This polypeptide was named Ezrin in recognition of Ezra Cornell University where it was purified (Louvet-Vallee, 2000). Independently, using an antibody directed against a synthetic peptide deduced from a cloned human endogenous retroviral gag-related DNA sequence, erv-1, a polypeptide of 75 kDa was identified in cell surface structures (Pakkanen et al., 1987). This protein, called cytovillin, was shown to be identical to Ezrin (Gould et al., 1989; Turunen et al., 1989). Ezrin was also identified in studies concerned with the regulation of acid secretion in parietal cells of gastric glands (Hanzel et al., 1991; Hanzel et al., 1989). Cloning and sequencing of the human Ezrin cDNA were reported in 1989 (Gould et al., 1989).

3.2.2.1 Introduction to Ezrin

Ezrin is a cytoplasmic peripheral membrane protein, which functions as a protein-tyrosine kinase substrate in microvilli and serves as a linker between the plasma membrane and the actin cytoskeleton. The gene encoding Ezrin is located on chromosome 6 at locus 6q25.3. The protein, Ezrin, plays a key role in cell surface structure organization, adhesion, migration and cell-signalling, by binding specifically to F-actin when in the activated form. Ezrin is a protein of 586 amino acids with an isoelectric point of 6.15 and a molecular mass of 69 kDa. It is a highly charged protein (38.5% of the residues are charged) (Louvet-Vallee, 2000).

3.2.2.2 Structure of Ezrin

Ezrin is characterized by the presence of an ~300 AA plasma membrane-associated domain in the N-terminus (called N-ERMAD or N-terminal ERM-association Domain), followed by a long region with a high α-helical propensity and terminating in a C-terminal domain (called C-ERMAD or C-terminal ERM-association Domain) which has the ability to bind the N-terminal ERMAD (in the closed conformation) or filamentous actin [F-actin] (in the open conformation), as shown in Fig 3.2.2.2 (Fehon et al., 2010). Thus, ERMAD refers to the two Association Domains present in Ezrin, Radixin and Moesin proteins, allowing the association of the N- and C- terminal domains either within a protein itself (leading to a closed conformation) or across multiple protein molecules, such that the C- and N- terminal domains of two distinct molecules are consecutively linked to form dimers or chain-like structures. Since not just Ezrin, Radixin and Moesin, but also the more distant members of the Band 4.1 protein superfamily show the presence of such a domain at the N-terminus, the N-ERMAD domain is also referred to as FERM (refer to Section 3.2.1.1). The N-terminal FERM domain can be divided into three subdomains (F1, F2 and F3) that have structural (but not sequence) homology to known protein folds. Specifically, F1 is structurally similar to ubiquitin, F2 to acyl CoA-binding protein and F3 to a pTB domain (Bretscher et al., 2002).

The C-terminal domain contains an F-actin-binding site in the last 34 residues of Ezrin (Bretscher et al., 2002).

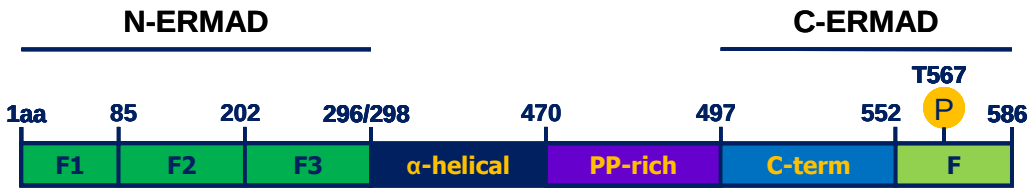

Fig 3.2.2.2. A schematic representation of the full-length Ezrin protein. F1, F2, F3 represent the three sub-domains of the N-terminal region, followed by an α-helical stretch and a polyproline-rich region (PP-rich). The C-terminal domain contains an F-actin binding site (F) at its very end, in which the residue T567 is phosphorylated (P) as part of the activation process of the protein. Upon phosphorylation, the N-terminal Ezrin-Radixin-Moesin Association Domain (N-ERMAD) and the C-terminal Ezrin-Radixin-Moesin Association Domain (C-ERMAD) dissociate from each other, resulting in complete activation of the protein into its fully-opened conformation.

Regulation of Ezrin function: Ezrin function is conformationally regulated by head to tail folding, i.e. binding of the C-ERMAD to the N-ERMAD, in such a way that the ~80 C-terminal residues of Ezrin - when bound tightly to the ~300 N-terminal residues - mask the F-actin-binding site (Fehon et al., 2010). It is now known that Ezrin exists in an apparently dormant, closed conformation and that release of the C-ERMAD from the N-ERMAD is necessary for full activation (Fehon et al., 2010). This then exposes binding sites within the N-ERMAD as well as the F-actin-binding site of the C-ERMAD and the molecule changes to an open conformation, allowing it to connect the plasma membrane with the underlying actin cytoskeleton. The first experiments indicating this mechanism (Algrain et al., 1993) showed that the N-terminal domain of Ezrin associates with the plasma membrane whereas the C-terminal domain associates with the cytoskeleton.

3.2.2.3 Functions of Ezrin

Ezrin mediates multiple interactions at the cell cortex and is involved in a wide variety of functions, as shown in Fig 3.2.2.3 below. For instance, Ezrin contributes to the functional organization of actin and plasma membrane proteins during the formation of microvilli in a polarized epithelial cell (Bretscher et al., 2002). Ezrin is believed to be necessary for exclusion of the glycoprotein CD43 from the immunological synapse (Takai et al., 2008). In the epithelial-cell and kidney-podocyte systems, the PDZ-containing proteins EBP50 and E3KARP are associated with Ezrin and may contribute to membrane linkage (Ingraffea et al., 2002).

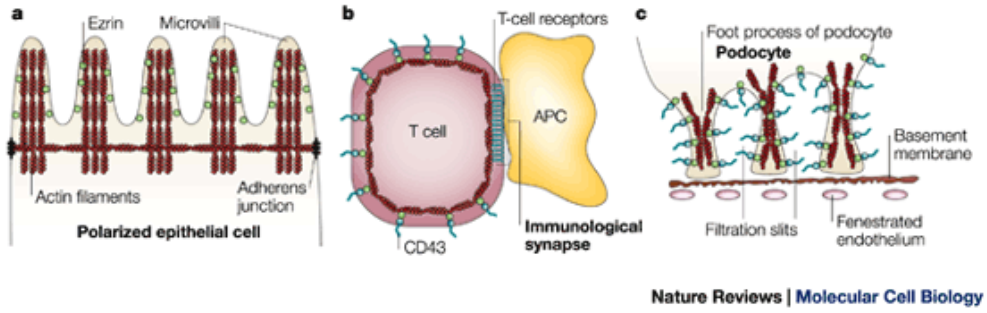

Fig 3.2.2.3. Diagram from Bretscher et al. 2002. Ezrin contributes to the functional organization of specific plasma-membrane domains. (A) The apical aspect of a polarized epithelial cell in which Ezrin links actin filaments laterally to the plasma membrane, specifically in microvilli. (B) A T-cell forming an immunological synapse with an antigen-presenting cell (APC). (C) The filtration barrier in the kidney glomerulus, in which the filtration slits between podocyte foot processes are believed to be maintained by restriction of podocalyxin to the apical membrane by Ezrin.

Formation of cell-surface structures and their role in membrane dynamics: Various studies have demonstrated multiple roles for Ezrin in membrane structure formation (Bretscher, 1989; Chen et al., 1994; Hanzel et al., 1991). As shown in Fig 3.2.2.3.A above, Ezrin links actin filaments laterally to the plasma membrane in microvilli, by using its C-terminal domain to bind specifically to F-actin and its N-terminal domain to bind to plasma membrane-associated proteins (e.g. phosphatidylinositol 4,5-bisphosphate, PIP2). Ezrin also connects cells together at gap-junctions, e.g. T cells and antigen-presenting cells (APCs), as shown in Fig 3.2.2.3.B. Furthermore, by restricting podocalyxin to the apical membrane, Ezrin helps to maintain the filtration slits between podocyte foot processes at the filtration barrier in the kidney glomerulus. Lastly, transfection experiments of different domains of Ezrin have identified the sites involved in membrane extension formations, namely residues 13–30, 280–310 and 566–585 (Martin et al., 1997).

Maintenance of cell shape and cell motility: Ezrin is a regulator of cell shape (Edwards et al., 1994). The role of Ezrin in cell shape maintenance and motility was characterized during Fos-mediated transformation of rat fibroblasts by micro-CALI (chromophore-assisted laser inactivation) (Lamb et al., 1997). In Fos-transformed rat cells, Ezrin was concentrated at the leading edge of extension and was mainly cytosolic. Functional ablation of Ezrin by micro-CALI blocked plasma membrane ruffling and motility of Fos-transformed fibroblasts. Ablation of Ezrin in normal rat cells caused a marked collapse of the leading edge of the cell. Thus, Ezrin is important in pseudopodial extension and maintains cell shape (Lamb et al., 1997).

Cell-substrate and cell-cell adhesion: The suppression of Ezrin expression by antisense oligonucleotides in thymoma cells as well as in mouse epithelial cells leads to the destruction of both cell-cell and cell-substrate adhesion (Takeuchi et al., 1994). The same result was obtained with two colorectal cancer cell lines in which Ezrin expression was inhibited by antisense oligonucleotides (Hiscox and Jiang, 1999). Overexpression of Ezrin in insect cells enhances cell adhesion (Martin et al., 1995). This modification of cell adhesion was also observed in other cell lines: immortalized fibroblasts overexpressing Ezrin lost their contact inhibition (Kaul et al., 1996).

Membrane trafficking: Ezrin and the actin cytoskeleton have a specialized function in the endocytic sorting of a subset of membrane proteins (Cao et al., 1999). Ezrin appears to be part of a minimal machinery that needs to be recruited by phagosomes from the cytoplasm for actin assembly (Defacque et al., 2000a; Defacque et al., 2000b).

Involvement in signaling pathways:

1) *Rho pathway*: Several studies have demonstrated that ERM activation is linked to the Rho signaling pathway. Rho, a small GTP-binding protein, is essential for the localization of Ezrin at the plasma membrane (Kotani et al., 1997). The RhoA-dependent phosphorylation of Ezrin occurs before its translocation to the membrane (Shaw et al., 1998). Ezrin is a downstream effector of Rho in the reorganization of the actin cytoskeleton (Mackay et al., 1997; Matsui et al., 1999). Rho regulates the interactions between the cell-surface glycoprotein - CD44 - and Ezrin (Hirao et al., 1996). This is of importance as CD44 and Ezrin have properties suggesting that they may play a role in the process of tumour–endothelium interactions, cell migration, cell adhesion, tumour progression and metastasis (Martin et al., 2003). RhoGDI (Rho GDP dissociation inhibitor) binds to the N-terminal domain of Ezrin (Takahashi et al., 1997). *In vivo* the RhoA-dependent phosphorylation of Ezrin and microvilli formation requires the kinase activity of PI4P5K (Matsui et al., 1999). It has also been shown that the interaction of the TSC1 tumor suppressor hamartin, a physiological binding partner of Ezrin, is required for activation of Rho by lysophosphatidic acid (LPA) (Lamb et al., 2000).

The model proposed to explain all these interactions is as follows: Upon extracellular activation of Rho, Rho in turn activates its targets, e.g. phosphatidylinositol-4-phosphate 5-kinase (PI4P5K), which induce an increase in phosphatidylinositol 4,5-bisphosphate (PIP2) levels. PIP2 binds to the N-terminal domain of Ezrin (and Ezrin-like protein, Radixin), thus inhibiting the interaction between the domains C-ERMAD and N-ERMAD. This causes the formation of an open configuration that allows the phosphorylation of a threonine in the C-

terminal domain. C-terminally phosphorylated Ezrin (or Radixin) is stabilized as the activated form and functions as a cross-linker between actin filaments and the plasma membrane to form microvilli. Once activated, Ezrin/Radixin can activate Rho: the N-terminal domain interacts with Dbl, a stimulatory GDP/GTP exchange protein of the Rho family (Takahashi et al., 1998). Rho GDI displaces Dbl from Ezrin/Radixin since it can also interact with the N-terminal domain. This interaction leads to the activation of Rho by releasing the Rho-GDI inhibition. Thus, Ezrin and its highly homologous proteins such as Radixin play an important role in the activation of Rho family members by recruiting their positive and negative regulators (Ivetic and Ridley, 2004).

2) *PI3-kinase/Akt pathway*: Phosphatidylinositol 3-kinase (PI3-kinase) is a critical component in survival signaling. In some culture conditions, LLC-PK1 cells form tubules and the overproduction of Ezrin can potentiate this process (Crepaldi et al., 1997). The replacement of Tyr-353 of Ezrin by phenylalanine induces cell apoptosis. It has been shown that Ezrin interacts with p85, the regulatory subunit of PI3-kinase (Gautreau et al., 1999). Two sites are involved in this interaction: the N-terminal domain containing the first 309 amino acids and the phosphorylated Tyr-353 residue, which binds to the C-terminal SH2 domain of p85. The activation of the PI3-kinase/Akt pathway, necessary for cell survival, requires phosphorylation of Ezrin at Tyr-353 (Gautreau et al., 1999). Thus, Ezrin determines the survival of epithelial cells by activating the PI3-kinase/Akt pathway.

3.2.2.4 Subcellular localization of Ezrin

Ezrin is highly concentrated in intestine, stomach, lung and kidney (Funayama et al., 1991; Tsukita and Hieda, 1989). It is present in the apical domain of polarized cells, a region usually characterized by the presence of microvilli, e.g. the brush border of the kidney proximal tubule epithelium (Berryman et al., 1993; Schwartz-Albiez et al., 1995). It has also been shown that the epithelial cells lining the bile ducts express Ezrin (Amieva et al., 1994). Although Ezrin is prominent in epithelial tissues and mesothelial cells, other cell types within the body can also express the protein, e.g. glia of the rostral migratory stream (Berryman et al., 1993; Schwartz-Albiez et al., 1995). Cultured cell lines usually express Ezrin (Amieva and Furthmayr, 1995; Sato et al., 1992). Immunofluorescence studies with specific antibodies have shown that Ezrin is particularly concentrated in actin-rich surface structures such as microvilli, membrane ruffles and filopodia (Amieva and Furthmayr, 1995; Franck et al., 1993). Immuno-electron microscopy of Ezrin in human placental syncytiotrophoblast and mouse mesothelia has shown that Ezrin is highly concentrated in the microvilli where it is associated with the cytoplasmic aspect of the plasma membrane (Berryman et al., 1993).

The relatively low level of Ezrin on adjacent regions of the apical membrane between microvilli supports the notion that Ezrin plays a special role in the attachment of microfilaments to the membrane, specifically within microvilli. Ezrin is also concentrated in adherens junctions (Takeuchi et al., 1994).

3.2.3 Production of Ezrin for downstream studies

In order to carry out extensive experiments on Ezrin and its role in inhibiting α-synuclein fibrillization, it was first necessary to produce large amounts of pure full-length Ezrin. The full-length Ezrin used in this study was tagged at its N-terminal end with a six-residue His sequence based on which it was subsequently purified. In brief, the Ezrin cDNA was cloned into a pDESTco vector and transformed into the *rosetta* strain of E. coli. Gene expression was induced by addition of IPTG to the growth medium overnight at 18°C. The following day, cells were harvested, lysed and subjected to purification on a HisTrap column for crude lysate (as described in Sections 2.2.2.9 and 2.2.2.10). The samples were further purified by gel filtration on a FPLC column and eluted into a standard physiological NaP buffer, free of imidazole and other salts. These samples were analyzed by SDS-PAGE and Coomassie staining (as shown in Fig. 3.2.3), before being pooled together and stored at -20°C.

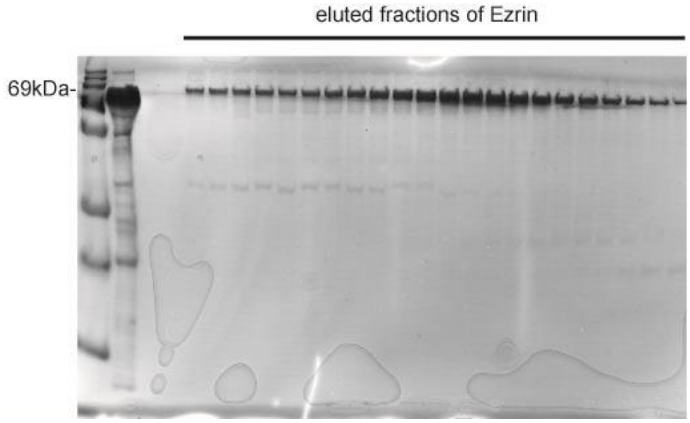

Fig 3.2.3 SDS-PAGE and Coomassie staining of the eluents containing full-length His-labelled Ezrin after gel-filtration, demonstrating the purity of the protein. The first lane represents the eluent from a HisTrap crude lysate column; the eluent was then subjected to gel filtration.

3.2.4 Ezrin reduces the formation of SDS-resistant higher-molecular-weight species of α-synuclein

To answer the question of whether Ezrin prevents the formation of pre-fibrillar species of α-synuclein such as trimers, tetramers, etc., samples of α-synuclein - in the presence and absence of Ezrin - were incubated for different lengths of time spanning the entire duration of the fibrillization assay (i.e. 0-65h). They were subjected to regular Thioflavin-T fluorescence measurements, before finally being removed for SDS-PAGE followed by immunoblotting. As

seen in Fig 3.2.4.A below, Ezrin does, indeed, inhibit the formation of higher molecular weight SDS-resistant species of α-synuclein which are clearly visible in samples of α-synuclein incubated alone. For example, the addition of Ezrin reduced the intensity of the 55 kDa (trimer), 72 kDa (tetramer) and 95 kDa (higher order species) α-synuclein bands at t=18h and t=24h, as shown in Fig 3.2.4.A below. Fig. 3.2.4.B depicts the corresponding Thioflavin-T fluorescence traces for the samples incubated for varying lengths of time. Additionally, Thioflavin-T fluorescence traces were generated for samples of α-synuclein incubated alone, to which Ezrin was added at different time-points, namely, after the onset of the exponential phase and before the onset of the plateau phase (in this experiment, 10h and 18h after the start of the assay, respectively). Fig. 3.2.4.C shows that the addition of Ezrin to the α-synuclein fibrillization assay at later time-points had no effect on α-synuclein fibrillization. Thus, the results suggest that Ezrin interferes with a relatively early step in the process of α-synuclein aggregation, thereby inhibiting the build-up of higher molecular weight species of α-synuclein which are seen when α-synuclein is allowed to aggregate alone.

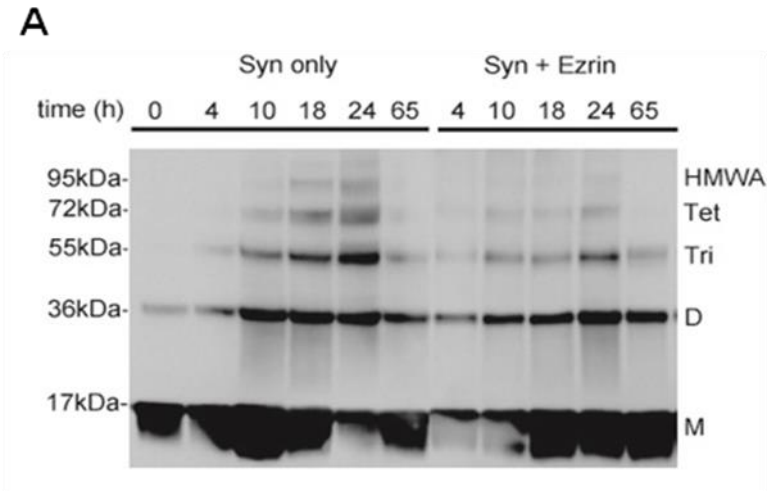

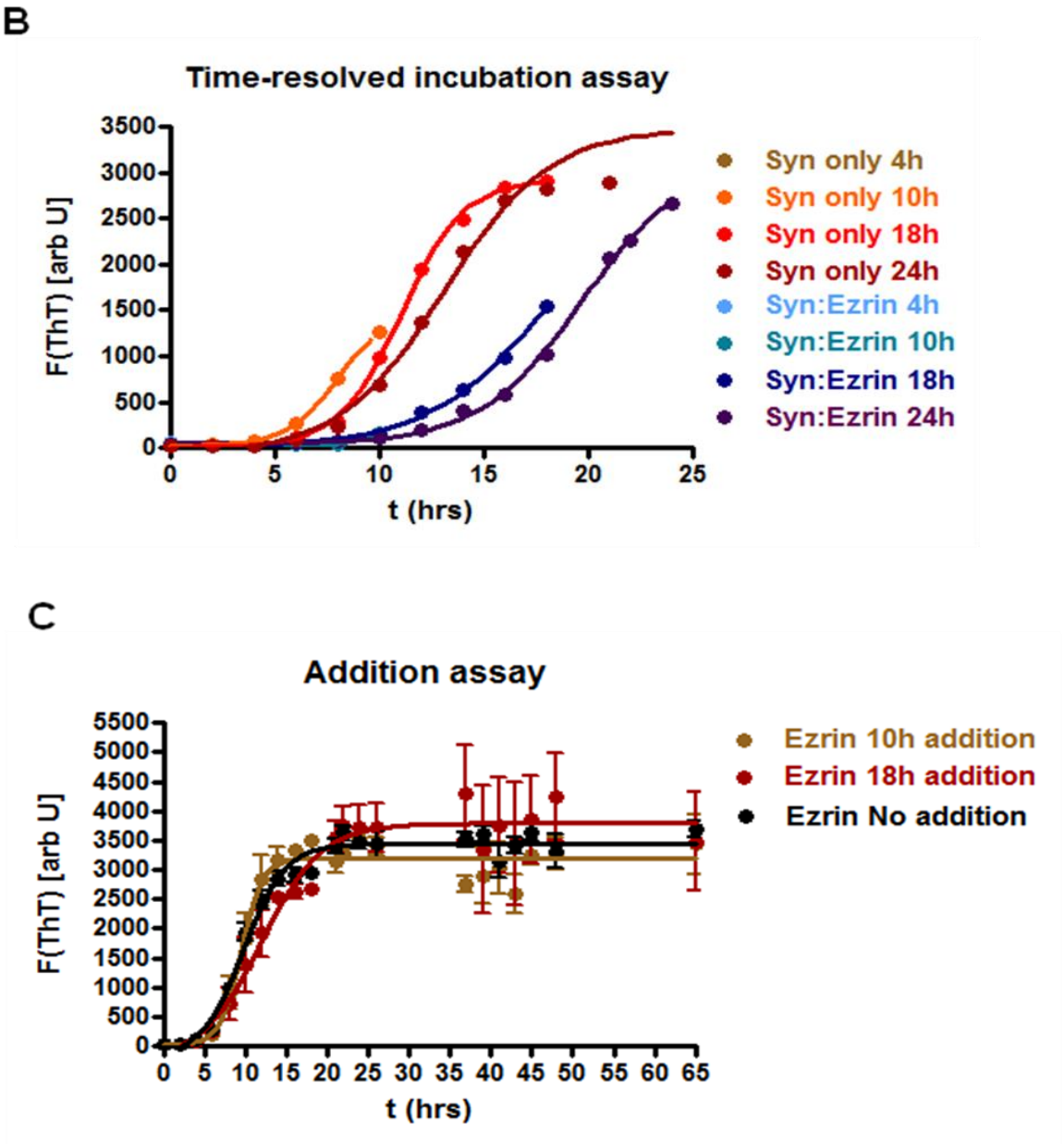

Fig 3.2.4 (A) SDS-PAGE and immunoblotting of samples of α-synuclein incubated alone (Syn only) or in the presence of Ezrin (Syn + Ezrin), for varying periods of time. α-synuclein alone over time showed a build-up of SDS-resistant higher molecular weight forms, which were significantly reduced when α-synuclein was incubated with Ezrin. The membrane was developed with an anti-α-synuclein mouse monoclonal antibody (sc-12767; Santa Cruz Biotechnology). HMWA = higher molecular weight aggregates; Tet = tetramer; Tri = trimer; D = dimer, M = monomer. (B) Thioflavin-T fluorescence data corresponding to the various time-periods shown in (A). (C) Thioflavin-T fluorescence data for samples of α-synuclein to which Ezrin was added at different time-points, i.e. before the start of the exponential phase and before the start of the plateau phase of aggregation. [α-synuclein:Ezrin 5:1]

3.2.5 Ezrin reduces the formation of SDS-resistant α-synuclein aggregates

Upon incubation at 37 ˚C in a shaker for extended periods of time, α-synuclein has been shown to form insoluble, SDS-resistant aggregates which are easily retained on a filter membrane and detected by the binding of relevant antibodies, referred to as a filter-retardation assay (Ehrnhoefer et al., 2008). Hence, samples of α-synuclein incubated for 65 hours with and without Ezrin were tested in a filter-retardation assay, to detect whether highly insoluble SDS-resistant aggregates of α-synuclein were also formed in the presence of Ezrin or whether Ezrin could inhibit the formation of such aggregates. As shown in Fig. 3.2.5 below, while α-synuclein incubated alone formed SDS-resistant aggregates that were retained on a filter membrane, α-synuclein incubated with Ezrin revealed an almost complete absence of aggregates on the membrane. Ezrin incubated alone, as a control, did not show detectable aggregates on the filter membrane. Thus, these studies indicate that Ezrin significantly inhibits the formation of SDS-resistant aggregates of α-synuclein.

Fig 3.2.5 Filter-retardation assay of 50 μM α-synuclein incubated alone (Syn only), α-synuclein incubated with Ezrin (Syn:Ezrin 5:1) and Ezrin incubated alone (Ezrin only) for a period of 65h. The sample containing α-synuclein alone clearly shows SDS-resistant aggregates retained on the membrane, which are absent in the samples of α-synuclein incubated with Ezrin and Ezrin incubated alone. The membrane was developed first with an anti-Ezrin mouse monoclonal antibody (sc-58758: Santa Cruz Biotechnology) and then with an anti-α-synuclein mouse monoclonal antibody (sc-12767; Santa Cruz Biotechnology).

3.2.6 Atomic force microscopy images suggest that Ezrin promotes the formation of atypical, non-fibrillar aggregates of α-synuclein

α-synuclein was incubated in the presence and absence of Ezrin, as previously described [molar ratio of α-synuclein:Ezrin 5:1] for up to 65h. The samples were then examined using atomic force microscopy at two different resolutions, as displayed below (see Fig. 3.2.6). The samples containing α-synuclein alone formed typical ß-sheet-rich fibrils, whereas the Ezrin-containing samples formed round, regular structures, suggesting that Ezrin may promote the formation of atypical and non-fibrillar aggregates of α-synuclein.

Syn only

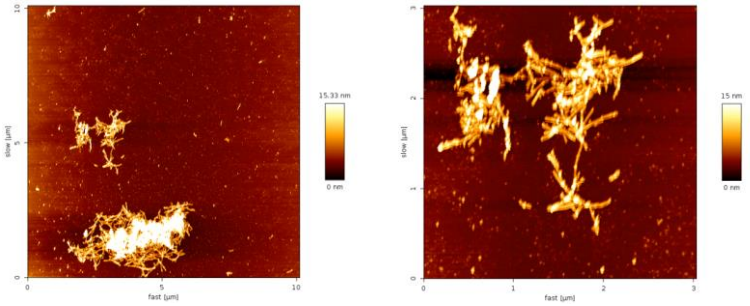

Syn:Ezrin 5:1

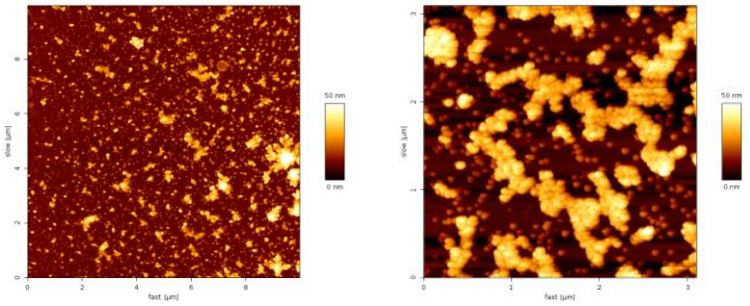

Fig 3.2.6 Atomic force microscopy of α-synuclein [Syn; 50 μM] incubated for 65 hours with and without Ezrin [10 μM]. α-synuclein alone forms aggregates with a typical fibrillar morphology, while α-synuclein incubated with Ezrin yields regular, spherical aggregates that tend to cluster together in large conglomerates. Images on the left are at a resolution of 10 μm X 10 μm, while those on the right are 3 μm X 3 μm.

3.2.7 Chapter Summary

The data presented in this section demonstrate that Ezrin is a potent inhibitor of α-synuclein fibrillization. Family members sharing high homology with Ezrin (e.g. Radixin) demonstrate a potent inhibition of α-synuclein fibrillization, while lower-homology proteins (e.g. Band 4.1) fail to do so, indicating that the modulatory effect of Ezrin on α-synuclein fibrillization may even be conserved across proteins with similar structure. Ezrin reduces the formation of higher molecular weight SDS-resistant oligomers and almost completely prevents the formation of SDS-resistant aggregates of α-synuclein. In addition, Ezrin mediates the formation of spherical and regular aggregates of α-synuclein, unlike the well-described fibrils found in the disease state (Bagchi et al., 2013). Thus, the next step in the study of Ezrin-mediated inhibition of α-synuclein fibrillization is to elucidate the mechanism by which Ezrin brings about its potent effect.

3.3 Time-resolved nuclear magnetic resonance (NMR) spectroscopy studies elucidate the mechanism by which Ezrin inhibits α-synuclein fibrillization

Nuclear magnetic resonance (NMR) is a physical phenomenon in which nuclei in a magnetic field absorb and re-emit electromagnetic radiation. NMR spectroscopy is a technique that exploits the magnetic properties of NMR-active atomic nuclei, e.g. ^{1}H and ^{15}N, and is used to investigate the properties of organic molecules such as proteins. In NMR spectroscopy, the chemical shift is the resonant frequency of a nucleus relative to a standard; often the position and number of chemical shifts are diagnostic of the structure of a molecule (Silverstein R.M., 1991). Chemical shift is calculated as follows:

$$\delta = \frac{\text{difference between a resonance fequency and that of a reference substance}}{\text{operating frequency of the spectrometer}}$$

Since the numerator is usually in Hertz (Hz) and the denominator in Megahertz (MHz), δ is usually expressed in parts per million (ppm) by frequency. The detected frequencies (in Hz) for ^{1}H-nuclei are usually referenced against TMS (tetramethylsilane) or DSS (4,4-dimethyl-4-silapentane-1-sulfonic acid), both of which are assigned the chemical shift of zero. Lastly, chemical shifts are very sensitive to the electronic environment of a nucleus (Higman, 2013). Perturbations in the chemical shift can be caused not only by a change in the covalent molecular structure, but also through non-covalent interactions with solvent molecules or binding partners. This makes chemical shifts a very sensitive probe for the identification of interaction surfaces in protein complexes, usually by a method referred to as chemical shift perturbation or mapping:

Chemical shift perturbation (CSP, chemical shift mapping or complexation-induced changes in chemical shift, CIS) follows changes in the chemical shifts of a protein when a ligand is added, and uses these to determine the location of the binding site, the affinity of the ligand and/or possibly the structure of the complex (Williamson, 2013). For determining the location of a bound ligand on the basis of shift change, the most appropriate method is usually to measure ^{15}N-HMQC spectra, calculate the geometrical distance moved by the peak, weighting ^{15}N shifts by a factor of about 0.14 compared to ^{1}H shifts, and select those residues for which the weighted shift-change is larger than the standard deviation of the shift for all residues (Williamson, 2013). However, there is no good way to distinguish changes in

chemical shift due to direct binding of the ligand from changes in chemical shift due to allosteric change (Williamson, 2013).

NMR spectroscopy is of particular use in yielding information about the interaction of α-synuclein with other proteins, for instance, the interaction between endosulfine-α (ENSA) and α-synuclein (Woods et al., 2007). This interaction was characterized in detail by NMR experiments, which demonstrated a highly selective interaction between ENSA and specific residues in the N-terminal helical domain of α-synuclein. This observation was extended to the demonstration of a similar interaction between α-synuclein and cAMP-regulated phosphoprotein 19 (ARPP-19), a protein highly related to ENSA which is also enriched in the brain (Woods et al., 2007). Hence, in order to elucidate the mechanism by which Ezrin inhibits the formation of Thioflavin-T-positive α-synuclein fibrils, solution-state NMR spectroscopy was employed to track the α-synuclein-Ezrin interaction systematically over time.

To this end, ^{15}N-labelled α-synuclein was incubated with Ezrin (α-synuclein:Ezrin 5:1), as previously described, and NMR measurements were carried out on the samples at regular time intervals, yielding a comprehensive, time-resolved and residue-specific dataset for α-synuclein. Experiments were carried out thrice to establish reproducibility. α-synuclein was also incubated alone and tracked by NMR over multiple time-points to obtain a suitable control for the experiment. The data generated from the NMR experiments are described in detail below.

As mentioned in Section 2.2.3.2, ^{15}N-labelled α-synuclein (as well as spectrometer-time) was a generous gift from Dr. Philipp Selenko (FMP). Spectrometer-operation, spectra-generation and raw-data conversion were done in collaboration with Dr. Silvia Verzini (FMP) without whom this work would not be possible. Both Dr. Philipp Selenko and Dr. Andres Binolfi contributed significantly to data-interpretation.

3.3.1 Establishment of a Thioflavin-T-based fluorescence-tracking assay for correlation with NMR spectroscopy

In order to be able to correlate any new NMR data with the data hitherto obtained, a Thioflavin-T-based 'tracking' assay was carried out in parallel with the NMR experiment. In brief, 50 μM ^{15}N-α-synuclein were incubated with and without Ezrin (α-synuclein:Ezrin 5:1) in NMR buffer (20 mM NaP, 150 mM NaCl, end-pH 6.4, filtered and de-gased) at 37˚C, shaking at 200 rpm. Samples destined for NMR experiments contained no Thioflavin-T, while samples intended for Thioflavin-T fluorescence assays contained 2 μM of the compound.

For the latter assay, Thioflavin-T fluorescence was measured at regular and systematic 4-5 hour time intervals which corresponded exactly to the time-intervals at which NMR measurements were taken. The two sample-sets were treated as being identical in all respects other than the type of measurements they were subjected to (i.e. NMR vs. fluorescence). Fig. 3.3.1 represents the fluorescence data obtained, which may also be used as a reference for the NMR experiments presented in the following sections.

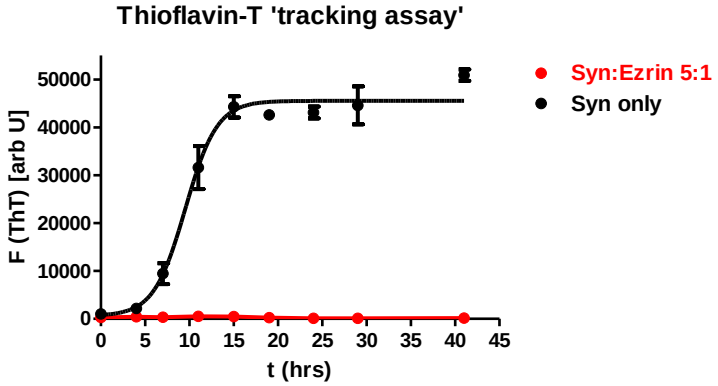

Fig 3.3.1 Thioflavin-T (ThT) 'tracking' assay of 50 μM α-synuclein incubated either alone (Syn only) or in the presence of Ezrin (Syn:Ezrin 5:1) at 37˚C, 200rpm, as a control for the NMR measurements being carried out in parallel. The NMR readings span the entire length of the aggregation curve of α-synuclein, from the initiation of the experiment to the end-stages of α-synuclein aggregation, i.e. several hours after a plateau has been established.

3.3.2 Time-resolved 1D-NMR reveals that Ezrin mediates the accelerated aggregation of α-synuclein

For the generation of 1D-NMR traces or ^{1}H-signal intensity profiles of ^{15}N-α-synuclein incubated alone and with Ezrin (Syn:Ezrin 5:1) in the absence of Thioflavin-T, samples were analyzed in the spectrometer at regular 4-5h intervals spanning a total time-period of 42 h. As shown in Fig. 3.3.2, 1D-NMR traces over multiple time-points revealed an unexpected trend: α-synuclein aggregated faster in the presence of Ezrin than when incubated alone. The 1D-NMR profiles below show selected time-points throughout the α-synuclein aggregation process including the start of the experiment (0 h), the exponential growth phase (21 h), the plateau phase (39 h) and the end of the reaction (66 h). The profiles clearly show that after 39 h incubation with Ezrin almost all the α-synuclein molecules have aggregated, as depicted by the nearly complete disappearance of monomeric α-synuclein ^{1}H-signal intensity. In contrast, in the absence of Ezrin, even after 66h of incubation, α-synuclein has not significantly aggregated, as evidenced by the high intensity of detectable ^{1}H-signal typical for monomeric α-synuclein. This suggests that Ezrin induces accelerated aggregation of α-synuclein.

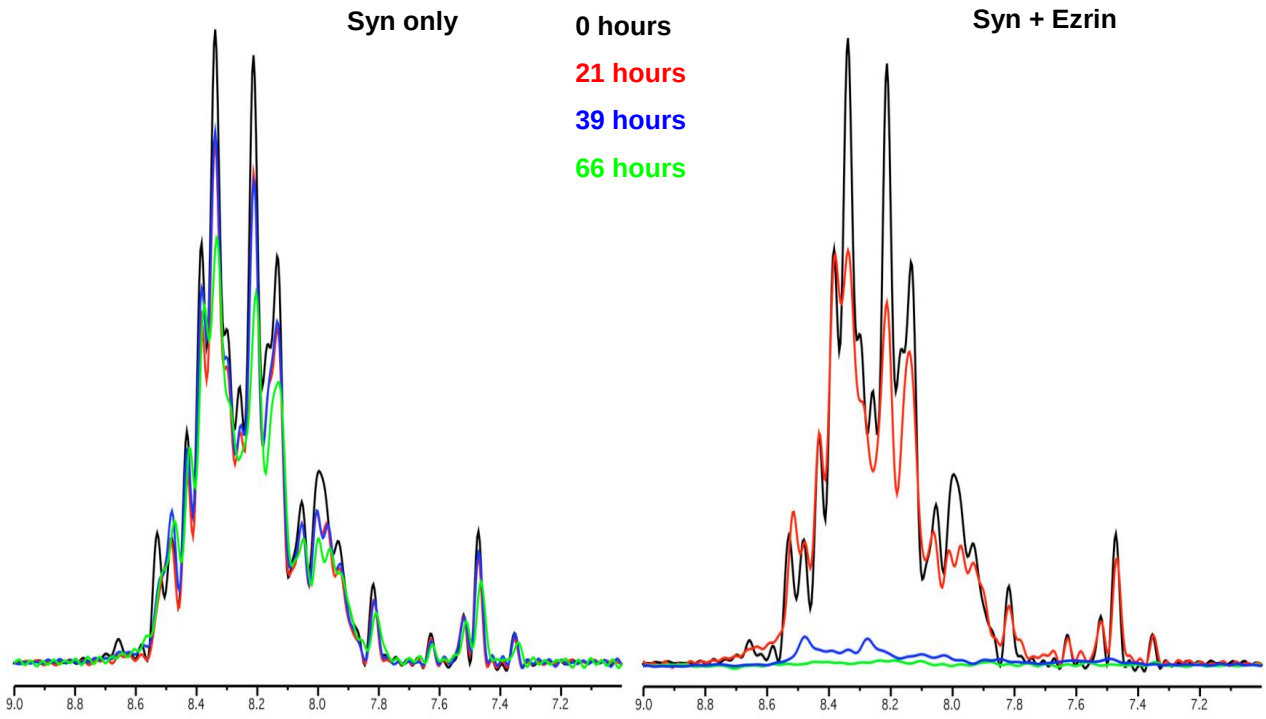

Fig 3.3.2 Representative 1D-NMR traces (or ^{1}H-signal intensity profiles) of 50 µM α-synuclein incubated in the presence and absence of Ezrin (Syn:Ezrin 5:1) generated at different time-points in the aggregation process. The four ^{1}H-signal intensity profiles for each test condition span the start (0 h), the exponential phase (21 h), the plateau phase (39 h) and the end (66 h) of the experiment and have been selected to highlight the dramatic *increase* in the rate of α-synuclein aggregation in the presence of Ezrin, as compared to the significantly *slower* rate of α-synuclein aggregation in the absence of Ezrin.

3.3.3 Residue-specific time-resolved ^{1}H-^{15}N HMQC values of α-synuclein incubated in the presence and absence of Ezrin

The Heteronuclear Multiple Quantum Coherence (HMQC) or Heteronuclear Multiple Quantum Correlation experiment, first described in 1980, is used frequently in NMR spectroscopy of organic molecules and is of particular significance in the field of protein NMR (Bodenhausen G, 1980). The resulting spectrum is two-dimensional with one axis for ^{1}H and the other for a heteronucleus (an atomic nucleus other than a proton), such as ^{15}N. The spectrum thus contains a peak for each unique proton attached to the heteronucleus being considered. In other words, as each residue of the protein (except proline) has an amide proton attached to a nitrogen in the peptide bond, the HMQC provides the correlation between the nitrogen and amide proton and each amide yields a peak in the HMQC spectra.

RESULTS

As described already in Section 3.3.1, 50 μM ^{15}N-α-synuclein were incubated with and without Ezrin (α-synuclein:Ezrin 5:1) in NMR buffer (20 mM NaP, 150 mM NaCl, end-pH 6.4, filtered and de-gased) at 37˚C, shaking at 200 rpm. The samples were subjected to ^{1}H-^{15}N HMQC experiments at regular 4-5 h intervals spanning a total time-period of 42 h. These ^{1}H-^{15}N HMQC (2D-NMR) analyses confirmed the accelerated rate of aggregation in the presence of Ezrin (^{1}H-signal intensity = 0 at time 39 h) as compared to α-synuclein incubated alone (^{1}H-signal intensity = ~80% of the original at time 39 h). Furthermore, examination of the residues across the length of the protein at various time-points revealed strikingly different phenomena of aggregation across the two conditions (see Fig. 3.3.3):

α-synuclein incubated alone showed a uniform loss of ^{1}H-signal intensity across the entire length of the molecule. A decrease in ^{1}H-signal intensity at the early-N-terminal region (also referred to as “broadening”) became prominent only at a very late stage of α-synuclein aggregation (66 h). In the presence of Ezrin, however, the α-synuclein molecule did not undergo uniform changes throughout its entire length. Ezrin treatment caused a pronounced broadening of early N-terminal residues in α-synuclein (AA 1-10) as early as 4h, with a nearly complete disappearance of these residues after 26 h of incubation, while the C-terminal residues (AA 96-140) remained clearly visible and showed essentially unchanged intensities even after 26 h of incubation, when the rest of the molecule was already significantly broadened. The NAC region showed a rate of loss of intensity which was intermediate between the rapid loss of the N-terminus and the considerably slower loss of the C-terminus. After 39 h of incubation, the α-synuclein with Ezrin sample had completely broadened (across *all* regions) and was therefore detected by NMR as a signal of marginal or nearly-zero ^{1}H-intensity, whereas the corresponding sample of α-synuclein incubated alone had an intensity that approached its baseline intensity, i.e. the intensity of α-synuclein alone at t=0h.

As a comparison to the NMR data, Thioflavin-T fluorescence data from the ‘tracking’ assay are presented in parallel in Fig. 3.3.3 below, highlighting certain disparities between the two types of results. While the Thioflavin-T data in Fig. 3.3.3.C seem to suggest that α-synuclein incubated alone has attained complete aggregation by 21h, the NMR data suggest that only a very small fraction of α-synuclein incubated alone for 21h has aggregated (visible by the minimal drop in I/Io in Fig. 3.3.3.B). Similarly, α-synuclein incubated alone for 39 h and examined by NMR indicates that the vast majority of the sample is still monomeric, with only a small sub-population that may have aggregated (visible as a slight drop in I/Io in Fig.

3.3.3.B), while the corresponding Thioflavin-T signal still shows maximal fluorescence, indicative of total aggregation of α-synuclein. This difference can be explained as follows:

The tiny fraction of α-synuclein which has aggregated after 21 h of being incubated alone (detected as a slight decrease in I/Io in Fig. 3.3.3.B) may be sufficient to bind all the available Thioflavin-T molecules in the solution, resulting in maximal fluorescence as detected by the 'tracking' assay. Thereby, a complete and saturated binding of *Thioflavin-T* by α-synuclein has been effected, rather than the complete aggregation of *α-synuclein* molecules. Thus, a maximal fluorescent signal is obtained from the 'tracking' assay for α-synuclein incubated alone, although only a small sub-population of α-synuclein has aggregated and the majority of the protein still exists as a monomer. This difference in sensitivity and accuracy of the two assays points towards the greater applicability and suitability of NMR spectroscopy for α-synuclein aggregation studies as compared to Thioflavin-T fluorescence measurements.

In the case of α-synuclein incubated with Ezrin (Fig 3.3.3.D and E), the Thioflavin-T data are in accordance with the NMR data as both experiments indicate that traditional cross-ß-pleated-sheet-containing fibrillar aggregates of α-synuclein are not formed in the presence of Ezrin. Thioflavin-T assays show no fluorescence whatsoever, indicating the absence of fibrillar aggregates in solution. Similarly, NMR data do not suggest typical fibril formation, as fibrillar aggregates would be detected by NMR as a uniform drop in intensity across the entire α-synuclein molecule, with no changes in the positions of the original resonance peaks of α-synuclein in the ^{1}H-^{15}N HMQC spectra (as observed for α-synuclein incubated alone).

In conclusion, an analysis of ^{1}H-signal intensity for each residue of α-synuclein across multiple time-points in its aggregation process confirmed that α-synuclein aggregates significantly faster in the presence of Ezrin than in its absence. The analysis also showed, rather unexpectedly, that the response of the aggregating protein to Ezrin is not uniform but varies considerably across the 3 regions of α-synuclein - the N-terminal, NAC and C-terminal regions. The N-terminal region – as the first region of α-synuclein to experience a change in the presence of Ezrin, namely, a rapid broadening – may be the first site of contact between Ezrin and α-synuclein and the changes that it undergoes may then lead to or facilitate additional conformational changes in the NAC – an effect which then continues down the length of the molecule to ultimately affect the C-terminal domain as well.

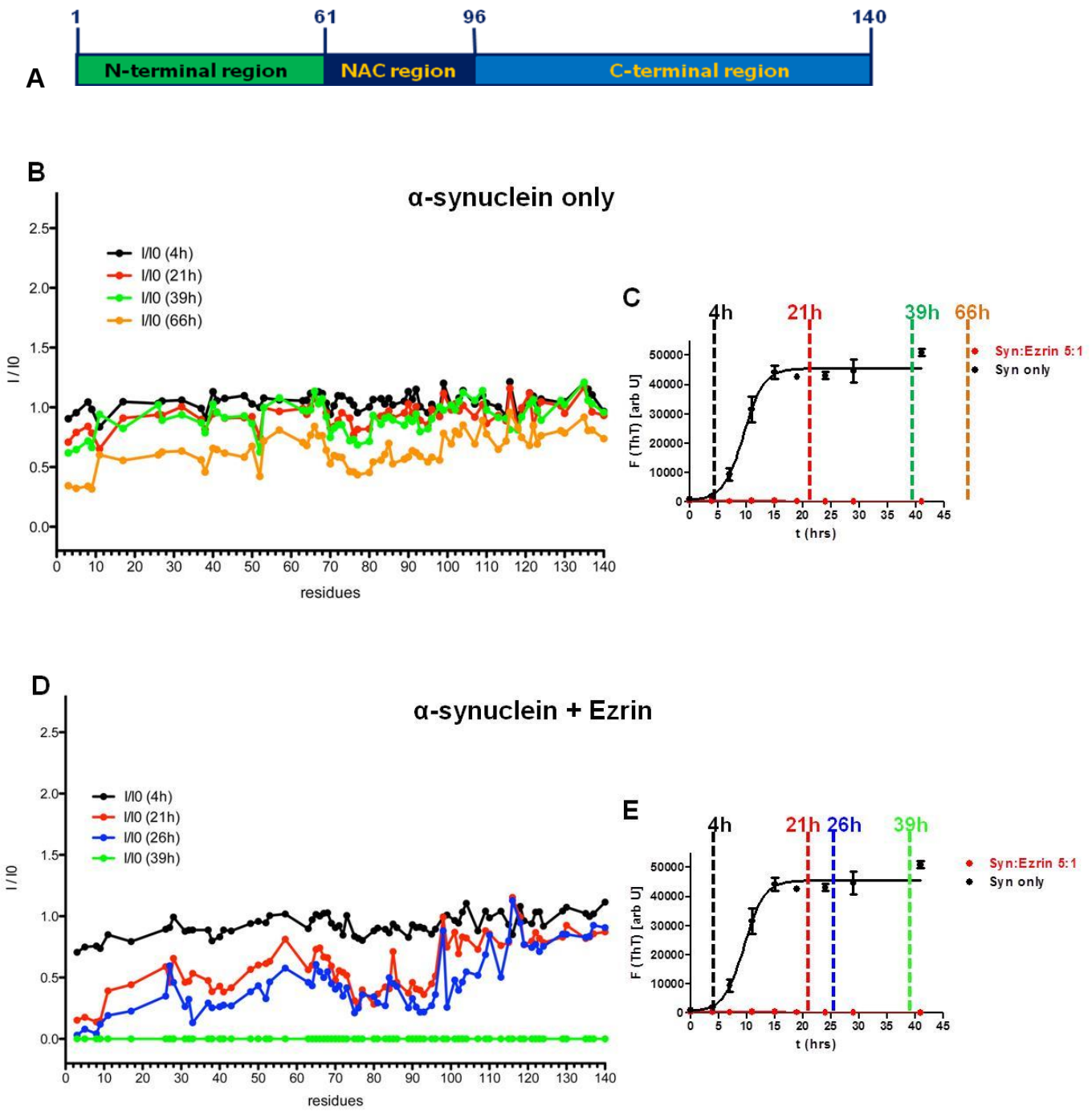

Fig 3.3.3. (A) A schematic representation of the three regions of the α-synuclein molecule: the N-terminus (Residues 1-60), the NAC region (Non-Amyloid Component; Residues 61-95) and the C-terminus (Residues 96-140). (B) ^{1}H-^{15}N HMQC-based intensity values for each residue of α-synuclein incubated alone at different time-points throughout the aggregation process. (C) Thioflavin-T 'tracking' assay fluorescence data corresponding to the time-points from the NMR experiment on α-synuclein incubated alone. (D) ^{1}H-^{15}N HMQC-based intensity values for each residue of α-synuclein incubated with Ezrin (α-synuclein:Ezrin 5:1) at different time-points throughout the aggregation process. (E) Thioflavin-T 'tracking' assay fluorescence data corresponding to the time-points from the NMR experiment on α-synuclein incubated with Ezrin (α-synuclein:Ezrin 5:1).

3.3.4 Time-resolved 2D-NMR reveals that the N-terminal, NAC and C-terminal regions of α-synuclein respond differently to Ezrin

The data from Fig. 3.3.3 suggest that the broadening of residues within the C-terminus, NAC and N-terminus of α-synuclein occurs at different time scales. Therefore, a more detailed, time-resolved analysis of residue-broadening was carried out for each of the three regions of α-synuclein (see Fig 3.3.4 below). This confirmed that the N-terminal (AA 1-60), the NAC (AA 61-95) and the C-terminal (AA 96-140) regions all show significantly differing trends over time, in the presence of Ezrin. The N-terminal domain of α-synuclein was the first part of the protein to undergo broadening in the presence of Ezrin and also demonstrated the most rapid broadening of all the 3 regions, as depicted in the graphs below. While the N-terminal intensity was reduced to less than half after only 11 h of incubation with Ezrin, the central NAC region showed a 50% intensity-loss only after 29 h and the C-terminal region lost over 50% intensity only after 41 h. Additionally, while the N-terminus showed an exponential loss of intensity, the NAC region showed a more gradual loss of intensity and the C-terminal region appeared to stay more-or-less consistent until right before the end of the experiment [i.e. at t=41 h or at the penultimate reading]. The final NMR measurement at t=42 h showed a complete disappearance of ^{1}H-^{15}N signal intensity across *all* regions of α-synuclein, hence, the data for this time-point have not been included in the graphs below. In fact, at 24 h and 29 h, the overall intensity value of the C-terminal region even approached its original value at t=0 h. The control sample of α-synuclein incubated alone, however, maintained a consistent intensity across all regions throughout the experiment (as depicted by the unwavering red line in Fig. 3.3.4. below). There was no indication of variation in the loss of intensity across the different regions, suggesting that this phenomenon was specific to α-synuclein incubated with Ezrin.

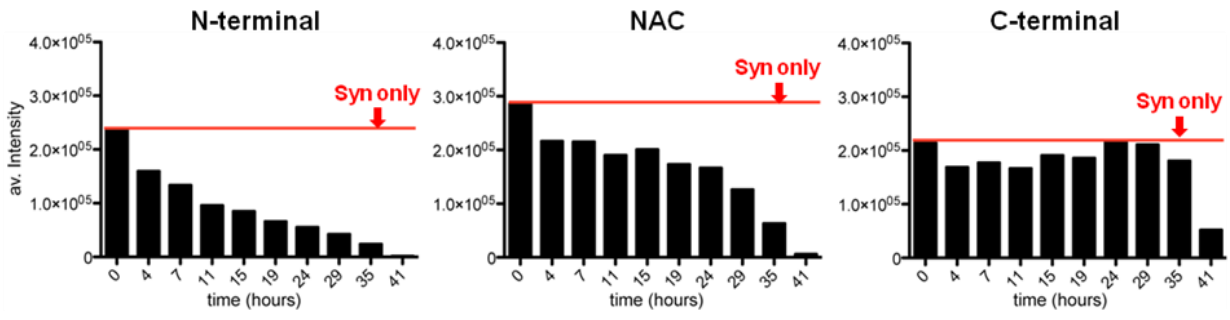

Fig 3.3.4. Total 1H-intensity values measured over time for the N-terminal, NAC and C-terminal regions of α-synuclein when incubated with Ezrin (black bar-graphs; α-synuclein:Ezrin 5:1). NMR measurements are shown for 10 different time-points. The corresponding 1H-intensity values of α-synuclein incubated alone are represented by the red line marked 'Syn only', signifying that the 1H-intensity of α-synuclein alone has not decreased even at the latest time-points and that there is no region-based difference in intensity

for α-synuclein incubated alone. α-synuclein incubated with Ezrin, however, shows a rapid drop in intensity at the N-terminal region over time, followed by a somewhat slower decrease in intensity at the NAC region. In contrast, the C-terminal region maintains a more-or-less constant intensity over a long period of time. However, the signal intensity is dramatically reduced at the penultimate time-point, 41 h, suggesting that this part of the molecule may be the last to be incorporated into higher-order structures or aggregates.

3.3.5 Time-resolved analysis of individual residues in the N-terminal, NAC and C-terminal regions of α-synuclein

An in-depth analysis of the N-terminal, NAC and C-terminal regions of α-synuclein revealed that even within a region different stretches of amino acids behave differently from their neighbours. Certain stretches appear to broaden significantly faster than neighbouring stretches (e.g. the motif MDVFMKGL, AA 1-8 in Fig 3.3.5.1), while other stretches show distinctive broadening trends even within the stretch (e.g. AA 69-73 and AA 75-83 in Fig 3.3.5.2). Furthermore, while overall intensity values represent general trends across a region, they fail to highlight that individual residues may actually show a behaviour opposite to the trend (e.g. the entire C-terminal region shows a similar overall intensity at 4 h and 35 h (refer to Fig. 3.3.4 above), yet AA 135-137 and 139-140 show an increase in intensity from 4 h to 35 h (Fig 3.3.5.3). Hence, it is critical to examine each region on a residue-specific level in order to obtain a truly representative picture of the behaviour of that region, and by extension, of the entire α-synuclein molecule.

1) N-terminal region (AA 1-60): The first 8 residues of α-synuclein along with the stretch from AA 30-49 show a reduction in intensity to less than one-third of the original value after only 24 h of incubation with Ezrin. While neighbouring residues also show a drop in intensity after 24 h, the values are not less than half the original value (e.g. AA 17 and 50).

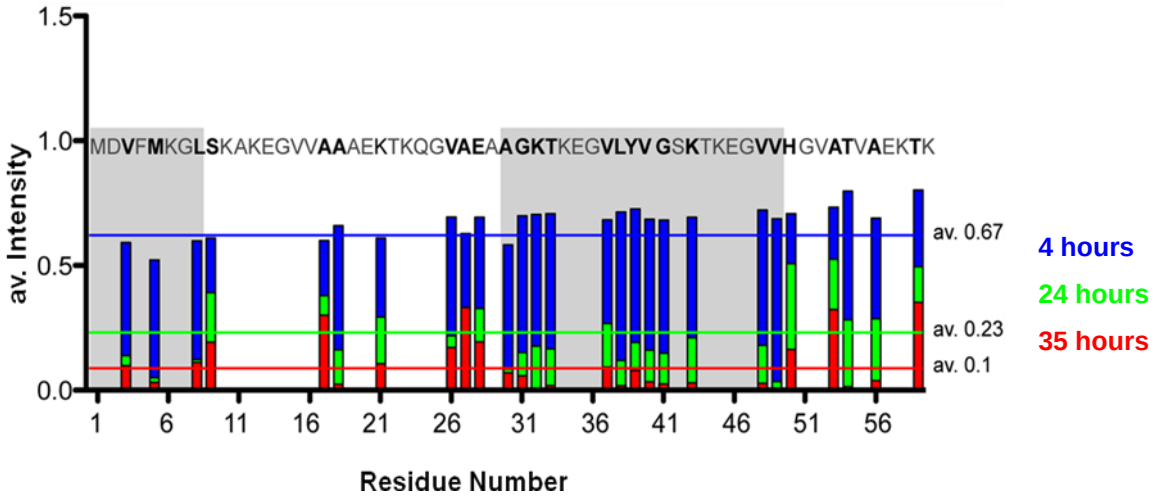

Fig 3.3.5.1. ^{1}H-intensity values of each residue of the N-terminal region of α-synuclein after treatment with Ezrin (α-synuclein:Ezrin 5:1). Three distinct time-points in the aggregation process are shown: 4 h (early phase), 24 h (mid-phase) and 35 h (end-phase). The regions shaded in grey represent stretches of amino aids that show a more rapid drop in intensity than their neighbours. The horizontal lines coloured blue, green and red represent the mean intensity of all the residues within this region at 4 h, 24 h and 35 h, respectively.

2) NAC region (AA 61-95): As mentioned previously, the NAC region shows an overall decrease in intensity which is slower than the decrease in intensity of the N-terminal region, yet faster than the decrease in intensity of the C-terminal region. However, within this region certain trends are clearly visible, demonstrating that not all the amino acids respond uniformly to the presence of Ezrin. For instance, the stretches AA 69-83 and AA 87-95 broaden much faster than their neighbours, but even within these stretches there is a clear trend visible, with AA 69-73 broadening relatively slower than AA 75-83 and AA 87-95, indicating a tendency of the latter part of the NAC region to broaden faster than the initial part.

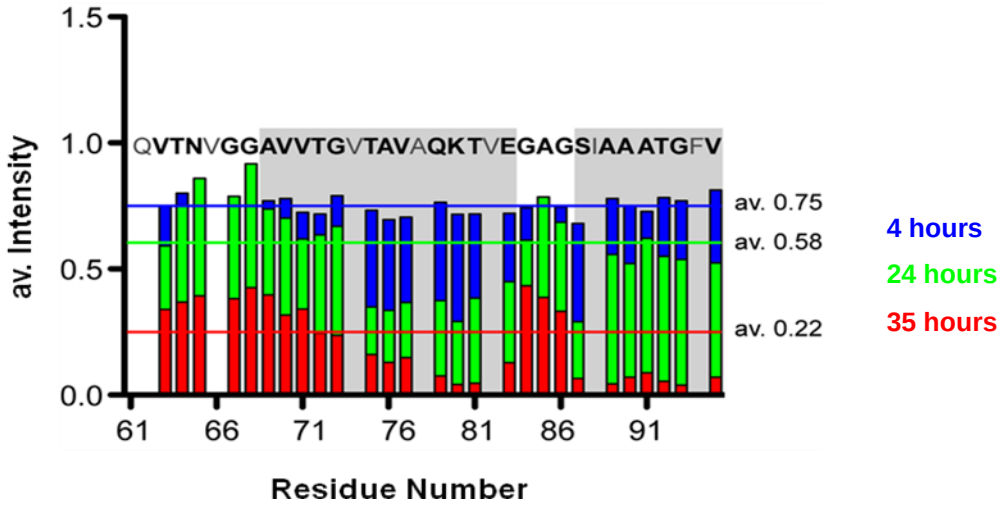

Fig 3.3.5.2 ^{1}H-intensity values of each residue of the NAC region of α-synuclein upon incubation with Ezrin (α-synuclein:Ezrin 5:1). Three distinct time-points in the aggregation process have been shown: 4 h (early phase), 24 h (mid-phase) and 35 h (end-phase). The regions shaded in grey represent stretches of AAs that show a more rapid drop in intensity than their neighbours and suggest that the mid-to-late NAC region may undergo broadening before the rest. The horizontal lines coloured blue, green and red represent the mean intensity of all the residues within this region at 4 h, 24 h and 35 h, respectively, highlighting the difference in drop in intensity of the NAC region with respect to the N-terminal region.

3) C-terminal region (AA 96-140): In contrast to the N-terminal and the NAC regions, the C-terminal region shows an overall intensity that stays more or less consistent until the penultimate time-point of 41 h. What is not evident from the overall intensity analyses,

however, is that certain residues actually show an increase in intensity at 24 h and 35 h (e.g. AA 110, 126 and 130) as compared to 0h. This indicates that although the overall intensity of the C-terminal region stays largely unchanged (24 h) or decreases slightly (35 h), certain residues become more flexible in the course of aggregation, resulting in greater visibility by NMR. This may be interpreted as follows: the C-terminal is the last region of the α-synuclein molecule to undergo Ezrin-mediated changes, indicating that its interaction with Ezrin may be minimal and certainly takes place after the interaction of the N-terminal and NAC domains with this modifier. This results in additional freedom and flexibility of this region of α-synuclein, which may also explain its relatively late broadening.

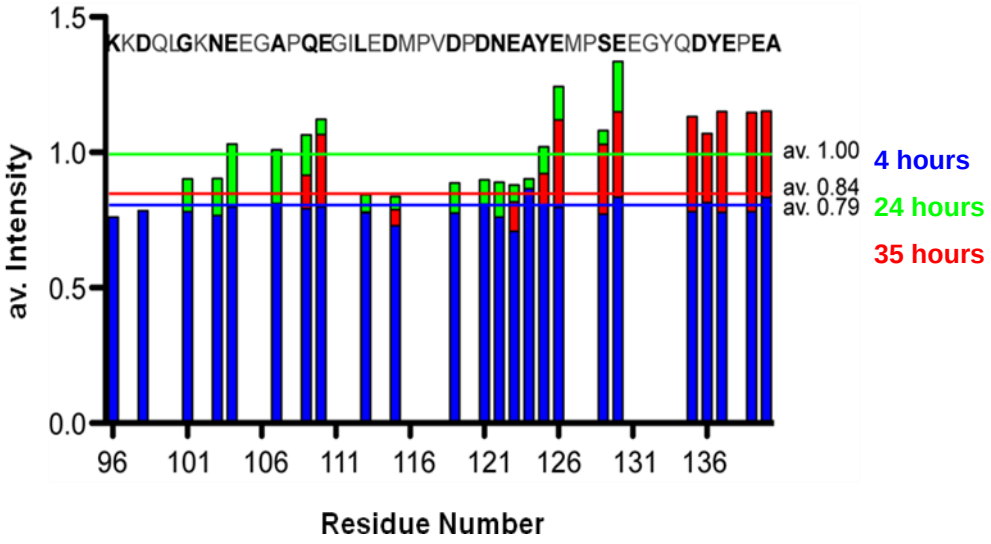

Fig 3.3.5.3 ^{1}H-intensity values of each residue of the C-terminal region of α-synuclein when incubated with Ezrin (α-synuclein:Ezrin 5:1) over 3 distinct time-points in the aggregation process: 4 h (early phase), 24 h (mid-phase) and 35 h (end-phase). The C-terminal region - in contrast to the N-terminal and the NAC regions - shows an overall intensity that stays practically consistent over the three time-points depicted in the diagram. Furthermore, at the later time-points of 24 h and 35 h, the intensity of certain C-terminal residues (e.g. AA 126 and 130) actually increases relative to the intensity at 0 h, indicating that these C-terminal AA may become more flexible in the course of aggregation. The horizontal lines coloured blue, green and red represent the mean intensity of all the residues within this region at 4 h, 24 h and 35 h, respectively.

3.3.6 Multiple, transient conformations of α-synuclein are generated in the presence of Ezrin

In order to better understand the effect of Ezrin on α-synuclein aggregation over time, the ^{1}H-^{15}N HMQC spectra for both α-synuclein incubated alone as well as for α-synuclein incubated with Ezrin were examined at each time-point at which NMR measurements were taken. Upon examination of the individual residues of α-synuclein at every step of the aggregation reaction (both in the presence as well as absence of Ezrin) certain trends in residue behavior became apparent, pointing towards a curious phenomenon:

At later time-points in the incubation process of α-synuclein with Ezrin (i.e. t=11 h onwards), secondary conformations or 'double-peaks' started to appear for many residues, indicative of chemical shift variations. These secondary conformations were transient, in that they appeared at a later stage of incubation, generally grew stronger in intensity before waning again and finally disappeared (sometimes before the disappearance of the original peak, and sometimes simultaneously with the disappearance of the original peak). Thus, at any given time-point in the mid to later stages of aggregation, variations in the chemical shifts of various residues of α-synuclein were detected, i.e. multiple conformations of α-synuclein were present. In other words, Ezrin appears to mediate the formation of various novel conformations of α-synuclein which have a typical NMR profile and which appear to co-exist with the monomeric form of α-synuclein, which is still detectable. This could be indicative of the formation of intermediates of α-synuclein which then go on to form the round, non-fibrillar aggregates of α-synuclein discussed in Section 3.2.6. In contrast, α-synuclein incubated alone shows only the conformation typical of monomeric, random-coil α-synuclein.

In Fig 3.3.6.A below, an overlay of a representative section of a spectrum of α-synuclein with Ezrin at time 15 h and time 0 h is shown, with the secondary conformations and corresponding original peaks clearly marked on it (within blue dashed circles). The development and disappearance of these secondary conformations was tracked over time for each residue that underwent a chemical shift variation. Only residues that showed the appearance and persistence of a secondary peak over at least 3 time-points were highlighted. Residues from all the different regions of the α-synuclein molecule (i.e. N-terminus, NAC and C-terminus) could be identified in this image, indicating that multiple residues undergo a change in chemical shift. In addition, sites on α-synuclein that undergo broadening in the presence of Ezrin have been marked in green in Fig. 3.3.6.A. In the interest of space, only the three most-broadened sites have been marked, which confirm again that broadening of α-synuclein in the presence of Ezrin initiates and is most rapid at the N-terminus of the protein.

Fig. 3.3.6.B in contrast, shows an overlay of α-synuclein incubated alone at 15 h and at 0 h, and clearly depicts the complete lack of chemical shift variation within this sample over time. Only histidine 50 (His-50) shows a slight change in chemical shift for the sample of α-synuclein incubated alone (marked in purple). However, His-50 is an amino acid which is extremely sensitive to even minor changes in its chemical environment (e.g. pH). As the pH of the incubation mixture varies slightly over the course of the experiment (due to marginal and unavoidable loss of water over the course of a 42 h incubation at 37˚C), it is not

unexpected that the His-50 residue would respond by undergoing a slight change in chemical shift. His-50 also undergoes a similar chemical shift variation in the sample of α-synuclein incubated with Ezrin, confirming that this effect is common in both conditions. However, in addition to this common chemical shift 'displacement', additional variations of the His-50 residue in the 'α-synuclein with Ezrin' sample are also visible, indicating a phenomenon of extensive chemical shift variations specific to α-synuclein incubated with Ezrin (see Fig. 3.3.6.A). Lastly, α-synuclein incubated alone shows practically no broadening at 15 h, in stark contrast to α-synuclein incubated with Ezrin, where the majority of the early N-terminal has broadened to the extent that it is completely invisible by NMR at 15 h.

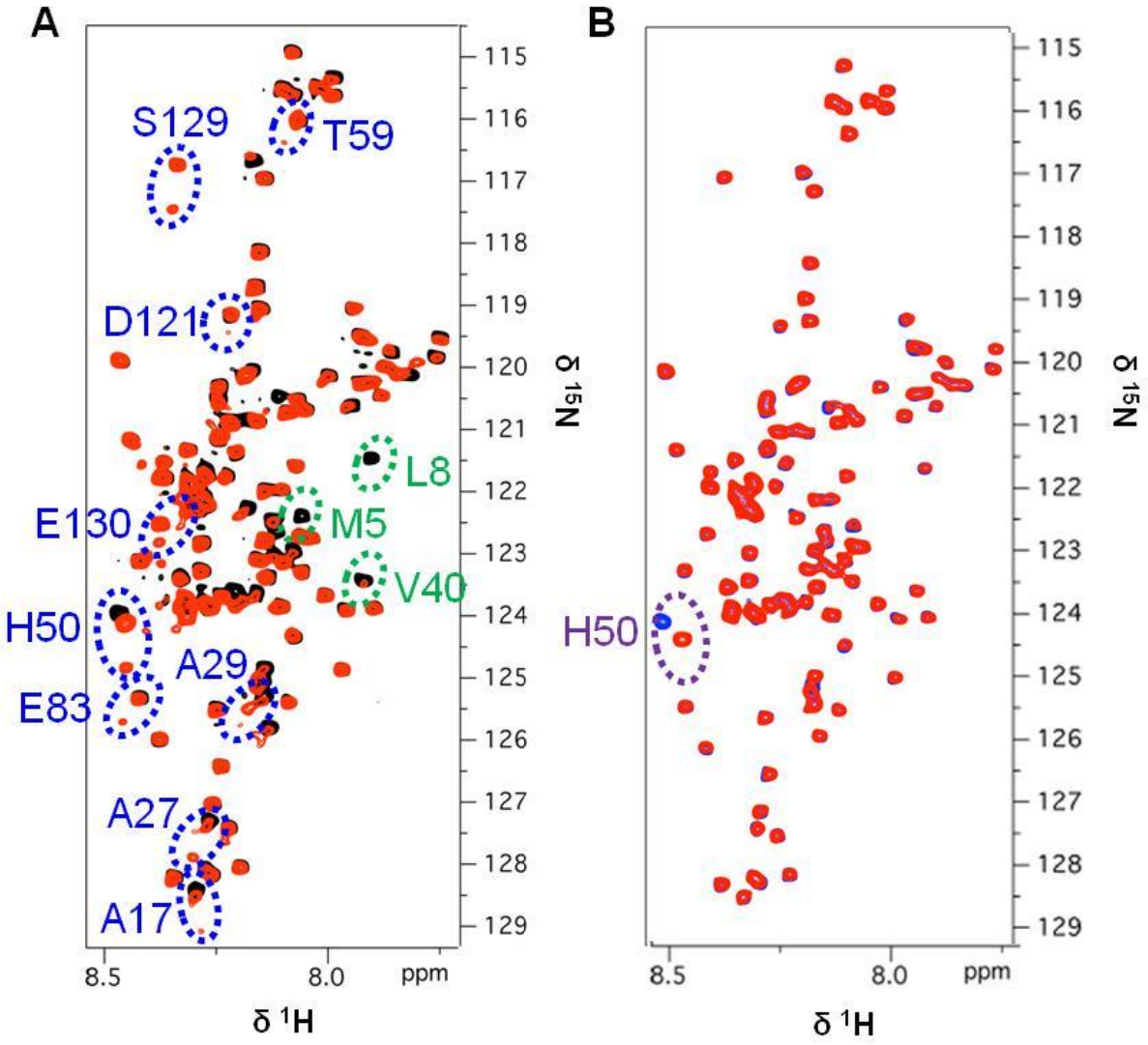

Fig 3.3.6.(A) ^{1}H-^{15}N HMQC spectrum of α-synuclein incubated in the presence of Ezrin for 15h (shown in red) overlaid on to the spectrum of α-synuclein with Ezrin at t=0h (black). Residues that show the formation of a second conformation in their vicinity are highlighted in blue dashed circles and named alongside. Residues that undergo broadening are highlighted in green dashed circles and also named alongside. For greater ease of viewing, only some of the residues undergoing conformational changes/ broadening have been circled, instead of all such residues. This representative selection incorporates

residues spanning the N-terminal, NAC and C-terminal regions of α-synuclein. (B) ^{1}H-^{15}N HMQC spectrum of α-synuclein incubated alone for 15h (shown in red) overlaid on to the spectrum of α-synuclein alone at t=0h (blue). His-50, a residue sensitive to fluctuations in its chemical environment, demonstrates a mild chemical shift 'displacement' as a result of perturbations in the pH of the incubation mixture and is highlighted by a purple dashed circle. Other chemical shift variations and/or broadening of residues within this sample are conspicuously absent.

3.3.7 Residue-specific chemical shift variation analysis across the N-terminal, NAC and C-terminal regions of α-synuclein

As mentioned above, the formation of secondary peaks was detected across the entire length of the α-synuclein molecule in the presence of Ezrin, prompting a detailed region-specific analysis of this large-scale variation. Fig 3.3.7.1 shows chemical shift variations upon 15h of incubation of α-synuclein with Ezrin across the 3 different regions of α-synuclein, clearly depicting that secondary conformations appear to cluster most strongly within the NAC region, as compared to the N-terminal and C-terminal regions. Even the flanking residues on either side of the NAC region, i.e. AA 59 and AA 97 undergo chemical shift variations.

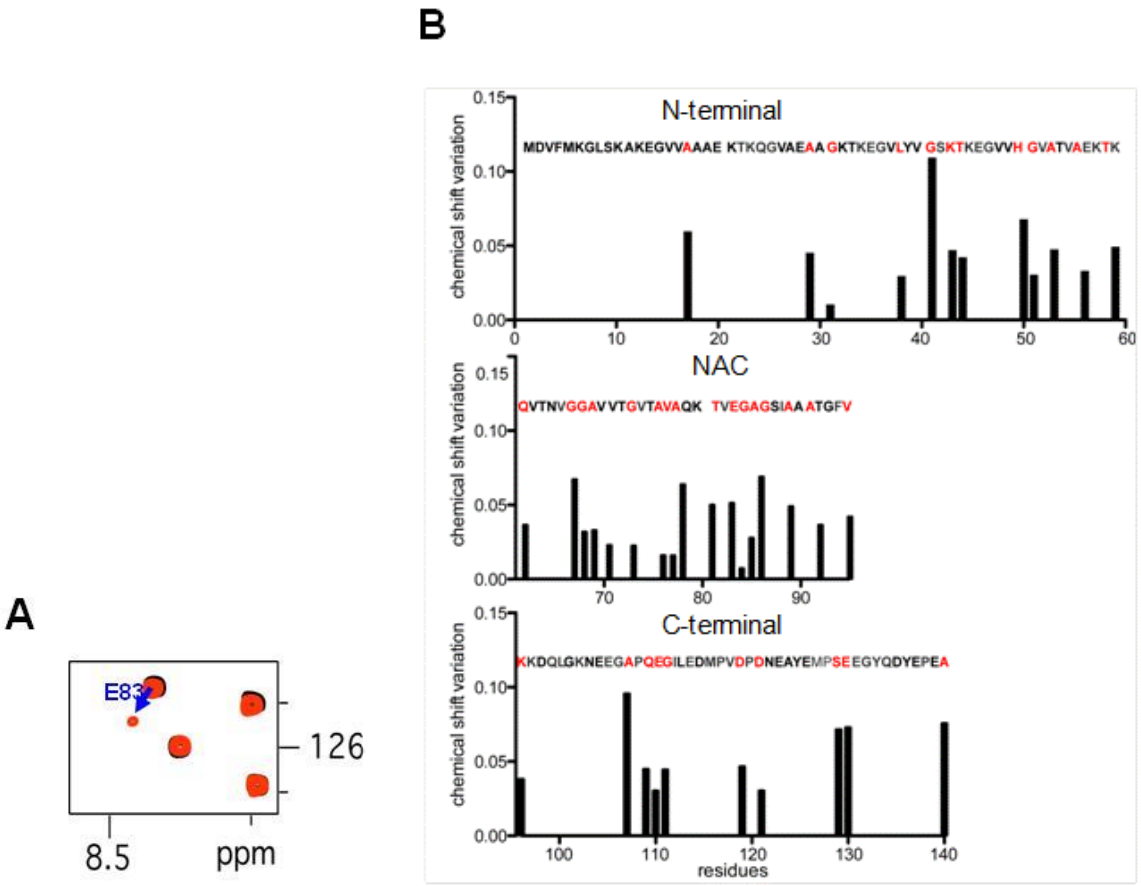

Fig 3.3.7.1. (A) An inset of the overlay depicted in Fig. 3.3.6.A - the ^{1}H-^{15}N HMQC spectrum of α-synuclein incubated in the presence of Ezrin for 15 h (shown in red) overlaid on to the spectrum of α-synuclein with

Ezrin at t=0 h (black). The inset highlights the chemical shift variation of one particular residue – E83 – in closer detail. The chemical shift variation is a function of the distance between the original peak and the secondary peak that has been formed in its immediate environment (pictorially represented by the blue arrow pointing from the original resonance to the newly-generated one). (B) Chemical shift variation values of all the secondary conformations of residues of α-synuclein when incubated with Ezrin for 15 h, represented region by region. While secondary conformations are detected for residues spanning the entire length of the α-synuclein molecule, there is evident clustering of a majority of these conformations in the central NAC region (and in the immediately flanking residues from the late N- and early C-terminals). Residues adopting secondary conformations are depicted in red. Those residues not adopting secondary conformations are represented in black. The absence of secondary conformations in these cases can be attributed to one of two causes, namely (i) those residues simply did not undergo a change in chemical shift, hence there were no secondary conformations corresponding to the original peak, e.g. M5, or (ii) the residue was present in a cluster of residues which were all too closely packed together to allow for unambiguous assignment of the correct original peak to each secondary conformation, e.g. A19 and L100.

Table 3.3.7.2 depicts the proportional distribution of secondary conformations across the different regions of the molecule, relative to the length of each region. The residues flanking the NAC region, referred to previously as T59 and K97, have been depicted as straddling the boundaries between the three regions, and have been both included and excluded from the overall NAC region analysis. This numerical approach shows that approximately half of the NAC region undergoes a change in chemical shift resulting in the formation of second conformations, as compared to ~20-25% of the N- and C- terminal regions each. These results suggest a special role for the NAC region in the process of α-synuclein fibrillization (or inhibition thereof), thereby paving the way for more detailed and qualitative analyses of the secondary conformations.

Table 3.3.7.2 Proportional distribution analysis of secondary conformations across the 3 regions of α-synuclein: N-terminus, NAC and C-terminus.

Region of the protein	Identity of AAs showing secondary conformations	# of AAs showing secondary conformations	Total # of AAs in the region	Percentage (%) of region showing secondary conformations
N-terminal	S9, A11, A17, A19, V26, A27, A29, V37, L38, K43, H50, G51, A53, A56,	14	60	23.33%
NAC	T59 Q61, G67, G68, A69, V71, T72, T75, A76, V77, T81, V82, E83, I88, G84, A89, A90, T92, V95	18 (+ 2 flanking residues) 18 (NAC only)	35 35	54.23% 48.57%
C-terminal	K97 A107, E110, D119, D121, N122, E126, S129, E130, A140	9	45	20.00%

3.3.8 Directionality analyses of chemical shift variation

Upon close observation of the development of variation in chemical shifts across the α-synuclein molecule over time in the presence of Ezrin, another feature became apparent, namely, the trends in directionality of the various chemical shift variations. Directionality of chemical shift variation (as represented in Fig. 3.3.8 below) is a function of the chemical shift of the residue at t=24 h (a time-point at which all the secondary conformations have been clearly and consistently detected by NMR) relative to the chemical shift of the same residue at t=0 h (a time-point at which no secondary conformations are detected). In other words, the variations in chemical shift appear to be taking place across all the different directions of the field: upwards, downwards, left-shift, right-shift and intermediates thereof (e.g. a downward left-shift, which is indicative of a de-shielding of electrons of the corresponding residues). This calls for a characterization of the directionality of chemical shift variations, whereby, once again, region-specific effects become evident.

Within the N-terminal region, chemical shift displacements seem to take place along both directions of the Δ15N-axis (i.e. upwards and downwards relative to the original residue). However, rightward displacements are never observed. Within the C-terminal region, there appears to be a converse trend of chemical shift displacements, with secondary conformations being formed upward and downward, but never leftward. However, the most striking effect is seen within the NAC region, namely, a uni-directionality of all chemical shift

variations in the left-downward direction (the exceptions being T81, I88, T92 and V95). Such uniformity of direction of chemical shift variation implies a symmetric change in the immediate environment of the NAC region. Such a homogenous effect is indicative of a de-shielding of electrons, which may occur as a result of hydrogen-bonding of the residues of the NAC region into ordered structures. This points towards the development of ß-sheets or aggregates within this region, suggesting a possible oligomerization of α-synuclein, brought about by an interaction of α-synuclein molecules. However, additional detailed NMR experiments are required to confirm this hypothesis.

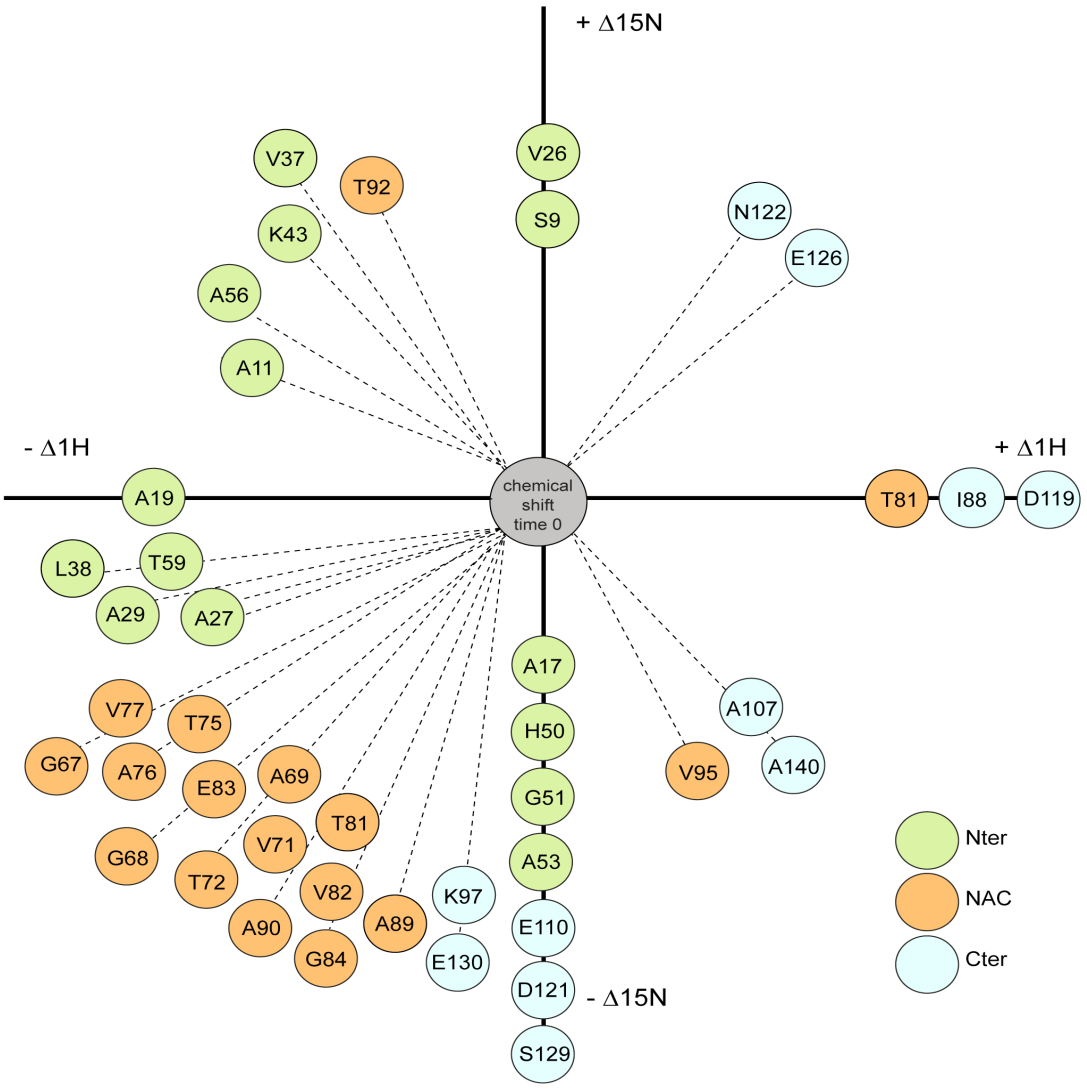

Fig 3.3.8. Directionality analysis of chemical shift variations across the three regions of α-synuclein. Directionality of chemical shift variation (shown as a dotted line) is a function of the chemical shift of the residue at t=24 h (shown as a circle containing the residue identity, e.g. E83) relative to the chemical shift of the same residue at t=0 h (shown as the grey circle at the center: 'chemical shift time 0'). N-terminal, NAC and C-terminal residues are coloured green, orange and blue, respectively. The majority of the NAC residues undergo a uni-directional, left-downward displacement as compared to residues in the N- and C-terminal regions.

3.3.9 Certain residues of α-synuclein give rise to three simultaneously-detectable conformations in the presence of Ezrin

Chemical shift variation analyses of late-to-end aggregation time-points (e.g. 24h onwards) revealed yet another unusual phenomenon: the formation of three different conformations of certain residues, i.e. “third” conformations or additional chemical shift variations of residues that had already undergone chemical shift variation once previously. Nine such ‘additional’ chemical shift variations were observed, distributed throughout the α-synuclein molecule: 2 in the N-terminal region (A29, L38); 4 in the NAC region (T81, E83, G84, A89) and 3 in the C-terminal region (A107, D119, E130), as shown below in Fig 3.3.9.A. Again, 4 of the 9 new conformations appeared to be closely clustered within the NAC region. The presence of ‘additional’ chemical shift variations confirms that α-synuclein adopts multiple conformations (of which at least three can be simultaneously detected for a single residue). These conformations appear to be in flux during the process of aggregation of α-synuclein into round, non-fibrillar structures in the presence of Ezrin. α-synuclein is constantly evolving from one state to another and simultaneously adopting multiple conformations in the presence of Ezrin, as can be seen for AA E83, shown in Fig. 3.3.9.B below. Both the second and third conformations of α-synuclein are best described as being transient, since they appear and disappear over the time-course of aggregation.

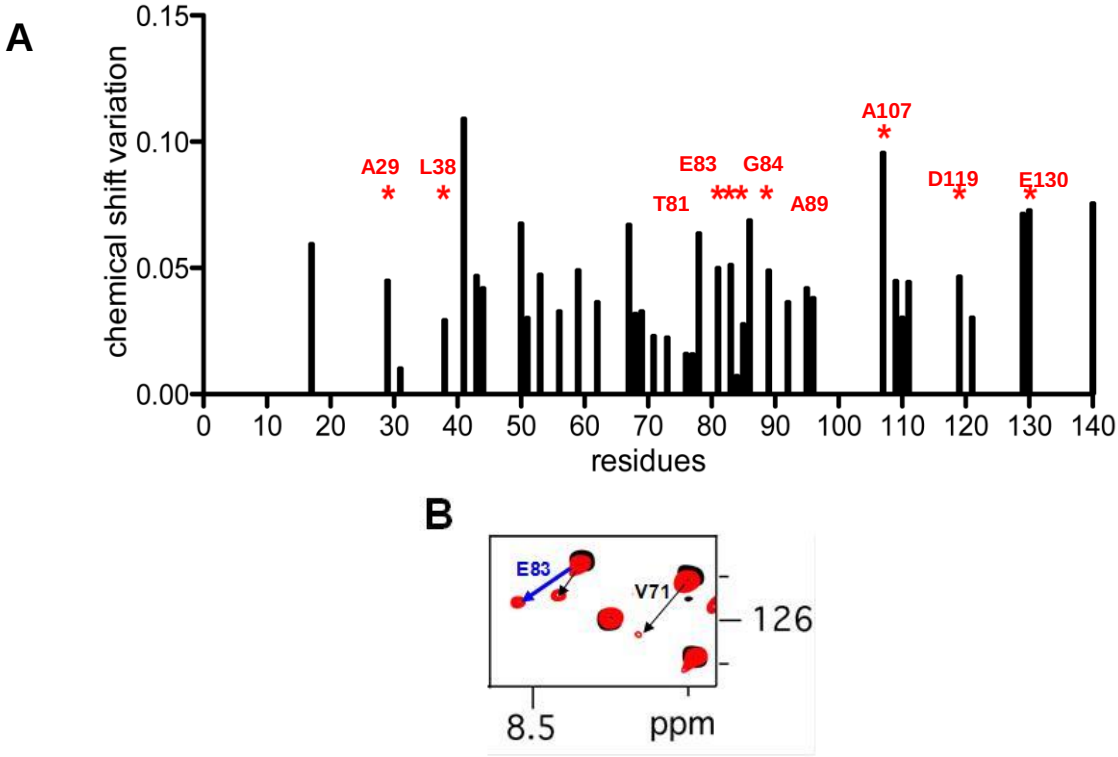

Fig 3.3.9. (A) Representation of the positions of third conformations of certain residues of α-synuclein (when incubated with Ezrin for 24 h). The asterisks and AA-identities of the third conformations (shown in red) are represented above the corresponding second conformation (black bars). (B) A subset of a ^{1}H-^{15}N HMQC spectrum of α-synuclein incubated with Ezrin for 24 h (red) overlaid onto the spectrum of α-

synuclein incubated with Ezrin at t=0 h (black) is shown. AA E83 is clearly seen to give rise to a third conformation (in contrast to V71 which only gives rise to two conformations).

3.3.10 Chapter Summary

In brief, time-resolved NMR was used to elucidate the mechanism by which Ezrin mediates the formation of off-pathway aggregates of α-synuclein. To this end, α-synuclein was incubated with Ezrin (α-synuclein:Ezrin 5:1) and analyzed every 4-5 h by NMR spectroscopy. This revealed that α-synuclein aggregates faster in the presence of sub-stoichiometric concentrations of Ezrin than in its absence. Furthermore, the N-terminal region, the NAC region and the C-terminal region of α-synuclein responded differently to the presence of Ezrin. The N-terminal region showed the first and most rapid broadening of residues, followed by the central NAC region, whereas the C-terminal region remained mostly visible, right up to the time-points preceding complete aggregation. On closer examination, differences within the 3 regions of α-synuclein (when incubated with Ezrin) also became evident. In contrast, α-synuclein incubated alone showed no differences across the different protein regions and broadening was observed at more-or-less the same rate across all residues (with the exception of the first few amino acids at later time-points).

At later stages of incubation, various residues of α-synuclein underwent chemical shifts to form second conformations, suggesting the presence of oligomeric assemblies of α-synuclein molecules. The presence of these additional conformations also showed regional differences. Clustering was predominantly observed in the NAC region and its flanking residues, while changes were also detected in the N- and C- terminal regions. Furthermore, the direction of chemical shift variation of these residues provided detailed information. Nearly all the second conformations of the NAC residues appeared to uniformly shift in a left-downward direction, indicative of electron-de-shielding or of hydrogen-bonding of the residues into structured forms, such as β-sheets or aggregates. Lastly, at later stages in the aggregation process, certain residues adopted yet another conformation, resulting in the simultaneous presence of three distinct populations of α-synuclein as detected by NMR spectroscopy. Once again, 4 of the 9 tertiary conformations were found within the NAC region, suggesting an important role for this region in the off-pathway aggregation of α-synuclein in the presence of Ezrin.

Thus, Ezrin mediates the accelerated formation of multiple off-pathway, transient and distinct species of α-synuclein with a typical NMR profile. Having established how Ezrin mediates its effect, the next question to be asked was whether these aggregates show reduced toxicity in a cellular context as compared to the toxic, on-pathway fibrillar forms of α-synuclein.

3.4 Ezrin is a potent inhibitor of α-synuclein-mediated toxicity

After having elucidated from NMR spectroscopy and biophysical analyses that Ezrin accelerates the formation of off-pathway aggregates of α-synuclein, the next question to be answered was whether these atypical aggregates are toxic to cells. To answer this question, LDH (lactate dehydrogenase) assays and MTT (3-(4,5-Dimethylthiazol-2-yl)-2,5-diphenyltetrazolium bromide) assays were conducted on rat primary neuronal cells (as described in Sections 2.2.4.2 and 2.2.4.3). Next, a *S. cerevisiae* model expressing the toxic α-synuclein mutant, A53T, was used to evaluate whether Ezrin affects α-synuclein toxicity *in vivo*. This revealed that Ezrin actually reduces the toxicity associated with α-synuclein in yeast. Lastly, Ezrin's effect on the formation of intracellular inclusions was analyzed by microscopy, using the same yeast model. Co-expression of Ezrin significantly reduced the number of A53T-α-synuclein inclusions in cells. Thus, Ezrin appears to modulate both α-synuclein-mediated toxicity and aggregation *in vivo*.

3.4.1 Ezrin reduces α-synuclein-mediated LDH release in primary neurons

In order to determine whether Ezrin is a modifier of α-synuclein *toxicity* as well as α-synuclein *aggregation,* cellular toxicity assays were employed. α-synuclein has been reported to aggregate into annular structures that form pores that disrupt membrane integrity (Lashuel et al., 2002a). Therefore, the lactate dehydrogenase (LDH) assay was employed to measure membrane integrity by monitoring the amount of cytoplasmic LDH released into the medium, thereby providing a readout of the viability of the cells. In other words, healthy, viable cells should have an intact membrane and thereby release only minimal amounts of LDH into the medium, whereas dying or compromised cells should have a weakened membrane, allowing for the release of larger amounts of LDH into the medium. The assay is based on the reduction of NAD (Nicotinamide Adenine Dinucleotide; a coenzyme found in all living cells) to NADH (the reduced form) by LDH. The NADH is then utilized in the stoichiometric conversion of a tetrazolium dye into a coloured compound, which is measured spectrophotometrically (Mosmann, 1983). The amount of LDH in cell-free aliquots of media from control- and test- samples can be used as an indicator of relative cell viability as well as a function of membrane integrity.

The LDH assay was utilized to measure whether Ezrin influences α-synuclein toxicity in cells. Hence, α-synuclein incubated with and without Ezrin for 42 h (i.e. the end-point samples from the NMR experiment described in Section 3.3 above) was added to the culture media surrounding primary rat neuronal cells, at a final concentration of 1 μM (n=3). After incubation at 37 ˚C for 24 h, the LDH assay was carried out.

As seen in Fig. 3.4.1, the α-synuclein-Ezrin sample (Syn:Ezrin 5:1) results in significantly reduced LDH release as compared to the α-synuclein sample without Ezrin (Syn only). This is indicative of greatly reduced toxicity in the α-synuclein-Ezrin sample. In fact, the LDH release of the α-synuclein-Ezrin sample is comparable to the LDH release of the buffer-only (healthy control) sample, indicating that Ezrin reduces α-synuclein-mediated toxicity to the level of the healthy control. Furthermore, cells incubated with Ezrin alone (Ezrin only) showed the same LDH release as the buffer-only healthy control. In conclusion, the presence of Ezrin at a substoichiometric (1:5) molar ratio during α-synuclein aggregation rescues α-synuclein-mediated toxicity and restores membrane integrity in primary neurons to that of healthy control cells.

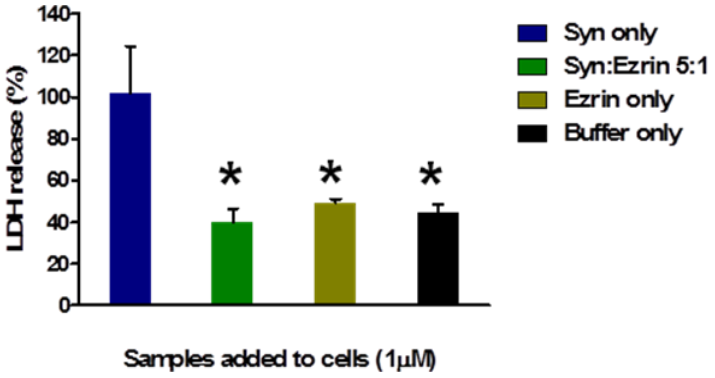

Fig 3.4.1 LDH release assay on primary neurons to which 1 μM samples of α-synuclein incubated with Ezrin (Syn:Ezrin 5:1) and without Ezrin (Syn only) for 42 h were delivered. The cells were then allowed to incubate with the samples for 24 h at 37˚C, before the assay was performed. All data were normalized to the values obtained for lysed cells (set to 100%). Cells incubated with Syn:Ezrin 5:1 showed a LDH release level consistent with that of cells to which only buffer had been added (Buffer only), i.e. the healthy control. In contrast, cells incubated with Syn only showed significantly higher levels of LDH release, often surpassing the LDH release levels of lysed cells or the positive control (i.e. 100%). Error bars represent s.e.m. * indicates P< 0.05. (n=3)

3.4.2 Ezrin incubated with α-synuclein increases MTT reduction in primary neurons

In order to confirm the results obtained from the LDH assay, another test of cellular toxicity, namely the MTT assay, was employed. The MTT assay is a colorimetric assay for measuring cellular proliferation. Cellular enzymes reduce the tetrazolium dye, MTT (3-(4,5-Dimethylthiazol-2-yl)-2,5-diphenyltetrazolium bromide, a yellow tetrazole), to insoluble formazan, giving a purple color. Efficient MTT reduction indicates high metabolic activity of the cells. If Ezrin were indeed capable of reducing the toxicity of α-synuclein, one would expect that cells incubated with the α-synuclein-Ezrin sample would generate more of the purple formazan produced by MTT reduction than cells incubated with α-synuclein only. A

solubilization solution containing SDS and dimethyl sulfoxide is added to cells to dissolve the insoluble purple formazan product into a colored solution, the absorbance of which is quantified by measuring the colour at a specific wavelength (around 560 nm) using a spectrophotometer. Reduction takes place only when mitochondrial reductase enzymes are active and therefore conversion can be directly related to the number of viable cells. Thus, the intensity of the absorbance is used as a readout of the number of metabolically active cells.

Similar to the LDH assay described above, α-synuclein was incubated with and without Ezrin (Syn:Ezrin 5.1) and delivered to primary cultures of rat neurons (n=3) for 24 h at three different concentrations, namely 4 µM, 2 µM and 1 µM. The MTT assay results (displayed in Fig 3.4.2 below) once again demonstrate that α-synuclein incubated with Ezrin results in significantly greater MTT reduction than α-synuclein incubated alone (which shows marginal MTT reduction). This is indicative of a toxicity-diminishing role for Ezrin within the cellular context. In fact, at higher concentrations, e.g. 4 µM, the α-synuclein-Ezrin mixture even appears to confer an advantage (i.e. increased MTT reduction) over control cells to which only buffer was added. This effect cannot simply be attributed to a beneficial role of Ezrin in the cells, as the 'Ezrin only' sample does not show a significantly larger MTT reduction as compared to the 'Buffer only' control. At lower concentrations of α-synuclein its toxicity decreases, which means that the difference in toxicity between α-synuclein incubated with Ezrin and α-synuclein incubated without Ezrin becomes less pronounced.

In all cases Ezrin rescued the metabolic activity at least to the level of control cells incubated with buffer only. In conclusion, and in keeping with expectations, when α-synuclein incubated with Ezrin was delivered to cells there was a significant rescue of metabolic activity, suggesting that co-incubation with Ezrin leads to an aggregation product that is non-toxic to cultured primary neurons. Thus, both cellular toxicity assays independently demonstrate that Ezrin significantly decreases the cytotoxicity of aggregated α-synuclein.

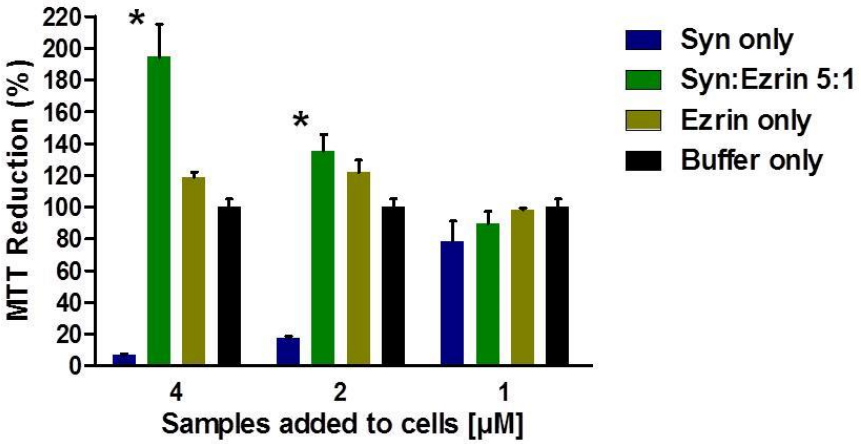

Fig 3.4.2 MTT reduction assay on primary neurons to which α-synuclein alone or α-synuclein incubated with Ezrin were delivered, over a range of concentrations. 4 µM α-synuclein incubated with Ezrin (Syn:Ezrin 5:1) showed a significantly greater MTT reduction than the same concentration of α-synuclein incubated alone (Syn only). A similar effect was observed for the experiment at 2 µM, whereas at a concentration of 1 µM the differences between the two α-synuclein conditions ceased to be significant. Ezrin incubated alone (Ezrin only) showed a value of MTT reduction that did not vary significantly from the 'Buffer only' control. Hence, Ezrin alone neither inhibited nor greatly enhanced MTT reduction. All data were normalized to the values obtained for cells to which only buffer was added ("Buffer only" control, set to 100%) and took into account the background MTT reduction observed even in lysed cells. Error bars represent s.e.m. * indicates P< 0.05 (n=3).

3.4.3 Ezrin rescues α-synuclein-mediated toxicity *in vivo* in *S. cerevisiae*

As mentioned in the introduction, baker's yeast - *S. cerevisiae*, one of the simplest eukaryotic organisms - is commonly used for modeling various intracellular processes that are of relevance even in higher species, such as rodents and humans (Karathia et al., 2011; Zakrajsek et al., 2011). It has been used extensively to model protein misfolding and toxicity in human neurodegenerative disorders (Miller-Fleming et al., 2008). The simplicity of the yeast genome allows many processes such as protein-protein interactions and intracellular aggregation of amyloidogenic proteins to be examined directly and easily in this organism. Keeping this in mind, certain research-groups have taken advantage of *S. cerevisiae* to develop a model for studying α-synuclein aggregation and toxicity *in vivo* (Outeiro and Lindquist, 2003). Briefly, in this model the gene coding for the highly toxic mutant of α-synuclein - A53T- was fused at its C-terminus to a GFP-construct and integrated into the yeast genome just after a galactose-inducible promoter (2 copies), such that addition of galactose to the growth medium induces the expression of α-synuclein. This α-synuclein protein is not only highly toxic to the yeast (as measured by growth assays) but also forms intracellular aggregates, which can be detected as large, GFP-positive inclusions using a fluorescence microscope (Outeiro and Lindquist, 2003). When grown in glucose-medium,

however, expression of mutant α-synuclein is not induced and the yeast cells remain healthy and inclusion-free. Upon transformation of the yeast cells with a pAG425-FLAG plasmid containing a galactose-inducible promoter and the Ezrin gene (or known toxicity enhancer- and suppressor- genes), it is possible to simultaneously induce the expression of a N-terminally Flag-tagged fusion protein (Ezrin/ toxicity enhancers/ toxicity suppressors) and α-synuclein in yeast cells grown in galactose-containing medium. This allows one to evaluate the effect of Ezrin *in vivo* on α-synuclein-mediated toxicity and aggregation.

3.4.3.1 Growth in galactose-containing medium results in the expression of A53T-α-synuclein and Ezrin

In order to confirm that neither α-synuclein nor Ezrin is produced in glucose-containing medium, but that both are expressed in galactose-containing medium, yeast cells were grown in parallel in both types of media, lysed and then analyzed by SDS-PAGE and immunoblotting using anti-α-synuclein and anti-Flag-tag antibodies. As seen in Fig 3.4.3.1, both proteins are expressed *only* in the presence of galactose in the medium and neither is expressed in glucose-containing medium, confirming the validity of the system as a suitable assay for gauging the effects of Ezrin on α-synuclein. Although A53T-α-synuclein is a small protein and usually resolves at 17-19 kDa, the presence of the large GFP-tag (~27 kDa) at its C-terminus causes it to resolve at 44-46 kDa. This is in accordance with the data in Fig. 3.4.3.1. Similarly, full-length wild-type Ezrin usually resolves at 69 kDa, and with the 1 kDa Flag-tag at its N-terminal end, it is expected to resolve at 70 kDa, which is in keeping with the results in Fig 3.4.3.1.

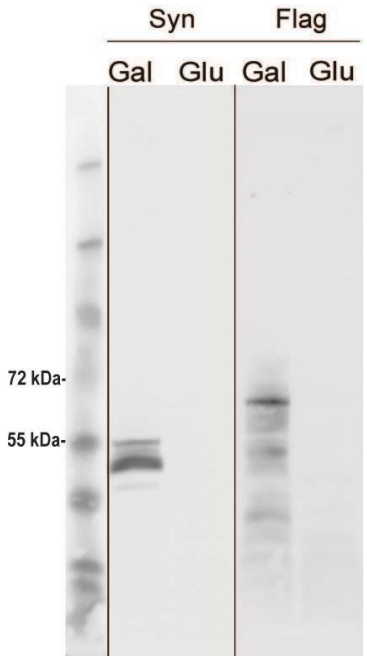

Fig 3.4.3.1 SDS-PAGE and immunoblotting of lysates of yeast cells grown for 24 h in galactose- and glucose-containing media. α-synuclein and Ezrin were detected with anti-α-synuclein and anti-Flag antibodies, respectively. As expected, the α-synuclein-GFP fusion protein resolved at ~46 kDa, while Flag-tagged Ezrin resolved at ~70 kDa. The smeary appearance of the Flag-tagged Ezrin (Gal lane) could be due to degradation of the protein, along with background noise contributed by proteins to which the anti-Flag antibody non-specifically binds. Similar background noise is detected at a lower level by the anti-Flag antibody even in the non-expressing condition (Glu lane).

3.4.3.2 Ezrin enhances the growth of A53T-α-synuclein-expressing yeast cells

After having confirmed that Ezrin and A53T-α-synuclein are co-expressed in galactose-containing medium, the next step was to carry out growth assays using yeast cells expressing both proteins, in order to determine whether Ezrin also acts as an inhibitor of α-synuclein toxicity in living organisms. To this end, two distinct types of growth tests were carried out to assess possible Ezrin-mediated changes in yeast growth, both qualitatively and quantitatively, as detailed below:

Growth tests on solid agar: As described in Section 2.2.5.5, serial dilutions of the yeast cultures were prepared in 96-well plates and stamped onto NBG -ut/ahl agar plates containing the carbon sources glucose or galactose. Plating on galactose activates the GAL-promoter that precedes the α-synuclein-GFP and blank-vector-GFP constructs integrated into the yeast genome, as well as the N-terminally Flag-tagged-gene in the plasmid transformed into the yeast, resulting in over-expression of α-synuclein-GFP and/or Flag-tagged fusion proteins. Plating on glucose, however, does not activate the GAL-promoter, thus, neither α-synuclein-GFP expression nor Flag-tagged fusion protein expression is induced. After 120 h of incubation at 30°C digital images of yeast colonies were taken, and colony growth was examined densitometrically.

The proteins ATP2C1 and NRG1 were used as negative controls as they are toxicity enhancers well-described in the literature and known to significantly inhibit the growth of yeast via their interaction with α-synuclein (Outeiro and Lindquist, 2003). As expected, the toxicity they induce in yeast cells - when expressed - was so strong that their growth on galactose-containing media (Rows 2 and 3 in Fig. 3.4.3.2.A below) was negligible. Similarly, the protein RAB1A, known to suppress α-synuclein-associated toxicity in yeast (Outeiro and Lindquist, 2003) was used in this study as a positive control for yeast growth. Coexpression with α-synuclein-GFP resulted in improved growth of yeast cells on galactose-containing medium (Row 4) as compared to A53T-Syn and Vector only (Row 5). Finally, yeast colonies expressing both A53T-Syn and Ezrin grew better than yeast cells expressing A53T-Syn and Vector only (Row 1 vs. Row 5, lower concentrations) and even grew better than the positive

control- A53T-Syn + Tox. Supp. (Row 1 vs. Row 5, lower concentrations), suggesting that Ezrin does, indeed, act as a suppressor of α-synuclein-mediated toxicity in living organisms.

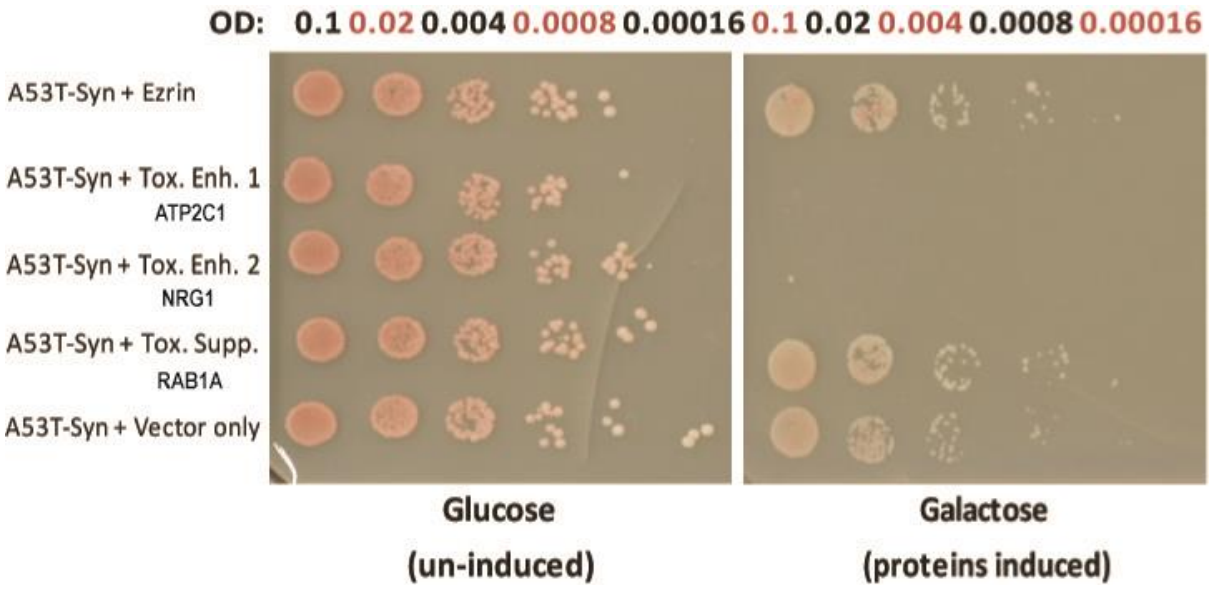

Fig 3.4.3.2.A Ezrin inhibits α-synuclein-mediated toxicity in yeast. Both the toxicity-enhancing proteins are only toxic in the galactose-induced condition in which α-synuclein is also expressed. Closer examination reveals that the galactose-induced Ezrin- and α-synuclein- expressing yeast strain contains numerous, large and distinct colonies at more than one concentration, indicating healthy growth of the yeast. This strain shows a significant increase in healthy, round colonies even at the lower dilutions, than the vector only- and Tox. Supp.- strains. N.B. Enhancers of toxicity are not toxic in the control-GFP-vector-containing strain which does not express α-synuclein. Expression vector: pAG425-FLAG (Gal promoter); yeast strain with gene expressing A53T-α-synuclein integrated in genome: a kind gift from Outeiro & Lindquist.

Growth tests in liquid culture: As described in Section 2.2.5.5, 100 ml each of glucose-containing and galactose-containing NBG -ut/ahl media were inoculated with yeast cultures to a starting OD_{600} of 0.01 and incubated at 30°C for 72 h, before the final OD_{600} was measured. The same proteins used as positive and negative controls in the previous growth test (namely, RAB1A, ATP2C1 and NRG1) were employed as toxicity suppressor/enhancers in this assay and they yielded identical results. A53T-Syn and NRG1 co-expression resulted in a significant decrease in yeast cell growth, whereas A53T-Syn and RAB1A co-expression partially rescued this effect, resulting in enhanced yeast cell growth as compared to the A53T-Syn and vector only sample. Similar to the results obtained from the growth tests on solid agar, the growth tests in liquid culture (see Fig. 3.4.3.2.B below) showed that yeast colonies expressing both A53T-Syn and Ezrin, grew better than yeast cells expressing A53T-Syn and the vector only. Furthermore, as expected, growth of the A53T-Syn + Ezrin sample was comparable to that of the A53T-Syn + toxicity suppressor sample, demonstrating that co-expression of Ezrin in A53T-α-synuclein-expressing yeast cells not

only rescues the toxicity-phenotype, but even enhances cell-growth to the level of the well-established toxicity-suppressor, RAB1A. Hence, examination of the same yeast strains and controls in multiple formats confirms a role for Ezrin as a potent suppressor of α-synuclein-mediated toxicity in yeast.

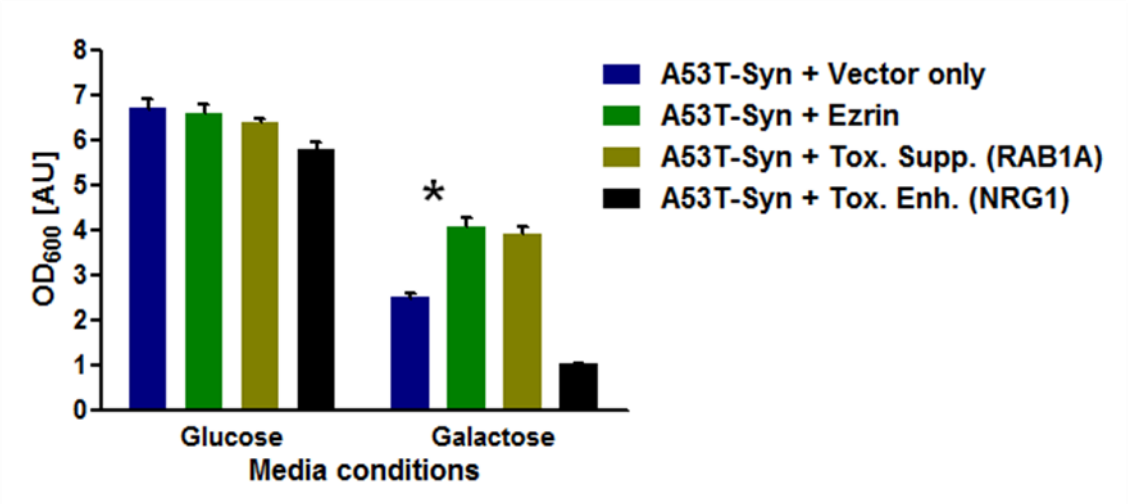

Fig 3.4.3.2.B Ezrin inhibits α-synuclein-mediated toxicity in liquid yeast cultures. OD_{600} measurements were carried out after 60 hours of incubation of the yeast cultures at 30˚C. In the galactose-induced condition, A53T-α-synuclein is seen to be highly toxic to the yeast cells, a condition which is further enhanced by the NRG1 protein (a known toxicity-enhancer), considerably suppressed by the RAB1A protein (a known toxicity-suppressor) and also significantly suppressed by Ezrin (to the level of toxicity-suppression seen for RAB1A, the positive control). Under conditions in which α-synuclein is not expressed, i.e. growth on a glucose-containing medium, all 4 types of yeast cultures show similar OD_{600} values (generally above 5.5 AU, with inter-sample variability being non-significant). Error bars represent s.e.m. * indicates P< 0.05. (n=3).

3.4.3.3 Ezrin inhibits A53T-α-synuclein aggregation in yeast

As mentioned above, 'A53T-α-synuclein-GFP' yeast cells carry 2 copies of the mutant- α-synuclein gene integrated into their genome. Galactose-inducible expression of A53T-α-synuclein-GFP results in the formation of foci or aggregates of α-synuclein within yeast cells (as seen in Fig 3.4.3.3.A below). Simultaneous co-expression of Ezrin significantly decreases the formation, size and numbers of such foci or aggregates. This was further confirmed by quantification, in which the number of aggregate-forming cells relative to the total number of α-synuclein-expressing cells (with and without Ezrin co-expression) was counted (refer to Fig 3.4.3.3.B). As expected, the proportion of yeast cells expressing A53T-Syn and Ezrin and containing aggregates was significantly lower than the proportion of yeast cells expressing A53T-Syn and vector only and containing aggregates. Thus, Ezrin not only

reduces α-synuclein-mediated toxicity in *S. cerevisiae* but also decreases the abundance of α-synuclein aggregates.

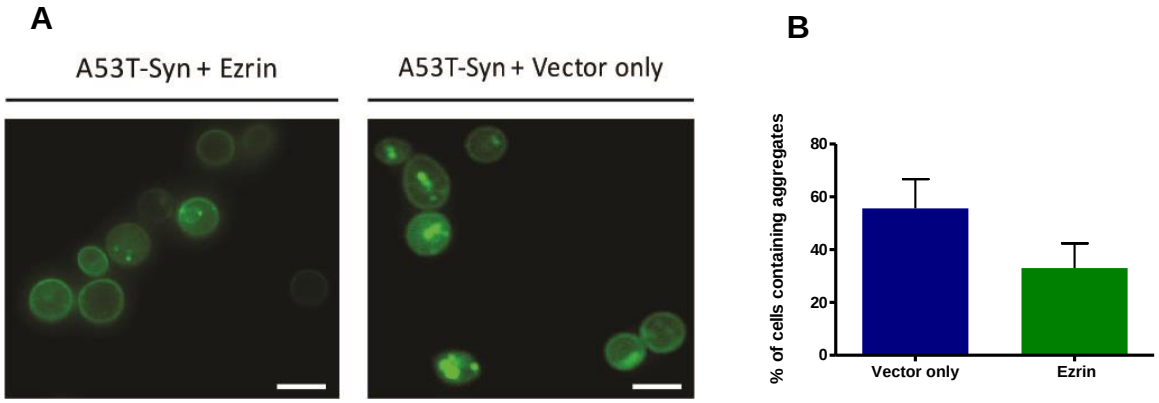

Fig 3.4.3.3 Ezrin inhibits aggregation of A53T-α-synuclein in yeast. (A) Co-expression of Ezrin significantly reduces the size and number of punctate aggregates formed in A53T-α-synuclein-expressing yeast cells. Also, the numbers of cells producing A53T-Syn aggregates under conditions of co-expression with Ezrin are greatly decreased. (B) Quantification of the numbers of aggregate-forming cells relative to total numbers of A53T-α-synuclein-expressing cells in the presence and absence of Ezrin (Ezrin and Vector only, respectively). Values are represented as the percentage of A53T-Syn-expressing cells containing aggregates. For each quantification, at least 100 A53T-Syn-expressing cells per condition were counted (n=3, where n refers to a single quantification per condition). Error bars represent s.e.m. * indicates P< 0.05.

3.4.4 Chapter Summary

In order to determine whether Ezrin can reduce α-synuclein-mediated *toxicity*- in addition to its role in modifying α-synuclein *aggregation*- it is necessary to examine the effect of Ezrin on α-synuclein aggregation in various *in vivo* settings. This has been approached in multiple ways, starting with the usage of two distinct cellular toxicity assays- the lactate dehydrogenase assay and the MTT assay. Both assays clearly demonstrate that α-synuclein fibrils are highly toxic to cells, whereas the aggregates of α-synuclein obtained in the presence of Ezrin are not. In fact, the lack of toxicity of Ezrin-mediated α-synuclein-aggregates on primary neuronal cultures is comparable to the toxicity levels of untreated control cells, indicating a complete rescue of α-synuclein toxicity under these conditions.

Furthermore, yeast cells that are capable of being induced to express both α-synuclein and Ezrin simultaneously provide the ideal *in vivo* environment in which to study the effect of Ezrin on α-synuclein toxicity and aggregation in a simple model organism. Co-expression of Ezrin rescues the toxicity mediated by A53T-α-synuclein when induced in liquid and plated yeast cultures, and simultaneously reduces the occurrence of large, intracellular aggregates

of A53T-α-synuclein in induced cultures. Thus, Ezrin plays a role in inhibiting the toxicity associated with typical aggregates of α-synuclein.

4. DISCUSSION

The formation of insoluble amyloidogenic protein aggregates is a characteristic hallmark of many neurodegenerative diseases, including Parkinson's disease. In this disease, α-synuclein is known to form not only the traditional amyloid fibrils referred to above, but also pre-fibrillar, small, soluble aggregates called oligomers, which are intermediates in the amyloid formation cascade and are thought to play an important role in disease pathogenesis. Despite large bodies of data implicating a role for α-synuclein in the pathogenesis of PD, and intensive analysis of the various forms of α-synuclein thought to mediate toxicity, there is presently no cure for the disease, and particularly, no treatment that targets the misfolding and deposition of the protein. Therefore, the aim of this project was to screen a large number of protein candidates in order to find novel modifiers that directly inhibit the aggregation of α-synuclein into the insoluble amyloid fibrils typical of PD and thereby help to identify new targets for therapeutic drugs that could interfere with early processes in the disease pathology.

4.1 An unbiased screen of 13,824 proteins reveals novel and potent modulators of α-synuclein fibrillization

An unbiased protein library encompassing 13,824 proteins had previously been generated by "shotgun cloning" for expression in *E.coli* (RZPD cDNA Library; Source: RZPD - Deutsches Ressourcenzentrum für Genomforschung [http://www.rzpd.de/]). The proteins in this library were expressed in pools of eight and then purified through His-tag affinity. As previously described in Section 2.2.2.16, α-synuclein was incubated with the various proteins together with the amyloid-binding fluorescent dye, Thioflavin-T, and aggregation kinetics were recorded so that an increase in fluorescence would act as a readout of amyloid formation. Several proteins were thus identified that strongly delayed or - in the case of Ezrin - completely prevented the formation of Thioflavin-T-binding fibrils, which indicated that the candidate protein in that mixture acted as an inhibitor of α-synuclein fibrillization. In this way, subsequent to successive rounds of screening, the following thirteen novel modifiers of α-synuclein fibrillization were identified: EZR, HMG20A, HMGN2, HNRPDL, IGSF4, NBL1, NONO, OTUD5, PABP1, PFDN5, PNMA1, RPL7 and RPS4X.

It was interesting to see that these modifiers were highly diverse proteins, in terms of size, localization, binding partners, etc., yet within this small sub-group of 'final hits', certain functional classes (e.g. RNA-binding) and particular expression patterns (e.g. expression in the testis) were strongly represented. Thus, by employing an unbiased screen, certain

categories of proteins seemed to emerge as inhibitors of α-synuclein fibrillization and one might speculate that these classes play an important (albeit undeciphered) role in this process. A minimum of 3 modifiers was deemed as being necessary to define a category which was 'strongly represented' among the hits from the screen.

Fig 4.1 below depicts the 'strongly represented' categories of protein modifiers, which can be further divided into 'functional' and 'expression-based' categories. The following discussion of modifiers and their properties has been based on information presented and referenced in the table presented in Section 3.1.6:

1) Functional categories: The top 13 modifiers from the screen were seen to be involved in multiple processes, of which '*RNA-processing/binding or poly(A)-related function*' was the most strongly represented, with six member proteins (see Fig. 4.1 below). The next functional class to be strongly represented was '*40S/60S ribosomal protein-associated*' with four members, followed by '*chaperone/UPS-associated*' proteins and '*cytoskeleton-associated*' proteins, with three members each. Interestingly, three of the 'hits' (namely, EZR, NONO and OTUD5) were already known to be indirectly associated with Parkinson's disease mutations (*PD mutant-associated*) as shown in Section 3.1.6, although no direct role had been demonstrated for their involvement in this disease. Four modifiers were known from the scientific literature to be '*neurological disorder- associated*' (i.e. HMG20A in mental retardation and nocturnal frontal lobe epilepsy; PNMA1 in paraneoplastic neurological disorders; RPS4X in Turner syndrome (rarely associated with cognitive deficits) and RPL7 in systemic lupus erythematosis (which may affect the brain and nervous system)). Four other modifiers were similarly known to play a role in cancer, i.e. EZR in metastasis; NBL1 as a suppressor of tumorigenicity; HMGN2 in tumour endothelial cells and IGSF4 as a tumour suppressor of non-small-cell lung cancer, were all termed '*cancer-associated*'.

2) Expression-based categories: Strikingly, the majority of the modifiers (eight in number, namely, EZR, HMG20A, HMGN2, IGSF4, NBL1, NONO, OTUD5 and PNMA1) were proteins showing '*brain expression*', while four modifiers (HMG20A, HMGN2, HNRPDL and NONO) unsurprisingly showed '*ubiquitous expression*'. It was unexpected that five modifiers were expressed in the testis, if not exclusively, then certainly in enriched proportions ('*testis expression*' of HMG20A, HMGN2, HNRPDL, IGSF4 and PNMA1). This was a novel finding and could be of potential interest for further studies.

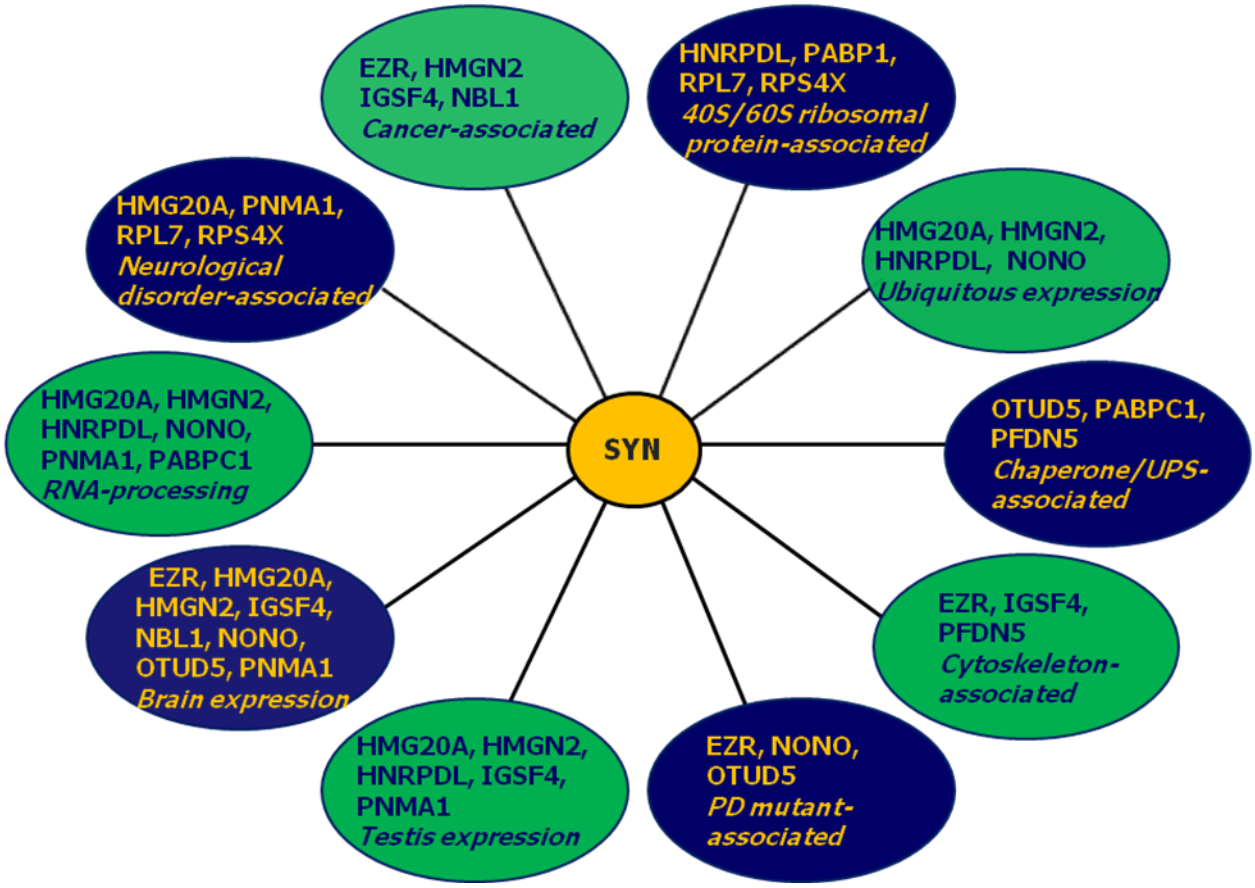

Fig. 4.1 Classification of the top 13 modifiers from the screen into functional and expression-based categories. The category name, e.g. RNA-processing, is shown in italics below the names of the genes that make up the category, while α-synuclein (SYN) is shown in the center.

In addition, it has been shown that the transcriptional co-factor high mobility group protein 1 (HMG1) is able to bind preferentially to aggregated α-synuclein and is present in α-synuclein filament-containing LBs isolated from brain tissue affected with LBD and PD (Lindersson et al., 2004). This is of particular interest as two high mobility group proteins: HMGN2 (nucleosomal binding domain 2) and HMG20A (protein 20A) were identified in the screen as being two of the most potent inhibitors of α-synuclein fibrillization. Further work on the family of HMG proteins and their striking involvement in α-synuclein fibrillization could shed more light on this issue.

It is also interesting to note that the screen did not reveal modulators that *increase* the rate of α-synuclein fibrillization, i.e. promoters of fibrillization. Many proteins have been reported to stimulate or speed up the fibrillization process of α-synuclein in the scientific literature: The list of these aggregation promoters includes tau protein (Giasson et al., 2002b), brain-specific protein p25α (Lindersson et al., 2005), and tubulin (Alim et al., 2002). However,

none of the proteins screened in this study appeared to significantly accelerate the rate of α-synuclein fibrillization, which may be explained as follows:

The presence of the stirring glass-bead brings about shearing forces within the solution, which results in the fragmentation of newly-formed or forming fibrils into smaller species, e.g. oligomers, proto-fibrils, etc. These act as nuclei for the available monomeric α-synuclein in the solution, which then also starts to fibrillize. So, instead of just one or a few nucleating centers being present within the solution, as shearing forces are generated by the stirring glass-bead over the course of α-synuclein fibril formation, multiple nucleating centers are generated, which seed the accelerated fibrillization of α-synuclein. In this case, the rate-limiting factor may be considered to be secondary seed formation through fibril fragmentation by the stirring bead (Knowles et al., 2009). Proteins that accelerate α-synuclein fibrillization by a similar mechanism may thus have been obscured.

4.2 Ezrin- the most potent inhibitor of α-synuclein fibrillization: Its role in the nervous system and diseases thereof

While all the thirteen modifiers represented in Fig 4.1 showed a concentration-dependent inhibition of α-synuclein fibrillization, Ezrin stood out as being the most potent modulator. The reason for this was that at concentrations as low as Ezrin:α-synuclein 1:5, fibrillization appeared to be completely inhibited. Thioflavin-T fluorescence was nearly completely absent even at the late stages of the reaction [refer to Section 3.1.6], suggesting that Ezrin may be sufficient to completely block or prevent the formation of fibrils with a typical cross-β-pleated-sheet structure. This was one of the major arguments for the selection of Ezrin as the modifier of choice for downstream experiments. Another reason for the selection of Ezrin was the presence of various studies from the scientific literature which suggested a role for Ezrin not just in the nervous system, but also in the pathogenesis of Parkinson's disease (as discussed in detail in Section 3.1.7).

In the following sections, the potential role of Ezrin in the brain and in brain-related diseases (Section 4.2.1) is examined, followed by a discussion of the biophysical and biochemical data that demonstrate the powerful inhibition of α-synuclein fibrillization by Ezrin (Section 4.2.2).

4.2.1 The role of Ezrin in the nervous system and in neurological disease

As mentioned previously in Section 3.1.7, various studies from the literature reveal a role for Ezrin in the nervous system, and in particular, a role in Parkinson's disease and other neurological diseases. For instance, phosphorylated Ezrin influences cortical neuron growth, morphology and motility *in vitro* (Li et al., 2007b). Ezrin expression is detected in the cerebrum at 20 weeks of gestation (Johnson et al., 2002) and later at 30 weeks of gestation (Johnson et al., 2002) indicating a role for Ezrin in neurogenesis. The phosphorylation of Ezrin by leucine-rich repeat kinase 2 (LRRK2) promotes the rearrangement of the actin cytoskeleton in neuronal morphogenesis (Parisiadou et al., 2009), which provides an indirect link to Parkinson's disease, as follows:

Variants of the LRRK2 gene are associated with an increased risk of Parkinson's disease (Paisan-Ruiz et al., 2004). Furthermore, the expression of LRRK2 mutants implicated in autosomal dominant Parkinson's disease causes shortening and simplification of the dendritic tree *in vivo* and in cultured neurons (MacLeod et al., 2006). The Gly2019Ser mutation in LRRK2 is a relatively common cause of familial Parkinson's disease in

Caucasians (Gilks et al., 2005) and may also cause sporadic Parkinson's disease. This mutation elicits post-synaptic calcium imbalance, leading to excess mitochondrial clearance from dendrites by mitophagy (Cherra et al., 2013). LRRK2 functions as a putative protein kinase of ezrin-family proteins, and the G2019S substitution in the kinase domain of LRRK2 further enhances their phosphorylation (Parisiadou et al., 2009). The phosphorylated proteins are restricted to the filopodia of growing neurites in which they tether filamentous actin (F-actin) to the cytoplasmic membrane and regulate the dynamics of filopodia protrusion. In cultured neurons derived from LRRK2 G2019S transgenic mice, the number of phosphorylated ezrin-family proteins and F-actin-enriched filopodia is significantly increased and this correlates with the retardation of neurite outgrowth.

Conversely, deletion of LRRK2, which lowers phosphorylated ezrin-family proteins and F-actin content in filopodia, promotes neurite outgrowth. Furthermore, inhibition of phosphorylation or actin polymerization rescues the G2019S-dependent neuronal growth defects. These data are supported by the finding that LRRK2 has been seen to phosphorylate Moesin (a protein with extremely high homology to Ezrin, described in detail in Section 3.2.1.3) at threonine-558, thereby characterizing how Parkinson’s disease mutants affect kinase activity (Jaleel et al., 2007). Lastly, an analysis of the susceptibility genes in Chinese pedigrees with early-onset familial Parkinson's disease (FPD) revealed two missense mutations, one of which was a single-nucleotide polymorphism at exon 5 of LRRK2 (Xu et al., 2010). Taken together, these studies suggest a potential involvement of Ezrin in some of the underlying mechanisms of Parkinson’s disease.

A final search for a direct connection linking α-synuclein and Ezrin did not readily appear in the literature (pointing once again to the novelty of this work), however an interesting connection of another nature was revealed: A study on aberrant expression of proteins in the hippocampus of patients with mesial temporal lobe epilepsy (MTLE) showed that although certain cytoskeleton proteins, e.g. tubulin α-1 chain, were significantly reduced, Ezrin levels were significantly increased in MTLE, as were the levels of synaptosomal proteins, e.g. synaptotagmin I and α-synuclein (Yang et al., 2006). The authors concluded that the findings may indicate cytoskeletal impairment and that altered synaptosomal protein expression possibly reflects simultaneous synaptic impairment in MTLE. Thus, while no studies exist in the literature that directly link α-synuclein with Ezrin, there is ample indirect evidence for a potential interaction of Ezrin with α-synuclein, and further, for a potential role of Ezrin in Parkinson’s disease.

4.2.2 The potent inhibition of α-synuclein fibrillization by Ezrin

In addition to the presence of Ezrin in the nervous system and its potential involvement in Parkinson's disease, the strong inhibition of α-synuclein fibrillization at sub-stoichiometric concentrations by Ezrin resulted in this protein being selected as the most promising modifier for downstream analyses. Various methods have been employed in this study to demonstrate that Ezrin inhibits the formation of traditional SDS-resistant higher-molecular-weight oligomers and aggregates by re-directing α-synuclein into off-pathway species instead.

Biochemical methods: Western blot analysis of samples of α-synuclein incubated with and without Ezrin for different lengths of time [refer to Section 3.2.4] and filter-retardation assays of end-point samples of α-synuclein incubated with and without Ezrin [refer to Section 3.2.5] clearly showed a significant decrease in the build-up of SDS-resistant higher-molecular-weight-oligomers and aggregates, respectively, in the presence of Ezrin.

Biophysical analysis: Atomic force microscopy (AFM) images clearly showed the formation of round, off-pathway aggregates of α-synuclein in the presence of Ezrin as opposed to the traditional long fibrils formed by α-synuclein when incubated alone [refer to Section 3.2.6].

Supporting evidence: This strong inhibitory effect on α-synuclein fibrillogenesis is not just limited to Ezrin, as protein family members sharing a high homology with Ezrin have an analogous effect on α-synuclein fibrillization, while proteins with lower homology to Ezrin do not [refer to Section 3.2.1.3]. Additionally, Ezrin affects early-stage oligomers or intermediates of α-synuclein – and not later-stage structures – as it only succeeds in inhibiting α-synuclein fibrillization when added to the solution at the early stages of incubation, i.e. before 10 hours of incubation have elapsed (refer to Section 3.2.4). Ezrin added later, i.e. 10 or more hours after the start of incubation, no longer has an effect on α-synuclein fibrillization.

In conclusion, Ezrin appears to directly modulate the fibrillization of α-synuclein. In the next section, therefore, we compare the effect of Ezrin on α-synuclein aggregation with that of other known modifiers of α-synuclein fibrillization, including small molecule inhibitors and chaperone proteins.

4.3 Comparison of the effect of Ezrin on α-synuclein fibrillogenesis with that of other known modifiers from the scientific literature

Keeping in mind the potency and nature of the effect of Ezrin on α-synuclein fibrillization, it may be of use to compare Ezrin with other known modifiers of α-synuclein fibrillization from the scientific literature. This may help to uncover common underlying features, if any, and also highlight striking differences in the actions of the different modifiers. For ease of analysis, this comparison has been divided into two sections:

4.3.1 Small molecule inhibitors of α-synuclein fibrillization

In the fields of pharmacology and biochemistry, a small molecule is a low-molecular-weight organic compound that may serve as a regulator of biological processes (Arkin et al., 2003). (The upper molecular weight limit for a small molecule is approximately 800 Daltons, which makes it possible for the molecule to rapidly diffuse across cell membranes so that it can reach intracellular sites of action (Veber et al., 2002)). In pharmacology, specifically, the term is usually restricted to a molecule that binds to a biopolymer such as a protein, nucleic acid, or polysaccharide and acts as an effector, thereby altering the activity or function of the biopolymer (Wilson and Arkin, 2011). Small molecules may function across a variety of cell types and may inhibit a specific function of a multifunctional protein or disrupt protein-protein interactions (Arkin and Wells, 2004). They may also have diverse biological functions, serving as cell-signalling molecules, tools in molecular biology and drugs in medicine, amongst others.

In this section, we provide an overview of different small molecules in order to introduce different possible mechanisms of intervention, e.g. inhibition of fibril formation, dissolution of large fibrils and induced formation of off-pathway aggregates or oligomers. Natural compounds, such as dopamine, baicalein and epigallocatechin gallate, as well as artificial compounds, e.g. rifampicin, have been provided as examples:

Dopamine and other catecholamines. The common pathway for both idiopathic and familial PD involves the damage and subsequent loss of dopaminergic neurons (Maguire-Zeiss and Federoff, 2003). This neurodegeneration, being accompanied by the formation of α-synuclein-containing LBs and LNs in the SN pars compacta (SNpc), clearly brings together α-synuclein, its aggregation and dopamine. The products of the oxidation of catecholamines, such as L-DOPA (L-3,4-dihydroxyphenylalanine) and dopamine, are inhibitors of α-synuclein fibrillization that are even more potent than the catecholamines themselves (Li et al., 2004a).

In a systematic analysis of the inhibitory effect of a library containing 169 drug-like molecules on α-synuclein fibrillization, it was established that all but one of 15 fibril inhibitors were catecholamines related to dopamine (Conway et al., 2001).

The inhibitory activity of dopamine was attributed to the formation of covalent adducts between the o-quinone derivative of dopamine and α-synuclein, causing an accumulation of covalently modified protofibrils that were unable to fibrillize (Conway et al., 2001). In agreement with this conclusion, it has recently been shown that in the initial phase of α-synuclein aggregation, dopamine *induces* soluble sodium dodecyl sulphate (SDS) - resistant oligomers which are non-amyloidogenic (Cappai et al., 2005). This is of interest when compared with the action of Ezrin (and homologous family members), as it is highly likely that Ezrin acts at exactly this initial phase of α-synuclein aggregation to *inhibit* the formation of sodium dodecyl sulphate - resistant oligomers, as presented in Section 3.2.4.

Baicalein. Baicalein, a component of the traditional Chinese herbal medicine *Scutellaria baicalensis*, is known to have multiple biological activities including anti-allergic, anti-carcinogenic and anti-HIV properties (Gao et al., 2001; Li et al., 2000). Micromolar concentrations of baicalein and its oxidized forms were shown to inhibit the formation of α-synuclein fibrils and to disaggregate the preformed fibrils *in vitro* giving rise to soluble oligomers (Zhu et al., 2004). In some ways, the effect of baicalein on α-synuclein also mirrors the effect of Ezrin on α-synuclein, as here, too, micromolar quantities are sufficient to almost completely inhibit α-synuclein fibrillization, and off-pathway, transient oligomeric species are generated during the process of α-synuclein aggregation, as shown in Section 3.3.6. However, unlike baicalein, Ezrin is unable to disaggregate preformed fibrils *in vitro*. Moreover, in contrast to the studies from the literature which show that the action of certain small molecules could actually result in increased toxicity, Ezrin – due to its unique mechanism of action – actually brings about the formation of distinct, non-toxic oligomers of α-synuclein and even reduces α-synuclein-mediated toxicity *in vivo* when delivered to neuronal cell cultures or expressed in yeast.

Rifampicin. Rifampicin is a semi-synthetic derivative of the rifamycins, a class of antibiotics that are fermentation products of *Nocardia mediterranei* (Furesz, 1970). Rifampicin was shown to inhibit α-synuclein fibrillization *in vitro* and to disaggregate preformed fibrils in a concentration-dependent manner, leading to the formation of soluble oligomers comprised of partially folded α-synuclein (Li et al., 2004b). This mechanism of inhibition would presumably vary significantly from the mechanism of action of Ezrin on α-synuclein, because

aggregates, and not oligomers, are the end-product of the Ezrin-α-synuclein incubation reaction, and because Ezrin does not disaggregate preformed fibrils, as discussed above.

Epigallocatechin gallate (EGCG): Also known as (-)-epigallocatechin-3-gallate, EGCG is the ester of epigallocatechin and gallic acid. EGCG is the most abundant catechin in tea and is a potent antioxidant. It is found in green tea but not in black tea, because during black tea production the catechins are converted to theaflavins and thearubigins (Lorenz et al., 2009). The polyphenol (-)-epigallocatechin gallate efficiently inhibits the fibrillogenesis of both α-synuclein and amyloid-ß by directly binding to natively unfolded polypeptides, preventing their conversion into toxic, on-pathway aggregation intermediates. Instead of ß-sheet-rich amyloid, the formation of unstructured, non-toxic α-synuclein and amyloid-ß oligomers of a new type is promoted, suggesting a generic effect on aggregation pathways in neurodegenerative diseases (Ehrnhoefer et al., 2008).

In some ways, this provides a parallel for the effect of Ezrin on α-synuclein, in that Ezrin also prevents the formation of the traditional, toxic, on-pathway aggregation intermediates of α-synuclein. Instead of ß-sheet-rich amyloid, the formation of round, non-toxic α-synuclein aggregates of a new type is promoted. The difference, of course, is that while EGCG binds to natively unfolded polypeptides, Ezrin appears not to do the same. The data suggest, instead, that Ezrin mediates its effect on early-stage oligomers of α-synuclein, diverting them into an alternative “off”-pathway. Additionally, while EGCG-induced α-synuclein aggregates are stable against SDS-denaturation, Ezrin reduces the formation of SDS-resistant aggregates (and other species) of α-synuclein. Furthermore, EGCG does not slow α-synuclein fibrillization at low sub-stoichiometric concentrations. Only at a 1:1 ratio of EGCG:α-synuclein does EGCG mediate its effect of complete inhibition of fibril-formation. Ezrin has quite the opposite effect, whereby rather low molar ratios of Ezrin:α-synuclein (1:5 and below) inhibit α-synuclein fibrillization and divert α-synuclein into “off-pathway” aggregate formation. Despite all these differences, Ezrin can still be considered to be most similar to EGCG in terms of overall mechanism of action and outcome.

4.3.2 Chaperone proteins

Molecular chaperones are proteins that assist in the non-covalent folding or unfolding and assembly or disassembly of other macromolecular structures, but do not form part of these structures when the structures are performing their normal biological functions after having completed the process of folding/assembly (Ellis, 2006). Because the tendency of proteins to aggregate increases with cellular stress, and elevated temperatures contribute strongly to

increased stress, it is no surprise that a large fraction of molecular chaperones are heat-shock proteins, e.g. Hsp70, Hsp90, Hsp104, etc., which are recruited in times of stress (Glover and Lindquist, 1998; Macario and Conway de Macario, 2000). Thus, chaperones play an important role in the cell's defence system against misfolded proteins. For example, chaperones may protect against neurodegeneration by converting toxic conformations of misfolded proteins into non-toxic forms which are tolerable for cells and which might be turned over more easily by the proteolytic machinery (as shown in Fig 4.3. below) (Maries et al., 2003).

Another characteristic feature of many chaperones, particularly heat-shock proteins such as Hsp104, Hsp110, Hsp40 and Hsp70, is their ATP-dependence (Shorter, 2011). In order to carry out their functions in the cell (for e.g. protein disaggregase and reactivation activity), many heat-shock proteins require energy in the form of ATP. Fig 4.3 below represents the interplay between multiple heat-shock proteins and their dependence on ATP.

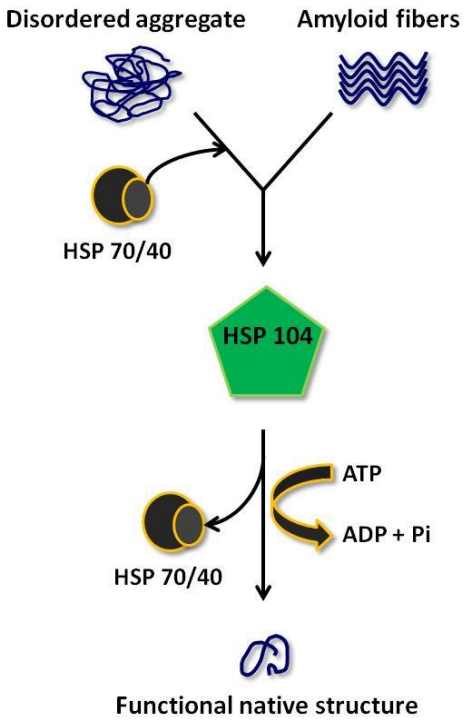

Fig 4.3 Protein disaggregation by Hsp104 (Vashist et al., 2010). Hsp104 couples energy from ATP-binding and hydrolysis to dissolve denatured protein aggregates and amyloid fibers. Hsp70 and Hsp40 co-ordinate the disaggregation of denatured protein aggregates, whereas they are less essential for the dissolution of amyloid structure.

4.3.2.1 The effect of chaperones on aggregating proteins

Molecular chaperones of the heat shock protein 70 (Hsp70) family have been shown to counteract protein misfolding in a variety of neurodegenerative disease models (Luk et al., 2008). *In vitro* assembly of α-synuclein fibrils was shown to be efficiently inhibited by substoichiometric concentrations of purified Hsp70 in the absence of cofactors (Luk et al., 2008). Further *in vitro* experiments have revealed that the chaperonin TRiC is a potent modulator of amyloid formation (Behrends et al., 2006; Kitamura et al., 2006; Tam et al., 2006). TRiC in combination with Hsp70 and Hsp40 prevents Huntingtin fibrillogenesis but stimulates the assembly of soluble polyglutamine-containing Huntingtin oligomers of a new type. These structures are non-toxic and are probably formed by an alternative aggregate formation pathway (Behrends et al., 2006). Additional *in vitro* studies have shown that the Hsp70/Hsp40 chaperone system inhibits the assembly of polyQ proteins into fibrils in an ATP-dependent manner (Muchowski et al., 2000).

Of particular relevance to this work is the fact that multiple studies indicate that chaperones play a beneficial role in inhibiting α-synuclein fibrillization and/or toxicity, for example:

(i) Studies involving heat-shock proteins: A groundbreaking study (Auluck et al., 2002) reported that directed expression of the molecular chaperone Hsp70 prevented dopaminergic neuronal loss associated with α-synuclein in *Drosophila melanogaster* and that interference with endogenous chaperone activity accelerated α-synuclein toxicity. Furthermore, the same study also showed that Lewy bodies in human postmortem tissue demonstrated positive immunostaining for molecular chaperones, thereby suggesting that chaperones may play a role in Parkinson's disease progression. Another study revealed that the molecular chaperone Hsp90 modulates intermediate steps of amyloid assembly of α-synuclein (Falsone et al., 2009), while Hsp104 was shown to antagonize α-synuclein aggregation and reduce dopaminergic degeneration in a rat model of Parkinson disease (Lo Bianco et al., 2008). [The role of heat-shock proteins in the inhibition of α-synuclein aggregation/neurotoxicity has been described in greater depth in the following section, and is, therefore, not analyzed in further detail here].

(ii) Studies involving chaperone-mediated autophagy: Various groups have shown that wild-type α-synuclein is degraded by chaperone-mediated autophagy and macroautophagy in neuronal cells (Vogiatzi et al., 2008). Aberrant α-synuclein is known to confer toxicity to neurons in part through inhibition of chaperone-mediated autophagy (Xilouri et al., 2009), while dopamine-modified α-synuclein blocks chaperone-mediated autophagy (Martinez-Vicente et al., 2008). Another groundbreaking study (Cuervo et al., 2004) showed that wild-

type α-synuclein was selectively translocated into lysosomes for degradation by the chaperone-mediated autophagy pathway, whereas the pathogenic A53T and A30P α-synuclein mutants bound to the receptor for this pathway on the lysosomal membrane, but appeared to act as uptake blockers, inhibiting both their own degradation and that of other substrates. This finding was thought to underlie the toxic gain-of-function by the mutants. Yet other studies indicated that regional deficiencies in chaperone-mediated autophagy underlie α-synuclein aggregation and neurodegeneration (Malkus and Ischiropoulos, 2012) and that boosting chaperone-mediated autophagy *in vivo* mitigates α-synuclein-induced neurodegeneration (Xilouri et al., 2013).

(iii) Studies involving other chaperones: Lastly, even less well-known chaperones have been linked with α-synuclein, for example, the mitochondrial chaperone protein TRAP1 (tumor necrosis factor receptor associated protein-1) has been shown to mitigate α-synuclein toxicity (Butler et al., 2012); a chemical chaperone, sodium 4-phenylbutyric acid, has been shown to attenuate the pathogenic potency in transgenic mice carrying two mutations of human α-synuclein, namely, A30P and A53T (Ono et al., 2009) and observations from another study (Zhou et al., 2006) confirm the suggestion that DJ-1 may act as an oxidative-stress-induced chaperone to prevent α-synuclein fibrillization. Since oxidative stress has been associated with PD, this last observation may explain why mutations of DJ-1 could be a contributing factor in PD.

In summary, a large number of chaperones has been associated with α-synuclein, giving rise to the question: “Does Ezrin also act as a chaperone, and is the mechanism of inhibition of α-synuclein fibrillization by Ezrin in any way similar to that of chaperones, particularly the heat-shock proteins?” The following section aims to answer this question.

4.3.2.2 The effect of heat-shock proteins on α-synuclein aggregation: a comparison with Ezrin

In this section, the effect of Ezrin on aggregating α-synuclein is compared in depth with the action of three distinct heat-shock proteins, namely, Hsp70 (together with Hsp40), Hsp90 and alphaB-crystallin on α-synuclein.

(i) Heat-shock protein 70: Various studies have indicated a role for Hsp70 in α-synuclein-mediated aggregation and/or toxicity. For instance, geldanamycin has been shown to induce Hsp70 and thereby prevent α-synuclein aggregation and toxicity *in vitro* (McLean et al., 2004), while chemically-induced Hsp70 has been shown to reduce α-synuclein aggregation in neuroglioma cells (Kilpatrick et al., 2013). In another study, introducing the

molecular chaperone Hsp70 into an *in vivo* model by breeding α-synuclein transgenic mice with Hsp70-overexpressing mice led to a significant reduction in both high molecular weight and detergent-insoluble α-synuclein species (Klucken et al., 2004). Concomitantly, Hsp70 overexpression *in vitro* similarly reduced detergent-insoluble α-synuclein species and protected cells from α-synuclein-induced cellular toxicity, leading the authors to conclude that the molecular chaperone Hsp70 can reduce the amount of misfolded, aggregated α-synuclein species *in vivo* and *in vitro* and protect cells against α-synuclein-dependent toxicity.

In many ways, the effect of Ezrin on α-synuclein is similar to that of Hsp70 on α-synuclein, in that Ezrin also led to a significant reduction in both high molecular weight and detergent-insoluble α-synuclein species, as depicted in Sections 3.2.4 and 3.2.5. In addition, Ezrin also protected cells from α-synuclein-induced cellular toxicity (refer to Sections 3.4.1 and 3.4.2). However, Ezrin did not *reduce* the total amount of aggregated α-synuclein, instead it mediated the *accelerated* aggregation of α-synuclein into off-pathway, non-toxic species, thereby reducing the amount of misfolded toxic α-synuclein aggregates. Furthermore, in neurons, Hsp70 and its Hsp40-like J-domain co-chaperones are the only known components of the chaperone network that use ATP to convert cytotoxic protein aggregates into harmless natively-refolded polypeptides (Hinault et al., 2010), which stands in direct contrast to Ezrin, which - as described in the previous section - mediates its effect on α-synuclein fibrillization in an ATP-independent manner (as no ATP was provided in the experimental set-up).

Lastly, chaperones such as Hsp40 and Hsp70 cause the formation of amorphous, detergent-soluble aggregates and are most effective when added in the lag-phase of the aggregation reaction (Muchowski et al., 2000). This mechanism of action shows similarities to the mechanism of action of Ezrin on α-synuclein. Within the scope of the incubation assay, the inhibition of α-synuclein fibrillization takes place only if Ezrin is added at the start or at latest during the lag-phase of the aggregation reaction [as shown in Section 3.2.4]. Ezrin added during or after the exponential growth phase fails to inhibit α-synuclein fibril formation.

(ii) Heat-shock protein 90: Chaperones such as Hsp90 (and Hsp70) have been found to be co-localized with Lewy bodies and the expression levels of Hsp90 have been found to be increased in brains of PD patients (Daturpalli et al., 2013). This group used various biophysical methods to reveal that Hsp90 prevents α-synuclein from aggregating in an ATP-independent manner and forms a strong complex with the transiently populated toxic oligomeric α-synuclein species formed along the aggregation pathway. It has also been

shown that, upon forming a complex with Hsp90, the oligomers are rendered harmless and non-toxic to cells. In many ways, this mechanism is similar to the mechanism of action of Ezrin on α-synuclein: Ezrin also acts in an ATP-independent manner (as no ATP was provided in the experimental set-up), and appears to complex with transient oligomers that are formed along the α-synuclein aggregation pathway (refer to Section 3.3.6). It thereby mediates the formation of harmless, non-toxic aggregates of α-synuclein, as determined from the toxicity assays detailed in Sections 3.4.1 and 3.4.2. However, unlike Hsp90, Ezrin does not *prevent* α-synuclein from aggregating; instead it *accelerates* off-pathway aggregation of α-synuclein by binding to early oligomeric species. It then directs them towards formation of non-toxic aggregates. Furthermore, it does not appear to form a strong complex with α-synuclein, as evidenced by the NMR data (refer to Section 3.3), appearing to form a transient complex instead. This type of mechanism has also been described elsewhere in the scientific literature and extends to other chaperones as well (Maries et al., 2003). Fig. 4.3.2 below details not just this mechanism but also the downstream effects and various outcomes of chaperone-mediated intervention at the oligomeric stage of the α-synuclein aggregation pathway, with a particular focus on toxicity.

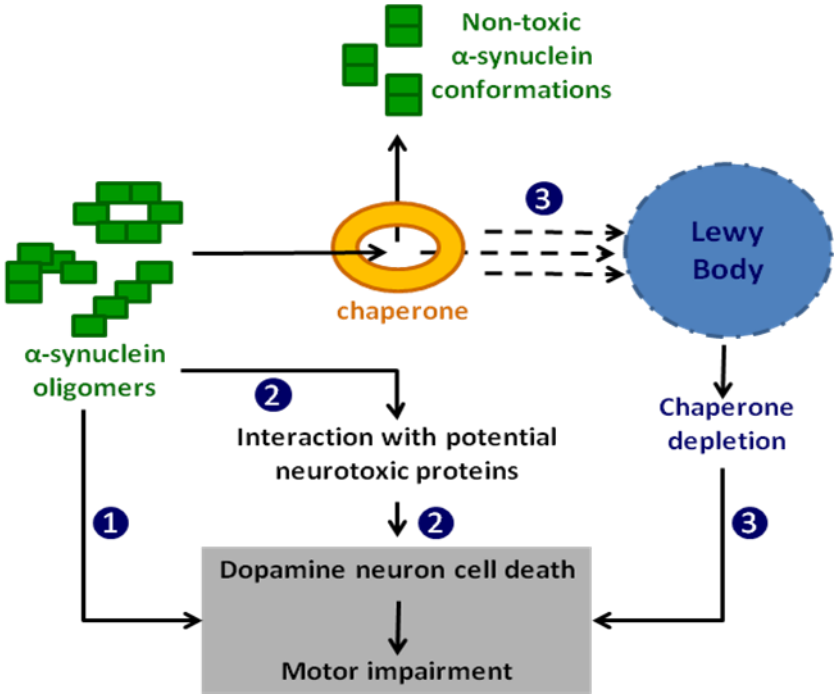

Fig 4.3.2 The relation between chaperones and α-synuclein aggregation and toxicity, adapted from (Maries et al., 2003). It has been proposed that chaperones may alter the conformation of highly toxic protofibrils or oligomers — the intermediates of fibril formation — and reduce their neurotoxicity through changes in protein structure (1). By modulating the structure of α-synuclein, chaperones inhibit their interaction with other neurotoxic proteins that would activate cell death pathways (2). In the synucleinopathies, chaperone molecules become sequestered in Lewy bodies and Lewy neurites, leading to chaperone depletion, which might be directly responsible for cell death (3).

(iii) alphaB-crystallin: alphaB-crystallin, a molecular chaperone also found in Lewy bodies has been shown to be a potent *in vitro* inhibitor of α-synuclein fibrillization, of both the wild-type and the two mutant forms (A30P and A53T) that cause familial, early onset PD (Rekas et al., 2004). Upon inhibiting α-synuclein fibrillization, large irregular aggregates of α-synuclein and alphaB-crystallin are formed, implying that alphaB-crystallin redirects α-synuclein from a fibril-formation pathway towards an amorphous aggregation pathway, thereby reducing the amount of physiologically stable amyloid deposits in favour of easily degradable amorphous aggregates. Once again, some similarities can be detected between the mechanism of inhibition of α-synuclein fibrillization by Ezrin as compared to that of alphaB-crystallin, namely, Ezrin also 'redirects α-synuclein from a fibril-formation pathway' towards an alternative pathway, thus reducing the amount of fibrillar deposits in favour of round, non-toxic aggregates. In addition, Ezrin does reduce the amount of SDS-stable amyloid deposits in favour of SDS-soluble aggregates (refer to Sections 3.2.4 and 3.2.5). However, as characterized by AFM in Section 3.2.6, the aggregates of α-synuclein formed in the presence of Ezrin are not particularly large, irregular or amorphous, and are better described as being round and regular instead.

In another study (Waudby et al., 2010), alphaB-crystallin was demonstrated to be an inhibitor of α-synuclein amyloid fibril formation in an ATP-independent manner *in vitro*. The authors investigated the mechanism underlying this inhibitory action of alphaB-crystallin and established by means of a variety of biophysical techniques that alphaB-crystallin interacts with α-synuclein, binding along the length of mature amyloid fibrils. This binding was shown to strongly inhibit further growth of fibrils and was also demonstrated to shift the monomer-fibril equilibrium in favour of dissociation. In certain aspects, Ezrin appears to mediate a similar effect, as it was also 'demonstrated to be an inhibitor of α-synuclein amyloid fibril formation in an ATP-independent manner *in vitro*'; however, its mechanism of action differs yet again from the chaperone in question. While alphaB-crystallin binds along the length of mature amyloid fibrils, Ezrin appears to bind to early oligomers of α-synuclein (refer to Section 3.3.6), thereby *preventing* the formation of amyloid fibrils. Furthermore, while alphaB-crystallin strongly inhibits further growth of fibrils, Ezrin appears to have no effect when added to the aggregation reaction at later stages which are indicative of the formation of protofibrils (refer to Results Section 3.2.4), thereby leading to the conclusion that Ezrin has no effect on fibril-elongation and is not capable of fibril-dissociation.

4.3.2.3 The effects of other chaperone (and non-chaperone) modifiers on α-synuclein

In a yeast model system, the mammalian ribosomal and chaperone protein RPS3A has been observed to counteract α-synuclein aggregation and toxicity (De Graeve et al., 2013). In other cell culture systems, the overexpression of heat shock proteins inhibits the formation of large inclusion bodies, resulting instead in detergent-soluble aggregates (Cashikar et al., 2005; Sittler et al., 2001). This phenomenon is also observed in the case of over-expression of Ezrin in yeast [see Section 3.4.3], where Ezrin not only reduces the toxicity mediated by α-synuclein in yeast, but also significantly inhibits the formation of large inclusion bodies.

Thus, in many ways, the effect of Ezrin on α-synuclein fibrillization closely resembles the effects of various chaperones on amyloid formation, while simultaneously differing from chaperone action in multiple ways. One of the most significant differences is the absence of ATP-dependence for mediation of the inhibition of α-synuclein fibrillization. The next questions to be asked, then, are, “Could it be that Ezrin is not a chaperone and mediates its effect, instead, via a related but inherently different mechanism? And are there other known non-chaperone protein modifiers of α-synuclein that mediate a similar effect?”

As an answer to these questions, in a related study, an evolutionarily highly conserved modifier of aggregation, MOAG-4/SERF (Modifier of aggregation-4/Small EDRK rich factor), was identified as being a positive regulator of aggregate formation in *C. elegans* models for polyglutamine diseases (van Ham et al., 2010). Inactivation of MOAG-4/SERF suppressed the formation of compact polyglutamine aggregation intermediates required for aggregate formation. The role of MOAG-4/SERF in driving aggregation extended to amyloid-ß and α-synuclein and appeared to be independent of heat-shock-factor-1-induced molecular chaperones, proteasomal degradation, and autophagy. A representative biophysical analysis of the human short isoform SERF1a:α-synuclein complex revealed that the amyloid-promoting activity resulted from an early and transient interaction (as is the case for Ezrin and α-synuclein as well), which was sufficient to provoke a massive increase of soluble α-synuclein amyloid nucleation templates (Falsone et al., 2012). Thus, MOAG-4 is similar to Ezrin in many aspects of its mechanism of action, although it ultimately enhances amyloid-formation as compared to the amyloid-inhibition mediated by Ezrin.

In summary, Ezrin appears to mediate the accelerated aggregation of α-synuclein into off-pathway, non-toxic species via an altogether novel, hitherto unknown mechanism of action, which is analysed based on its own merit in the following section.

4.4 Ezrin mediates the accelerated formation of off-pathway aggregates of α-synuclein via a unique mechanism

NMR spectroscopy has long been known for its ability to characterize macromolecular structures, as well as molecular and supramolecular dynamics (Pellechia et al., 2004). It is, therefore, a powerful technique for investigating both static and transient features of various reactions, for e.g. the α-synuclein-Ezrin incubation reaction. NMR has the advantages of being able to detect and quantify interactions of various natures with high sensitivity, without requiring prior knowledge of the details of the interaction. Hence, a transient interaction such as the association between Ezrin and α-synuclein is best suited to analysis using NMR methods. Indeed, this is the only technology that can be utilized to study such a fluctuating interaction, as traditional methods, such as co-immunoprecipitation, do not serve their purpose in a scenario where Ezrin does not bind to monomeric α-synuclein, and where early-stage α-synuclein intermediates are practically impossible to stabilize for the duration of a co-immunoprecipitation experiment. Thus, the high-resolution, bio-structural technique of NMR spectroscopy has been availed of to elucidate the mechanism of the Ezrin-α-synuclein interaction, in this study. Based on the collective results from the biochemical, biophysical and NMR-based experiments, the following mechanism is proposed to explain the inhibition of α-synuclein fibrillization by Ezrin.

4.4.1 Structural basis of α-synuclein aggregation

Structural properties of α-synuclein in solution: Solution-state NMR studies propose that the N-terminus and the C-terminus of the molecule engage in transient long-range contacts, while the C-terminal and NAC region are involved in hydrophobic contacts, in such a way that the entire ensemble masks the aggregation-prone NAC region (see Fig 4.4.1) (McClendon et al., 2009). The disruption of these interactions by heating, stress, action of other proteins, etc. may increase the propensity of random-coil monomeric α-synuclein to aggregate. Such an increase in aggregation may be caused directly by the release of the contacts themselves, or indirectly, by an increase in overall hydrophobicity as a result of disruption of the contacts (McClendon et al., 2009).

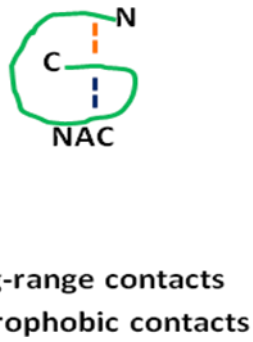

Fig 4.4.1 Schematic representation of the intra-molecular contacts within monomeric α-synuclein. The N-terminus and C-terminus engage in long-range contacts, while the C-terminus and NAC region are involved in hydrophobic contacts, thereby shielding the aggregation-prone NAC region.

Supporting evidence from the literature: Even in the absence of endogenous factors, there is equilibrium between the natively unfolded and the partially folded conformations in α-synuclein. Therefore, high protein concentration may result in an accelerated fibril growth (Uversky et al., 2001b), if there is excessive disruption of the intramolecular contacts within the α-synuclein molecule as a result of molecular crowding. For instance, a large family developed autosomal dominant PD associated with the triplication of the α-synuclein locus, which led to an elevated level of α-synuclein production (Farrer et al., 2004; Singleton et al., 2004; Singleton et al., 2003). Thus, it is possible that disruption of long-range and hydrophobic contacts within α-synuclein - due to high concentrations of the protein - result in increased overall hydrophobicity and give rise to a pre-molten globule-like α-synuclein conformation. This has also been described elsewhere in the scientific literature: A pre-molten globule-like conformation was stabilized by a highly selective self-assembly process during prolonged incubation of α-synuclein at elevated temperatures, and these oligomers have been thought to evolve into the fibril nucleus (Uversky et al., 2001a). Furthermore, early stages of fibril formation involve the formation of a highly fibrillization-prone pre-molten globule-like conformation of α-synuclein, which represents a critical intermediate in the fibrillization pathway (Uversky et al., 2001b). The fact that *in vitro* oligomerization produced the same oligomeric species as those found in human LB preparations suggested that this *in vitro* process may in fact reflect the *in vivo* mechanism of α-synuclein aggregation in the early stages of PD pathogenesis (Uversky et al., 2001a). Hence, factors (e.g. point mutations) that shift the equilibrium in favor of this conformation facilitate fibril formation.

Structural mechanism of inhibition of α-synuclein fibrillization by Ezrin: Once a certain concentration of these globular forms has been reached, the binding of Ezrin to this otherwise-minor population can be detected by NMR spectroscopy. This binding of Ezrin

appears to be mediated primarily at the N-terminus of α-synuclein (particularly, residues 1-10), which is the first region to undergo broadening of its residues as revealed by NMR [see Sections 3.3.3 and 3.3.4]. When these N-C long-range contacts are disturbed, the NAC region becomes more exposed to the environment and may adopt a number of alternative conformations due to its hydrophobic nature. These conformations may be detected by NMR as multiple, simultaneous resonances for the same residue [see Section 3.3.6]. These resonances appear only transiently and disappear at later time-points when large insoluble aggregates are formed that cannot be detected by NMR. The energetically-unfavourable exposure of the hydrophobic NAC region may result in the faster formation of aggregates, in an attempt to mask or bury the hydrophobic regions from the water-containing solvent, thereby explaining the accelerated rate of α-synuclein aggregation in the presence of Ezrin [refer to Section 3.3.2].

Lastly, the exposure of the NAC region would also affect the C-terminal-NAC hydrophobic contacts, releasing them. This could then result in increased freedom or flexibility of the C-terminus in the later stages of aggregation, once all the contacts have been disrupted. This is, indeed, what is reported by NMR. At the later stages of aggregation, not only is the ^{1}H-intensity strongest for the C-terminus, as compared to the rest of the molecule, but it is equivalent in value to the ^{1}H-intensity at time 0 hours [see Section 3.3.4]. This is consistent with the proposition put forth above that disruption of the C-terminal-NAC hydrophobic contacts results in an increased flexibility of the newly-released C-terminus. Additionally, right upto the penultimate NMR measurement, i.e. the measurement preceding complete aggregation, the *only* residues detectable by NMR lie in the C-terminal region, in keeping with expectations [see Section 3.3.4]. The aggregates formed through incubation with Ezrin would then be different from the traditional fibrillar aggregates of α-synuclein alone, as confirmed elsewhere by AFM experiments [refer to Section 3.2.6]. α-synuclein incubated alone shows no broadening of N-terminal residues, and therefore, presumably, no significant disruption of long-range N-C contacts [see Section 3.3.3]. This explains the absence of multiple transient species with a typical NMR profile when α-synuclein aggregates in the absence of Ezrin [see Section 3.3.6]. It also explains the uniform loss of intensity across all regions of the α-synuclein molecule in the absence of Ezrin, with no extensive flexibility of the C-terminus [see Section 3.3.3].

4.4.2 Mechanism of Ezrin-mediated aggregation of α-synuclein

As described in Section 3.3, NMR spectroscopy was used to elucidate the mechanism by which Ezrin mediates inhibition of α-synuclein fibrillization. By generating ^{1}H-^{15}N HMQC

spectra of α-synuclein incubated in the absence and presence of Ezrin (α-synuclein:Ezrin 5:1), at regular 4-5hr intervals until 42hrs (i.e. for the duration of the entire experiment), it became evident that Ezrin mediates the *accelerated* aggregation of α-synuclein into off-pathway species. As seen from NMR spectroscopy at 0 hours of incubation, Ezrin does *not* bind monomeric α-synuclein. It follows that Ezrin binds to early intermediates of fibrillization, e.g. early-stage oligomers. Binding to these oligomers would correspond to the broadening of α-synuclein residues visible in NMR spectra after 4 hours of incubation. The altered ^{1}H-^{15}N HMQC spectrum of α-synuclein in the presence of Ezrin thereafter, with multiple resonances being detected for a single peak and appearing/disappearing over time, indicates that Ezrin mediates the formation of multiple conformations of α-synuclein. This could alternatively be interpreted as the binding of Ezrin to multiple conformations of α-synuclein, resulting in the accelerated aggregation of α-synuclein in the presence of Ezrin as compared to α-synuclein aggregated alone. This may explain the transient nature of many of these conformations, as Ezrin could bind to them and thereby draw them out of the available pool for on-pathway aggregation, detected by NMR as a loss of the species over time.

In this way, by mediating and/or binding to altered forms of α-synuclein, Ezrin ensures that none of the early-stage intermediates is available for traditional on-pathway aggregation into fibrils, which would be detectable as an increase in Thioflavin-T fluorescence over time. Instead, the complete *lack* of Thioflavin-T signal at a molar concentration of Ezrin 5-fold lower than α-synuclein, seems to confirm the absence of early-stage intermediates (e.g. oligomers) available for traditional fibrillization. Having bound to various oligomeric or proto-oligomeric states of α-synuclein, it is also more probable that sub-stoichiometric concentrations of Ezrin are able to effect such a potent inhibition of α-synuclein, as the α-synuclein protein has already started grouping into “clusters” before it becomes suitable for the action of Ezrin. Smaller amounts of Ezrin are required for targeting oligomers than for targeting monomeric α-synuclein, explaining the extreme potency of the effect of this modifier on α-synuclein fibrillization. The accelerated formation of such α-synuclein “clusters” may induce the formation of successive α-synuclein “clusters”, leading to the rapid formation of off-pathway “supra-clusters” or aggregates. The two pathways proposed for α-synuclein fibrillization and non-typical aggregation of α-synuclein in the presence of Ezrin, respectively, have been schematically represented in Fig 4.4.2 below.

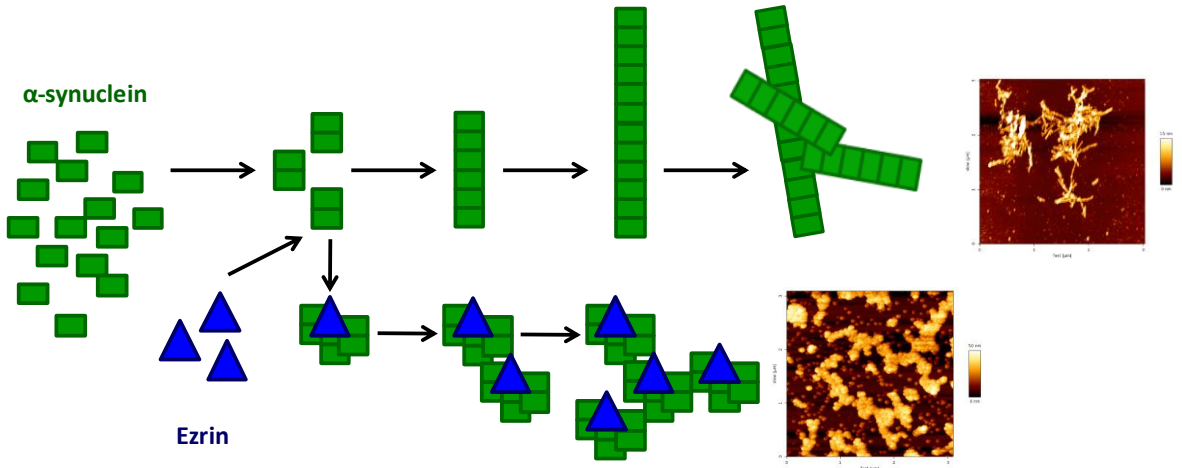

Fig 4.4.2 A proposed mechanism for the off-pathway aggregation of α-synuclein into alternate non-toxic species in the presence of Ezrin.

4.4.3 Comparison of α-synuclein with the ß- and γ- synucleins

Having previously discussed the effect of proteins highly homologous to Ezrin on α-synuclein fibrillization, it may now be useful to closely examine proteins highly homologous to *α-synuclein,* to better understand the structural details of α-synuclein fibrillization. Human ß- and γ-synucleins, which are 78% and 60% identical to α-synuclein, respectively, preserve some characteristic features of α-synuclein, while missing others (see Fig 4.4.3). The ß- and γ- synucleins share a conserved C-terminus with three identically placed tyrosine residues. However, ß-synuclein lacks 11 residues within the NAC region (Clayton and George, 1998; Lucking and Brice, 2000) and γ-synuclein specifically lacks the tyrosine rich C-terminal signature of α- and ß- synucleins (Clayton and George, 1998).

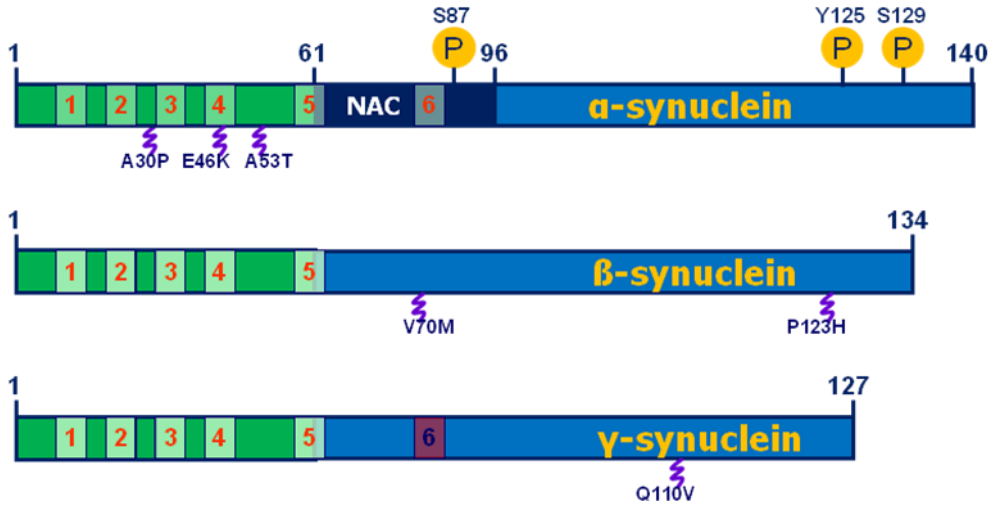

Fig. 4.4.3 The synucleins, adapted from (Mukaetova-Ladinska and McKeith, 2006). Synuclein mutations ( ) and phosphorylation sites ( ) are represented, along with the imperfect repeats of 11 amino acids containing a KTKEGV core ( ), conserved across all the 3 synucleins.

Comparison of the structural properties of the members of the synuclein family by several physicochemical methods revealed that although all three synucleins behaved as typical 'natively unfolded' proteins, they possessed some structural variability. ß-synuclein exhibited the properties of a typical random coil, whereas α- and γ-synucleins were slightly more compact and structured (Uversky et al., 2002b), as represented in Fig 4.4.3. Hence, one could question whether Ezrin could possibly have a similar effect on the less-structured ß-synuclein, which lacks the long-range N-C termini contacts of α-synuclein to start with. Both α- and γ-synucleins were shown to form fibrils, whereas ß-synuclein did not fibrillate when incubated under the same conditions (Uversky et al., 2002b). However, even apparently 'non-amyloidogenic' ß-synuclein can be forced to fibrillate in the presence of metals, such as Zn2+, Pb2+, and Cu2+ (Uversky et al., 2002c) or pesticides (Yamin et al., 2005). Furthermore, the metal-induced fibrillization of ß-synuclein was further accelerated by the addition of glycosaminoglycans (GAG) or high concentrations of macromolecular crowding agents (Yamin et al., 2005). Intriguingly, the addition of either ß-synuclein or γ-synuclein in a 1:1 molar ratio to α-synuclein substantially increased the duration of the lag-time and dramatically reduced the elongation rate of α-synuclein fibrillization (Uversky et al., 2002b). Fibrillization was completely inhibited at a 4:1 molar excess of ß-synuclein or γ-synuclein over α-synuclein (Uversky et al., 2002b). In contrast, the addition of excess α-synuclein to a solution only serves to speed up the process of aggregation further and shorten the lag phase even more, underlining a fundamental difference in the properties of ß- and γ-synucleins from α-synuclein. ß-synuclein inhibited α-synuclein aggregation in animal models, too (Hashimoto et al., 2001). This suggests that ß-synuclein and γ-synuclein may act as regulators of α-synuclein fibrillization *in vivo*, potentially acting as chaperones (Uversky et al., 2002b) and thereby exhibiting similarity to the action of Ezrin on α-synuclein fibril formation.

4.5 Ezrin rescues α-synuclein-mediated toxicity

As proteins whose expression has been detected in the brain (Moon et al., 2012; Persson et al., 2010; Solano et al., 2000; Wirdefeldt et al., 2001), both α-synuclein and Ezrin are relevant for study in neuronal cell cultures. Multiple assays that assess different readouts of toxicity reveal that Ezrin rescues the toxicity mediated by α-synuclein in rat primary neurons [see Sections 3.4.1 and 3.4.2]. Furthermore, *in vivo* studies of the effect of Ezrin on α-synuclein using the model organism, yeast, show that Ezrin indeed rescues the toxicity mediated by α-synuclein, at an organismal level. Multiple growth assays on α-synuclein- and Ezrin- expressing yeast cells, strengthened by microscopy analyses & quantifications, confirm once again that Ezrin has a protective role *in vivo* in terms of α-synuclein-mediated toxicity and aggregation. In order to analyze the mechanism underlying the reduction in α-synuclein toxicity by Ezrin, the 'off'-pathway aggregates of α-synuclein generated in the presence of Ezrin are compared, below, to other pre-fibrillar aggregates, oligomers and intermediates of α-synuclein previously described in the literature.

Although fibrillar α-synuclein is a major component of Lewy bodies (LBs), recent data implicate prefibrillar, oligomeric intermediates as the toxic species in PD (Colla et al., 2012; Outeiro et al., 2008). These studies indicate that some small prefibrillar α-synuclein species are highly neurotoxic, a theory commonly referred to as the 'toxic oligomer hypothesis'. A recent study used bimolecular fluorescence complementation (BiFC) to directly visualize α-synuclein oligomerization in living mammalian cells, allowing the study of the initial events leading to α-synuclein oligomerization, the precursor to aggregate formation. Stabilization of α-synuclein oligomers via BiFC resulted in increased cytotoxicity, which could be rescued by Hsp70 in a process that reduced the formation of α-synuclein oligomers. Another study (Lashuel et al., 2002a) showed that mutant amyloid proteins associated with familial Alzheimer's and Parkinson's diseases form morphologically indistinguishable annular protofibrils that resemble a class of pore-forming bacterial toxins, suggesting that inappropriate membrane permeabilization might be the cause of cell dysfunction and even cell death in amyloid diseases. Yet another study (Lashuel et al., 2002b) showed that two mutations in the α-synuclein gene (A30P and A53T) that are linked to autosomal dominant early-onset Parkinson's disease promote the formation of transient protofibrils (prefibrillar oligomers), suggesting that protofibrils are linked to cytotoxicity. Even wild-type α-synuclein after extended incubation forms annular protofibrils.

After evaluating the results of these studies, it would appear that halting the fibrillization process at early stages associated with the formation of small oligomers could create more

harm than benefit, as these species are potentially more neurotoxic than neuroprotective. Similarly, small molecules that are able to disaggregate fibrils to smaller oligomers or soluble aggregates could also promote neurodegeneration. In this respect, the finding of a modifier such as Ezrin, which actually diverts the fibrillization pathway away from the traditional, toxic oligomeric species towards the formation of off-pathway, non-toxic and non-seeding oligomers, confers some advantages. Not only is the traditional fibrillization process altered, but also the outcome of the alternative process - here, the formation of off-pathway aggregates - reduces the toxicity otherwise associated with fibrillar α-synuclein. Furthermore, the AFM data described in this work provide evidence that the Ezrin-mediated 'off'-pathway aggregates are not annular protofibrils, but rather regular, round aggregates, and the various cellular assays show clearly that these aggregates are not linked to cytotoxicity and do not give rise to cell dysfunction or death as a result of inappropriate membrane permeabilization. Instead, Ezrin actually reduces α-synuclein-mediated toxicity. Thus, it is plausible that Ezrin may reduce α-synuclein-mediated toxicity by diverting the fibrillization pathway away from the formation of toxic, protofibrillar, cytotoxicity-causing oligomers to give rise to round, non-toxic 'off'-pathway aggregates of α-synuclein instead.

4.6 Parkinson's disease in the gut: a possible physiological relevance of the α-synuclein-Ezrin interaction

α-synuclein is primarily a neuronally-expressed protein and even Ezrin expression has been detected in the brain. Furthermore, various studies have indicated an indirect role for Ezrin and Ezrin-like proteins in Parkinson's disease [see Section 3.1.7]. Thus, there is already plentiful evidence from the scientific literature for an association of Ezrin with Parkinson's disease in the brain. On the other hand, Ezrin was first identified (and is most abundantly expressed) in gastro-intestinal tissues, so it may be of interest to examine the role of α-synuclein in the gut (i.e. the natural habitat of Ezrin) and a possible role of the gastrointestinal tract in the pathology of PD. The rest of this section, therefore, deals with PD in the gut and any potential physiological relevance that the α-synuclein-Ezrin interaction may have within this region.

It is now well established that PD lesions occur outside the CNS and, in particular, in the enteric nervous system or ENS (Lebouvier et al., 2009). A majority of PD patients present with disorders of gastric motility or suffer from other gastro-intestinal (GI) problems (Lebouvier et al., 2009). Since Ezrin is expressed predominantly in the gut, there may be multiple possibilities for a neuroprotective role of Ezrin in PD, spanning both the CNS and ENS. While a role for Ezrin-mediated inhibition of α-synuclein fibrillization in the gut is indeed speculative at this stage, there is no ambiguity about the involvement of the gut and the ENS in Parkinson's disease, as described in detail in the following sections:

4.6.1 The Enteric Nervous System viewed as "a second brain"

The postulate that the gut is a second brain arose in the early 1900s, when it was found that the ENS control of intestinal motility and secretion was largely independent of influences from the CNS. The ENS contains as many neurons as the spinal cord (approximately 80–100 million) and the functional and chemical diversity of enteric neurons closely resembles that of the CNS (Benarroch, 2007; Goyal and Hirano, 1996). There is also a relatively small proportion of dopaminergic neurons in the ENS. Enteric dopaminergic neurons, which express tyrosine hydroxylase (TH) and the dopamine transporter but lack dopamine ß-hydroxylase, have been identified in mice, guinea pigs (Li et al., 2004c) and humans (Anlauf et al., 2003). Moreover, all subtypes of dopaminergic receptors (D1–D5) are expressed by enteric neurons (Li et al., 2004c). Approximately 10–13% of both myenteric and submucosal neurons in the ileum and bowel of mice are dopaminergic (Li et al., 2004c). In humans, a detailed survey of the proportion of dopaminergic neurons has clearly demonstrated that

these neurons are distributed along an oral–aboral gradient. Dopaminergic neurons are abundant in both plexuses of the upper GI tract, accounting for 14–20% of the total enteric neurons, whereas their proportion decreases to 1–6% in the lower small intestine and large intestine (Anlauf et al., 2003). A comprehensive review of the putative role of dopaminergic neurons in the ENS has been recently published (Natale et al., 2008). Although their precise function remains largely unclear, it has been suggested that enteric dopaminergic neurons exert an inhibitory effect upon motility because: (i) dopamine transporter knockout mice show a decrease in electrically induced contractions of colonic smooth muscle (Walker et al., 2000); and (ii) mice invalidated for the gene encoding D2 have an increase in intestinal motility (Li et al., 2006).

4.6.2 The ENS of patients is affected by the pathological process of PD

It has become increasingly evident that PD is a multicentric neurodegenerative process that affects several neuronal structures outside the SN (Braak and Del Tredici, 2008; Braak and Del Tredici, 2009). Various reports suggest that among the structures affected outside the CNS, the ENS is affected by the pathological process of PD (Braak and Del Tredici, 2008; Braak and Del Tredici, 2009). In a seminal paper (Qualman et al., 1984), the authors compared the neuropathological features in autopsies of 22 PD patients and 50 controls matched for age and sex. Among PD patients, three suffered from upper GI tract symptoms, especially dysphagia. Lewy Bodies (LBs) were found in the myenteric plexus (MP) in two of three PD patients suffering from dysphagia. In contrast, no LBs were identified in the GI tracts of PD patients without dysphagia or in controls. A subsequent case report showed the presence of LBs in the colonic submucosal and myenteric neurons of a patient with PD and colon motility disorders (Kupsky et al., 1987), further supporting the assumption that LBs are present in the ENS of PD patients with GI symptoms. These first observations led to further systematic assessment of the presence of LBs in the ENS of PD patients.

In a further study (Wakabayashi et al., 1988), the authors found LBs in the GI tracts of seven consecutive autopsied PD patients. The LBs were distributed widely in both the MP and SMP (sub-mucosal plexus), from the upper oesophagus to the rectum. They occurred in neuronal cell bodies and processes, and were most frequent and numerous in the MP of the lower oesophagus. In eight of 24 age-matched controls, the LBs were fewer in number, and in the remaining control cases they were absent. The same group then performed additional immunohistochemical analyses of specimens from three autopsied patients with PD (Wakabayashi et al., 1992). In a post-mortem survey (Braak et al., 2006), the authors systematically compared the gastric MP and SMP from five individuals with LB diseases of

increasing severity with corresponding samples from five individuals whose brains were devoid of inclusions. α-synuclein-immunoreactive inclusions were found in both the MP and the SMP of all LB disease individuals. The inclusions observed in the SMP were reminiscent of Lewy neurites, whereas the ones observed in the MP were similar to Lewy bodies. This led Braak to make the assumption that the ENS could be targeted by the pathological process at a very early stage of the disease (Braak et al., 2006). Immunohistochemical staining with an antibody against phosphorylated α-synuclein revealed that four of five PD patients had phospho-α-synuclein-immunoreactive neurites, a pattern that was absent in all control patients (Lebouvier et al., 2008).

In addition to the pathological studies on PD patients described above, which suggest that PD pathology progresses from the enteric nervous system and the olfactory bulb into the central nervous system, it has recently been shown that the resection of the autonomic nerves stops this progression (Pan-Montojo et al., 2012). This study also indicated that environmental toxins such as rotenone promote the release of α-synuclein by enteric neurons, which is then taken up by presynaptic sympathetic neuritis, and retrogradely transported to the soma, where it accumulates. These results strongly suggested that the progression of PD pathology is based on the transneuronal and retrograde axonal transport of α-synuclein, initiating within the enteric nervous system. Fig 4.6 below exemplifies the details of such a pathway initiating in the ENS and continuing upward to specific regions of the CNS.

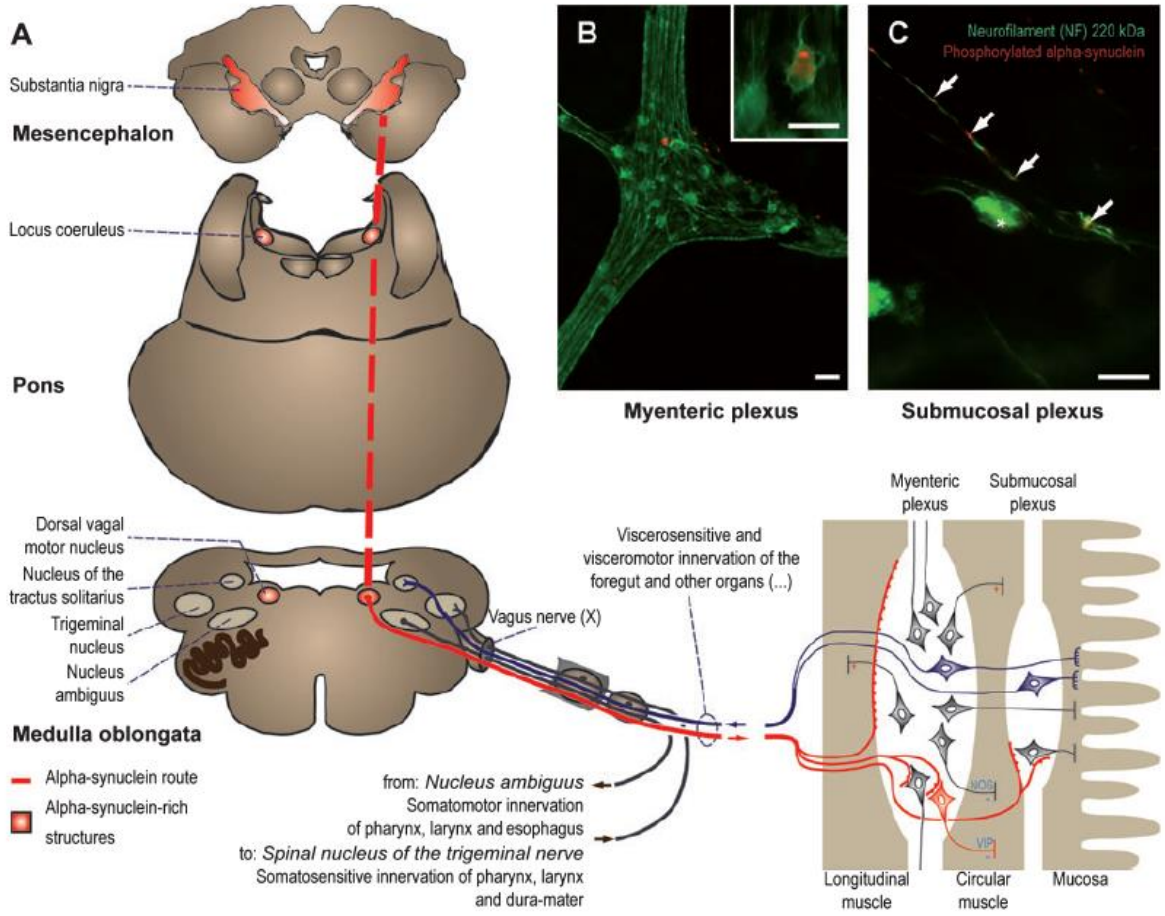

Fig. 4.6. Parkinson's disease in the gut (Lebouvier et al., 2009). (A) α-synuclein pathway: along the CNS-ENS axis. A high endogenous content of α-synuclein seems to predispose the neural structures to the degenerative changes observed in PD. Within the brainstem, the dorsal motor nucleus of the vagus nerve, locus coeruleus and substantia nigra (shaded red) are intrinsically rich in α-synuclein. Interestingly, vagal efferent axons (red), which are the only ones to degenerate in PD, are differentiated from the afferent fibers (blue) by selective α-synuclein expression. Here, a neuron is depicted in red in the myenteric plexus (MP). Hence, a putative retrograde and ascending pathway following α-synuclein-rich structures can be drawn from the ENS towards the CNS. (B) Whole mount of colonic MP from an end-stage PD patient (autopsy sample). Double-labeling with antibodies against neurofilament and phosphorylated α-synuclein reveals some Lewy neurites (arrow) in most of the myenteric ganglia, and occasional Lewy bodies (insert). (C) Whole mount of colonic submucosal plexus from a living PD patient (colonoscopic biopsy). Although no intrinsic submucosal neuron seems to be affected, the same immunolabeling shows degenerative changes within presumably extrinsic fibers (arrows). Asterisk: submucosal ganglion. NOS, nitric oxide synthase.

4.6.3 Evidence for neuronal loss in the ENS of PD patients

In an interesting study (Singaram et al., 1995), the authors compared colonic tissue from 11 patients with advanced PD to that from 22 controls (17 patients with adenocarcinoma, and five who underwent colectomy for severe constipation). Using anti-dopamine antibodies,

they showed that nine of 11 PD patients had fewer myenteric dopaminergic neurons than the controls. This was associated with a reduction in submucosal dopaminergic neurons in PD patients, but this difference did not reach statistical significance. In the particular context of experimental parkinsonism, in mice acutely treated with 1-methyl-4-phenyl-1,2,3,6-tetrahydropyridine (MPTP), the numbers of dopamine-immunoreactive neurons in the SN were dramatically reduced at day 4 after MPTP, and further markedly reduced at day 25 (Mori et al., 1988). However, such a dramatic drop in the numbers of dopaminergic neurons described in PD patients should be interpreted cautiously and requires further confirmation: In contrast to the results of the aforementioned autopsy survey, other studies found no neuronal loss and, especially, no dopaminergic neuronal loss in the SMP of PD patients (Lebouvier et al., 2008). However, the main limitation of such studies was the lack of access to myenteric ganglia, which, is likely to be primarily affected by the pathological process during PD.

4.6.4 The consequences of the lesions of the ENS in PD

The presence of the lesions in the ENS during PD occurs at an early stage of the disease. Hence, they could play a central role in the pathophysiology of the disease per se, namely, in the spread of the pathological process from the gut to the brain. These lesions could also explain, at least in part, the GI dysfunction frequently encountered by PD patients. Since the neurons of the ENS are directly in contact with the environment, they could represent a route of entry for a putative environmental factor to initiate the pathological process (Hawkes et al., 2007). Braak and co-workers determined that the appearance of α-synuclein-positive Lewy pathology initially occurs in the earliest stage of PD in the ENS (Braak et al., 2003). This led Braak to put forth the general proposal that PD may be produced by an environmental pathogen that breaches the mucosal barrier of the GI tract and that the pathological process further spreads to the CNS via the vagal preganglionic innervation of the gut (Braak et al., 2006; Hawkes et al., 2007), as has already been demonstrated for scrapie (McBride et al., 2001) and neural tracers (Powley et al., 1987).

If Braak's theory is true, an uninterrupted pathway that expresses α-synuclein throughout its trajectory should allow the retrograde transport of the pathological process from the GI mucosa to the CNS. A very elegant study has demonstrated that such a pathway indeed exists: A group of researchers performed an in-depth characterization of α-synuclein-immunoreactive neurons in the ENS of rats, and showed that vagal efferent axons and terminals are positive for α-synuclein, and that some of these preganglionic efferent neurons synapse on α-synuclein-positive intrinsic neurons in the MP of both the stomach and

duodenum (Phillips et al., 2008). Further reinforcing the role of these neurons in the spread of the pathological process is the occurrence of α-synuclein inclusions in the DMV (Dorsal Motor nucleus of the Vagus) neurons of rats that received intragastric injections of a proteasome-inhibitor (Miwa et al., 2006). The identification of such a pathway provides support for the development and spread of Lewy pathology in PD.

4.6.5 The pathophysiology of GI dysfunction in PD

The lesions of the ENS are commonly considered to be responsible for the debilitating digestive symptoms (Pfeiffer, 2003). However, due to the paucity of available data on the structural and neurochemical alterations of myenteric neurons, it could also be argued that the lesions of the medullar, spinal and peripheral autonomic nervous system, which are also present in PD patients, are sufficient to induce GI dysfunction (Benarroch et al., 2005; Wakabayashi and Takahashi, 1997). It is likely that the respective roles of intrinsic and extrinsic innervation in GI dysfunction during PD could be difficult to resolve. In this regard, multiple system atrophy, a neurodegenerative disorder belonging to the atypical parkinsonian syndromes, provides some interesting clues concerning the respective roles of extrinsic and intrinsic innervations in the pathophysiology of GI dysfunction.

Multiple system atrophy is characterized by an early and severe pan-dysautonomia, due to the massive degeneration of the autonomic nucleus of the brainstem and spinal cord (Benarroch et al., 2006a; Benarroch et al., 2006b; Benarroch et al., 2007). In contrast to PD, where postsynaptic peripheral neurons degenerate first (including those from the ENS), multiple system atrophy can be considered a paradigmatic extrinsic dysautonomia. In this disorder, the postsynaptic intrinsic neurons are indeed spared or affected later, in a centrifugal pattern (Sone et al., 2005). Interestingly, GI dysfunction in general, and constipation in particular, have the same prevalence and severity in multiple system atrophy and PD, suggesting that extrinsic lesions prevail in causing digestive symptoms (Stocchi et al., 2000; Wenning et al., 1994).

4.6.6 A putative role for Ezrin in the context of PD in the gut

Several reports strongly support the idea that α-synuclein could indeed be a key element in the spread of the pathological process during PD: α-synuclein has been shown to be secreted by neuronal cells *in vitro*, and this secreted α-synuclein is prone to aggregate (Lee et al., 2005). In a recent, compelling study (Pan-Montojo et al., 2012), it has been demonstrated that an environmental toxin (i.e. rotenone) promotes the release of α-synuclein by enteric neurons and that released enteric α-synuclein is up-taken by

presynaptic sympathetic neurites and retrogradely transported to the soma, where it accumulates. This could provide the perfect setting for Ezrin and α-synuclein to meet in the gut, as the α-synuclein excreted by the ENS neurons would naturally find itself in the epithelial cell space where Ezrin is abundantly expressed. Furthermore, the Ezrin towards the basal end of the epithelial cells (where the ENS neurons innervate) is predominantly unphosphoryated, or in its inactivated form, identical to the form of Ezrin used in this study. The phosphorylated or activated Ezrin, by virtue of its binding to F-actin and to membrane-associated proteins, is localized at the apical end of the epithelial cell, further removed from the ENS innervation.

These “secreted” aggregates of α-synuclein can be taken up from the extracellular space by neurons (Liu et al., 2009; Sung et al., 2001) and induce cell death in human neuroblastoma cells (Sung et al., 2001), suggesting that α-synuclein secreted into or present in the extracellular space may exert its cytotoxic effect on neighbouring neuronal cells. If α-synuclein is released into the epithelial cell environment where it interacts with Ezrin, which prevents it from aggregating into on-pathway species, its toxicity to neighbouring neurons would also be correspondingly diminished. Thus, Ezrin would bring about a decrease in α-synuclein-mediated toxicity in an *in vivo* environment.

It could then be further postulated that when excessive amounts of α-synuclein accumulate inside neurons, which eventually die, its aggregates leak out of the dead neurons and spread its cytotoxic effect to the neighboring cells. Such a hypothesis is further reinforced by the recent description of LBs in grafted neurons in PD patients. Three patients who had long-term survival of transplanted fetal mesencephalic dopaminergic neurons, for more than 10 years, developed LBs in grafted neurons (Kordower et al., 2008a; Kordower et al., 2008b; Li et al., 2008). Taken together, these results support a prion disease-like mechanism in the spread of the Lewy pathology, relying on α-synuclein misfolding and post-translational changes, which may account for the transmission of the pathological process from the ENS to the CNS (Haik et al., 2004). This could provide a potential environment in which Ezrin is brought into close contact with α-synuclein, where it could presumably mediate its inhibitory effect on α-synuclein aggregation and thereby reduce α-synuclein-mediated toxicity, before being overpowered by large amounts of misfolded or otherwise abnormal forms of α-synuclein, resulting in the spread of pathology upwards from the ENS towards the CNS.

4.7 Significance of the study

The principal problem with Parkinson's disease is two-sided, in that there exists neither a cure for the disease, nor a detailed understanding of what exactly causes it. Due to lack of appropriate medications, long-term-hazardous side-effects from the existing symptomatic treatments, and an ever-increasing pool of patients, it is quite critical to explore different avenues in search of a suitable therapeutic target. The real problem with drugs that inhibit α-synuclein fibrillization or which promote the disaggregation of preformed fibrils is the lack of a clear understanding of the mechanisms of aggregation-related neurotoxicity, coupled with the observation that not a single drug has succeeded in curing or halting the process of Parkinson's disease. Screens for drugs against α-synuclein aggregation or for small molecule inhibitors of α-synuclein fibrillization also face the standard challenges of establishing safety, efficacy, absence of side-effects, etc. The discovery of a non-chaperone, CNS-expressed protein modifier confers some advantages in this respect, and can thus be thought of as a potential new drug target:

Implications for potential therapeutic intervention: A naturally produced biomolecule such as Ezrin, which of its own accord does not give rise to any disorders or debilitating conditions (i.e. it is not an oncogene, or otherwise detrimental protein), may bypass some of the toxicity concerns associated with using drugs or other proteins that are known to play a role in cancer. As an example, a comprehensive study of the direct transactivating effects of heat-shock factor 1 (HSF1) in cancer revealed that HSF1 regulates diverse cellular processes that extend far beyond heat-shock genes, and that HSF1 activation in multiple cancers is strongly associated with metastasis and death (Mendillo et al., 2012). Heat-Shock Factor 1 – although a master regulator of the heat-shock response – facilitates malignant transformation, cancer cell survival, and proliferation in model systems. Hence, upregulating either HSF1 or chaperone-levels through HSF1 is not the optimal strategy to suppress α-synuclein fibrillization. Ezrin, in contrast to HSF1, actually reduces α-synuclein-mediated toxicity *in vivo,* thereby providing a much more viable option for potential therapeutic intervention.

As the field of gene therapy develops further, Ezrin may provide an alternative strategy in the future to the classical drug-development paradigm for treating PD. The fact that ATP is not necessary for the effect mediated by Ezrin on α-synuclein and that sub-stoichiometric concentrations of the protein are sufficient to re-direct the harmful fibrillization process of α-synuclein to an alternative, rapid, non-toxic and structurally-defined pathway is already a positive indicator for the applicability of Ezrin to future studies with a therapeutic focus.

Novelty of the work: At the time of production of this work, no study has provided evidence of such a structurally-detailed, time-resolved, multi-component and fundamentally unique mechanism of inhibition of an aggregating protein. Ezrin would appear to be the first modifier of its kind, which requires neither high concentrations nor ATP to mediate an effect that is very potent. In addition, this effect is not mediated on monomeric α-synuclein, but rather on early-stage oligomers or intermediates of the fibril formation pathway, adding to the novelty of the mechanism.

4.8 Outlook

In this study, we have aimed to identify, characterize and explain the effect of a novel protein modulator on the fibrillization of α-synuclein, with particular emphasis on the physiological relevance of this phenomenon. In order to confirm a role for Ezrin in Parkinson's disease, it would be extremely informative to examine pathological brain tissue for changes in expression of Ezrin, for the presence of Ezrin in Lewy bodies or for co-immunoprecipitation of Ezrin with α-synuclein. Furthermore, studies on other model organisms, such as *C. elegans* or *D. melanogaster*, in which α-synuclein has been engineered to aggregate, may confirm the effect of Ezrin on α-synuclein fibrillization that was observed in yeast, thereby establishing a conserved role for this protein in protection against neurodegeneration. In terms of cellular work, Chevalier and co-workers (Chevalier et al., 2008) developed primary cultures of ENS whose enteric neurons expressed α-synuclein. This may provide the ideal setting in which to study the effects of Ezrin on α-synuclein aggregation. Not only could the effect of Ezrin on α-synuclein aggregation and toxicity be monitored in a physiologically relevant environment, but also its interaction with α-synuclein (or early-stage, on-pathway species thereof) could be confirmed, by employing standard pull-down experiments or co-immunoprecipitation assays.

From a structural perspective, it may be useful to generate fragments of the Ezrin protein for use in Thioflavin-T-based α-synuclein fibrillization assays or for incubation with α-synuclein as examined by NMR spectroscopy, to determine the region/s of the protein important for mediating this effect. A comparison in this study with Radixin, Moesin and Band 4.1 proteins could serve to pinpoint those residues/stretches of amino acids that are critical for inhibiting α-synuclein fibrillization. Fibrillization assays with permanently-phosphorylated and inducibly-phosphorylatable forms of Ezrin may also shed light on structural aspects of Ezrin-mediated α-synuclein-inhibition, as well as on possible internal cellular mechanisms of Ezrin regulation. Lastly, generating and employing ^{15}N-Ezrin in solution-state NMR spectroscopy experiments may explain many structural details of the process of inhibition of α-synuclein-fibrillization.

Finally, solid-state NMR spectroscopy of the Ezrin-mediated α-synuclein aggregates may provide additional insights into the structure of these species. Together with CD spectroscopy, electron microscopy and other biophysical tools, it is possible to draw up a highly-detailed picture of the nature of α-synuclein aggregates formed in the presence of Ezrin. Thus, additional downstream experiments could provide a more complete understanding of various facets of Ezrin-mediated inhibition of α-synuclein fibrillization.

5. ABSTRACT/ ZUSAMMENFASSUNG

5.1 Abstract

α-synuclein - a key protein involved in Parkinson's disease (PD) - forms large insoluble deposits of amyloid fibrils that are toxic and cause the loss of dopaminergic neurons - a hallmark characteristic of PD. Some proteins (e.g. heat-shock proteins) interact with α-synuclein and interfere with aggregate formation, thereby providing a source of potential neuroprotective intervention. In this study, a library of 13,824 proteins was screened *in vitro* to detect inhibitors of α-synuclein fibrillization. After several stringent rounds of screening, the cytoskeletal linker protein, Ezrin, was identified as being the most potent modulator of α-synuclein aggregation. An arsenal of biophysical and biochemical assays, including atomic force microscopy, SDS-PAGE and *in vitro* fibrillization assays was then used to demonstrate the potency of Ezrin and closely-related family members as powerful modulators of α-synuclein fibrillization. Nuclear magnetic resonance (NMR) spectroscopy studies were employed to elucidate the novel and unique mechanism by which Ezrin mediates its effect on α-synuclein fibrillization. Namely, Ezrin interacts with early-stage oligomers of α-synuclein rather than monomers to divert the protein into off-pathway, regular aggregates, structurally distinct from fibrils. Additionally, multiple cell-based assays demonstrated that Ezrin significantly reduced α-synuclein-mediated toxicity in primary neuronal cell cultures. Yeast cells overexpressing α-synuclein and Ezrin served to confirm this rescue of α-synuclein-mediated toxicity by Ezrin in an *in vivo* setting. Lastly, microscopy studies revealed a decrease in the number of α-synuclein aggregates formed in yeast in the presence of co-expressed Ezrin.

The discovery of a novel mechanism of regulation of α-synuclein fibrillization by a cytoskeletal protein may provide insight into the cellular mechanisms of regulation of α-synuclein fibril formation. In the long run, this could uncover new aspects of the misregulation of this process in PD patients. It could also lead to a better understanding of hitherto unknown processes that may be involved in the neuropathology seen in brain tissue from PD patients. Lastly, as Ezrin is strongly expressed in the gastro-intestinal tract – a site believed by many to be the primary location for the initation of PD pathology – additional studies may shed light on the physiological onset and progression of PD as a condition that is quite commonly thought to originate in the gut.

5.2 Zusammenfassung

α-Synuclein – ein Schlüsselprotein in der Parkinson Krankheit (PD) – bildet große unlösliche Ablagerungen bestehend aus Amyloidfibrillen. Diese sind toxisch und verursachen den Verlust von dopaminergen Neuronen – ein Charakteristikum der PD. Manche Proteine (z.B. Hitzeschock-Proteine) interagieren mit α-Synuclein und verhindern dessen Aggregatbildung. Sie sind somit ein Ausgangspunkt für weiterführende therapeutische Untersuchungen. In dieser Arbeit wurde daher in einer Bibliothek bestehend aus 13.824 Proteinen nach Inhibitoren der α-Synuclein Fibrillenbildung gesucht. Nach mehreren sehr stringenten Screening-Runden wurde das Zytoskelettprotein Ezrin als ein Modulator mit dem höchsten Potential identifiziert. Dieses Potential wurde durch zahlreiche biophysikalische und biochemische Methoden einschließlich Rasterkraftmikroskopie, SDS-PAGE und *in vitro* Fibrillisierung überprüft. Außerdem wurde auch gezeigt, dass nahverwandte Mitglieder der Ezrin-Familie, als starke Fibrillisierungsmodulatoren wirken. Nuklear-Magnet-Resonanz (NMR) Spektroskopie wurde eingesetzt, um den neuartigen Wirkmechanismus von Ezrin bei der α-Synuclein Aggregation zu untersuchen. Es konnte gezeigt werden, dass Ezrin mit kleinen, krankheitsrelevanten α-Synuclein Oligomeren aber nicht mit Monomeren interagiert. Dies führt zur Bildung von off-pathway α-Synuclein Aggregaten, die sich strukturell von Fibrillen unterscheiden. Außerdem wurde in zellbasierten Versuchen mehrfach demonstriert, dass Ezrin die α-Synuclein vermittelte Toxizität auf primäre Neurone in Kultur signifikant verringern kann. Diese Ergebnisse wurden auch in einem Hefezellmodell erfolgreich bestätigt. Schließlich konnte auch durch Mikroskopie-Studien eine Abnahme von α-Synuclein Aggregaten in Ezrin co-exprimierenden Hefezellen gezeigt werden.

Zusammenfassend kann gesagt werden, dass in dieser Arbeit ein neuartiger, sehr potenter α-Synuclein Fibrillisierungsinhibitor identifiziert wurde. Das Protein Ezrin wurde im Detail charakterisiert und die durchgeführten Untersuchungen lieferten wichtige Einblicke in den Mechanismus der spontanen α-Synuclein Aggregation. Gleichzeitig beweist die Arbeit durch Zell-basierte und *in vivo* Studien, dass Ezrin die Toxizität von α-Synuclein Aggregaten in Zellen reduzieren kann. Das Protein ist somit ein wichtiger neuer Ansatzpunkt für weiterführende therapeutische Studien. Des Weiteren führten die Untersuchungen der α-Synuclein Fibrillisierung mit Ezrin zu neuen Einblicken in die zellulären Regulations-mechanismen der α-Synuclein Fibrillenbildung in Zellen. Die Studien werfen ein neues Licht auf die Fehlregulation dieses Prozesses in PD Patienten und könnten längerfristig zu einem besseren Verständnis der Pathogenese bei PD führen. Da Ezrin verstärkt im gastro-intestinal Trakt exprimiert wird, einem Areal in dem viele Forscher den Ursprung der PD

Pathologie vermuten, könnten weiterführende Studien zur Aufklärung der potentiellen Krankheitsmechanismen im Darm beitragen.

6. REFERENCES

(WHO), W.H.O. 2009. Death and DALY estimates for 2004 by cause for WHO Member States (Persons, all ages).

Alexi, T., C.V. Borlongan, R.L. Faull, C.E. Williams, R.G. Clark, P.D. Gluckman, and P.E. Hughes. 2000. Neuroprotective strategies for basal ganglia degeneration: Parkinson's and Huntington's diseases. *Progress in neurobiology*. 60:409-470.

Algrain, M., O. Turunen, A. Vaheri, D. Louvard, and M. Arpin. 1993. Ezrin contains cytoskeleton and membrane binding domains accounting for its proposed role as a membrane-cytoskeletal linker. *The Journal of cell biology*. 120:129-139.

Alim, M.A., M.S. Hossain, K. Arima, K. Takeda, Y. Izumiyama, M. Nakamura, H. Kaji, T. Shinoda, S. Hisanaga, and K. Ueda. 2002. Tubulin seeds alpha-synuclein fibril formation. *The Journal of biological chemistry*. 277:2112-2117.

Alim, M.A., Q.L. Ma, K. Takeda, T. Aizawa, M. Matsubara, M. Nakamura, A. Asada, T. Saito, H. Kaji, M. Yoshii, S. Hisanaga, and K. Ueda. 2004. Demonstration of a role for alpha-synuclein as a functional microtubule-associated protein. *J Alzheimers Dis*. 6:435-442; discussion 443-439.

Alvarez-Erviti, L., M.C. Rodriguez-Oroz, J.M. Cooper, C. Caballero, I. Ferrer, J.A. Obeso, and A.H. Schapira. 2010. Chaperone-mediated autophagy markers in Parkinson disease brains. *Archives of neurology*. 67:1464-1472.

Amieva, M.R., and H. Furthmayr. 1995. Subcellular localization of moesin in dynamic filopodia, retraction fibers, and other structures involved in substrate exploration, attachment, and cell-cell contacts. *Experimental cell research*. 219:180-196.

Amieva, M.R., K.K. Wilgenbus, and H. Furthmayr. 1994. Radixin is a component of hepatocyte microvilli in situ. *Experimental cell research*. 210:140-144.

Andrekopoulos, C., H. Zhang, J. Joseph, S. Kalivendi, and B. Kalyanaraman. 2004. Bicarbonate enhances alpha-synuclein oligomerization and nitration: intermediacy of carbonate radical anion and nitrogen dioxide radical. *The Biochemical journal*. 378:435-447.

Anlauf, M., M.K. Schafer, L. Eiden, and E. Weihe. 2003. Chemical coding of the human gastrointestinal nervous system: cholinergic, VIPergic, and catecholaminergic phenotypes. *The Journal of comparative neurology*. 459:90-111.

Arkin, M.R., M. Randal, W.L. DeLano, J. Hyde, T.N. Luong, J.D. Oslob, D.R. Raphael, L. Taylor, J. Wang, R.S. McDowell, J.A. Wells, and A.C. Braisted. 2003. Binding of small molecules to an adaptive protein-protein interface. *Proceedings of the National Academy of Sciences of the United States of America*. 100:1603-1608.

Arkin, M.R., and J.A. Wells. 2004. Small-molecule inhibitors of protein-protein interactions: progressing towards the dream. *Nature reviews. Drug discovery*. 3:301-317.

Artegiani, B., C. Labbaye, A. Sferra, M.T. Quaranta, P. Torreri, G. Macchia, M. Ceccarini, T.C. Petrucci, and P. Macioce. 2010. The interaction with HMG20a/b proteins suggests a potential role for beta-dystrobrevin in neuronal differentiation. *The Journal of biological chemistry*. 285:24740-24750.

Auluck, P.K., H.Y. Chan, J.Q. Trojanowski, V.M. Lee, and N.M. Bonini. 2002. Chaperone suppression of alpha-synuclein toxicity in a Drosophila model for Parkinson's disease. *Science*. 295:865-868.

Ayala, A., J.L. Venero, J. Cano, and A. Machado. 2007. Mitochondrial toxins and neurodegenerative diseases. *Front Biosci*. 12:986-1007.

Baba, M., S. Nakajo, P.H. Tu, T. Tomita, K. Nakaya, V.M. Lee, J.Q. Trojanowski, and T. Iwatsubo. 1998. Aggregation of alpha-synuclein in Lewy bodies of sporadic Parkinson's disease and dementia with Lewy bodies. *Am J Pathol*. 152:879-884.

Bagchi, D.P., L. Yu, J.S. Perlmutter, J. Xu, R.H. Mach, Z. Tu, and P.T. Kotzbauer. 2013. Binding of the radioligand SIL23 to alpha-synuclein fibrils in Parkinson disease brain

tissue establishes feasibility and screening approaches for developing a Parkinson disease imaging agent. *PloS one*. 8:e55031.

Banich MT, C.R. 2011. Motor control. *Cognitive neuroscience*:108-144.

Bartels, T., J.G. Choi, and D.J. Selkoe. 2011. alpha-Synuclein occurs physiologically as a helically folded tetramer that resists aggregation. *Nature*. 477:107-110.

Behm-Ansmant, I., D. Gatfield, J. Rehwinkel, V. Hilgers, and E. Izaurralde. 2007. A conserved role for cytoplasmic poly(A)-binding protein 1 (PABPC1) in nonsense-mediated mRNA decay. *The EMBO journal*. 26:1591-1601.

Behrends, C., C.A. Langer, R. Boteva, U.M. Bottcher, M.J. Stemp, G. Schaffar, B.V. Rao, A. Giese, H. Kretzschmar, K. Siegers, and F.U. Hartl. 2006. Chaperonin TRiC promotes the assembly of polyQ expansion proteins into nontoxic oligomers. *Molecular cell*. 23:887-897.

Benarroch, E.E. 2007. Enteric nervous system: functional organization and neurologic implications. *Neurology*. 69:1953-1957.

Benarroch, E.E., A.M. Schmeichel, P.A. Low, B.F. Boeve, P. Sandroni, and J.E. Parisi. 2005. Involvement of medullary regions controlling sympathetic output in Lewy body disease. *Brain : a journal of neurology*. 128:338-344.

Benarroch, E.E., A.M. Schmeichel, P. Sandroni, P.A. Low, and J.E. Parisi. 2006a. Differential involvement of hypothalamic vasopressin neurons in multiple system atrophy. *Brain : a journal of neurology*. 129:2688-2696.

Benarroch, E.E., A.M. Schmeichel, P. Sandroni, P.A. Low, and J.E. Parisi. 2006b. Involvement of vagal autonomic nuclei in multiple system atrophy and Lewy body disease. *Neurology*. 66:378-383.

Benarroch, E.E., A.M. Schmeichel, P. Sandroni, P.A. Low, and J.E. Parisi. 2007. Involvement of hypocretin neurons in multiple system atrophy. *Acta neuropathologica*. 113:75-80.

Bergman, H., and G. Deuschl. 2002. Pathophysiology of Parkinson's disease: from clinical neurology to basic neuroscience and back. *Movement disorders : official journal of the Movement Disorder Society*. 17 Suppl 3:S28-40.

Berryman, M., Z. Franck, and A. Bretscher. 1993. Ezrin is concentrated in the apical microvilli of a wide variety of epithelial cells whereas moesin is found primarily in endothelial cells. *Journal of cell science*. 105 (Pt 4):1025-1043.

Bertoncini, C.W., C.O. Fernandez, C. Griesinger, T.M. Jovin, and M. Zweckstetter. 2005. Familial mutants of alpha-synuclein with increased neurotoxicity have a destabilized conformation. *The Journal of biological chemistry*. 280:30649-30652.

Betarbet, R., T.B. Sherer, G. MacKenzie, M. Garcia-Osuna, A.V. Panov, and J.T. Greenamyre. 2000. Chronic systemic pesticide exposure reproduces features of Parkinson's disease. *Nature neuroscience*. 3:1301-1306.

Beyer, K. 2006. Alpha-synuclein structure, posttranslational modification and alternative splicing as aggregation enhancers. *Acta neuropathologica*. 112:237-251.

Biggiogera, M., M.L. Von Schack, T.E. Martin, J. Gordon, M. Muller, and S. Fakan. 1993. Immunoelectron microscope localization of snRNP, hnRNP, and ribosomal proteins in mouse spermatogenesis. *Molecular reproduction and development*. 35:261-271.

Bodenhausen G, R.D.J. 1980. Natural abundance nitrogen-15 NMR by enhanced heteronuclear spectroscopy. *Chemical Physics Letters*. 69:185-189.

Bodles, A.M., D.J. Guthrie, B. Greer, and G.B. Irvine. 2001. Identification of the region of non-Abeta component (NAC) of Alzheimer's disease amyloid responsible for its aggregation and toxicity. *J Neurochem*. 78:384-395.

Bodner, R.A., D.E. Housman, and A.G. Kazantsev. 2006a. New directions for neurodegenerative disease therapy: using chemical compounds to boost the formation of mutant protein inclusions. *Cell Cycle*. 5:1477-1480.

Bodner, R.A., T.F. Outeiro, S. Altmann, M.M. Maxwell, S.H. Cho, B.T. Hyman, P.J. McLean, A.B. Young, D.E. Housman, and A.G. Kazantsev. 2006b. Pharmacological promotion of inclusion formation: a therapeutic approach for Huntington's and Parkinson's

diseases. *Proceedings of the National Academy of Sciences of the United States of America*. 103:4246-4251.

Bonifati, V., P. Rizzu, F. Squitieri, E. Krieger, N. Vanacore, J.C. van Swieten, A. Brice, C.M. van Duijn, B. Oostra, G. Meco, and P. Heutink. 2003. DJ-1(PARK7), a novel gene for autosomal recessive, early onset parkinsonism. *Neurological sciences : official journal of the Italian Neurological Society and of the Italian Society of Clinical Neurophysiology*. 24:159-160.

Bonini, N.M., and B.I. Giasson. 2005. Snaring the function of alpha-synuclein. *Cell*. 123:359-361.

Braak, H., and E. Braak. 2000. Pathoanatomy of Parkinson's disease. *Journal of neurology*. 247 Suppl 2:II3-10.

Braak, H., R.A. de Vos, J. Bohl, and K. Del Tredici. 2006. Gastric alpha-synuclein immunoreactive inclusions in Meissner's and Auerbach's plexuses in cases staged for Parkinson's disease-related brain pathology. *Neuroscience letters*. 396:67-72.

Braak, H., and K. Del Tredici. 2008. Invited Article: Nervous system pathology in sporadic Parkinson disease. *Neurology*. 70:1916-1925.

Braak, H., and K. Del Tredici. 2009. Neuroanatomy and pathology of sporadic Parkinson's disease. *Advances in anatomy, embryology, and cell biology*. 201:1-119.

Braak, H., U. Rub, W.P. Gai, and K. Del Tredici. 2003. Idiopathic Parkinson's disease: possible routes by which vulnerable neuronal types may be subject to neuroinvasion by an unknown pathogen. *J Neural Transm*. 110:517-536.

Bretscher, A. 1983. Purification of an 80,000-dalton protein that is a component of the isolated microvillus cytoskeleton, and its localization in nonmuscle cells. *The Journal of cell biology*. 97:425-432.

Bretscher, A. 1989. Rapid phosphorylation and reorganization of ezrin and spectrin accompany morphological changes induced in A-431 cells by epidermal growth factor. *The Journal of cell biology*. 108:921-930.

Bretscher, A., K. Edwards, and R.G. Fehon. 2002. ERM proteins and merlin: integrators at the cell cortex. *Nature reviews. Molecular cell biology*. 3:586-599.

Bruzzone, F., M. Vallarino, G. Berruti, and C. Angelini. 2008. Expression of the deubiquitinating enzyme mUBPy in the mouse brain. *Brain research*. 1195:56-66.

Bucciantini, M., G. Calloni, F. Chiti, L. Formigli, D. Nosi, C.M. Dobson, and M. Stefani. 2004. Prefibrillar amyloid protein aggregates share common features of cytotoxicity. *The Journal of biological chemistry*. 279:31374-31382.

Bucciantini, M., E. Giannoni, F. Chiti, F. Baroni, L. Formigli, J. Zurdo, N. Taddei, G. Ramponi, C.M. Dobson, and M. Stefani. 2002. Inherent toxicity of aggregates implies a common mechanism for protein misfolding diseases. *Nature*. 416:507-511.

Burre, J., M. Sharma, T. Tsetsenis, V. Buchman, M.R. Etherton, and T.C. Sudhof. 2010. Alpha-synuclein promotes SNARE-complex assembly in vivo and in vitro. *Science*. 329:1663-1667.

Busch, A., S. Engemann, R. Lurz, H. Okazawa, H. Lehrach, and E.E. Wanker. 2003. Mutant huntingtin promotes the fibrillogenesis of wild-type huntingtin: a potential mechanism for loss of huntingtin function in Huntington's disease. *The Journal of biological chemistry*. 278:41452-41461.

Butler, E.K., A. Voigt, A.K. Lutz, J.P. Toegel, E. Gerhardt, P. Karsten, B. Falkenburger, A. Reinartz, K.F. Winklhofer, and J.B. Schulz. 2012. The mitochondrial chaperone protein TRAP1 mitigates alpha-Synuclein toxicity. *PLoS genetics*. 8:e1002488.

Canet-Aviles, R.M., M.A. Wilson, D.W. Miller, R. Ahmad, C. McLendon, S. Bandyopadhyay, M.J. Baptista, D. Ringe, G.A. Petsko, and M.R. Cookson. 2004. The Parkinson's disease protein DJ-1 is neuroprotective due to cysteine-sulfinic acid-driven mitochondrial localization. *Proc Natl Acad Sci U S A*. 101:9103-9108.

Cao, T.T., H.W. Deacon, D. Reczek, A. Bretscher, and M. von Zastrow. 1999. A kinase-regulated PDZ-domain interaction controls endocytic sorting of the beta2-adrenergic receptor. *Nature*. 401:286-290.

REFERENCES

Cappai, R., S.L. Leck, D.J. Tew, N.A. Williamson, D.P. Smith, D. Galatis, R.A. Sharples, C.C. Curtain, F.E. Ali, R.A. Cherny, J.G. Culvenor, S.P. Bottomley, C.L. Masters, K.J. Barnham, and A.F. Hill. 2005. Dopamine promotes alpha-synuclein aggregation into SDS-resistant soluble oligomers via a distinct folding pathway. *FASEB journal : official publication of the Federation of American Societies for Experimental Biology*. 19:1377-1379.

Cashikar, A.G., M. Duennwald, and S.L. Lindquist. 2005. A chaperone pathway in protein disaggregation. Hsp26 alters the nature of protein aggregates to facilitate reactivation by Hsp104. *The Journal of biological chemistry*. 280:23869-23875.

Castagnet, P.I., M.Y. Golovko, G.C. Barcelo-Coblijn, R.L. Nussbaum, and E.J. Murphy. 2005. Fatty acid incorporation is decreased in astrocytes cultured from alpha-synuclein gene-ablated mice. *Journal of neurochemistry*. 94:839-849.

Caughey, B., and P.T. Lansbury. 2003. Protofibrils, pores, fibrils, and neurodegeneration: separating the responsible protein aggregates from the innocent bystanders. *Annual review of neuroscience*. 26:267-298.

Chandra, S., G. Gallardo, R. Fernandez-Chacon, O.M. Schluter, and T.C. Sudhof. 2005. Alpha-synuclein cooperates with CSPalpha in preventing neurodegeneration. *Cell*. 123:383-396.

Charles, V., E. Mezey, P.H. Reddy, A. Dehejia, T.A. Young, M.H. Polymeropoulos, M.J. Brownstein, and D.A. Tagle. 2000. Alpha-synuclein immunoreactivity of huntingtin polyglutamine aggregates in striatum and cortex of Huntington's disease patients and transgenic mouse models. *Neuroscience letters*. 289:29-32.

Chartier-Harlin, M.C., J. Kachergus, C. Roumier, V. Mouroux, X. Douay, S. Lincoln, C. Levecque, L. Larvor, J. Andrieux, M. Hulihan, N. Waucquier, L. Defebvre, P. Amouyel, M. Farrer, and A. Destee. 2004. Alpha-synuclein locus duplication as a cause of familial Parkinson's disease. *Lancet*. 364:1167-1169.

Chaudhuri, K.R., and A.H. Schapira. 2009. Non-motor symptoms of Parkinson's disease: dopaminergic pathophysiology and treatment. *Lancet neurology*. 8:464-474.

Chen, H.L., and S.R. D'Mello. 2010. Induction of neuronal cell death by paraneoplastic Ma1 antigen. *Journal of neuroscience research*. 88:3508-3519.

Chen, J., R.B. Doctor, and L.J. Mandel. 1994. Cytoskeletal dissociation of ezrin during renal anoxia: role in microvillar injury. *The American journal of physiology*. 267:C784-795.

Cheng, L., K. Itoh, and V. Lemmon. 2005. L1-mediated branching is regulated by two ezrin-radixin-moesin (ERM)-binding sites, the RSLE region and a novel juxtamembrane ERM-binding region. *The Journal of neuroscience : the official journal of the Society for Neuroscience*. 25:395-403.

Cherra, S.J., 3rd, E. Steer, A.M. Gusdon, K. Kiselyov, and C.T. Chu. 2013. Mutant LRRK2 elicits calcium imbalance and depletion of dendritic mitochondria in neurons. *The American journal of pathology*. 182:474-484.

Cherukuri, S., R. Hock, T. Ueda, F. Catez, M. Rochman, and M. Bustin. 2008. Cell cycle-dependent binding of HMGN proteins to chromatin. *Molecular biology of the cell*. 19:1816-1824.

Chevalier, J., P. Derkinderen, P. Gomes, R. Thinard, P. Naveilhan, P. Vanden Berghe, and M. Neunlist. 2008. Activity-dependent regulation of tyrosine hydroxylase expression in the enteric nervous system. *The Journal of physiology*. 586:1963-1975.

Chiba-Falek, O., G.J. Lopez, and R.L. Nussbaum. 2006. Levels of alpha-synuclein mRNA in sporadic Parkinson disease patients. *Movement disorders : official journal of the Movement Disorder Society*. 21:1703-1708.

Chinta, S.J., and J.K. Andersen. 2005. Dopaminergic neurons. *The international journal of biochemistry & cell biology*. 37:942-946.

Clayton, D.F., and J.M. George. 1998. The synucleins: a family of proteins involved in synaptic function, plasticity, neurodegeneration and disease. *Trends in neurosciences*. 21:249-254.

REFERENCES

Clayton, D.F., and J.M. George. 1999. Synucleins in synaptic plasticity and neurodegenerative disorders. *Journal of neuroscience research*. 58:120-129.

Cleary, M.A., N. Uboha, M.R. Picciotto, and R.D. Beech. 2006. Expression of ezrin in glial tubes in the adult subventricular zone and rostral migratory stream. *Neuroscience*. 143:851-861.

Cole, N.B., D.D. Murphy, T. Grider, S. Rueter, D. Brasaemle, and R.L. Nussbaum. 2002. Lipid droplet binding and oligomerization properties of the Parkinson's disease protein alpha-synuclein. *The Journal of biological chemistry*. 277:6344-6352.

Colla, E., P.H. Jensen, O. Pletnikova, J.C. Troncoso, C. Glabe, and M.K. Lee. 2012. Accumulation of toxic alpha-synuclein oligomer within endoplasmic reticulum occurs in alpha-synucleinopathy in vivo. *The Journal of neuroscience : the official journal of the Society for Neuroscience*. 32:3301-3305.

Conway, K.A., J.D. Harper, and P.T. Lansbury, Jr. 2000a. Fibrils formed in vitro from alpha-synuclein and two mutant forms linked to Parkinson's disease are typical amyloid. *Biochemistry*. 39:2552-2563.

Conway, K.A., S.J. Lee, J.C. Rochet, T.T. Ding, J.D. Harper, R.E. Williamson, and P.T. Lansbury, Jr. 2000b. Accelerated oligomerization by Parkinson's disease linked alpha-synuclein mutants. *Annals of the New York Academy of Sciences*. 920:42-45.

Conway, K.A., S.J. Lee, J.C. Rochet, T.T. Ding, R.E. Williamson, and P.T. Lansbury, Jr. 2000c. Acceleration of oligomerization, not fibrillization, is a shared property of both alpha-synuclein mutations linked to early-onset Parkinson's disease: implications for pathogenesis and therapy. *Proceedings of the National Academy of Sciences of the United States of America*. 97:571-576.

Conway, K.A., J.C. Rochet, R.M. Bieganski, and P.T. Lansbury, Jr. 2001. Kinetic stabilization of the alpha-synuclein protofibril by a dopamine-alpha-synuclein adduct. *Science*. 294:1346-1349.

Cookson, M.R. 2005. The biochemistry of Parkinson's disease. *Annual review of biochemistry*. 74:29-52.

Cooper, A.A., A.D. Gitler, A. Cashikar, C.M. Haynes, K.J. Hill, B. Bhullar, K. Liu, K. Xu, K.E. Strathearn, F. Liu, S. Cao, K.A. Caldwell, G.A. Caldwell, G. Marsischky, R.D. Kolodner, J. Labaer, J.C. Rochet, N.M. Bonini, and S. Lindquist. 2006. Alpha-synuclein blocks ER-Golgi traffic and Rab1 rescues neuron loss in Parkinson's models. *Science*. 313:324-328.

Crepaldi, T., A. Gautreau, P.M. Comoglio, D. Louvard, and M. Arpin. 1997. Ezrin is an effector of hepatocyte growth factor-mediated migration and morphogenesis in epithelial cells. *The Journal of cell biology*. 138:423-434.

Cuervo, A.M., L. Stefanis, R. Fredenburg, P.T. Lansbury, and D. Sulzer. 2004. Impaired degradation of mutant alpha-synuclein by chaperone-mediated autophagy. *Science*. 305:1292-1295.

Daher, J.P., M. Ying, R. Banerjee, R.S. McDonald, M.D. Hahn, L. Yang, M. Flint Beal, B. Thomas, V.L. Dawson, T.M. Dawson, and D.J. Moore. 2009. Conditional transgenic mice expressing C-terminally truncated human alpha-synuclein (alphaSyn119) exhibit reduced striatal dopamine without loss of nigrostriatal pathway dopaminergic neurons. *Molecular neurodegeneration*. 4:34.

Dalmau, J., S.H. Gultekin, R. Voltz, R. Hoard, T. DesChamps, C. Balmaceda, T. Batchelor, E. Gerstner, J. Eichen, J. Frennier, J.B. Posner, and M.R. Rosenfeld. 1999. Ma1, a novel neuron- and testis-specific protein, is recognized by the serum of patients with paraneoplastic neurological disorders. *Brain : a journal of neurology*. 122 (Pt 1):27-39.

Damrath, E., M.V. Heck, S. Gispert, M. Azizov, J. Nowock, C. Seifried, U. Rub, M. Walter, and G. Auburger. 2012. ATXN2-CAG42 sequesters PABPC1 into insolubility and induces FBXW8 in cerebellum of old ataxic knock-in mice. *PLoS genetics*. 8:e1002920.

Danno, A., W. Fukuda, M. Yoshida, R. Aki, T. Tanaka, T. Kanai, T. Imanaka, and S. Fujiwara. 2008. Expression profiles and physiological roles of two types of prefoldins from the hyperthermophilic archaeon Thermococcus kodakaraensis. *Journal of molecular biology*. 382:298-311.

Daturpalli, S., C.A. Waudby, S. Meehan, and S.E. Jackson. 2013. Hsp90 Inhibits alpha-Synuclein Aggregation by Interacting with Soluble Oligomers. *Journal of molecular biology*.

Dauer, W., N. Kholodilov, M. Vila, A.C. Trillat, R. Goodchild, K.E. Larsen, R. Staal, K. Tieu, Y. Schmitz, C.A. Yuan, M. Rocha, V. Jackson-Lewis, S. Hersch, D. Sulzer, S. Przedborski, R. Burke, and R. Hen. 2002. Resistance of alpha -synuclein null mice to the parkinsonian neurotoxin MPTP. *Proceedings of the National Academy of Sciences of the United States of America*. 99:14524-14529.

Davidson, W.S., A. Jonas, D.F. Clayton, and J.M. George. 1998. Stabilization of alpha-synuclein secondary structure upon binding to synthetic membranes. *The Journal of biological chemistry*. 273:9443-9449.

Davis, G.C., A.C. Williams, S.P. Markey, M.H. Ebert, E.D. Caine, C.M. Reichert, and I.J. Kopin. 1979. Chronic Parkinsonism secondary to intravenous injection of meperidine analogues. *Psychiatry Res*. 1:249-254.

De Graeve, S., S. Marinelli, F. Stolz, J. Hendrix, J. Vandamme, Y. Engelborghs, P. Van Dijck, and J.M. Thevelein. 2013. Mammalian ribosomal and chaperone protein RPS3A counteracts alpha-Synuclein aggregation and toxicity in a yeast model system. *The Biochemical journal*.

de Laureto, P.P., L. Tosatto, E. Frare, O. Marin, V.N. Uversky, and A. Fontana. 2006. Conformational properties of the SDS-bound state of alpha-synuclein probed by limited proteolysis: unexpected rigidity of the acidic C-terminal tail. *Biochemistry*. 45:11523-11531.

Defacque, H., M. Egeberg, A. Antzberger, W. Ansorge, M. Way, and G. Griffiths. 2000a. Actin assembly induced by polylysine beads or purified phagosomes: quantitation by a new flow cytometry assay. *Cytometry*. 41:46-54.

Defacque, H., M. Egeberg, A. Habermann, M. Diakonova, C. Roy, P. Mangeat, W. Voelter, G. Marriott, J. Pfannstiel, H. Faulstich, and G. Griffiths. 2000b. Involvement of ezrin/moesin in de novo actin assembly on phagosomal membranes. *The EMBO journal*. 19:199-212.

Deng, L.X., G.X. Wu, Y. Cao, B. Fan, X. Gao, L. Luo, and N. Huang. 2011. The chromosomal protein HMGN2 mediates lipopolysaccharide-induced expression of beta-defensins in A549 cells. *The FEBS journal*. 278:2152-2166.

Dev, K.K., K. Hofele, S. Barbieri, V.L. Buchman, and H. van der Putten. 2003. Part II: alpha-synuclein and its molecular pathophysiological role in neurodegenerative disease. *Neuropharmacology*. 45:14-44.

Devi, L., V. Raghavendran, B.M. Prabhu, N.G. Avadhani, and H.K. Anandatheerthavarada. 2008. Mitochondrial import and accumulation of alpha-synuclein impair complex I in human dopaminergic neuronal cultures and Parkinson disease brain. *J Biol Chem*. 283:9089-9100.

Devine, M.J., M. Ryten, P. Vodicka, A.J. Thomson, T. Burdon, H. Houlden, F. Cavaleri, M. Nagano, N.J. Drummond, J.W. Taanman, A.H. Schapira, K. Gwinn, J. Hardy, P.A. Lewis, and T. Kunath. 2011. Parkinson's disease induced pluripotent stem cells with triplication of the alpha-synuclein locus. *Nat Commun*. 2:440.

Di Fonzo, A., C.F. Rohe, J. Ferreira, H.F. Chien, L. Vacca, F. Stocchi, L. Guedes, E. Fabrizio, M. Manfredi, N. Vanacore, S. Goldwurm, G. Breedveld, C. Sampaio, G. Meco, E. Barbosa, B.A. Oostra, and V. Bonifati. 2005. A frequent LRRK2 gene mutation associated with autosomal dominant Parkinson's disease. *Lancet*. 365:412-415.

Dick, F.D., G. De Palma, A. Ahmadi, N.W. Scott, G.J. Prescott, J. Bennett, S. Semple, S. Dick, C. Counsell, P. Mozzoni, N. Haites, S.B. Wettinger, A. Mutti, M. Otelea, A.

Seaton, P. Soderkvist, and A. Felice. 2007. Environmental risk factors for Parkinson's disease and parkinsonism: the Geoparkinson study. *Occup Environ Med*. 64:666-672.

Dickson, D.W., H. Fujishiro, C. Orr, A. DelleDonne, K.A. Josephs, R. Frigerio, M. Burnett, J.E. Parisi, K.J. Klos, and J.E. Ahlskog. 2009. Neuropathology of non-motor features of Parkinson disease. *Parkinsonism Relat Disord*. 15 Suppl 3:S1-5.

Dickson, D.W., D. Ruan, H. Crystal, M.H. Mark, P. Davies, Y. Kress, and S.H. Yen. 1991. Hippocampal degeneration differentiates diffuse Lewy body disease (DLBD) from Alzheimer's disease: light and electron microscopic immunocytochemistry of CA2-3 neurites specific to DLBD. *Neurology*. 41:1402-1409.

Dong, X., C. Yu, O. Shynlova, J.R. Challis, P.S. Rennie, and S.J. Lye. 2009. p54nrb is a transcriptional corepressor of the progesterone receptor that modulates transcription of the labor-associated gene, connexin 43 (Gja1). *Mol Endocrinol*. 23:1147-1160.

Dong, Z., B. Ferger, J. Feldon, and H. Bueler. 2002. Overexpression of Parkinson's disease-associated alpha-synucleinA53T by recombinant adeno-associated virus in mice does not increase the vulnerability of dopaminergic neurons to MPTP. *Journal of neurobiology*. 53:1-10.

Drescher, M., M. Huber, and V. Subramaniam. 2012. Hunting the chameleon: structural conformations of the intrinsically disordered protein alpha-synuclein. *Chembiochem : a European journal of chemical biology*. 13:761-768.

Drolet, R.E., B. Behrouz, K.J. Lookingland, and J.L. Goudreau. 2004. Mice lacking alpha-synuclein have an attenuated loss of striatal dopamine following prolonged chronic MPTP administration. *Neurotoxicology*. 25:761-769.

Duncan, K.A., P. Jimenez, and L.L. Carruth. 2009. The selective estrogen receptor-alpha coactivator, RPL7, and sexual differentiation of the songbird brain. *Psychoneuroendocrinology*. 34 Suppl 1:S30-38.

Dunker, A.K., J.D. Lawson, C.J. Brown, R.M. Williams, P. Romero, J.S. Oh, C.J. Oldfield, A.M. Campen, C.M. Ratliff, K.W. Hipps, J. Ausio, M.S. Nissen, R. Reeves, C. Kang, C.R. Kissinger, R.W. Bailey, M.D. Griswold, W. Chiu, E.C. Garner, and Z. Obradovic. 2001. Intrinsically disordered protein. *Journal of molecular graphics & modelling*. 19:26-59.

Edwards, K.A., R.A. Montague, S. Shepard, B.A. Edgar, R.L. Erikson, and D.P. Kiehart. 1994. Identification of Drosophila cytoskeletal proteins by induction of abnormal cell shape in fission yeast. *Proceedings of the National Academy of Sciences of the United States of America*. 91:4589-4593.

Ehrnhoefer, D.E., J. Bieschke, A. Boeddrich, M. Herbst, L. Masino, R. Lurz, S. Engemann, A. Pastore, and E.E. Wanker. 2008. EGCG redirects amyloidogenic polypeptides into unstructured, off-pathway oligomers. *Nature structural & molecular biology*. 15:558-566.

Eliezer, D., E. Kutluay, R. Bussell, Jr., and G. Browne. 2001. Conformational properties of alpha-synuclein in its free and lipid-associated states. *Journal of molecular biology*. 307:1061-1073.

Ellis, R.J. 2006. Molecular chaperones: assisting assembly in addition to folding. *Trends in biochemical sciences*. 31:395-401.

Engelender, S., Z. Kaminsky, X. Guo, A.H. Sharp, R.K. Amaravi, J.J. Kleiderlein, R.L. Margolis, J.C. Troncoso, A.A. Lanahan, P.F. Worley, V.L. Dawson, T.M. Dawson, and C.A. Ross. 1999. Synphilin-1 associates with alpha-synuclein and promotes the formation of cytosolic inclusions. *Nature genetics*. 22:110-114.

Enomoto, H., T. Ozaki, E. Takahashi, N. Nomura, S. Tabata, H. Takahashi, N. Ohnuma, M. Tanabe, J. Iwai, H. Yoshida, and et al. 1994. Identification of human DAN gene, mapping to the putative neuroblastoma tumor suppressor locus. *Oncogene*. 9:2785-2791.

REFERENCES

Esler, W.P., E.R. Stimson, J.R. Ghilardi, A.M. Felix, Y.A. Lu, H.V. Vinters, P.W. Mantyh, and J.E. Maggio. 1997. A beta deposition inhibitor screen using synthetic amyloid. *Nature biotechnology*. 15:258-263.

Falkenburger, B.H., and J.B. Schulz. 2006. Limitations of cellular models in Parkinson's disease research. *J Neural Transm Suppl*:261-268.

Falsone, S.F., A.J. Kungl, A. Rek, R. Cappai, and K. Zangger. 2009. The molecular chaperone Hsp90 modulates intermediate steps of amyloid assembly of the Parkinson-related protein alpha-synuclein. *The Journal of biological chemistry*. 284:31190-31199.

Falsone, S.F., N.H. Meyer, E. Schrank, G. Leitinger, C.L. Pham, M.T. Fodero-Tavoletti, M. Holmberg, M. Dulle, B. Scicluna, B. Gesslbauer, H.M. Ruckert, G.E. Wagner, D.A. Merle, E.A. Nollen, A.J. Kungl, A.F. Hill, R. Cappai, and K. Zangger. 2012. SERF protein is a direct modifier of amyloid fiber assembly. *Cell reports*. 2:358-371.

Fan, G.H., H.Y. Zhou, H. Yang, and S.D. Chen. 2006. Heat shock proteins reduce alpha-synuclein aggregation induced by MPP+ in SK-N-SH cells. *FEBS letters*. 580:3091-3098.

Farrer, M., J. Kachergus, L. Forno, S. Lincoln, D.S. Wang, M. Hulihan, D. Maraganore, K. Gwinn-Hardy, Z. Wszolek, D. Dickson, and J.W. Langston. 2004. Comparison of kindreds with parkinsonism and alpha-synuclein genomic multiplications. *Annals of neurology*. 55:174-179.

Fauvet, B., M.K. Mbefo, M.B. Fares, C. Desobry, S. Michael, M.T. Ardah, E. Tsika, P. Coune, M. Prudent, N. Lion, D. Eliezer, D.J. Moore, B. Schneider, P. Aebischer, O.M. El-Agnaf, E. Masliah, and H.A. Lashuel. 2012. alpha-Synuclein in central nervous system and from erythrocytes, mammalian cells, and Escherichia coli exists predominantly as disordered monomer. *The Journal of biological chemistry*. 287:15345-15364.

Feany, M.B., and W.W. Bender. 2000. A Drosophila model of Parkinson's disease. *Nature*. 404:394-398.

Fehon, R.G., A.I. McClatchey, and A. Bretscher. 2010. Organizing the cell cortex: the role of ERM proteins. *Nature reviews. Molecular cell biology*. 11:276-287.

Fiorillo, A.A., T.R. Medler, Y.B. Feeney, Y. Liu, K.L. Tommerdahl, and C.V. Clevenger. 2011. HMGN2 inducibly binds a novel transactivation domain in nuclear PRLr to coordinate Stat5a-mediated transcription. *Mol Endocrinol*. 25:1550-1564.

Fisher, E.M., P. Beer-Romero, L.G. Brown, A. Ridley, J.A. McNeil, J.B. Lawrence, H.F. Willard, F.R. Bieber, and D.C. Page. 1990. Homologous ribosomal protein genes on the human X and Y chromosomes: escape from X inactivation and possible implications for Turner syndrome. *Cell*. 63:1205-1218.

Foley, P., M. Gerlach, K.L. Double, and P. Riederer. 2004. Dopamine receptor agonists in the therapy of Parkinson's disease. *J Neural Transm*. 111:1375-1446.

Fornai, F., O.M. Schluter, P. Lenzi, M. Gesi, R. Ruffoli, M. Ferrucci, G. Lazzeri, C.L. Busceti, F. Pontarelli, G. Battaglia, A. Pellegrini, F. Nicoletti, S. Ruggieri, A. Paparelli, and T.C. Sudhof. 2005. Parkinson-like syndrome induced by continuous MPTP infusion: convergent roles of the ubiquitin-proteasome system and alpha-synuclein. *Proceedings of the National Academy of Sciences of the United States of America*. 102:3413-3418.

Forno, L.S. 1996. Neuropathology of Parkinson's disease. *Journal of neuropathology and experimental neurology*. 55:259-272.

Forno, L.S.a.E.C.A., Jr. 1974. Depigmentation in the nerve cells of the substantia nigra and locus ceruleus in Parkinsonism. *Advances in neurology*:195-202.

Fortin, D.L., M.D. Troyer, K. Nakamura, S. Kubo, M.D. Anthony, and R.H. Edwards. 2004. Lipid rafts mediate the synaptic localization of alpha-synuclein. *The Journal of neuroscience : the official journal of the Society for Neuroscience*. 24:6715-6723.

Frame, M.C., H. Patel, B. Serrels, D. Lietha, and M.J. Eck. 2010. The FERM domain: organizing the structure and function of FAK. *Nature reviews. Molecular cell biology*. 11:802-814.

Franck, Z., R. Gary, and A. Bretscher. 1993. Moesin, like ezrin, colocalizes with actin in the cortical cytoskeleton in cultured cells, but its expression is more variable. *Journal of cell science*. 105 (Pt 1):219-231.

Freed, C.R., N.L. Rosenberg, S.A. Schneck, and R.E. Breeze. 1992. Improved drug responsiveness following fetal tissue implant for Parkinson's disease. *Neurochemistry international*. 20 Suppl:321S-327S.

Frigerio, R., K.R. Sanft, B.R. Grossardt, B.J. Peterson, A. Elbaz, J.H. Bower, J.E. Ahlskog, M. de Andrade, D.M. Maraganore, and W.A. Rocca. 2006. Chemical exposures and Parkinson's disease: a population-based case-control study. *Mov Disord*. 21:1688-1692.

Fuchs, J., C. Nilsson, J. Kachergus, M. Munz, E.M. Larsson, B. Schule, J.W. Langston, F.A. Middleton, O.A. Ross, M. Hulihan, T. Gasser, and M.J. Farrer. 2007. Phenotypic variation in a large Swedish pedigree due to SNCA duplication and triplication. *Neurology*. 68:916-922.

Fukuda, T. 2001. Neurotoxicity of MPTP. *Neuropathology : official journal of the Japanese Society of Neuropathology*. 21:323-332.

Funayama, N., A. Nagafuchi, N. Sato, and S. Tsukita. 1991. Radixin is a novel member of the band 4.1 family. *The Journal of cell biology*. 115:1039-1048.

Furesz, S. 1970. Chemical and biological properties of rifampicin. *Antibiotics and chemotherapy*. 16:316-351.

Furutani, Y., H. Matsuno, M. Kawasaki, T. Sasaki, K. Mori, and Y. Yoshihara. 2007. Interaction between telencephalin and ERM family proteins mediates dendritic filopodia formation. *The Journal of neuroscience : the official journal of the Society for Neuroscience*. 27:8866-8876.

Gao, Z., K. Huang, and H. Xu. 2001. Protective effects of flavonoids in the roots of Scutellaria baicalensis Georgi against hydrogen peroxide-induced oxidative stress in HS-SY5Y cells. *Pharmacological research : the official journal of the Italian Pharmacological Society*. 43:173-178.

Garcia-Reitbock, P., O. Anichtchik, A. Bellucci, M. Iovino, C. Ballini, E. Fineberg, B. Ghetti, L. Della Corte, P. Spano, G.K. Tofaris, M. Goedert, and M.G. Spillantini. 2010. SNARE protein redistribution and synaptic failure in a transgenic mouse model of Parkinson's disease. *Brain*. 133:2032-2044.

Gautreau, A., P. Poullet, D. Louvard, and M. Arpin. 1999. Ezrin, a plasma membrane-microfilament linker, signals cell survival through the phosphatidylinositol 3-kinase/Akt pathway. *Proceedings of the National Academy of Sciences of the United States of America*. 96:7300-7305.

George, J.M. 2002. The synucleins. *Genome Biol*. 3:REVIEWS3002.

Gerlach-Bank, L.M., A.D. Ellis, B. Noonen, and K.F. Barald. 2002. Cloning and expression analysis of the chick DAN gene, an antagonist of the BMP family of growth factors. *Developmental dynamics : an official publication of the American Association of Anatomists*. 224:109-115.

Gerlitz, G. 2010. HMGNs, DNA repair and cancer. *Biochimica et biophysica acta*. 1799:80-85.

Gershanik, O.S., and T.G. Nygaard. 1990. Parkinson's disease beginning before age 40. *Advances in neurology*. 53:251-258.

Giasson, B.I., J.E. Duda, S.M. Quinn, B. Zhang, J.Q. Trojanowski, and V.M. Lee. 2002a. Neuronal alpha-synucleinopathy with severe movement disorder in mice expressing A53T human alpha-synuclein. *Neuron*. 34:521-533.

Giasson, B.I., H. Ischiropoulos, V.M. Lee, and J.Q. Trojanowski. 2002b. The relationship between oxidative/nitrative stress and pathological inclusions in Alzheimer's and Parkinson's diseases. *Free radical biology & medicine*. 32:1264-1275.

Gilks, W.P., P.M. Abou-Sleiman, S. Gandhi, S. Jain, A. Singleton, A.J. Lees, K. Shaw, K.P. Bhatia, V. Bonifati, N.P. Quinn, J. Lynch, D.G. Healy, J.L. Holton, T. Revesz, and N.W. Wood. 2005. A common LRRK2 mutation in idiopathic Parkinson's disease. *Lancet*. 365:415-416.

Gitler, A.D., B.J. Bevis, J. Shorter, K.E. Strathearn, S. Hamamichi, L.J. Su, K.A. Caldwell, G.A. Caldwell, J.C. Rochet, J.M. McCaffery, C. Barlowe, and S. Lindquist. 2008. The Parkinson's disease protein alpha-synuclein disrupts cellular Rab homeostasis. *Proc Natl Acad Sci U S A*. 105:145-150.

Glenner, G.G., and M.A. Murphy. 1989. Amyloidosis of the nervous system. *Journal of the neurological sciences*. 94:1-28.

Glover, J.R., and S. Lindquist. 1998. Hsp104, Hsp70, and Hsp40: a novel chaperone system that rescues previously aggregated proteins. *Cell*. 94:73-82.

Goedert, M. 2001. Alpha-synuclein and neurodegenerative diseases. *Nat Rev Neurosci*. 2:492-501.

Golovko, M.Y., N.J. Faergeman, N.B. Cole, P.I. Castagnet, R.L. Nussbaum, and E.J. Murphy. 2005. Alpha-synuclein gene deletion decreases brain palmitate uptake and alters the palmitate metabolism in the absence of alpha-synuclein palmitate binding. *Biochemistry*. 44:8251-8259.

Gonzalez-Navajas, J.M., J. Law, K.P. Nguyen, M. Bhargava, M.P. Corr, N. Varki, L. Eckmann, H.M. Hoffman, J. Lee, and E. Raz. 2010. Interleukin 1 receptor signaling regulates DUBA expression and facilitates Toll-like receptor 9-driven antiinflammatory cytokine production. *The Journal of experimental medicine*. 207:2799-2807.

Gosavi, N., H.J. Lee, J.S. Lee, S. Patel, and S.J. Lee. 2002. Golgi fragmentation occurs in the cells with prefibrillar alpha-synuclein aggregates and precedes the formation of fibrillar inclusion. *The Journal of biological chemistry*. 277:48984-48992.

Gould, K.L., A. Bretscher, F.S. Esch, and T. Hunter. 1989. cDNA cloning and sequencing of the protein-tyrosine kinase substrate, ezrin, reveals homology to band 4.1. *The EMBO journal*. 8:4133-4142.

Gould, K.L., J.A. Cooper, A. Bretscher, and T. Hunter. 1986. The protein-tyrosine kinase substrate, p81, is homologous to a chicken microvillar core protein. *The Journal of cell biology*. 102:660-669.

Gouras, G.K., D. Tampellini, R.H. Takahashi, and E. Capetillo-Zarate. 2010. Intraneuronal beta-amyloid accumulation and synapse pathology in Alzheimer's disease. *Acta neuropathologica*. 119:523-541.

Gousseva, N., and R.T. Baker. 2003. Gene structure, alternate splicing, tissue distribution, cellular localization, and developmental expression pattern of mouse deubiquitinating enzyme isoforms Usp2-45 and Usp2-69. *Gene expression*. 11:163-179.

Gowers, W.R., and A.E. Barker. 1886. On a Case of Abscess of the Temporo-Sphenoidal Lobe of the Brain, Due to Otitis Media, Successfully Treated by Trephining and Drainage. *British medical journal*. 2:1154-1156.

Goyal, R.K., and I. Hirano. 1996. The enteric nervous system. *The New England journal of medicine*. 334:1106-1115.

Gutekunst, C.A., S.H. Li, H. Yi, J.S. Mulroy, S. Kuemmerle, R. Jones, D. Rye, R.J. Ferrante, S.M. Hersch, and X.J. Li. 1999. Nuclear and neuropil aggregates in Huntington's disease: relationship to neuropathology. *The Journal of neuroscience : the official journal of the Society for Neuroscience*. 19:2522-2534.

Haas, M.A., J.C. Vickers, and T.C. Dickson. 2007. Rho kinase activates ezrin-radixin-moesin (ERM) proteins and mediates their function in cortical neuron growth, morphology and motility in vitro. *Journal of neuroscience research*. 85:34-46.

Haik, S., B.A. Faucheux, and J.J. Hauw. 2004. Brain targeting through the autonomous nervous system: lessons from prion diseases. *Trends in molecular medicine*. 10:107-112.

Hanzel, D., H. Reggio, A. Bretscher, J.G. Forte, and P. Mangeat. 1991. The secretion-stimulated 80K phosphoprotein of parietal cells is ezrin, and has properties of a membrane cytoskeletal linker in the induced apical microvilli. *The EMBO journal*. 10:2363-2373.

Hanzel, D.K., T. Urushidani, W.R. Usinger, A. Smolka, and J.G. Forte. 1989. Immunological localization of an 80-kDa phosphoprotein to the apical membrane of gastric parietal cells. *The American journal of physiology*. 256:G1082-1089.

Hardy, J.A., and G.A. Higgins. 1992. Alzheimer's disease: the amyloid cascade hypothesis. *Science*. 256:184-185.

Harper, J.D., S.S. Wong, C.M. Lieber, and P.T. Lansbury, Jr. 1999. Assembly of A beta amyloid protofibrils: an in vitro model for a possible early event in Alzheimer's disease. *Biochemistry*. 38:8972-8980.

Hashimoto, M., E. Rockenstein, M. Mante, M. Mallory, and E. Masliah. 2001. beta-Synuclein inhibits alpha-synuclein aggregation: a possible role as an anti-parkinsonian factor. *Neuron*. 32:213-223.

Hawkes, C.H., K. Del Tredici, and H. Braak. 2007. Parkinson's disease: a dual-hit hypothesis. *Neuropathology and applied neurobiology*. 33:599-614.

Hayashi, T., K. Sentani, N. Oue, S. Ohara, J. Teishima, K. Anami, N. Sakamoto, A. Matsubara, and W. Yasui. 2013. The Search for Secreted Proteins in Prostate Cancer by the Escherichia coli Ampicillin Secretion Trap: Expression of NBL1 Is Highly Restricted to the Prostate and Is Related to Cancer Progression. *Pathobiology : journal of immunopathology, molecular and cellular biology*. 80:60-69.

Heiser, V., S. Engemann, W. Brocker, I. Dunkel, A. Boeddrich, S. Waelter, E. Nordhoff, R. Lurz, N. Schugardt, S. Rautenberg, C. Herhaus, G. Barnickel, H. Bottcher, H. Lehrach, and E.E. Wanker. 2002. Identification of benzothiazoles as potential polyglutamine aggregation inhibitors of Huntington's disease by using an automated filter retardation assay. *Proceedings of the National Academy of Sciences of the United States of America*. 99 Suppl 4:16400-16406.

Higman, V.A. 2013. Proteins in solution and at interfaces: Methods and Applications in Biotechnology and Materials Science.

Hinault, M.P., A.F. Cuendet, R.U. Mattoo, M. Mensi, G. Dietler, H.A. Lashuel, and P. Goloubinoff. 2010. Stable alpha-synuclein oligomers strongly inhibit chaperone activity of the Hsp70 system by weak interactions with J-domain co-chaperones. *The Journal of biological chemistry*. 285:38173-38182.

Hirao, M., N. Sato, T. Kondo, S. Yonemura, M. Monden, T. Sasaki, Y. Takai, and S. Tsukita. 1996. Regulation mechanism of ERM (ezrin/radixin/moesin) protein/plasma membrane association: possible involvement of phosphatidylinositol turnover and Rho-dependent signaling pathway. *The Journal of cell biology*. 135:37-51.

Hiscox, S., and W.G. Jiang. 1999. Ezrin regulates cell-cell and cell-matrix adhesion, a possible role with E-cadherin/beta-catenin. *Journal of cell science*. 112 Pt 18:3081-3090.

Hoffmann, L.A., S. Jarius, H.L. Pellkofer, M. Schueller, M. Krumbholz, F. Koenig, W. Johannis, C. la Fougere, T. Newman, A. Vincent, and R. Voltz. 2008. Anti-Ma and anti-Ta associated paraneoplastic neurological syndromes: 22 newly diagnosed patients and review of previous cases. *Journal of neurology, neurosurgery, and psychiatry*. 79:767-773.

Hofmann, I., M. Casella, M. Schnolzer, T. Schlechter, H. Spring, and W.W. Franke. 2006. Identification of the junctional plaque protein plakophilin 3 in cytoplasmic particles containing RNA-binding proteins and the recruitment of plakophilins 1 and 3 to stress granules. *Molecular biology of the cell*. 17:1388-1398.

Holbert, S., I. Denghien, T. Kiechle, A. Rosenblatt, C. Wellington, M.R. Hayden, R.L. Margolis, C.A. Ross, J. Dausset, R.J. Ferrante, and C. Neri. 2001. The Gln-Ala repeat transcriptional activator CA150 interacts with huntingtin: neuropathologic and

genetic evidence for a role in Huntington's disease pathogenesis. *Proceedings of the National Academy of Sciences of the United States of America*. 98:1811-1816.

Hosoda, N., F. Lejeune, and L.E. Maquat. 2006. Evidence that poly(A) binding protein C1 binds nuclear pre-mRNA poly(A) tails. *Molecular and cellular biology*. 26:3085-3097.

Hsu, L.J., Y. Sagara, A. Arroyo, E. Rockenstein, A. Sisk, M. Mallory, J. Wong, T. Takenouchi, M. Hashimoto, and E. Masliah. 2000. alpha-synuclein promotes mitochondrial deficit and oxidative stress. *Am J Pathol*. 157:401-410.

Huang, O.W., X. Ma, J. Yin, J. Flinders, T. Maurer, N. Kayagaki, Q. Phung, I. Bosanac, D. Arnott, V.M. Dixit, S.G. Hymowitz, M.A. Starovasnik, and A.G. Cochran. 2012. Phosphorylation-dependent activity of the deubiquitinase DUBA. *Nature structural & molecular biology*. 19:171-175.

Hung, W.T., F.J. Wu, C.J. Wang, and C.W. Luo. 2012. DAN (NBL1) specifically antagonizes BMP2 and BMP4 and modulates the actions of GDF9, BMP2, and BMP4 in the rat ovary. *Biology of reproduction*. 86:158, 151-159.

Hunter, T., and J.A. Cooper. 1981. Epidermal growth factor induces rapid tyrosine phosphorylation of proteins in A431 human tumor cells. *Cell*. 24:741-752.

Hyun, D.H., M. Lee, B. Halliwell, and P. Jenner. 2003. Proteasomal inhibition causes the formation of protein aggregates containing a wide range of proteins, including nitrated proteins. *Journal of neurochemistry*. 86:363-373.

Ingraffea, J., D. Reczek, and A. Bretscher. 2002. Distinct cell type-specific expression of scaffolding proteins EBP50 and E3KARP: EBP50 is generally expressed with ezrin in specific epithelia, whereas E3KARP is not. *European journal of cell biology*. 81:61-68.

Ito, A., M. Hagiyama, and J. Oonuma. 2008. Nerve-mast cell and smooth muscle-mast cell interaction mediated by cell adhesion molecule-1, CADM1. *Journal of smooth muscle research = Nihon Heikatsukin Gakkai kikanshi*. 44:83-93.

Ivetic, A., and A.J. Ridley. 2004. Ezrin/radixin/moesin proteins and Rho GTPase signalling in leucocytes. *Immunology*. 112:165-176.

Jaleel, M., R.J. Nichols, M. Deak, D.G. Campbell, F. Gillardon, A. Knebel, and D.R. Alessi. 2007. LRRK2 phosphorylates moesin at threonine-558: characterization of how Parkinson's disease mutants affect kinase activity. *The Biochemical journal*. 405:307-317.

Janus, C., J. Pearson, J. McLaurin, P.M. Mathews, Y. Jiang, S.D. Schmidt, M.A. Chishti, P. Horne, D. Heslin, J. French, H.T. Mount, R.A. Nixon, M. Mercken, C. Bergeron, P.E. Fraser, P. St George-Hyslop, and D. Westaway. 2000. A beta peptide immunization reduces behavioural impairment and plaques in a model of Alzheimer's disease. *Nature*. 408:979-982.

Jao, C.C., A. Der-Sarkissian, J. Chen, and R. Langen. 2004. Structure of membrane-bound alpha-synuclein studied by site-directed spin labeling. *Proceedings of the National Academy of Sciences of the United States of America*. 101:8331-8336.

Jellinger, K.A. 2003. Neuropathological spectrum of synucleinopathies. *Mov Disord*. 18 Suppl 6:S2-12.

Jenco, J.M., A. Rawlingson, B. Daniels, and A.J. Morris. 1998. Regulation of phospholipase D2: selective inhibition of mammalian phospholipase D isoenzymes by alpha- and beta-synucleins. *Biochemistry*. 37:4901-4909.

Jensen, P.H., M.S. Nielsen, R. Jakes, C.G. Dotti, and M. Goedert. 1998. Binding of alpha-synuclein to brain vesicles is abolished by familial Parkinson's disease mutation. *The Journal of biological chemistry*. 273:26292-26294.

Jin, J., G.J. Li, J. Davis, D. Zhu, Y. Wang, C. Pan, and J. Zhang. 2007. Identification of novel proteins associated with both alpha-synuclein and DJ-1. *Molecular & cellular proteomics : MCP*. 6:845-859.

Jo, E., A.A. Darabie, K. Han, A. Tandon, P.E. Fraser, and J. McLaurin. 2004. alpha-Synuclein-synaptosomal membrane interactions: implications for fibrillogenesis. *European journal of biochemistry / FEBS*. 271:3180-3189.

Jo, E., J. McLaurin, C.M. Yip, P. St George-Hyslop, and P.E. Fraser. 2000. alpha-Synuclein membrane interactions and lipid specificity. *The Journal of biological chemistry*. 275:34328-34334.

Johnson, M.W., H. Miyata, and H.V. Vinters. 2002. Ezrin and moesin expression within the developing human cerebrum and tuberous sclerosis-associated cortical tubers. *Acta neuropathologica*. 104:188-196.

Just, W., C. Geerkens, K.R. Held, and W. Vogel. 1992. Expression of RPS4X in fibroblasts from patients with structural aberrations of the X chromosome. *Human genetics*. 89:240-242.

Kalivendi, S.V., D. Yedlapudi, C.J. Hillard, and B. Kalyanaraman. 2010. Oxidants induce alternative splicing of alpha-synuclein: Implications for Parkinson's disease. *Free Radic Biol Med*. 48:377-383.

Kamei, D., N. Tsuchiya, M. Yamazaki, H. Meguro, and M. Yamada. 1999. Two forms of expression and genomic structure of the human heterogeneous nuclear ribonucleoprotein D-like JKTBP gene (HNRPDL). *Gene*. 228:13-22.

Kamp, F., and K. Beyer. 2006. Binding of alpha-synuclein affects the lipid packing in bilayers of small vesicles. *The Journal of biological chemistry*. 281:9251-9259.

Karathia, H., E. Vilaprinyo, A. Sorribas, and R. Alves. 2011. Saccharomyces cerevisiae as a model organism: a comparative study. *PloS one*. 6:e16015.

Kaul, S.C., Y. Mitsui, Y. Komatsu, R.R. Reddel, and R. Wadhwa. 1996. A highly expressed 81 kDa protein in immortalized mouse fibroblast: its proliferative function and identity with ezrin. *Oncogene*. 13:1231-1237.

Kawamura, H., Y. Tomozoe, T. Akagi, D. Kamei, M. Ochiai, and M. Yamada. 2002. Identification of the nucleocytoplasmic shuttling sequence of heterogeneous nuclear ribonucleoprotein D-like protein JKTBP and its interaction with mRNA. *The Journal of biological chemistry*. 277:2732-2739.

Kayagaki, N., Q. Phung, S. Chan, R. Chaudhari, C. Quan, K.M. O'Rourke, M. Eby, E. Pietras, G. Cheng, J.F. Bazan, Z. Zhang, D. Arnott, and V.M. Dixit. 2007. DUBA: a deubiquitinase that regulates type I interferon production. *Science*. 318:1628-1632.

Kegel, K.B., A.R. Meloni, Y. Yi, Y.J. Kim, E. Doyle, B.G. Cuiffo, E. Sapp, Y. Wang, Z.H. Qin, J.D. Chen, J.R. Nevins, N. Aronin, and M. DiFiglia. 2002. Huntingtin is present in the nucleus, interacts with the transcriptional corepressor C-terminal binding protein, and represses transcription. *The Journal of biological chemistry*. 277:7466-7476.

Kilpatrick, K., J.A. Novoa, T. Hancock, C.J. Guerriero, P. Wipf, J.L. Brodsky, and L. Segatori. 2013. Chemical Induction of Hsp70 Reduces alpha-Synuclein Aggregation in Neuroglioma Cells. *ACS chemical biology*.

Kim, A.S., and S.J. Pleasure. 2003. Expression of the BMP antagonist Dan during murine forebrain development. *Brain research. Developmental brain research*. 145:159-162.

Kim, H.S., C.D. Bae, and J. Park. 2010. Glutamate receptor-mediated phosphorylation of ezrin/radixin/moesin proteins is implicated in filopodial protrusion of primary cultured hippocampal neuronal cells. *Journal of neurochemistry*. 113:1565-1576.

Kim, T.Y., C.W. Ha, and W.K. Huh. 2009. Differential subcellular localization of ribosomal protein L7 paralogs in Saccharomyces cerevisiae. *Molecules and cells*. 27:539-546.

Kim, Y.S., E. Laurine, W. Woods, and S.J. Lee. 2006. A novel mechanism of interaction between alpha-synuclein and biological membranes. *Journal of molecular biology*. 360:386-397.

Kimura, M., K. Ishida, S. Kashiwabara, and T. Baba. 2009. Characterization of two cytoplasmic poly(A)-binding proteins, PABPC1 and PABPC2, in mouse spermatogenic cells. *Biology of reproduction*. 80:545-554.

Kirik, D., L.E. Annett, C. Burger, N. Muzyczka, R.J. Mandel, and A. Bjorklund. 2003. Nigrostriatal alpha-synucleinopathy induced by viral vector-mediated overexpression of human alpha-synuclein: a new primate model of Parkinson's disease. *Proceedings of the National Academy of Sciences of the United States of America*. 100:2884-2889.

Kirik, D., C. Rosenblad, C. Burger, C. Lundberg, T.E. Johansen, N. Muzyczka, R.J. Mandel, and A. Bjorklund. 2002. Parkinson-like neurodegeneration induced by targeted overexpression of alpha-synuclein in the nigrostriatal system. *The Journal of neuroscience : the official journal of the Society for Neuroscience*. 22:2780-2791.

Kisilevsky, R., and M. Axelrad. 1976. The pathogenesis of amyloid deposition: a new hypothesis. *Medical hypotheses*. 2:233-237.

Kitada, T., S. Asakawa, N. Hattori, H. Matsumine, Y. Yamamura, S. Minoshima, M. Yokochi, Y. Mizuno, and N. Shimizu. 1998. Mutations in the parkin gene cause autosomal recessive juvenile parkinsonism. *Nature*. 392:605-608.

Kitamura, A., H. Kubota, C.G. Pack, G. Matsumoto, S. Hirayama, Y. Takahashi, H. Kimura, M. Kinjo, R.I. Morimoto, and K. Nagata. 2006. Cytosolic chaperonin prevents polyglutamine toxicity with altering the aggregation state. *Nature cell biology*. 8:1163-1170.

Klucken, J., Y. Shin, E. Masliah, B.T. Hyman, and P.J. McLean. 2004. Hsp70 Reduces alpha-Synuclein Aggregation and Toxicity. *The Journal of biological chemistry*. 279:25497-25502.

Knowles, T.P., C.A. Waudby, G.L. Devlin, S.I. Cohen, A. Aguzzi, M. Vendruscolo, E.M. Terentjev, M.E. Welland, and C.M. Dobson. 2009. An analytical solution to the kinetics of breakable filament assembly. *Science*. 326:1533-1537.

Koller, W., R. O'Hara, W. Weiner, A. Lang, J. Nutt, Y. Agid, A.M. Bonnet, and J. Jankovic. 1987. Relationship of aging to Parkinson's disease. *Advances in neurology*. 45:317-321.

Kontopoulos, E., J.D. Parvin, and M.B. Feany. 2006. α-synuclein acts in the nucleus to inhibit histone acetylation and promote neurotoxicity. *Human Molecular Genetics*. 15:3012-3023.

Kordower, J.H., Y. Chu, R.A. Hauser, T.B. Freeman, and C.W. Olanow. 2008a. Lewy body-like pathology in long-term embryonic nigral transplants in Parkinson's disease. *Nature medicine*. 14:504-506.

Kordower, J.H., Y. Chu, R.A. Hauser, C.W. Olanow, and T.B. Freeman. 2008b. Transplanted dopaminergic neurons develop PD pathologic changes: a second case report. *Movement disorders : official journal of the Movement Disorder Society*. 23:2303-2306.

Kotani, H., K. Takaishi, T. Sasaki, and Y. Takai. 1997. Rho regulates association of both the ERM family and vinculin with the plasma membrane in MDCK cells. *Oncogene*. 14:1705-1713.

Kowall, N.W., P. Hantraye, E. Brouillet, M.F. Beal, A.C. McKee, and R.J. Ferrante. 2000. MPTP induces alpha-synuclein aggregation in the substantia nigra of baboons. *Neuroreport*. 11:211-213.

Kruger, R., W. Kuhn, T. Muller, D. Woitalla, M. Graeber, S. Kosel, H. Przuntek, J.T. Epplen, L. Schols, and O. Riess. 1998. Ala30Pro mutation in the gene encoding alpha-synuclein in Parkinson's disease. *Nat Genet*. 18:106-108.

Kupsky, W.J., M.M. Grimes, J. Sweeting, R. Bertsch, and L.J. Cote. 1987. Parkinson's disease and megacolon: concentric hyaline inclusions (Lewy bodies) in enteric ganglion cells. *Neurology*. 37:1253-1255.

Laemmli, U.K. 1970. Cleavage of structural proteins during the assembly of the head of bacteriophage T4. *Nature*. 227:680-685.

Lakso, M., S. Vartiainen, A.M. Moilanen, J. Sirvio, J.H. Thomas, R. Nass, R.D. Blakely, and G. Wong. 2003. Dopaminergic neuronal loss and motor deficits in Caenorhabditis elegans overexpressing human alpha-synuclein. *J Neurochem*. 86:165-172.

Lamb, R.F., B.W. Ozanne, C. Roy, L. McGarry, C. Stipp, P. Mangeat, and D.G. Jay. 1997. Essential functions of ezrin in maintenance of cell shape and lamellipodial extension in normal and transformed fibroblasts. *Current biology : CB*. 7:682-688.

Lamb, R.F., C. Roy, T.J. Diefenbach, H.V. Vinters, M.W. Johnson, D.G. Jay, and A. Hall. 2000. The TSC1 tumour suppressor hamartin regulates cell adhesion through ERM proteins and the GTPase Rho. *Nature cell biology*. 2:281-287.

Langston, J.W., P. Ballard, J.W. Tetrud, and I. Irwin. 1983. Chronic Parkinsonism in humans due to a product of meperidine-analog synthesis. *Science*. 219:979-980.

Lansbury, P.T., Jr. 1999. Evolution of amyloid: what normal protein folding may tell us about fibrillogenesis and disease. *Proceedings of the National Academy of Sciences of the United States of America*. 96:3342-3344.

Larsen, K.E., Y. Schmitz, M.D. Troyer, E. Mosharov, P. Dietrich, A.Z. Quazi, M. Savalle, V. Nemani, F.A. Chaudhry, R.H. Edwards, L. Stefanis, and D. Sulzer. 2006. Alpha-synuclein overexpression in PC12 and chromaffin cells impairs catecholamine release by interfering with a late step in exocytosis. *The Journal of neuroscience : the official journal of the Society for Neuroscience*. 26:11915-11922.

Lashuel, H.A., D. Hartley, B.M. Petre, T. Walz, and P.T. Lansbury, Jr. 2002a. Neurodegenerative disease: amyloid pores from pathogenic mutations. *Nature*. 418:291.

Lashuel, H.A., B.M. Petre, J. Wall, M. Simon, R.J. Nowak, T. Walz, and P.T. Lansbury, Jr. 2002b. Alpha-synuclein, especially the Parkinson's disease-associated mutants, forms pore-like annular and tubular protofibrils. *Journal of molecular biology*. 322:1089-1102.

Latourelle, J.C., N. Pankratz, A. Dumitriu, J.B. Wilk, S. Goldwurm, G. Pezzoli, C.B. Mariani, A.L. DeStefano, C. Halter, J.F. Gusella, W.C. Nichols, R.H. Myers, and T. Foroud. 2009. Genomewide association study for onset age in Parkinson disease. *BMC medical genetics*. 10:98.

Lavedan, C. 1998. The synuclein family. *Genome research*. 8:871-880.

Lebouvier, T., T. Chaumette, P. Damier, E. Coron, Y. Touchefeu, S. Vrignaud, P. Naveilhan, J.P. Galmiche, S. Bruley des Varannes, P. Derkinderen, and M. Neunlist. 2008. Pathological lesions in colonic biopsies during Parkinson's disease. *Gut*. 57:1741-1743.

Lebouvier, T., T. Chaumette, S. Paillusson, C. Duyckaerts, S. Bruley des Varannes, M. Neunlist, and P. Derkinderen. 2009. The second brain and Parkinson's disease. *The European journal of neuroscience*. 30:735-741.

Lee, H.J., C. Choi, and S.J. Lee. 2002a. Membrane-bound alpha-synuclein has a high aggregation propensity and the ability to seed the aggregation of the cytosolic form. *The Journal of biological chemistry*. 277:671-678.

Lee, H.J., M.S. Kim, J.M. Shin, T.J. Park, H.M. Chung, and K.H. Baek. 2006. The expression patterns of deubiquitinating enzymes, USP22 and Usp22. *Gene expression patterns : GEP*. 6:277-284.

Lee, H.J., S. Patel, and S.J. Lee. 2005. Intravesicular localization and exocytosis of alpha-synuclein and its aggregates. *The Journal of neuroscience : the official journal of the Society for Neuroscience*. 25:6016-6024.

Lee, J.H., I.H. Lee, Y.J. Choe, S. Kang, H.Y. Kim, W.P. Gai, J.S. Hahn, and S.R. Paik. 2009. Real-time analysis of amyloid fibril formation of alpha-synuclein using a fibrillation-state-specific fluorescent probe of JC-1. *The Biochemical journal*. 418:311-323.

Lee, J.T., T.C. Wheeler, L. Li, and L.S. Chin. 2008. Ubiquitination of alpha-synuclein by Siah-1 promotes alpha-synuclein aggregation and apoptotic cell death. *Hum Mol Genet*. 17:906-917.

Lee, M.K., W. Stirling, Y. Xu, X. Xu, D. Qui, A.S. Mandir, T.M. Dawson, N.G. Copeland, N.A. Jenkins, and D.L. Price. 2002b. Human alpha-synuclein-harboring familial Parkinson's disease-linked Ala-53 --> Thr mutation causes neurodegenerative disease with alpha-synuclein aggregation in transgenic mice. *Proceedings of the National Academy of Sciences of the United States of America*. 99:8968-8973.

Lee, Y., R.S. Smith, W. Jordan, B.L. King, J. Won, J.M. Valpuesta, J.K. Naggert, and P.M. Nishina. 2011. Prefoldin 5 is required for normal sensory and neuronal development in a murine model. *The Journal of biological chemistry*. 286:726-736.

LeVine, H., 3rd. 1999. Quantification of beta-sheet amyloid fibril structures with thioflavin T. *Methods in enzymology*. 309:274-284.

Levy, G. 2007. The relationship of Parkinson disease with aging. *Archives of neurology*. 64:1242-1246.

Lewy, F.H. 1912. Paralysis agitans. *Handbuch der Neurologie*. I:920-933.

Li, D., R. Belusa, S. Nowicki, and A. Aperia. 2000. Arachidonic acid metabolic pathways regulating activity of renal Na(+)-K(+)-ATPase are age dependent. *American journal of physiology. Renal physiology*. 278:F823-829.

Li, H.T., H.N. Du, L. Tang, J. Hu, and H.Y. Hu. 2002a. Structural transformation and aggregation of human alpha-synuclein in trifluoroethanol: non-amyloid component sequence is essential and beta-sheet formation is prerequisite to aggregation. *Biopolymers*. 64:221-226.

Li, J., V.N. Uversky, and A.L. Fink. 2001. Effect of familial Parkinson's disease point mutations A30P and A53T on the structural properties, aggregation, and fibrillation of human alpha-synuclein. *Biochemistry*. 40:11604-11613.

Li, J., V.N. Uversky, and A.L. Fink. 2002b. Conformational behavior of human alpha-synuclein is modulated by familial Parkinson's disease point mutations A30P and A53T. *Neurotoxicology*. 23:553-567.

Li, J., M. Zhu, A.B. Manning-Bog, D.A. Di Monte, and A.L. Fink. 2004a. Dopamine and L-dopa disaggregate amyloid fibrils: implications for Parkinson's and Alzheimer's disease. *FASEB journal : official publication of the Federation of American Societies for Experimental Biology*. 18:962-964.

Li, J., M. Zhu, S. Rajamani, V.N. Uversky, and A.L. Fink. 2004b. Rifampicin inhibits alpha-synuclein fibrillation and disaggregates fibrils. *Chemistry & biology*. 11:1513-1521.

Li, J.Y., E. Englund, J.L. Holton, D. Soulet, P. Hagell, A.J. Lees, T. Lashley, N.P. Quinn, S. Rehncrona, A. Bjorklund, H. Widner, T. Revesz, O. Lindvall, and P. Brundin. 2008. Lewy bodies in grafted neurons in subjects with Parkinson's disease suggest host-to-graft disease propagation. *Nature medicine*. 14:501-503.

Li, W.W., R. Yang, J.C. Guo, H.M. Ren, X.L. Zha, J.S. Cheng, and D.F. Cai. 2007a. Localization of alpha-synuclein to mitochondria within midbrain of mice. *Neuroreport*. 18:1543-1546.

Li, Y., T. Harada, Y.T. Juang, V.C. Kyttaris, Y. Wang, M. Zidanic, K. Tung, and G.C. Tsokos. 2007b. Phosphorylated ERM is responsible for increased T cell polarization, adhesion, and migration in patients with systemic lupus erythematosus. *J Immunol*. 178:1938-1947.

Li, Z.S., T.D. Pham, H. Tamir, J.J. Chen, and M.D. Gershon. 2004c. Enteric dopaminergic neurons: definition, developmental lineage, and effects of extrinsic denervation. *The Journal of neuroscience : the official journal of the Society for Neuroscience*. 24:1330-1339.

Li, Z.S., C. Schmauss, A. Cuenca, E. Ratcliffe, and M.D. Gershon. 2006. Physiological modulation of intestinal motility by enteric dopaminergic neurons and the D2 receptor: analysis of dopamine receptor expression, location, development, and function in wild-type and knock-out mice. *The Journal of neuroscience : the official journal of the Society for Neuroscience*. 26:2798-2807.

Lill, C.M., J.T. Roehr, M.B. McQueen, F.K. Kavvoura, S. Bagade, B.M. Schjeide, L.M. Schjeide, E. Meissner, U. Zauft, N.C. Allen, T. Liu, M. Schilling, K.J. Anderson, G. Beecham, D. Berg, J.M. Biernacka, A. Brice, A.L. DeStefano, C.B. Do, N. Eriksson, S.A. Factor, M.J. Farrer, T. Foroud, T. Gasser, T. Hamza, J.A. Hardy, P. Heutink, E.M. Hill-Burns, C. Klein, J.C. Latourelle, D.M. Maraganore, E.R. Martin, M. Martinez, R.H. Myers, M.A. Nalls, N. Pankratz, H. Payami, W. Satake, W.K. Scott, M. Sharma, A.B. Singleton, K. Stefansson, T. Toda, J.Y. Tung, J. Vance, N.W. Wood, C.P.

Zabetian, P. Young, R.E. Tanzi, M.J. Khoury, F. Zipp, H. Lehrach, J.P. Ioannidis, and L. Bertram. 2012. Comprehensive research synopsis and systematic meta-analyses in Parkinson's disease genetics: The PDGene database. *PLoS genetics*. 8:e1002548.

Lindersson, E., D. Lundvig, C. Petersen, P. Madsen, J.R. Nyengaard, P. Hojrup, T. Moos, D. Otzen, W.P. Gai, P.C. Blumbergs, and P.H. Jensen. 2005. p25alpha Stimulates alpha-synuclein aggregation and is co-localized with aggregated alpha-synuclein in alpha-synucleinopathies. *The Journal of biological chemistry*. 280:5703-5715.

Lindersson, E.K., P. Hojrup, W.P. Gai, D. Locker, D. Martin, and P.H. Jensen. 2004. alpha-Synuclein filaments bind the transcriptional regulator HMGB-1. *Neuroreport*. 15:2735-2739.

Linke, A.T., B. Marchant, P. Marsh, G. Frampton, J. Murphy, and M.L. Rose. 2001. Screening of a HUVEC cDNA library with transplant-associated coronary artery disease sera identifies RPL7 as a candidate autoantigen associated with this disease. *Clinical and experimental immunology*. 126:173-179.

Liu, D., L. Jin, H. Wang, H. Zhao, C. Zhao, C. Duan, L. Lu, B. Wu, S. Yu, P. Chan, Y. Li, and H. Yang. 2008. Silencing alpha-synuclein gene expression enhances tyrosine hydroxylase activity in MN9D cells. *Neurochem Res*. 33:1401-1409.

Liu, J., J.P. Zhang, M. Shi, T. Quinn, J. Bradner, R. Beyer, S. Chen, and J. Zhang. 2009. Rab11a and HSP90 regulate recycling of extracellular alpha-synuclein. *The Journal of neuroscience : the official journal of the Society for Neuroscience*. 29:1480-1485.

Lo Bianco, C., J. Shorter, E. Regulier, H. Lashuel, T. Iwatsubo, S. Lindquist, and P. Aebischer. 2008. Hsp104 antagonizes alpha-synuclein aggregation and reduces dopaminergic degeneration in a rat model of Parkinson disease. *The Journal of clinical investigation*. 118:3087-3097.

Loeb, V., E. Yakunin, A. Saada, and R. Sharon. 2010. The transgenic overexpression of alpha-synuclein and not its related pathology associates with complex I inhibition. *J Biol Chem*. 285:7334-7343.

Lorenz, M., J. Urban, U. Engelhardt, G. Baumann, K. Stangl, and V. Stangl. 2009. Green and black tea are equally potent stimuli of NO production and vasodilation: new insights into tea ingredients involved. *Basic research in cardiology*. 104:100-110.

Louvet-Vallee, S. 2000. ERM proteins: from cellular architecture to cell signaling. *Biology of the cell / under the auspices of the European Cell Biology Organization*. 92:305-316.

Lucey, M.M., Y. Wang, M. Bustin, and M.K. Duncan. 2008. Differential expression of the HMGN family of chromatin proteins during ocular development. *Gene expression patterns : GEP*. 8:433-437.

Lucking, C.B., and A. Brice. 2000. Alpha-synuclein and Parkinson's disease. *Cellular and molecular life sciences : CMLS*. 57:1894-1908.

Luk, K.C., I.P. Mills, J.Q. Trojanowski, and V.M. Lee. 2008. Interactions between Hsp70 and the hydrophobic core of alpha-synuclein inhibit fibril assembly. *Biochemistry*. 47:12614-12625.

Lundvig, D., E. Lindersson, and P.H. Jensen. 2005. Pathogenic effects of alpha-synuclein aggregation. *Brain research. Molecular brain research*. 134:3-17.

Macario, A.J., and E. Conway de Macario. 2000. Stress and molecular chaperones in disease. *International journal of clinical & laboratory research*. 30:49-66.

Mackay, D.J., F. Esch, H. Furthmayr, and A. Hall. 1997. Rho- and rac-dependent assembly of focal adhesion complexes and actin filaments in permeabilized fibroblasts: an essential role for ezrin/radixin/moesin proteins. *The Journal of cell biology*. 138:927-938.

MacLeod, D., J. Dowman, R. Hammond, T. Leete, K. Inoue, and A. Abeliovich. 2006. The familial Parkinsonism gene LRRK2 regulates neurite process morphology. *Neuron*. 52:587-593.

Madine, J., A.J. Doig, and D.A. Middleton. 2006. A study of the regional effects of alpha-synuclein on the organization and stability of phospholipid bilayers. *Biochemistry*. 45:5783-5792.

Maekawa, M., C. Ito, Y. Toyama, F. Suzuki-Toyota, E. Fujita, T. Momoi, and K. Toshimori. 2011. Localisation of RA175 (Cadm1), a cell adhesion molecule of the immunoglobulin superfamily, in the mouse testis, and analysis of male infertility in the RA175-deficient mouse. *Andrologia*. 43:180-188.

Maguire-Zeiss, K.A., and H.J. Federoff. 2003. Convergent pathobiologic model of Parkinson's disease. *Annals of the New York Academy of Sciences*. 991:152-166.

Malkus, K.A., and H. Ischiropoulos. 2012. Regional deficiencies in chaperone-mediated autophagy underlie alpha-synuclein aggregation and neurodegeneration. *Neurobiology of disease*. 46:732-744.

Maries, E., B. Dass, T.J. Collier, J.H. Kordower, and K. Steece-Collier. 2003. The role of alpha-synuclein in Parkinson's disease: insights from animal models. *Nature reviews. Neuroscience*. 4:727-738.

Maroteaux, L., J.T. Campanelli, and R.H. Scheller. 1988. Synuclein: a neuron-specific protein localized to the nucleus and presynaptic nerve terminal. *The Journal of neuroscience : the official journal of the Society for Neuroscience*. 8:2804-2815.

Martin, I., V.L. Dawson, and T.M. Dawson. 2011. Recent advances in the genetics of Parkinson's disease. *Annual review of genomics and human genetics*. 12:301-325.

Martin, L.J., Y. Pan, A.C. Price, W. Sterling, N.G. Copeland, N.A. Jenkins, D.L. Price, and M.K. Lee. 2006. Parkinson's disease alpha-synuclein transgenic mice develop neuronal mitochondrial degeneration and cell death. *J Neurosci*. 26:41-50.

Martin, M., C. Andreoli, A. Sahuquet, P. Montcourrier, M. Algrain, and P. Mangeat. 1995. Ezrin NH2-terminal domain inhibits the cell extension activity of the COOH-terminal domain. *The Journal of cell biology*. 128:1081-1093.

Martin, M., C. Roy, P. Montcourrier, A. Sahuquet, and P. Mangeat. 1997. Three determinants in ezrin are responsible for cell extension activity. *Molecular biology of the cell*. 8:1543-1557.

Martin, T.A., G. Harrison, R.E. Mansel, and W.G. Jiang. 2003. The role of the CD44/ezrin complex in cancer metastasis. *Critical reviews in oncology/hematology*. 46:165-186.

Martinez-Vicente, M., Z. Talloczy, S. Kaushik, A.C. Massey, J. Mazzulli, E.V. Mosharov, R. Hodara, R. Fredenburg, D.C. Wu, A. Follenzi, W. Dauer, S. Przedborski, H. Ischiropoulos, P.T. Lansbury, D. Sulzer, and A.M. Cuervo. 2008. Dopamine-modified alpha-synuclein blocks chaperone-mediated autophagy. *The Journal of clinical investigation*. 118:777-788.

Masino, L., and A. Pastore. 2002. Glutamine repeats: structural hypotheses and neurodegeneration. *Biochemical Society transactions*. 30:548-551.

Masliah, E., E. Rockenstein, I. Veinbergs, M. Mallory, M. Hashimoto, A. Takeda, Y. Sagara, A. Sisk, and L. Mucke. 2000. Dopaminergic loss and inclusion body formation in alpha-synuclein mice: implications for neurodegenerative disorders. *Science*. 287:1265-1269.

Matsui, T., S. Yonemura, and S. Tsukita. 1999. Activation of ERM proteins in vivo by Rho involves phosphatidyl-inositol 4-phosphate 5-kinase and not ROCK kinases. *Current biology : CB*. 9:1259-1262.

Mazzio, E.A., F. Close, and K.F. Soliman. 2011. The biochemical and cellular basis for nutraceutical strategies to attenuate neurodegeneration in Parkinson's disease. *International journal of molecular sciences*. 12:506-569.

McBride, P.A., W.J. Schulz-Schaeffer, M. Donaldson, M. Bruce, H. Diringer, H.A. Kretzschmar, and M. Beekes. 2001. Early spread of scrapie from the gastrointestinal tract to the central nervous system involves autonomic fibers of the splanchnic and vagus nerves. *Journal of virology*. 75:9320-9327.

McClendon, S., C.C. Rospigliosi, and D. Eliezer. 2009. Charge neutralization and collapse of the C-terminal tail of alpha-synuclein at low pH. *Protein science : a publication of the Protein Society*. 18:1531-1540.

McLean, P.J., H. Kawamata, S. Ribich, and B.T. Hyman. 2000. Membrane association and protein conformation of alpha-synuclein in intact neurons. Effect of Parkinson's disease-linked mutations. *The Journal of biological chemistry*. 275:8812-8816.

McLean, P.J., H. Kawamata, S. Shariff, J. Hewett, N. Sharma, K. Ueda, X.O. Breakefield, and B.T. Hyman. 2002. TorsinA and heat shock proteins act as molecular chaperones: suppression of alpha-synuclein aggregation. *Journal of neurochemistry*. 83:846-854.

McLean, P.J., J. Klucken, Y. Shin, and B.T. Hyman. 2004. Geldanamycin induces Hsp70 and prevents alpha-synuclein aggregation and toxicity in vitro. *Biochemical and biophysical research communications*. 321:665-669.

Mendillo, M.L., S. Santagata, M. Koeva, G.W. Bell, R. Hu, R.M. Tamimi, E. Fraenkel, T.A. Ince, L. Whitesell, and S. Lindquist. 2012. HSF1 drives a transcriptional program distinct from heat shock to support highly malignant human cancers. *Cell*. 150:549-562.

Meredith, G.E., S. Totterdell, E. Petroske, K. Santa Cruz, R.C. Callison, Jr., and Y.S. Lau. 2002. Lysosomal malfunction accompanies alpha-synuclein aggregation in a progressive mouse model of Parkinson's disease. *Brain research*. 956:156-165.

Miller-Fleming, L., F. Giorgini, and T.F. Outeiro. 2008. Yeast as a model for studying human neurodegenerative disorders. *Biotechnology journal*. 3:325-338.

Miller, D.W., S.M. Hague, J. Clarimon, M. Baptista, K. Gwinn-Hardy, M.R. Cookson, and A.B. Singleton. 2004. Alpha-synuclein in blood and brain from familial Parkinson disease with SNCA locus triplication. *Neurology*. 62:1835-1838.

Miwa, H., T. Kubo, A. Suzuki, and T. Kondo. 2006. Intragastric proteasome inhibition induces alpha-synuclein-immunopositive aggregations in neurons in the dorsal motor nucleus of the vagus in rats. *Neuroscience letters*. 401:146-149.

Moon, Y., J.Y. Kim, S.Y. Choi, H.M. Cho, H. Kim, and W. Sun. 2012. Expression of ezrin in subventricular zone neural stem cells and their progeny in adult and developing mice. *Histochemistry and cell biology*.

Mooseker, M.S. 1983. Actin binding proteins of the brush border. *Cell*. 35:11-13.

Mori, S., J. Fujitake, S. Kuno, and Y. Sano. 1988. Immunohistochemical evaluation of the neurotoxic effects of 1-methyl-4-phenyl-1,2,3,6-tetrahydropyridine (MPTP) on dopaminergic nigrostriatal neurons of young adult mice using dopamine and tyrosine hydroxylase antibodies. *Neuroscience letters*. 90:57-62.

Mosmann, T. 1983. Rapid colorimetric assay for cellular growth and survival: application to proliferation and cytotoxicity assays. *Journal of immunological methods*. 65:55-63.

Muchowski, P.J., G. Schaffar, A. Sittler, E.E. Wanker, M.K. Hayer-Hartl, and F.U. Hartl. 2000. Hsp70 and hsp40 chaperones can inhibit self-assembly of polyglutamine proteins into amyloid-like fibrils. *Proceedings of the National Academy of Sciences of the United States of America*. 97:7841-7846.

Mukaetova-Ladinska, E.B., and I.G. McKeith. 2006. Pathophysiology of synuclein aggregation in Lewy body disease. *Mechanisms of ageing and development*. 127:188-202.

Murakami, Y. 2008. [Involvement of a cell adhesion molecule, CADM1/TSLC1 in oncogenesis and spermatogenesis]. *Seikagaku. The Journal of Japanese Biochemical Society*. 80:81-93.

Myung, J.K., L. Afjehi-Sadat, M. Felizardo-Cabatic, I. Slavc, and G. Lubec. 2004. Expressional patterns of chaperones in ten human tumor cell lines. *Proteome science*. 2:8.

Nalls, M.A., V. Plagnol, D.G. Hernandez, M. Sharma, U.M. Sheerin, M. Saad, J. Simon-Sanchez, C. Schulte, S. Lesage, S. Sveinbjornsdottir, K. Stefansson, M. Martinez, J. Hardy, P. Heutink, A. Brice, T. Gasser, A.B. Singleton, and N.W. Wood. 2011.

Imputation of sequence variants for identification of genetic risks for Parkinson's disease: a meta-analysis of genome-wide association studies. *Lancet*. 377:641-649.

Natale, G., O. Kastsiuchenka, L. Pasquali, S. Ruggieri, A. Paparelli, and F. Fornai. 2008. MPTP- but not methamphetamine-induced parkinsonism extends to catecholamine neurons in the gut. *Annals of the New York Academy of Sciences*. 1139:345-349.

Necula, M., C.N. Chirita, and J. Kuret. 2003. Rapid anionic micelle-mediated alpha-synuclein fibrillization in vitro. *The Journal of biological chemistry*. 278:46674-46680.

Nemani, V.M., W. Lu, V. Berge, K. Nakamura, B. Onoa, M.K. Lee, F.A. Chaudhry, R.A. Nicoll, and R.H. Edwards. 2010. Increased expression of alpha-synuclein reduces neurotransmitter release by inhibiting synaptic vesicle reclustering after endocytosis. *Neuron*. 65:66-79.

Neumann, M., P.J. Kahle, B.I. Giasson, L. Ozmen, E. Borroni, W. Spooren, V. Muller, S. Odoy, H. Fujiwara, M. Hasegawa, T. Iwatsubo, J.Q. Trojanowski, H.A. Kretzschmar, and C. Haass. 2002. Misfolded proteinase K-resistant hyperphosphorylated alpha-synuclein in aged transgenic mice with locomotor deterioration and in human alpha-synucleinopathies. *The Journal of clinical investigation*. 110:1429-1439.

Nieto, M., F.J. Gil-Bea, E. Dalfo, M. Cuadrado, F. Cabodevilla, B. Sanchez, S. Catena, T. Sesma, E. Ribe, I. Ferrer, M.J. Ramirez, and T. Gomez-Isla. 2006. Increased sensitivity to MPTP in human alpha-synuclein A30P transgenic mice. *Neurobiology of aging*. 27:848-856.

Norris, E.H., K. Uryu, S. Leight, B.I. Giasson, J.Q. Trojanowski, and V.M. Lee. 2007. Pesticide exposure exacerbates alpha-synucleinopathy in an A53T transgenic mouse model. *The American journal of pathology*. 170:658-666.

Nucifora, F.C., Jr., M. Sasaki, M.F. Peters, H. Huang, J.K. Cooper, M. Yamada, H. Takahashi, S. Tsuji, J. Troncoso, V.L. Dawson, T.M. Dawson, and C.A. Ross. 2001. Interference by huntingtin and atrophin-1 with cbp-mediated transcription leading to cellular toxicity. *Science*. 291:2423-2428.

Olakowski, M., T. Tyszkiewicz, M. Jarzab, R. Krol, M. Oczko-Wojciechowska, M. Kowalska, M. Kowal, G.M. Gala, M. Kajor, D. Lange, E. Chmielik, E. Gubala, P. Lampe, and B. Jarzab. 2009. NBL1 and anillin (ANLN) genes over-expression in pancreatic carcinoma. *Folia histochemica et cytobiologica / Polish Academy of Sciences, Polish Histochemical and Cytochemical Society*. 47:249-255.

Olanow, C.W., C.G. Goetz, J.H. Kordower, A.J. Stoessl, V. Sossi, M.F. Brin, K.M. Shannon, G.M. Nauert, D.P. Perl, J. Godbold, and T.B. Freeman. 2003. A double-blind controlled trial of bilateral fetal nigral transplantation in Parkinson's disease. *Annals of neurology*. 54:403-414.

Omnus, D.J., S. Mehrtens, B. Ritter, K. Resch, M. Yamada, R. Frank, M. Nourbakhsh, and M.R. Reboll. 2011. JKTBP1 is involved in stabilization and IRES-dependent translation of NRF mRNAs by binding to 5' and 3' untranslated regions. *Journal of molecular biology*. 407:492-504.

Omoe, K., and A. Endo. 1994. Expression level of Rps4 mRNA in 39,X mice and 40,XX mice. *Cytogenetics and cell genetics*. 67:52-54.

Ono, K., M. Ikemoto, T. Kawarabayashi, M. Ikeda, T. Nishinakagawa, M. Hosokawa, M. Shoji, M. Takahashi, and M. Nakashima. 2009. A chemical chaperone, sodium 4-phenylbutyric acid, attenuates the pathogenic potency in human alpha-synuclein A30P + A53T transgenic mice. *Parkinsonism & related disorders*. 15:649-654.

Outeiro, T.F., and S. Lindquist. 2003. Yeast cells provide insight into alpha-synuclein biology and pathobiology. *Science*. 302:1772-1775.

Outeiro, T.F., P. Putcha, J.E. Tetzlaff, R. Spoelgen, M. Koker, F. Carvalho, B.T. Hyman, and P.J. McLean. 2008. Formation of toxic oligomeric alpha-synuclein species in living cells. *PloS one*. 3:e1867.

Paisan-Ruiz, C., S. Jain, E.W. Evans, W.P. Gilks, J. Simon, M. van der Brug, A. Lopez de Munain, S. Aparicio, A.M. Gil, N. Khan, J. Johnson, J.R. Martinez, D. Nicholl, I.M. Carrera, A.S. Pena, R. de Silva, A. Lees, J.F. Marti-Masso, J. Perez-Tur, N.W.

Wood, and A.B. Singleton. 2004. Cloning of the gene containing mutations that cause PARK8-linked Parkinson's disease. *Neuron*. 44:595-600.

Pakkanen, R., K. Hedman, O. Turunen, T. Wahlstrom, and A. Vaheri. 1987. Microvillus-specific Mr 75,000 plasma membrane protein of human choriocarcinoma cells. *The journal of histochemistry and cytochemistry : official journal of the Histochemistry Society*. 35:809-816.

Pan-Montojo, F., M. Schwarz, C. Winkler, M. Arnhold, G.A. O'Sullivan, A. Pal, J. Said, G. Marsico, J.M. Verbavatz, M. Rodrigo-Angulo, G. Gille, R.H. Funk, and H. Reichmann. 2012. Environmental toxins trigger PD-like progression via increased alpha-synuclein release from enteric neurons in mice. *Scientific reports*. 2:898.

Parisiadou, L., C. Xie, H.J. Cho, X. Lin, X.L. Gu, C.X. Long, E. Lobbestael, V. Baekelandt, J.M. Taymans, L. Sun, and H. Cai. 2009. Phosphorylation of ezrin/radixin/moesin proteins by LRRK2 promotes the rearrangement of actin cytoskeleton in neuronal morphogenesis. *The Journal of neuroscience : the official journal of the Society for Neuroscience*. 29:13971-13980.

Parkinson, J. 2002. An essay on the shaking palsy. 1817. *J Neuropsychiatry Clin Neurosci*. 14:223-236; discussion 222.

Pavao, M., Y.H. Huang, L.J. Hafer, R.B. Moreland, and A.M. Traish. 2001. Immunodetection of nmt55/p54nrb isoforms in human breast cancer. *BMC cancer*. 1:15.

Pellechia, P.J., J. Gao, Y. Gu, H.J. Ploehn, and C.J. Murphy. 2004. Platinum ion uptake by dendrimers: an NMR and AFM study. *Inorganic chemistry*. 43:1421-1428.

Pellkofer, H., A.S. Schubart, R. Hoftberger, N. Schutze, M. Pagany, M. Schuller, H. Lassmann, R. Hohlfeld, R. Voltz, and C. Linington. 2004. Modelling paraneoplastic CNS disease: T-cells specific for the onconeuronal antigen PNMA1 mediate autoimmune encephalomyelitis in the rat. *Brain : a journal of neurology*. 127:1822-1830.

Peng, X., R. Tehranian, P. Dietrich, L. Stefanis, and R.G. Perez. 2005. Alpha-synuclein activation of protein phosphatase 2A reduces tyrosine hydroxylase phosphorylation in dopaminergic cells. *J Cell Sci*. 118:3523-3530.

Perez, R.G., J.C. Waymire, E. Lin, J.J. Liu, F. Guo, and M.J. Zigmond. 2002. A role for alpha-synuclein in the regulation of dopamine biosynthesis. *J Neurosci*. 22:3090-3099.

Perrin, R.J., W.S. Woods, D.F. Clayton, and J.M. George. 2001. Exposure to long chain polyunsaturated fatty acids triggers rapid multimerization of synucleins. *The Journal of biological chemistry*. 276:41958-41962.

Persson, A., C. Lindwall, M.A. Curtis, and H.G. Kuhn. 2010. Expression of ezrin radixin moesin proteins in the adult subventricular zone and the rostral migratory stream. *Neuroscience*. 167:312-322.

Perutz, M.F., T. Johnson, M. Suzuki, and J.T. Finch. 1994. Glutamine repeats as polar zippers: their possible role in inherited neurodegenerative diseases. *Proceedings of the National Academy of Sciences of the United States of America*. 91:5355-5358.

Petit, A., T. Kawarai, E. Paitel, N. Sanjo, M. Maj, M. Scheid, F. Chen, Y. Gu, H. Hasegawa, S. Salehi-Rad, L. Wang, E. Rogaeva, P. Fraser, B. Robinson, P. St George-Hyslop, and A. Tandon. 2005. Wild-type PINK1 prevents basal and induced neuronal apoptosis, a protective effect abrogated by Parkinson disease-related mutations. *J Biol Chem*. 280:34025-34032.

Petrucelli, L., C. O'Farrell, P.J. Lockhart, M. Baptista, K. Kehoe, L. Vink, P. Choi, B. Wolozin, M. Farrer, J. Hardy, and M.R. Cookson. 2002. Parkin protects against the toxicity associated with mutant alpha-synuclein: proteasome dysfunction selectively affects catecholaminergic neurons. *Neuron*. 36:1007-1019.

Pfeiffer, R.F. 2003. Gastrointestinal dysfunction in Parkinson's disease. *Lancet neurology*. 2:107-116.

Phillips, R.J., G.C. Walter, S.L. Wilder, E.A. Baronowsky, and T.L. Powley. 2008. Alpha-synuclein-immunopositive myenteric neurons and vagal preganglionic terminals: autonomic pathway implicated in Parkinson's disease? *Neuroscience*. 153:733-750.

Poirier, M.A., H. Li, J. Macosko, S. Cai, M. Amzel, and C.A. Ross. 2002. Huntingtin spheroids and protofibrils as precursors in polyglutamine fibrilization. *The Journal of biological chemistry*. 277:41032-41037.

Polesello, C., and F. Payre. 2004. Small is beautiful: what flies tell us about ERM protein function in development. *Trends in cell biology*. 14:294-302.

Polymeropoulos, M.H., C. Lavedan, E. Leroy, S.E. Ide, A. Dehejia, A. Dutra, B. Pike, H. Root, J. Rubenstein, R. Boyer, E.S. Stenroos, S. Chandrasekharappa, A. Athanassiadou, T. Papapetropoulos, W.G. Johnson, A.M. Lazzarini, R.C. Duvoisin, G. Di Iorio, L.I. Golbe, and R.L. Nussbaum. 1997. Mutation in the alpha-synuclein gene identified in families with Parkinson's disease. *Science*. 276:2045-2047.

Pountney, D.L., R. Lowe, M. Quilty, J.C. Vickers, N.H. Voelcker, and W.P. Gai. 2004. Annular alpha-synuclein species from purified multiple system atrophy inclusions. *Journal of neurochemistry*. 90:502-512.

Pountney, D.L., T.M. Treweek, T. Chataway, Y. Huang, F. Chegini, P.C. Blumbergs, M.J. Raftery, and W.P. Gai. 2005. Alpha B-crystallin is a major component of glial cytoplasmic inclusions in multiple system atrophy. *Neurotoxicity research*. 7:77-85.

Powley, T.L., E.A. Fox, and H.R. Berthoud. 1987. Retrograde tracer technique for assessment of selective and total subdiaphragmatic vagotomies. *The American journal of physiology*. 253:R361-370.

Qualman, S.J., H.M. Haupt, P. Yang, and S.R. Hamilton. 1984. Esophageal Lewy bodies associated with ganglion cell loss in achalasia. Similarity to Parkinson's disease. *Gastroenterology*. 87:848-856.

Rajan, R.S., M.E. Illing, N.F. Bence, and R.R. Kopito. 2001. Specificity in intracellular protein aggregation and inclusion body formation. *Proceedings of the National Academy of Sciences of the United States of America*. 98:13060-13065.

Ramakrishnan, M., P.H. Jensen, and D. Marsh. 2003. Alpha-synuclein association with phosphatidylglycerol probed by lipid spin labels. *Biochemistry*. 42:12919-12926.

Rathke-Hartlieb, S., P.J. Kahle, M. Neumann, L. Ozmen, S. Haid, M. Okochi, C. Haass, and J.B. Schulz. 2001. Sensitivity to MPTP is not increased in Parkinson's disease-associated mutant alpha-synuclein transgenic mice. *Journal of neurochemistry*. 77:1181-1184.

Rattner, B.P., T. Yusufzai, and J.T. Kadonaga. 2009. HMGN proteins act in opposition to ATP-dependent chromatin remodeling factors to restrict nucleosome mobility. *Molecular cell*. 34:620-626.

Reboll, M.R., A. Oumard, A.C. Gazdag, I. Renger, B. Ritter, M. Schwarzer, H. Hauser, M. Wood, M. Yamada, K. Resch, and M. Nourbakhsh. 2007. NRF IRES activity is mediated by RNA binding protein JKTBP1 and a 14-nt RNA element. *RNA*. 13:1328-1340.

Rekas, A., C.G. Adda, J. Andrew Aquilina, K.J. Barnham, M. Sunde, D. Galatis, N.A. Williamson, C.L. Masters, R.F. Anders, C.V. Robinson, R. Cappai, and J.A. Carver. 2004. Interaction of the molecular chaperone alphaB-crystallin with alpha-synuclein: effects on amyloid fibril formation and chaperone activity. *Journal of molecular biology*. 340:1167-1183.

Ritossa, P. 1962. [Problems of prophylactic vaccinations of infants]. *Rivista dell'Istituto sieroterapico italiano*. 37:79-108.

Robertson, D.C., O. Schmidt, N. Ninkina, P.A. Jones, J. Sharkey, and V.L. Buchman. 2004. Developmental loss and resistance to MPTP toxicity of dopaminergic neurones in substantia nigra pars compacta of gamma-synuclein, alpha-synuclein and double alpha/gamma-synuclein null mutant mice. *Journal of neurochemistry*. 89:1126-1136.

Rosenfeld, M.R., J.G. Eichen, D.F. Wade, J.B. Posner, and J. Dalmau. 2001. Molecular and clinical diversity in paraneoplastic immunity to Ma proteins. *Annals of neurology*. 50:339-348.

Sakiyama, S., and T. Ozaki. 1997. [DAN gene]. *Gan to kagaku ryoho. Cancer & chemotherapy*. 24:1465-1470.

Samii, A., J.G. Nutt, and B.R. Ransom. 2004. Parkinson's disease. *Lancet*. 363:1783-1793.

Sampathu, D.M., B.I. Giasson, A.C. Pawlyk, J.Q. Trojanowski, and V.M. Lee. 2003. Ubiquitination of alpha-synuclein is not required for formation of pathological inclusions in alpha-synucleinopathies. *The American journal of pathology*. 163:91-100.

Satake, W., Y. Nakabayashi, I. Mizuta, Y. Hirota, C. Ito, M. Kubo, T. Kawaguchi, T. Tsunoda, M. Watanabe, A. Takeda, H. Tomiyama, K. Nakashima, K. Hasegawa, F. Obata, T. Yoshikawa, H. Kawakami, S. Sakoda, M. Yamamoto, N. Hattori, M. Murata, Y. Nakamura, and T. Toda. 2009. Genome-wide association study identifies common variants at four loci as genetic risk factors for Parkinson's disease. *Nature genetics*. 41:1303-1307.

Sato, N., N. Funayama, A. Nagafuchi, S. Yonemura, and S. Tsukita. 1992. A gene family consisting of ezrin, radixin and moesin. Its specific localization at actin filament/plasma membrane association sites. *Journal of cell science*. 103 (Pt 1):131-143.

Scherzer, C.R., R.V. Jensen, S.R. Gullans, and M.B. Feany. 2003. Gene expression changes presage neurodegeneration in a Drosophila model of Parkinson's disease. *Human molecular genetics*. 12:2457-2466.

Schiffner, S., N. Zimara, R. Schmid, and A.K. Bosserhoff. 2011. p54nrb is a new regulator of progression of malignant melanoma. *Carcinogenesis*. 32:1176-1182.

Schluter, O.M., F. Fornai, M.G. Alessandri, S. Takamori, M. Geppert, R. Jahn, and T.C. Sudhof. 2003. Role of alpha-synuclein in 1-methyl-4-phenyl-1,2,3,6-tetrahydropyridine-induced parkinsonism in mice. *Neuroscience*. 118:985-1002.

Schmitt, E., M. Gehrmann, M. Brunet, G. Multhoff, and C. Garrido. 2007. Intracellular and extracellular functions of heat shock proteins: repercussions in cancer therapy. *Journal of leukocyte biology*. 81:15-27.

Schuller, M., D. Jenne, and R. Voltz. 2005. The human PNMA family: novel neuronal proteins implicated in paraneoplastic neurological disease. *Journal of neuroimmunology*. 169:172-176.

Schwartz-Albiez, R., A. Merling, H. Spring, P. Moller, and K. Koretz. 1995. Differential expression of the microspike-associated protein moesin in human tissues. *European journal of cell biology*. 67:189-198.

Scott, D.A., I. Tabarean, Y. Tang, A. Cartier, E. Masliah, and S. Roy. 2010. A pathologic cascade leading to synaptic dysfunction in alpha-synuclein-induced neurodegeneration. *J Neurosci*. 30:8083-8095.

Seshadri, T., J.A. Uzman, J. Oshima, and J. Campisi. 1993. Identification of a transcript that is down-regulated in senescent human fibroblasts. Cloning, sequence analysis, and regulation of the human L7 ribosomal protein gene. *The Journal of biological chemistry*. 268:18474-18480.

Sharon, R., I. Bar-Joseph, G.E. Mirick, C.N. Serhan, and D.J. Selkoe. 2003. Altered fatty acid composition of dopaminergic neurons expressing alpha-synuclein and human brains with alpha-synucleinopathies. *The Journal of biological chemistry*. 278:49874-49881.

Shashidharan, P., P.F. Good, A. Hsu, D.P. Perl, M.F. Brin, and C.W. Olanow. 2000a. TorsinA accumulation in Lewy bodies in sporadic Parkinson's disease. *Brain research*. 877:379-381.

Shashidharan, P., B.C. Kramer, R.H. Walker, C.W. Olanow, and M.F. Brin. 2000b. Immunohistochemical localization and distribution of torsinA in normal human and rat brain. *Brain research*. 853:197-206.

Shaw, R.J., M. Henry, F. Solomon, and T. Jacks. 1998. RhoA-dependent phosphorylation and relocalization of ERM proteins into apical membrane/actin protrusions in fibroblasts. *Molecular biology of the cell*. 9:403-419.

Shendelman, S., A. Jonason, C. Martinat, T. Leete, and A. Abeliovich. 2004. DJ-1 is a redox-dependent molecular chaperone that inhibits alpha-synuclein aggregate formation. *PLoS biology*. 2:e362.

Sherer, T.B., J.H. Kim, R. Betarbet, and J.T. Greenamyre. 2003. Subcutaneous rotenone exposure causes highly selective dopaminergic degeneration and alpha-synuclein aggregation. *Experimental neurology*. 179:9-16.

Shimura, H., N. Hattori, S. Kubo, Y. Mizuno, S. Asakawa, S. Minoshima, N. Shimizu, K. Iwai, T. Chiba, K. Tanaka, and T. Suzuki. 2000. Familial Parkinson disease gene product, parkin, is a ubiquitin-protein ligase. *Nat Genet*. 25:302-305.

Shinbo, J., T. Ozaki, T. Nakagawa, K. Watanabe, Y. Nakamura, M. Yamazaki, H. Moriya, A. Nakagawara, and S. Sakiyama. 2002. p73-dependent expression of DAN during cisplatin-induced cell death and osteoblast differentiation. *Biochemical and biophysical research communications*. 295:501-507.

Shorter, J. 2011. The mammalian disaggregase machinery: Hsp110 synergizes with Hsp70 and Hsp40 to catalyze protein disaggregation and reactivation in a cell-free system. *PloS one*. 6:e26319.

Silva, B.A., L. Breydo, and V.N. Uversky. 2012. Targeting the Chameleon: a Focused Look at alpha-Synuclein and Its Roles in Neurodegeneration. *Molecular neurobiology*.

Silverstein R.M., B.G.C., and Morrill T. C. 1991. Spectrometric identification of organic compounds.

Silvestri, L., V. Caputo, E. Bellacchio, L. Atorino, B. Dallapiccola, E.M. Valente, and G. Casari. 2005. Mitochondrial import and enzymatic activity of PINK1 mutants associated to recessive parkinsonism. *Hum Mol Genet*. 14:3477-3492.

Simon-Sanchez, J., C. Schulte, J.M. Bras, M. Sharma, J.R. Gibbs, D. Berg, C. Paisan-Ruiz, P. Lichtner, S.W. Scholz, D.G. Hernandez, R. Kruger, M. Federoff, C. Klein, A. Goate, J. Perlmutter, M. Bonin, M.A. Nalls, T. Illig, C. Gieger, H. Houlden, M. Steffens, M.S. Okun, B.A. Racette, M.R. Cookson, K.D. Foote, H.H. Fernandez, B.J. Traynor, S. Schreiber, S. Arepalli, R. Zonozi, K. Gwinn, M. van der Brug, G. Lopez, S.J. Chanock, A. Schatzkin, Y. Park, A. Hollenbeck, J. Gao, X. Huang, N.W. Wood, D. Lorenz, G. Deuschl, H. Chen, O. Riess, J.A. Hardy, A.B. Singleton, and T. Gasser. 2009. Genome-wide association study reveals genetic risk underlying Parkinson's disease. *Nature genetics*. 41:1308-1312.

Simons, C.T., A. Staes, H. Rommelaere, C. Ampe, S.A. Lewis, and N.J. Cowan. 2004. Selective contribution of eukaryotic prefoldin subunits to actin and tubulin binding. *The Journal of biological chemistry*. 279:4196-4203.

Singaram, C., W. Ashraf, E.A. Gaumnitz, C. Torbey, A. Sengupta, R. Pfeiffer, and E.M. Quigley. 1995. Dopaminergic defect of enteric nervous system in Parkinson's disease patients with chronic constipation. *Lancet*. 346:861-864.

Singleton, A., K. Gwinn-Hardy, Y. Sharabi, S.T. Li, C. Holmes, R. Dendi, J. Hardy, A. Crawley, and D.S. Goldstein. 2004. Association between cardiac denervation and parkinsonism caused by alpha-synuclein gene triplication. *Brain : a journal of neurology*. 127:768-772.

Singleton, A.B., M. Farrer, J. Johnson, A. Singleton, S. Hague, J. Kachergus, M. Hulihan, T. Peuralinna, A. Dutra, R. Nussbaum, S. Lincoln, A. Crawley, M. Hanson, D. Maraganore, C. Adler, M.R. Cookson, M. Muenter, M. Baptista, D. Miller, J. Blancato, J. Hardy, and K. Gwinn-Hardy. 2003. alpha-Synuclein locus triplication causes Parkinson's disease. *Science*. 302:841.

Sittler, A., R. Lurz, G. Lueder, J. Priller, H. Lehrach, M.K. Hayer-Hartl, F.U. Hartl, and E.E. Wanker. 2001. Geldanamycin activates a heat shock response and inhibits huntingtin aggregation in a cell culture model of Huntington's disease. *Human molecular genetics*. 10:1307-1315.

Smith, W.W., Z. Liu, Y. Liang, N. Masuda, D.A. Swing, N.A. Jenkins, N.G. Copeland, J.C. Troncoso, M. Pletnikov, T.M. Dawson, L.J. Martin, T.H. Moran, M.K. Lee, D.R. Borchelt, and C.A. Ross. 2010. Synphilin-1 attenuates neuronal degeneration in the A53T alpha-synuclein transgenic mouse model. *Human molecular genetics*. 19:2087-2098.

Snyder, H., K. Mensah, C. Theisler, J. Lee, A. Matouschek, and B. Wolozin. 2003. Aggregated and monomeric alpha-synuclein bind to the S6' proteasomal protein and inhibit proteasomal function. *J Biol Chem*. 278:11753-11759.

Solano, S.M., D.W. Miller, S.J. Augood, A.B. Young, and J.B. Penney, Jr. 2000. Expression of alpha-synuclein, parkin, and ubiquitin carboxy-terminal hydrolase L1 mRNA in human brain: genes associated with familial Parkinson's disease. *Annals of neurology*. 47:201-210.

Sone, M., M. Yoshida, Y. Hashizume, N. Hishikawa, and G. Sobue. 2005. alpha-Synuclein-immunoreactive structure formation is enhanced in sympathetic ganglia of patients with multiple system atrophy. *Acta neuropathologica*. 110:19-26.

Song, D.D., C.W. Shults, A. Sisk, E. Rockenstein, and E. Masliah. 2004. Enhanced substantia nigra mitochondrial pathology in human alpha-synuclein transgenic mice after treatment with MPTP. *Experimental neurology*. 186:158-172.

Soto, C. 2003. Unfolding the role of protein misfolding in neurodegenerative diseases. *Nature reviews. Neuroscience*. 4:49-60.

Speck, O., S.C. Hughes, N.K. Noren, R.M. Kulikauskas, and R.G. Fehon. 2003. Moesin functions antagonistically to the Rho pathway to maintain epithelial integrity. *Nature*. 421:83-87.

Spillantini, M.G., M.L. Schmidt, V.M. Lee, J.Q. Trojanowski, R. Jakes, and M. Goedert. 1997. Alpha-synuclein in Lewy bodies. *Nature*. 388:839-840.

St Martin, J.L., J. Klucken, T.F. Outeiro, P. Nguyen, C. Keller-McGandy, I. Cantuti-Castelvetri, T.N. Grammatopoulos, D.G. Standaert, B.T. Hyman, and P.J. McLean. 2007. Dopaminergic neuron loss and up-regulation of chaperone protein mRNA induced by targeted over-expression of alpha-synuclein in mouse substantia nigra. *Journal of neurochemistry*. 100:1449-1457.

Stefanis, L., K.E. Larsen, H.J. Rideout, D. Sulzer, and L.A. Greene. 2001. Expression of A53T mutant but not wild-type alpha-synuclein in PC12 cells induces alterations of the ubiquitin-dependent degradation system, loss of dopamine release, and autophagic cell death. *J Neurosci*. 21:9549-9560.

Steffan, J.S., A. Kazantsev, O. Spasic-Boskovic, M. Greenwald, Y.Z. Zhu, H. Gohler, E.E. Wanker, G.P. Bates, D.E. Housman, and L.M. Thompson. 2000. The Huntington's disease protein interacts with p53 and CREB-binding protein and represses transcription. *Proceedings of the National Academy of Sciences of the United States of America*. 97:6763-6768.

Stocchi, F., D. Badiali, L. Vacca, L. D'Alba, F. Bracci, S. Ruggieri, M. Torti, A. Berardelli, and E. Corazziari. 2000. Anorectal function in multiple system atrophy and Parkinson's disease. *Movement disorders : official journal of the Movement Disorder Society*. 15:71-76.

Subramanian, M., R.W. Gonzalez, H. Patil, T. Ueda, J.H. Lim, K.H. Kraemer, M. Bustin, and M. Bergel. 2009. The nucleosome-binding protein HMGN2 modulates global genome repair. *The FEBS journal*. 276:6646-6657.

Sumoy, L., L. Carim, M. Escarceller, M. Nadal, M. Gratacos, M.A. Pujana, X. Estivill, and B. Peral. 2000. HMG20A and HMG20B map to human chromosomes 15q24 and 19p13.3 and constitute a distinct class of HMG-box genes with ubiquitous expression. *Cytogenetics and cell genetics*. 88:62-67.

Sung, J.Y., J. Kim, S.R. Paik, J.H. Park, Y.S. Ahn, and K.C. Chung. 2001. Induction of neuronal cell death by Rab5A-dependent endocytosis of alpha-synuclein. *The Journal of biological chemistry*. 276:27441-27448.

Taira, T., Y. Saito, T. Niki, S.M. Iguchi-Ariga, K. Takahashi, and H. Ariga. 2004. DJ-1 has a role in antioxidative stress to prevent cell death. *EMBO Rep*. 5:213-218.

Takahashi, K., T. Sasaki, A. Mammoto, I. Hotta, K. Takaishi, H. Imamura, K. Nakano, A. Kodama, and Y. Takai. 1998. Interaction of radixin with Rho small G protein GDP/GTP exchange protein Dbl. *Oncogene*. 16:3279-3284.

Takahashi, K., T. Sasaki, A. Mammoto, K. Takaishi, T. Kameyama, S. Tsukita, and Y. Takai. 1997. Direct interaction of the Rho GDP dissociation inhibitor with ezrin/radixin/moesin initiates the activation of the Rho small G protein. *The Journal of biological chemistry*. 272:23371-23375.

Takai, Y., K. Kitano, S. Terawaki, R. Maesaki, and T. Hakoshima. 2008. Structural basis of the cytoplasmic tail of adhesion molecule CD43 and its binding to ERM proteins. *Journal of molecular biology*. 381:634-644.

Takeuchi, K., N. Sato, H. Kasahara, N. Funayama, A. Nagafuchi, S. Yonemura, and S. Tsukita. 1994. Perturbation of cell adhesion and microvilli formation by antisense oligonucleotides to ERM family members. *The Journal of cell biology*. 125:1371-1384.

Tam, S., R. Geller, C. Spiess, and J. Frydman. 2006. The chaperonin TRiC controls polyglutamine aggregation and toxicity through subunit-specific interactions. *Nature cell biology*. 8:1155-1162.

Tanaka, Y., S. Engelender, S. Igarashi, R.K. Rao, T. Wanner, R.E. Tanzi, A. Sawa, L.D. V, T.M. Dawson, and C.A. Ross. 2001. Inducible expression of mutant alpha-synuclein decreases proteasome activity and increases sensitivity to mitochondria-dependent apoptosis. *Hum Mol Genet*. 10:919-926.

Tanner, C.M., G.W. Ross, S.A. Jewell, R.A. Hauser, J. Jankovic, S.A. Factor, S. Bressman, A. Deligtisch, C. Marras, K.E. Lyons, G.S. Bhudhikanok, D.F. Roucoux, C. Meng, R.D. Abbott, and J.W. Langston. 2009. Occupation and risk of parkinsonism: a multicenter case-control study. *Archives of neurology*. 66:1106-1113.

Thayanidhi, N., J.R. Helm, D.C. Nycz, M. Bentley, Y. Liang, and J.C. Hay. 2010. Alpha-synuclein delays endoplasmic reticulum (ER)-to-Golgi transport in mammalian cells by antagonizing ER/Golgi SNAREs. *Mol Biol Cell*. 21:1850-1863.

Thomas, B., A.S. Mandir, N. West, Y. Liu, S.A. Andrabi, W. Stirling, V.L. Dawson, T.M. Dawson, and M.K. Lee. 2011. Resistance to MPTP-neurotoxicity in alpha-synuclein knockout mice is complemented by human alpha-synuclein and associated with increased beta-synuclein and Akt activation. *PloS one*. 6:e16706.

Todi, S.V., B.J. Winborn, K.M. Scaglione, J.R. Blount, S.M. Travis, and H.L. Paulson. 2009. Ubiquitination directly enhances activity of the deubiquitinating enzyme ataxin-3. *The EMBO journal*. 28:372-382.

Tofaris, G.K., P. Garcia Reitbock, T. Humby, S.L. Lambourne, M. O'Connell, B. Ghetti, H. Gossage, P.C. Emson, L.S. Wilkinson, M. Goedert, and M.G. Spillantini. 2006. Pathological changes in dopaminergic nerve cells of the substantia nigra and olfactory bulb in mice transgenic for truncated human alpha-synuclein(1-120): implications for Lewy body disorders. *The Journal of neuroscience : the official journal of the Society for Neuroscience*. 26:3942-3950.

Tompa, P. 2002. Intrinsically unstructured proteins. *Trends in biochemical sciences*. 27:527-533.

Tretiakoff, C. 1919. Contribution à l'étude de l'anatomie pathologique du locus niger de Soemmering avec quelques deductions relatives à la pathogénie des troubles du tonus muscolaire et de la maladie de Parkinson. *Univ. Paris*.

Trofatter, J.A., M.M. MacCollin, J.L. Rutter, J.R. Murrell, M.P. Duyao, D.M. Parry, R. Eldridge, N. Kley, A.G. Menon, K. Pulaski, and et al. 1993. A novel moesin-, ezrin-, radixin-like gene is a candidate for the neurofibromatosis 2 tumor suppressor. *Cell*. 75:826.

Trojanowski, J.Q., M. Goedert, T. Iwatsubo, and V.M. Lee. 1998. Fatal attractions: abnormal protein aggregation and neuron death in Parkinson's disease and Lewy body dementia. *Cell death and differentiation*. 5:832-837.

Trojanowski, J.Q., and V.M. Lee. 2000. "Fatal attractions" of proteins. A comprehensive hypothetical mechanism underlying Alzheimer's disease and other neurodegenerative disorders. *Annals of the New York Academy of Sciences*. 924:62-67.

Tsai, J., J. Grutzendler, K. Duff, and W.B. Gan. 2004. Fibrillar amyloid deposition leads to local synaptic abnormalities and breakage of neuronal branches. *Nature neuroscience*. 7:1181-1183.

Tsuchiya, N., D. Kamei, A. Takano, T. Matsui, and M. Yamada. 1998. Cloning and characterization of a cDNA encoding a novel heterogeneous nuclear ribonucleoprotein-like protein and its expression in myeloid leukemia cells. *Journal of biochemistry*. 123:499-507.

Tsukita, S., and Y. Hieda. 1989. A new 82-kD barbed end-capping protein (radixin) localized in the cell-to-cell adherens junction: purification and characterization. *The Journal of cell biology*. 108:2369-2382.

Turunen, O., R. Winqvist, R. Pakkanen, K.H. Grzeschik, T. Wahlstrom, and A. Vaheri. 1989. Cytovillin, a microvillar Mr 75,000 protein. cDNA sequence, prokaryotic expression, and chromosomal localization. *The Journal of biological chemistry*. 264:16727-16732.

Ueda, K., H. Fukushima, E. Masliah, Y. Xia, A. Iwai, M. Yoshimoto, D.A. Otero, J. Kondo, Y. Ihara, and T. Saitoh. 1993. Molecular cloning of cDNA encoding an unrecognized component of amyloid in Alzheimer disease. *Proceedings of the National Academy of Sciences of the United States of America*. 90:11282-11286.

Ulmer, T.S., and A. Bax. 2005. Comparison of structure and dynamics of micelle-bound human alpha-synuclein and Parkinson disease variants. *The Journal of biological chemistry*. 280:43179-43187.

Ulmer, T.S., A. Bax, N.B. Cole, and R.L. Nussbaum. 2005. Structure and dynamics of micelle-bound human alpha-synuclein. *The Journal of biological chemistry*. 280:9595-9603.

Uversky, V.N. 2003. A protein-chameleon: conformational plasticity of alpha-synuclein, a disordered protein involved in neurodegenerative disorders. *Journal of biomolecular structure & dynamics*. 21:211-234.

Uversky, V.N. 2007. Neuropathology, biochemistry, and biophysics of alpha-synuclein aggregation. *Journal of neurochemistry*. 103:17-37.

Uversky, V.N., M.C. E, K.S. Bower, J. Li, and A.L. Fink. 2002a. Accelerated alpha-synuclein fibrillation in crowded milieu. *FEBS letters*. 515:99-103.

Uversky, V.N., H.J. Lee, J. Li, A.L. Fink, and S.J. Lee. 2001a. Stabilization of partially folded conformation during alpha-synuclein oligomerization in both purified and cytosolic preparations. *The Journal of biological chemistry*. 276:43495-43498.

Uversky, V.N., J. Li, and A.L. Fink. 2001b. Evidence for a partially folded intermediate in alpha-synuclein fibril formation. *The Journal of biological chemistry*. 276:10737-10744.

Uversky, V.N., J. Li, P. Souillac, I.S. Millett, S. Doniach, R. Jakes, M. Goedert, and A.L. Fink. 2002b. Biophysical properties of the synucleins and their propensities to fibrillate: inhibition of alpha-synuclein assembly by beta- and gamma-synucleins. *The Journal of biological chemistry*. 277:11970-11978.

Uversky, V.N., S.E. Permyakov, V.E. Zagranichny, I.L. Rodionov, A.L. Fink, A.M. Cherskaya, L.A. Wasserman, and E.A. Permyakov. 2002c. Effect of zinc and temperature on the conformation of the gamma subunit of retinal phosphodiesterase: a natively unfolded protein. *Journal of proteome research*. 1:149-159.

van Ham, T.J., M.A. Holmberg, A.T. van der Goot, E. Teuling, M. Garcia-Arencibia, H.E. Kim, D. Du, K.L. Thijssen, M. Wiersma, R. Burggraaff, P. van Bergeijk, J. van

Rheenen, G. Jerre van Veluw, R.M. Hofstra, D.C. Rubinsztein, and E.A. Nollen. 2010. Identification of MOAG-4/SERF as a regulator of age-related proteotoxicity. *Cell*. 142:601-612.

Vashist, S., M. Cushman, and J. Shorter. 2010. Applying Hsp104 to protein-misfolding disorders. *Biochemistry and cell biology = Biochimie et biologie cellulaire*. 88:1-13.

Veber, D.F., S.R. Johnson, H.Y. Cheng, B.R. Smith, K.W. Ward, and K.D. Kopple. 2002. Molecular properties that influence the oral bioavailability of drug candidates. *Journal of medicinal chemistry*. 45:2615-2623.

Venda, L.L., S.J. Cragg, V.L. Buchman, and R. Wade-Martins. 2010. alpha-Synuclein and dopamine at the crossroads of Parkinson's disease. *Trends in neurosciences*. 33:559-568.

Vogiatzi, T., M. Xilouri, K. Vekrellis, and L. Stefanis. 2008. Wild type alpha-synuclein is degraded by chaperone-mediated autophagy and macroautophagy in neuronal cells. *The Journal of biological chemistry*. 283:23542-23556.

Volles, M.J., and P.T. Lansbury, Jr. 2002. Vesicle permeabilization by protofibrillar alpha-synuclein is sensitive to Parkinson's disease-linked mutations and occurs by a pore-like mechanism. *Biochemistry*. 41:4595-4602.

Volles, M.J., and P.T. Lansbury, Jr. 2003. Zeroing in on the pathogenic form of alpha-synuclein and its mechanism of neurotoxicity in Parkinson's disease. *Biochemistry*. 42:7871-7878.

Voltz, R., S.H. Gultekin, M.R. Rosenfeld, E. Gerstner, J. Eichen, J.B. Posner, and J. Dalmau. 1999. A serologic marker of paraneoplastic limbic and brain-stem encephalitis in patients with testicular cancer. *The New England journal of medicine*. 340:1788-1795.

von Mikecz, A., P. Hemmerich, E. Neu, H.H. Peter, and U. Krawinkel. 1994. [Ribosomal protein L7 as an autoantigen in patients with systemic lupus erythematosus, mixed collagen disease and rheumatoid arthritis]. *Zeitschrift fur arztliche Fortbildung*. 88:501-503.

Waelter, S., A. Boeddrich, R. Lurz, E. Scherzinger, G. Lueder, H. Lehrach, and E.E. Wanker. 2001. Accumulation of mutant huntingtin fragments in aggresome-like inclusion bodies as a result of insufficient protein degradation. *Molecular biology of the cell*. 12:1393-1407.

Wakabayashi, K., and H. Takahashi. 1997. Neuropathology of autonomic nervous system in Parkinson's disease. *European neurology*. 38 Suppl 2:2-7.

Wakabayashi, K., H. Takahashi, K. Obata, and F. Ikuta. 1992. Immunocytochemical localization of synaptic vesicle-specific protein in Lewy body-containing neurons in Parkinson's disease. *Neuroscience letters*. 138:237-240.

Wakabayashi, K., H. Takahashi, S. Takeda, E. Ohama, and F. Ikuta. 1988. Parkinson's disease: the presence of Lewy bodies in Auerbach's and Meissner's plexuses. *Acta neuropathologica*. 76:217-221.

Walker, J.K., R.R. Gainetdinov, A.W. Mangel, M.G. Caron, and M.A. Shetzline. 2000. Mice lacking the dopamine transporter display altered regulation of distal colonic motility. *American journal of physiology. Gastrointestinal and liver physiology*. 279:G311-318.

Walker, R.H., M.F. Brin, D. Sandu, P. Gujjari, P.R. Hof, C. Warren Olanow, and P. Shashidharan. 2001. Distribution and immunohistochemical characterization of torsinA immunoreactivity in rat brain. *Brain research*. 900:348-354.

Walsh, D.T., L. Bresciani, D. Saunders, M.F. Manca, A. Jen, S.M. Gentleman, and L.S. Jen. 2005. Amyloid beta peptide causes chronic glial cell activation and neuro-degeneration after intravitreal injection. *Neuropathology and applied neurobiology*. 31:491-502.

Wang, W., I. Perovic, J. Chittuluru, A. Kaganovich, L.T. Nguyen, J. Liao, J.R. Auclair, D. Johnson, A. Landeru, A.K. Simorellis, S. Ju, M.R. Cookson, F.J. Asturias, J.N. Agar, B.N. Webb, C. Kang, D. Ringe, G.A. Petsko, T.C. Pochapsky, and Q.Q. Hoang. 2011. A soluble alpha-synuclein construct forms a dynamic tetramer. *Proceedings of*

the National Academy of Sciences of the United States of America. 108:17797-17802.

Watabe, K., A. Ito, Y.I. Koma, and Y. Kitamura. 2003. IGSF4: a new intercellular adhesion molecule that is called by three names, TSLC1, SgIGSF and SynCAM, by virtue of its diverse function. *Histology and histopathology*. 18:1321-1329.

Watanabe, M., A.R. Zinn, D.C. Page, and T. Nishimoto. 1993. Functional equivalence of human X- and Y-encoded isoforms of ribosomal protein S4 consistent with a role in Turner syndrome. *Nature genetics*. 4:268-271.

Waudby, C.A., T.P. Knowles, G.L. Devlin, J.N. Skepper, H. Ecroyd, J.A. Carver, M.E. Welland, J. Christodoulou, C.M. Dobson, and S. Meehan. 2010. The interaction of alphaB-crystallin with mature alpha-synuclein amyloid fibrils inhibits their elongation. *Biophysical journal*. 98:843-851.

Weinreb, P.H., W. Zhen, A.W. Poon, K.A. Conway, and P.T. Lansbury, Jr. 1996. NACP, a protein implicated in Alzheimer's disease and learning, is natively unfolded. *Biochemistry*. 35:13709-13715.

Wenning, G.K., Y. Ben Shlomo, M. Magalhaes, S.E. Daniel, and N.P. Quinn. 1994. Clinical features and natural history of multiple system atrophy. An analysis of 100 cases. *Brain : a journal of neurology*. 117 (Pt 4):835-845.

West, K.L., Y. Ito, Y. Birger, Y. Postnikov, H. Shirakawa, and M. Bustin. 2001. HMGN3a and HMGN3b, two protein isoforms with a tissue-specific expression pattern, expand the cellular repertoire of nucleosome-binding proteins. *The Journal of biological chemistry*. 276:25959-25969.

Wetzel, R. 1996. For protein misassembly, it's the "I" decade. *Cell*. 86:699-702.

Williamson, M.P. 2013. Using chemical shift perturbation to characterise ligand binding. *Progress in nuclear magnetic resonance spectroscopy*. 73:1-16.

Willingham, S., T.F. Outeiro, M.J. DeVit, S.L. Lindquist, and P.J. Muchowski. 2003. Yeast genes that enhance the toxicity of a mutant huntingtin fragment or alpha-synuclein. *Science*. 302:1769-1772.

Wilson, C.G., and M.R. Arkin. 2011. Small-molecule inhibitors of IL-2/IL-2R: lessons learned and applied. *Current topics in microbiology and immunology*. 348:25-59.

Wirdefeldt, K., N. Bogdanovic, L. Westerberg, H. Payami, M. Schalling, and G. Murdoch. 2001. Expression of alpha-synuclein in the human brain: relation to Lewy body disease. *Brain research. Molecular brain research*. 92:58-65.

Wolters, E. 2009. Non-motor extranigral signs and symptoms in Parkinson's disease. *Parkinsonism Relat Disord*. 15 Suppl 3:S6-12.

Wood-Kaczmar, A., S. Gandhi, and N.W. Wood. 2006. Understanding the molecular causes of Parkinson's disease. *Trends in molecular medicine*. 12:521-528.

Wood, S.J., J. Wypych, S. Steavenson, J.C. Louis, M. Citron, and A.L. Biere. 1999. alpha-synuclein fibrillogenesis is nucleation-dependent. Implications for the pathogenesis of Parkinson's disease. *The Journal of biological chemistry*. 274:19509-19512.

Woods, W.S., J.M. Boettcher, D.H. Zhou, K.D. Kloepper, K.L. Hartman, D.T. Ladror, Z. Qi, C.M. Rienstra, and J.M. George. 2007. Conformation-specific binding of alpha-synuclein to novel protein partners detected by phage display and NMR spectroscopy. *The Journal of biological chemistry*. 282:34555-34567.

Wu, S., J.N. De Croos, and K.B. Storey. 2008. Cold acclimation-induced up-regulation of the ribosomal protein L7 gene in the freeze tolerant wood frog, Rana sylvatica. *Gene*. 424:48-55.

Wynder, C., M.A. Hakimi, J.A. Epstein, A. Shilatifard, and R. Shiekhattar. 2005. Recruitment of MLL by HMG-domain protein iBRAF promotes neural differentiation. *Nature cell biology*. 7:1113-1117.

Xilouri, M., O.R. Brekk, N. Landeck, P.M. Pitychoutis, T. Papasilekas, Z. Papadopoulou-Daifoti, D. Kirik, and L. Stefanis. 2013. Boosting chaperone-mediated autophagy in vivo mitigates alpha-synuclein-induced neurodegeneration. *Brain : a journal of neurology*. 136:2130-2146.

REFERENCES

Xilouri, M., T. Vogiatzi, K. Vekrellis, D. Park, and L. Stefanis. 2009. Abberant alpha-synuclein confers toxicity to neurons in part through inhibition of chaperone-mediated autophagy. *PloS one*. 4:e5515.

Xu, C., J. Xu, Y. Zhang, J. Ma, H. Kawakami, H. Maruyama, and M. Kamada. 2010. Analysis on the susceptibility genes in two chinese pedigrees with familial Parkinson's disease. *Neurology research international*. 2010:674740.

Xu, J., S.Y. Kao, F.J. Lee, W. Song, L.W. Jin, and B.A. Yankner. 2002. Dopamine-dependent neurotoxicity of alpha-synuclein: a mechanism for selective neurodegeneration in Parkinson disease. *Nature medicine*. 8:600-606.

Xu, Z., Y. Zheng, Y. Zhu, X. Kong, and L. Hu. 2011. Evidence for OTUD-6B participation in B lymphocytes cell cycle after cytokine stimulation. *PloS one*. 6:e14514.

Yagi, H., E. Kusaka, K. Hongo, T. Mizobata, and Y. Kawata. 2005. Amyloid fibril formation of alpha-synuclein is accelerated by preformed amyloid seeds of other proteins: implications for the mechanism of transmissible conformational diseases. *The Journal of biological chemistry*. 280:38609-38616.

Yamada, M., T. Iwatsubo, Y. Mizuno, and H. Mochizuki. 2004. Overexpression of alpha-synuclein in rat substantia nigra results in loss of dopaminergic neurons, phosphorylation of alpha-synuclein and activation of caspase-9: resemblance to pathogenetic changes in Parkinson's disease. *Journal of neurochemistry*. 91:451-461.

Yamin, G., L.A. Munishkina, M.A. Karymov, Y.L. Lyubchenko, V.N. Uversky, and A.L. Fink. 2005. Forcing nonamyloidogenic beta-synuclein to fibrillate. *Biochemistry*. 44:9096-9107.

Yang, J.W., T. Czech, M. Felizardo, C. Baumgartner, and G. Lubec. 2006. Aberrant expression of cytoskeleton proteins in hippocampus from patients with mesial temporal lobe epilepsy. *Amino acids*. 30:477-493.

Yang, Y.S., J.H. Hanke, L. Carayannopoulos, C.M. Craft, J.D. Capra, and P.W. Tucker. 1993. NonO, a non-POU-domain-containing, octamer-binding protein, is the mammalian homolog of Drosophila nonAdiss. *Molecular and cellular biology*. 13:5593-5603.

Youdim, M.B., D. Edmondson, and K.F. Tipton. 2006. The therapeutic potential of monoamine oxidase inhibitors. *Nature reviews. Neuroscience*. 7:295-309.

Zakrajsek, T., P. Raspor, and P. Jamnik. 2011. Saccharomyces cerevisiae in the stationary phase as a model organism--characterization at cellular and proteome level. *Journal of proteomics*. 74:2837-2845.

Zarranz, J.J., J. Alegre, J.C. Gomez-Esteban, E. Lezcano, R. Ros, I. Ampuero, L. Vidal, J. Hoenicka, O. Rodriguez, B. Atares, V. Llorens, E. Gomez Tortosa, T. del Ser, D.G. Munoz, and J.G. de Yebenes. 2004. The new mutation, E46K, of alpha-synuclein causes Parkinson and Lewy body dementia. *Ann Neurol*. 55:164-173.

Zekri, L., E. Huntzinger, S. Heimstadt, and E. Izaurralde. 2009. The silencing domain of GW182 interacts with PABPC1 to promote translational repression and degradation of microRNA targets and is required for target release. *Molecular and cellular biology*. 29:6220-6231.

Zhang, W., Q.B. Tian, Q.K. Li, J.M. Wang, C.N. Wang, T. Liu, D.W. Liu, and M.W. Wang. 2011. Lysine 92 amino acid residue of USP46, a gene associated with 'behavioral despair' in mice, influences the deubiquitinating enzyme activity. *PloS one*. 6:e26297.

Zhang, Y., J. Gao, K.K. Chung, H. Huang, V.L. Dawson, and T.M. Dawson. 2000. Parkin functions as an E2-dependent ubiquitin- protein ligase and promotes the degradation of the synaptic vesicle-associated protein, CDCrel-1. *Proceedings of the National Academy of Sciences of the United States of America*. 97:13354-13359.

Zhou, R.M., Y.X. Huang, X.L. Li, C. Chen, Q. Shi, G.R. Wang, C. Tian, Z.Y. Wang, Y.Y. Jing, C. Gao, and X.P. Dong. 2010. Molecular interaction of alpha-synuclein with tubulin influences on the polymerization of microtubule in vitro and structure of microtubule in cells. *Mol Biol Rep*. 37:3183-3192.

Zhou, W., M. Zhu, M.A. Wilson, G.A. Petsko, and A.L. Fink. 2006. The oxidation state of DJ-1 regulates its chaperone activity toward alpha-synuclein. *Journal of molecular biology*. 356:1036-1048.

Zhu, M., and A.L. Fink. 2003. Lipid binding inhibits alpha-synuclein fibril formation. *The Journal of biological chemistry*. 278:16873-16877.

Zhu, M., J. Li, and A.L. Fink. 2003. The association of alpha-synuclein with membranes affects bilayer structure, stability, and fibril formation. *The Journal of biological chemistry*. 278:40186-40197.

Zhu, M., Z.J. Qin, D. Hu, L.A. Munishkina, and A.L. Fink. 2006. Alpha-synuclein can function as an antioxidant preventing oxidation of unsaturated lipid in vesicles. *Biochemistry*. 45:8135-8142.

Zhu, M., S. Rajamani, J. Kaylor, S. Han, F. Zhou, and A.L. Fink. 2004. The flavonoid baicalein inhibits fibrillation of alpha-synuclein and disaggregates existing fibrils. *The Journal of biological chemistry*. 279:26846-26857.

Zimprich, A., S. Biskup, P. Leitner, P. Lichtner, M. Farrer, S. Lincoln, J. Kachergus, M. Hulihan, R.J. Uitti, D.B. Calne, A.J. Stoessl, R.F. Pfeiffer, N. Patenge, I.C. Carbajal, P. Vieregge, F. Asmus, B. Muller-Myhsok, D.W. Dickson, T. Meitinger, T.M. Strom, Z.K. Wszolek, and T. Gasser. 2004. Mutations in LRRK2 cause autosomal-dominant parkinsonism with pleomorphic pathology. *Neuron*. 44:601-607.

Zinn, A.R., R.K. Alagappan, L.G. Brown, I. Wool, and D.C. Page. 1994. Structure and function of ribosomal protein S4 genes on the human and mouse sex chromosomes. *Molecular and cellular biology*. 14:2485-2492.

7. LIST OF ABBREVIATIONS

°C	degrees Celsius
µg	microgram
µl	microliter
µM	micromolar
3-AT	3-amino-1,2,4-triazole
6-OHDA	6-hydroxydopamine
A30P	α-synuclein mutation (alanine [A] to proline [P] at position 30)
A53T	α-synuclein mutation (alanine [A] to threonine [T] at position 53)
AD	Alzheimer's disease
ADP	adenosine diphosphate
ALS	amyotrophic lateral sclerosis
Amp	ampicillin
ATP	adenosine triphosphate
AU	arbitrary units
β-gal	ß-galactosidase
BD	DNA-binding domain
bp	base pair
C. elegans	*Caenorhabditis elegans*
CD	circular dichroism
cDNA	complementary DNA
CMA	chaperone-mediated autophagy
CNS	central nervous system
co-IP	co-immunoprecipitation
D. melanogaster	*Drosophila melanogaster*
ddH_2O	double-distilled water
DLB	dementia with Lewy bodies
DMSO	dimethyl sulphoxide
DNA	deoxyribonucleic acid
DTT	dithiothreitol
E46K	α-synuclein mutation (glutamic acid [E] to lysine [K] at position 46)
E. coli	*Escherichia coli*
EDTA	ethylene diamine tetraacetic acid
ENS	enteric nervous system
ER	endoplasmic reticulum
g	Earth's gravity
GAG	glycosaminoglycan

LIST OF ABBREVIATIONS

GCI	glial cytoplasmic inclusion
GFP	green fluorescent protein
GI	gastro-intestinal
GWAS	genome-wide association studies
h	hour
HD	Huntington's disease
HEK	Human Embryonic Kidney 293 cells
HEPES	4-(2-hydroxyethyl)-1-piperazineethanesulphonic acid
HSF1	heat-shock factor 1
Htt	Huntingtin
Kan	kanamycin
kDa	kilodalton
L-DOPA	L-3,4-dihydroxyphenylalanine
LB	Lysogeny broth / Lewy body
LBD	Lewy body disease
LDH	lactate dehydrogenase
LN	Lewy neurite
MATα	yeast mating type α
MATa	yeast mating type a
mg	milligram
min	minutes
ml	milliliter
MP	myenteric plexus
MPTP	1-methyl-4-phenyl-1,2,3,6-tetrahydropyridine
mRNA	messenger ribonucleic acid
MS	mass spectrometry
MTP	microtiter plate
MTT	3-(4,5-dimethylthiazol-2-yl)-2,5-diphenyltetrazolium bromide
NAC	non-Aβ component of AD amyloid
NGF	nerve growth factor
nm	nanometer
NMR	nuclear magnetic resonance
NOS	nitric oxide synthase
OD_{600}	optical density at a wavelength of 600nm
ORF	open reading frame
PBS	phospho-buffered saline
PCR	polymerase chain reaction

LIST OF ABBREVIATIONS

PD	Parkinson's disease
PPI	protein-protein interaction
PTM	post-translational modification
ROS	reactive oxygen species
RNAi	RNA interference
S. cerevisiae	*Saccharomyces cerevisiae*
SCA	spinocerebellar ataxias
SD	synthetically defined broth
SDS	sodium dodecyl sulfate
SDS-PAGE	sodium dodecyl sulfate polyacrylamide gel electrophoresis
siRNA	small interfering ribonucleic acid
SMP	sub-mucosal plexus
SNCA	gene encoding α-synuclein
SN	substantia nigra
SNpc	substantia nigra pars compacta
Tet	tetracycline
TH	tyroxine hydroxylase
TF	transcription factor
TNF	tumor necrosis factor
Tris	tris(hydroxymethyl)aminomethane
U	unit of enzyme activity
UPS	ubiquitin-proteasome system
WB	Western blot
WT	wild-type
Y2H	yeast two-hybrid
YPD	yeast full medium

8. LEBENSLAUF

Der Lebenslauf ist in der Online-Version aus Gründen des Datenschutzes nicht enthalten.

LEBENSLAUF

Der Lebenslauf ist in der Online-Version aus Gründen des Datenschutzes nicht enthalten.